Heft 20-1
München, Oktober 1985

International Federation of Surveyors
– F I G –

Proceedings

Inertial, Doppler and GPS Measurements for National and Engineering Surveys

Joint Meeting of Study Groups 5B and 5C
July 1-3, 1985

Editors: W. M. Welsch
L. A. Lapine

SCHRIFTENREIHE

Universitärer Studiengang Vermessungswesen
Universität der Bundeswehr München

UniBw

Heft 20-1
München, Oktober 1985

International Federation of Surveyors
– F I G –

Proceedings

Inertial, Doppler and GPS Measurements for National and Engineering Surveys

Joint Meeting of Study Groups 5B and 5C
July 1-3, 1985

Editors: W. M. Welsch
L. A. Lapine

SCHRIFTENREIHE

Universitärer Studiengang Vermessungswesen
Universität der Bundeswehr München

UniBw

Der Druck dieses Heftes wurde aus Haushaltsmitteln der Hochschule der Bundeswehr München gefördert.

Auflagenhöhe: 900 Exemplare

Verantwortlich für die Herausgabe der Schriftenreihe:

Der Prodekan des Universitären Studiengangs Vermessungswesen

Bezugsnachweis:

Universität der Bundeswehr München
Fakultät für Bauingenieur- und Vermessungswesen
Universitärer Studiengang Vermessungswesen
Werner-Heisenberg-Weg 39
8014 Neubiberg

ISSN 0173-1009

P R E F A C E

On behalf of the International Federation of Surveyors (FIG) and the FIG Commission 5 "Survey Instruments and Methods" the joint meeting of Study Group 5B "Survey Control Networks" and 5C "Satellite and Inertial Survey Systems" was organized.

The basis for this meeting are the recommendations of the last FIG-Congress in Sofia, 1983, which read

R 503: "Recognizing the basic importance of control networks for many tasks of surveying, considering the fact, that increasingly not only conventional terrestrial networks but also networks established on the basis of Doppler, inertial and interferometric techniques serve as fundamental control networks, and regarding the recommendations of the Meeting of Study Group 5B in Aalborg (Denmark), 1982, refering to general topics of current scientific and practical interest, the FIG recommends to continue the work of Study Group 5B "Survey Control Networks" with special emphasis on an adequate integration and densification of all kinds of fundamental control networks (hybrid networks) to the benefit of existing national and other control networks."

R 504: "Considering the fact that "Satellite and Inertial Survey Systems" are relatively new high technology systems with important applications for developing countries with large unmapped areas, and that some of these survey systems also have worldwide applications for the connection of national survey networks, the FIG recommends that Study Group 5C continues its work to investigate all satellite and inertial survey systems with an emphasis on practical applications, use and data reduction by land surveyors. In the event that other high technology systems become available to the surveyor prior to the XVIIIth Congress, 1986, these systems should also be studied and reported on that time."

In fulfilment of these requirements the joint meeting has been given the title "Inertial, Doppler and GPSD Measurements for National and Engineering Surveys".

The topics of the symposium have been fairly wide-spanned. They cover two substantially different sources of geodetic measurements: inertial survey

systems and satellite aided survey systems. To begin with the latter:

Right now there is a transition zone between the use of the TRANSIT and the NAVSTAR satellite system. The first has been exploited extensively by measurements based on the Doppler-effect since many years. It is representing the second generation of satellites applied to geodetic measurements.

The first was the PAGEOS-satellite. In those early times of satellite aided positioning it took as much as two or three months to determine the position of a point with an accuracy of 5 - 8 m. The observation process was purely photographic.

The second generation has, as mentioned before, made use of the TRANSIT satellites since 10 years or so. It takes some days or 70 to 100 satellite passes to determine point positions with an accuracy of 1 m or better absolutely or - applying differential techniques - an accuracy as good as 0.1 m relatively.

The new, third generation of satellites for geodetic applications coming into use since some years, the so-called Global Positioning System (GPS), requires an observation time of only a few hours for the time being. The accuracy received by different modes of processing can reach the subdecimeter region; even cm-accuracy can be achieved as test measurements have proven. The GPS allows not only static measurements, also the dynamic mode is possible. This mode can be utilized for tracking tasks. A target of the future is "millimeters within seconds" as expressed by a paper given at the First International Symposium on Precise Positioning with the Global Positioning System in Rockville in April 1985. The GPS is still in a nascent state. It was only recently that GPS ground control was switched from interim to operational status. This apparently means that the full worldwide tracking network will be used from now on to compute satellite ephemeris and should lead to some more consistent results. Summarizing, compared with the TRANSIT system, in differential positioning it will provide about 10 times the accuracy in 1/10 the time. But - is TRANSIT dead?

Inertial survey systems are of quite a different nature. They provide satellite independent information of positioning, and are therefore somehow independent of political constellations. The state of the art in inertial surveying has been under development for over two decades, is widely used in

military and civilian applications, and is well documented in the technical literature. However, inertial systems are not typically stand-alone systems. In many applications, in navigation as well as in geodesy, the combination of an inertial navigation system (INS) and satellite aided systems offer particular advantages, and integrated GPS - INS are being developed to capitalize on these advantages.

When information of this symposium was spread and papers were called for, the answer was clearly on the side of GPS-applications. It is a new and fascinating technology to scientists and practitioners as well. The other techniques, however, should not be forgotten.

The joint meeting of FIG Study Group 5B and 5C the proceedings of which have been published in these two volumes intended to contribute to the knowledge of inertial and satellite aided survey systems.

W.M. Welsch L.A. Lapine

TABLE OF CONTENTS

Volume 1

		Page
Preface		1
INERTIAL MEASUREMENTS		9
Caspary, W.	- Review Paper - Inertial Positioning - Principals and Procedures	11
Boedecker, G.	Inertial Gravimetry: Results of a Test-net Observation Campaign with Ferranti FILS MK II	21
Lechner, W.	Azimuth Determination with Inertial Systems	35
Möhlenbrink, W.	Drift Effects in Inertial Measurement Systems (Resulting from Nonlinear Terms in the Equations of Motions)	51
Penton, C.R.	Inertial Measurements for National Control	71
Schödlbauer, A.	Inertial Survey Platforms and their Geodetic Relevant Coordinate Systems	89
NNSS DOPPLER MEASUREMENTS - The Navy Navigation Satellite System -		113
Richardus, P.	- Review Paper - Transit Doppler Satellite Positioning for National and Engineering Control Surveys	115
Ádám, J.	On the Consistency of the Station Coordinates Derived from Satellite Doppler Observations	123
Joó, I.	Improvement of the Hungarian National Geodetic Control Network by Satellite Doppler Positioning	145
Mihály, S., Borza, T., Fejes, I.	Practical Results of Interferometric Processing of NNSS Doppler Observations	163

		Page
GPS MEASUREMENTS		177
- The Global Positioning System -		
Wells, D.E.	Recommended GPS Terminology	179
Hartl, Ph., Schöller, W., Thiel, K.-H.	- Review Paper - GPS - Technology and Methodology for Geodetic Applications	109
Krakiwsky, E.J.	- Review Paper - Satellite and Inertial Surveying: Trends and Prospects	227
Beier, W.	A C/A Code GPS-Receiver for Navigation	241
Borutta, H., Heister, H.	Optimal Design for GPS 3-D Differential Positioning	257
Eissfeller, B.	The Estimation of Orthometric Heights from GPS Baseline Vectors Using Gravity Field Information and Least-Squares Collocation	277
Evans, A.G.	The Global Positioning System: An Alternative to Six Degrees-of-Freedom Inertial Navigation	279
Fritzensmeier, K., Kloth, G., Niemeier, W., Eichholz, K.	Simulation Studies on the Improvement of Terrestrial 2-D-Networks by Additional GPS-Information	291

Volume 2

		Page
Gerlach, B.E.	Positioning with a GPS Pseudorange Receiver - Functional Model Test Results -	315
Gervaise, J., Mayoud, M., Beutler, G., Gurtner, W.	Test of GPS on the CERN-LEP Control Network	337
Grafarend, E.W., Lindlohr, W., Stomma, A.	Improved Second Order Design of the Global Positioning System - Ephemerides, Clocks and Atmospheric Influences -	359
Gründig, L., Neureither, M., Bahndorf, J.	Including Macrometer-Type Observables into a Standard 3D Adjustment Program	377
Hartl, Ph., Schöller, W., Thiel, K.-H.	GPS Related Activities of the INS	391
Hein, G.W.	From the Phase Observables of the Global Positioning System to 3D-Baseline Components	403
Henson, D.J., Collier, E.A., Schneider, K.R.	Geodetic Applications of the Texas Instruments TI 4100 GPS Navigator	405
Hofmann-Wellenhof, B.	GPS in Practice - from Measurements to Results	425
Hofmann-Wellenhof, B., Remondi, B.W.	Determination of the Trajectory of a Moving Platform Using GPS Carrier Phase	443
Landau, H.	GPS Baseline Vectors in an Integrated Threedimensional Adjustment	463
Le Cocq, C., Boucher, C.	Geodetic Applications of the SERCEL TR5S GPS Receiver	465
Papo, H.B., Perelmuter, A.	Should Our Concept of Geodetic Datum Change with the Introduction of GPS ?	475
Seeber, G., Wübbena, G.	Geodetic Measurements with TI 4100 GPS Receivers	487

		Page
Stansell, T.A.Jr., Chamberlain, S.M., Brunner, F.K.	The First Wild-Magnavox GPS Satellite Surveying Equipment: WM 101	503
Stiller, A.	Development of Civilian GPS Receivers in the Federal Republic of Germany for Different Applications	525
Strauß, R.	On the Variation of the Transformation Parameters between GPS and the German Horizontal Network	545
Wübbena, G.	Model and Program Developements for cm-Positioning with GPS	553
THE MODERN TECHNIQUES FOR DEVELOPING COUNTRIES		567
Wassef, A.M.	- Review Paper - Modern Techniques for Developing Countries	569
Jonsson, B.	Doppler Observations in Zambia	577
Seeber, G.	Some Examples of Doppler Measurements for Control Surveys in Latin America	599
Vote of Thanks		609
Closing Remarks		611
After Dinner Speech		615
List of Participants		617

Inertial Measurements

- Review Paper -

INERTIAL POSITIONING - PRINCIPLES AND PROCEDURES

by

Wilhelm CASPARY

Institut für Geodäsie
Universität der Bundeswehr München
Werner-Heisenberg-Weg 39
D-8014 Neubiberg, F.R. Germany

ABSTRACT

The principle of inertial surveying systems is outlined and its mechanizations are discussed. The different types of platforms including the basic functions of gyros and accelerometers are explained.

Special attention is paid to the disturbing forces and to the error budget of the instruments. Observation schemes and signal processing procedures for on-line filter and for post mission smoothing are presented.

ZUSAMMENFASSUNG

Das Prinzip inertialer Vermessungssysteme und seine Realisierung werden erläutert. Die unterschiedlichen Plattformen einschließlich der Funktionsweise von Kreiseln und Beschleunigungsmessern werden behandelt.

Besondere Aufmerksamkeit wird den Störkräften und dem Fehlerhaushalt der Instrument gewidmet. Beobachtungsverfahren und Signalverarbeitungsmethoden werden dargelegt.

1. INTRODUCTION

Inertial surveying systems (ISS) are modified versions of inertial navigation platforms. In the western world three companies manufacture such instruments which are available on the civil market.

Since 1974/75 the firm LITTON has been selling its Autosurveyor originally designed as the Position and Azimuth Determining System (PADS) for the Artillery of the United States Army. A short time later the British firm FERRANTI presented the Ferranti Inertial Land Surveyor (FILS), which was originally developed as the PADS for the British Army. The GEO-SPIN of the Avionics Division of HONEYWELL which came around 1980 is modified from the SPN/GEANS platform installed in the United States Air Force B-52 bombers.

From the beginning this entirely new principle of geodetic observation has found ample interest in the surveying community. The most attractive properties of ISS are the independence of a line of sight and of external sources of information, and the rapidity of performance. The accuracy ranges between 0.02 and 0.60 m standard deviation depending on the type of instrument, the observation procedure and the density of control points. The high cost between 0.5 and 1.2 million US $ for one ISS, however, makes the use only economical, when the surveying project is sufficiently large.

During the past 10 years this new surveying technology has been used extensively by governmental agencies in the USA and in Canada, and by a number of private companies, which operate in all parts of the world. The main field of application is the establishment of lower order control for cadastral and for mapping projects. The published reports claim that savings of about 50 % in cost and considerably savings in time are typical, so that the instruments pay for themselves within two years.

2. THE BASIC PRINCIPLE

Consider a mass point in space moving along a trajectory as depicted in Fig. 1. If the acceleration a of the point in respect to the coordinate system is measured continuously, then it is possible to compute the way by a double integration over the time.

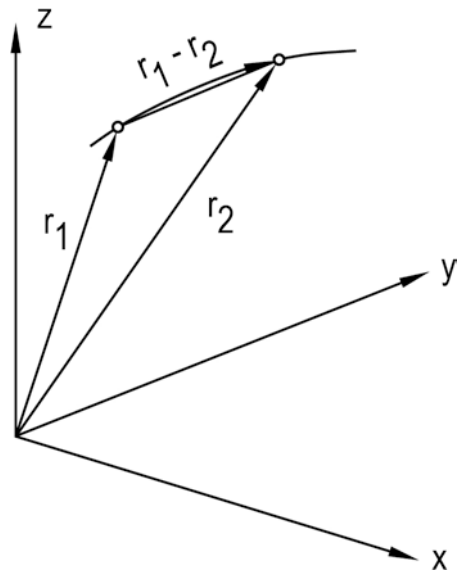

Fig. 1: Motion of a mass point in space

$$r_2 - r_1 = \iint_{t_1}^{t_2} a(t)\, dtdt$$

where the way is defined as the difference vector in the reference frame. Newton's laws of motion provide the basis for the mechanization of the basic idea. The second law gives the well-known relationship between an acting force F, a mass m and the acceleration a

$$F = m \cdot a$$

where the assumption is made that the observation refers to an inertial frame, i.e. a reference frame that is fixed in space.

3. INERTIAL PLATFORMS

In order to apply the basic principle for the fixing of positions on the earth, it is necessary to mechanize a measurement frame with known orientation in respect to an inertial reference frame. In this system three accelerometers can be used to measure the three components of acceleration. The realization of this idea is the so-called inertial platform. It is basically a stable element on which three mutually orthogonal accelerometers and three single-degree of freedom gyros (or two two-degrees of freedom gyros) are mounted. The platform is isolated from its case and from the host vehicle, on which it is being carried, by a system of three or four gimbals, see Fig. 2.

The gyros control the attitude of the platform in respect to the inertial reference frame, thus providing the rotational information needed to perform the transformation of the signals from the inertial frame to a geodetic coordinate system. The principle of a gimbal mounted two-degrees of freedom gyro is depicted in Fig. 3.

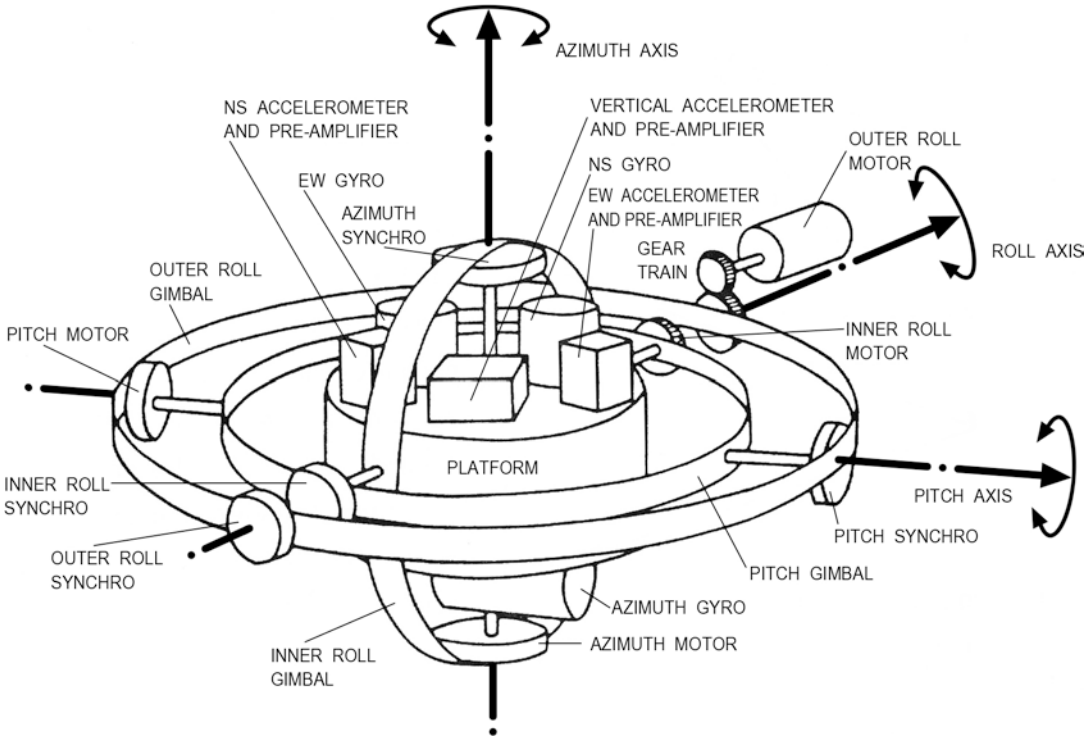

Fig. 2: Schematic of a Gimballed Platform (FILS), Deren (1981)

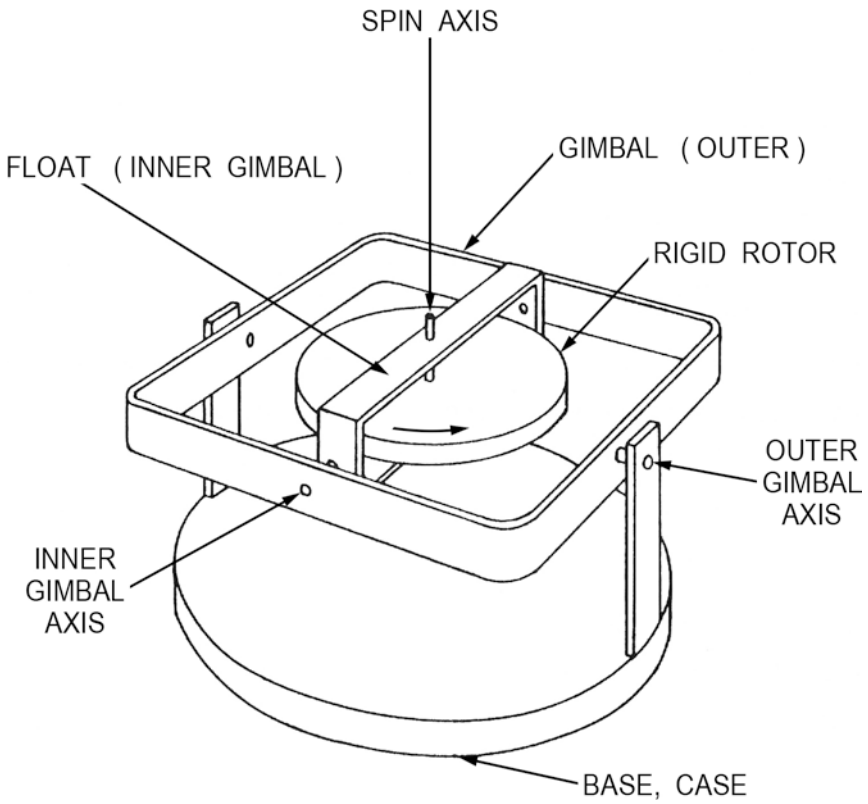

Fig. 3: Gimbal mounted TDF Gyro, Rüeger (1982)

When the rotor is spinning fast and no disturbing torque is applied, then the spin axis will preserve indefinitely its orientation in inertial space. If on the other hand a torque acts upon the outer gimbal axis, an angular rate precession of the inner gimbal (float) about its axis results. Thus the gyro can be used to stabilize the platform or to manipulate its attitude in any desired way.

The accelerometers are precision measuring devices containing a mass that is coupled to a case through an elastic or an electromagnetic constraint. Actually it senses the specific force being the resultant of the inertial reaction force due to vehicle accelerations and of the gravitational and various disturbing forces. Fig. 4 shows in a simplified manner the principle of an accelerometer.

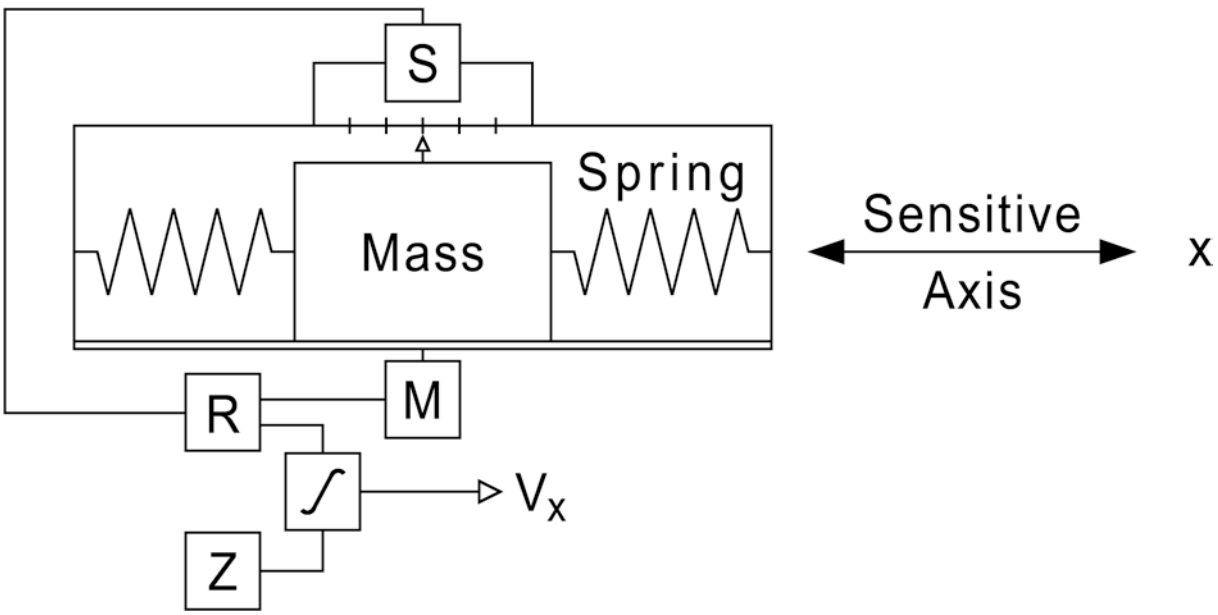

Fig. 4: Schematic of an Accelerometer

Three types of inertial platforms have been developed which differ in the way of control of the accelerometer triad.

The space-stabilized platform maintains its orientation between two alignments. Thus the accelerations refer to a frame which is fixed in space. The conversion of the position differences into a geodetic coordinate system is carried out by on-line transformations. The GEO-SPIN of Honeywell is an example of a space-stabilized system.

The local-level platform is continuously torqued to keep the z - axis parallel to the local normal of the reference ellipsoid and to hold its horizontal axes always pointing towards north and east, respectively. This type of platform control is realized in the Litton Autosurveyor and in the Ferranti Inertial Land Surveyor.

The strap-down platform follows all movements of the host vehicle. The rotations are sensed by gyros and accounted for computationally. No strap-down platform has been modified so far for geodetic position fixing.

4. THE ERROR BUDGET

The implementation of the very simple principle of inertial positioning requires the overcoming of a number of difficulties originating from the fact that the earth rotates, that the measurements are performed in the earth gravity field and that the mechanical and the electronic realization cannot be accomplished without small biases. Consequently the measured acceleration is the sum of the signal and various bias and noise terms

$$F = a_r + \sum a_d + g + \sum b_I + \sum \varepsilon \ , \quad m = 1$$

These terms can be grouped according to the way they are dealt with.

The first group, $\sum a_d$, consists of systematic effects which are completely known and can therefore be compensated for by strict mathematical corrections. The Coriolis, the centripetal and the tangential accelerations belong to this group. They occur since the measurements are carried out on the rotating earth. The influence of the gravity field, g, on the sensor output can be considered here as well. The normal gravity is compensated strictly. The remaining gravity disturbances belong to the second group, being formed by systematic effects which vary with time or position and can be estimated during the mission. Especially instrumental biases, $\sum b_I$, as zero offsets, scale factors, gyro drifts, non-orthogonality of sensitive axes and alignment errors pertain to this group. First estimates of these biases are computed in the pre-mission calibration phase. A Kalman-filter or similar approximation procedures are employed to update these instrumental errors for proper correction of the signals. If these biases are not controlled on-line they grow rapidly since the double integration of the signals amplifies all disturbances dramatically. The observations necessary

for the filter are taken at regular stops in intervals of 3 - 5 minutes. In the absence of vehicle accelerations the corrected signals of the horizontal sensors should be zero. The actual readings are used to update the filter (zero velocity update: ZUPT).

The third group of errors, $\sum\varepsilon$, is formed by random noise and by pseudo-random errors remaining after applying estimated corrections and reductions. These errors propagate statistically. They are accounted for in post-mission smoothing and adjustment procedures. Additional self-calibrating parameters are estimated if the error pattern is of systematic nature.

5. OBSERVATION PROCEDURES

Inertial surveying systems are usually operated from a helicopter or a land vehicle, but there are also applications using vessels and aeroplanes.

A mission begins with a platform alignment which is carried out automatically under computer control. When the position, the elevation and additional parameters for time, coordinate system etc. have been entered into the instrument, the platform is levelled to the gravity field by use of the horizontal accelerometers and it is aligned to the local astronomical coordinate system by a technique known as gyrocompassing. During this process of alignment an initial calibration is being performed to estimate the actual biases and drift rates of gyros and accelerometers. For this pre-mission alignment/calibration 30 - 60 minutes are needed. At the same time the system attains its operating temperature which has to be maintained during the whole mission. While for the Autosurveyor and the GEO-SPIN usually one alignment at the beginning of a working day suffices, it is necessary to repeat the procedure for the FILS every 90 - 120 minutes. A re-alignment is necessary for all platforms after a switch off or break down of the system.

The mission commences in the survey mode over a known control point and proceeds by driving along the traverse stopping at all points where geodetic parameters are required and between points for ZUPTs if the spacing is too wide. The internal measurements for a ZUPT of for a coordinate fix last 20 - 30 seconds. If it is not possible to centre the reference point of the platform on the survey mark it is required to measure the excentri-

city in position and height. Efficient auxiliary equipment has been developed for this purpose, so that the stops are usually shorter than two minutes. The mission must be terminated over a known control point, different from the starting point.

At the terminal station the differences between the predicted and the known coordinates are used by a smoother to compute corrected coordinates for all intermediate points. Since most of the systematic errors are functions of the time or the distance travelled very simple on-line smoothing models are applied. As a protection against gross errors and for the elimination of course dependent biases all traverses are run forward and reverse.

Independent of the type of the ISS the following rules are to be considered in order to get most accurate results

- the time between control points should not exceed two hours
- the traverses should be fairly straight
- the points should be evenly spaced
- ZUPT stops should be made every three minutes.

6. POST MISSION PROCEDURES

The two terminal points of a traverse do not provide enough information to develop a sophisticated error model. To this end a higher degree of redundancy is necessary, which is achieved by combining traverses to a network with a sufficient number of cross-overs. In the ideal design all points belong to two traverses, thus creating a network of grid pattern. Fig. 5 shows as an example the network "Ebersberger Forst" which has been established to test different inertial platforms (CASPARY, BORUTTA, KÖNIG, 1985).

The method of modelling systematic errors in a post mission adjustment is similar to the well known self calibration approach in photogrammetry. The problem is mainly one of selecting suitable nuisance parameters to absorb efficiently the systematic errors. Simulation studies with different observation schemes using both, polynomial error models and those based on known error sources, have been published by HANNAH and PAVLIS 1980 and ARDEN and SCHWARZ 1983.

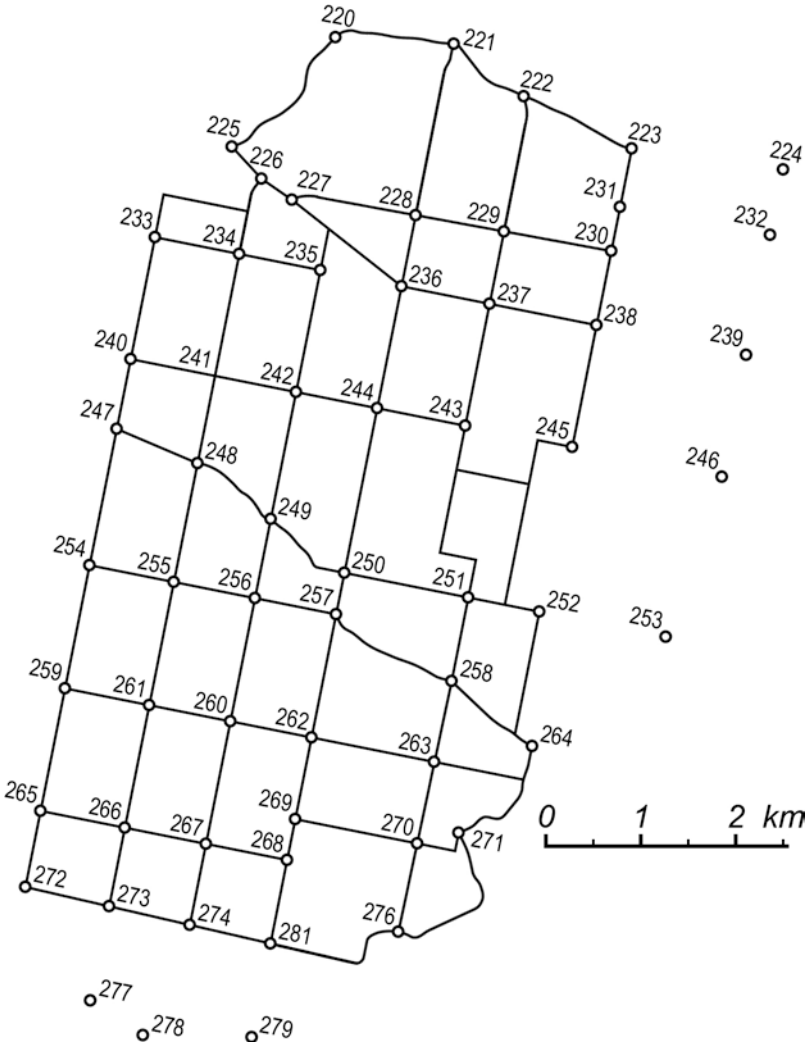

Fig. 5: Test network "Ebersberger Forst"

7. CONCLUSION

The inertial surveying systems being in use during the last 10 years proved their capability for a variety of geodetic applications. They have established their place in the geodetic arsenal, and their use is most successful if projects of sufficient extent are considered. Since progress in the electronic industry has been tremendous in this time it appears that a second generation of platforms is due. The users hope for improved instruments with more accurate sensors, being compacter, less power requiring and less expensive. This would open new fields for a much wider application of inertial surveying systems.

8. REFERENCES

ARDEN, I.A.G., SCHWARZ, K.P.: ***Optimizing Field Procedures for Inertial Network.*** XVIII. General Assembly of the IUUG, Hamburg, 1983

BOEDECKER, G.: ***Inertialvermessung.*** Beitrag zum IX. Internationalen Kurs für Ingenieurvermessung, 1984, A 17

CASPARY, W.: ***Inertiale Vermessungssysteme.*** Vermessungswesen und Raumordnung, S. 169-189, 1983

CASPARY, W., BORUTTA, H., KÖNIG, R.: ***Network Densification by Inertial Positioning.*** 7th Symposium on Geodetic Computations, Cracow, June 18 - 21, 1985

DEREN, G.: ***The Ferranti Inertial Land Surveyor and its Applications.*** Proceedings 2nd ISS-Symposium, Banff, 1981

GONTHIER, M.: ***Smoothing procedures for inertial survey systems of local level type.*** UCSE Reports Number 20008, 1984

HANNAH, J.: ***Inertial surveying systems and their use in geodetic positioning.*** Journal of the surveying engineering, p. 39-48, 1984

HANNAH, J., PAVLIS, D.E.: ***Post Mission Adjustment Techniques for Inertial Surveys.*** Report of the Department of Geodetic Science and Surveying No. 305, Ohio State University

MILBERT, D.G.: ***Inert 1: A Program for Planning and Simultaneous Adjustment of Inertial Surveys.*** Proceedings ASCM 42nd Meeting, S. 173-183, 1982

MUELLER, I.I.: ***Inertial Survey Systems in the Geodetic Arsenal.*** 2nd ISS, Banff, 1981

MÜLLER, HANNAH, PAVLIS: ***Inertial technology for surveying.*** FIG XVI. International Congress Montreux, 501.4, 1981

ROOF, E.F.: ***Inertial survey applications to civil works.*** U.S. Army Corps of Engineering ETL - 0309, 1983

RÜEGER, J.M.: ***Inertial Sensors, Part I: Gyroscopes.*** Edited by K.P. Schwarz, Division of Surveying Engineering, Publ. 1982

RÜEGER, J.M.: ***Evaluation of an Inertial Surveying System.*** Australian Surveyor, p. 78-98, 1984

SCHWARZ, K.O.: ***Inertial Surveying and Geodesy.*** Review of Geophysics and Space Physics, Vol. 21, No. 878-890, 1983

INERTIAL GRAVIMETRY:
RESULTS OF A TESTNET OBSERVATION CAMPAIGN
WITH FERRANTI FILS MKII

by
Gerd BOEDECKER

Bayerische Kommission für die Internationale Erdmessung
Marstallplatz 8, D-8000 München 22
Fed. Rep. of Germany

Abstract

With a Ferranti FILS MKII an inertial observation campaign was carried out on a testnet in Bavaria including 40 stations and two long traverses in the Alpine foreland. Data have been preprocessed by own software utilizing the two step method with smoothing splines for the error velocity function. The network data then were fitted to 5 control stations. A comparison with other control stations exhibit mean square deviations of 30 cm in latitude, 40 cm in longitude and 25 cm in height. Through improved operation layout and software these values could be reduced to about 50 %. For the most rugged part of the alpine traverses gravity values were derived from the inertial data with an accuracy of about 6 mGal.

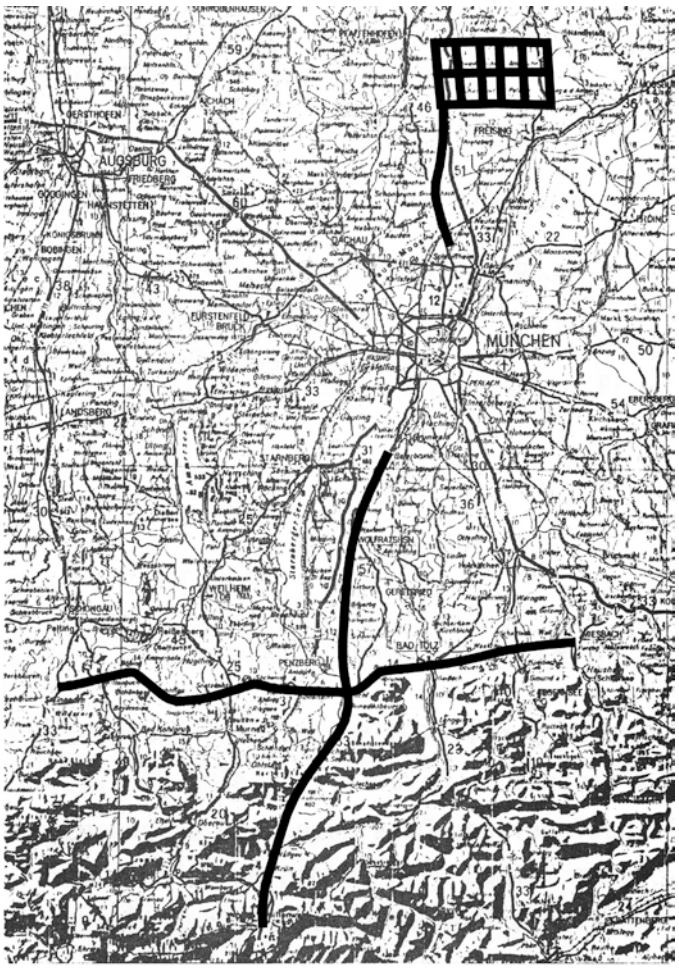

Figure 1: Inertial test net

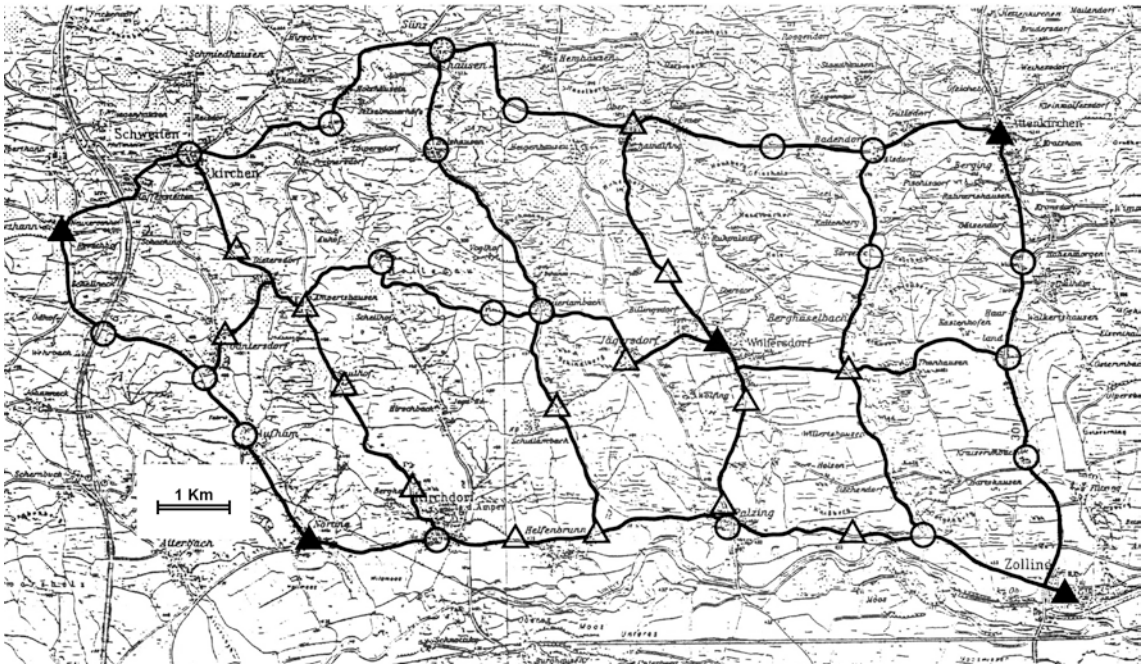

1. PRINCIPLES OF INERTIAL POSITIONING

As an introduction to the investigations in this paper we first recall some basic equations as published e.g. in ***BOEDECKER*** **[1983]** and **[1984]**. In view of the later application we shall restrict ourselves to the local level mechanisation Inertial Measuring Unit (IMU).

Starting from

$$\underline{r}_i = \underline{R}_i^l \, \underline{r}_l \tag{1-1}$$

$\underline{r}_i$ position vector in inertial space

$\underline{r}_l$ position vector in local reference system with identical origin to $\underline{r}_i$ at some initial time epoch

$\underline{R}_i^l$ rotation from local to inertial reference

we arrive at

$$\ddot{\underline{r}}_i = \underline{R}_i^l \left[\ddot{\underline{r}}_l + 2\,\underline{\Omega}\,\dot{\underline{r}}_l + \left(\underline{\Omega}\,\underline{\Omega} + \dot{\underline{\Omega}}\right) \underline{r}_l \right]. \tag{1-2}$$

with

$\underline{\Omega}$ Earth rotation.

In the sequel we shall assume the change of the Earth's rotation $\dot{\underline{\Omega}} = \underline{0}$. $\ddot{\underline{r}}_i$ can be obtained from a combination of the specific force vector $\underline{f}$ to be determined by means of accelerometers of the IMU and the vector of gravitation $\underline{g}'$.

$$\ddot{\underline{r}}_i = \underline{R}_i^l \left(\underline{f}_l - \underline{g}'_l \right) \tag{1-3}$$

Combination of equations (1-2), (1-3) yields

$$\ddot{\underline{r}}_l = \underline{f}_l - 2\,\underline{\Omega}\,\dot{\underline{r}}_l - \left(\underline{g}' + \underline{\Omega}\,\underline{\Omega}\,\underline{r}_l \right) . \tag{1-4}$$

In eq. (1-4) the second term $2\,\underline{\Omega}\,\dot{\underline{r}}_l = \underline{c}$ denotes the Coriolis acceleration, the term in brackets $\underline{g}' + \underline{\Omega}\,\underline{\Omega}\,\underline{r}_l = \underline{g}$ comprises gravitation and centrifugal

acceleration and can thus be identified as the gravity $\underline{g}$. Therefore (1-4) can be shortened to

$$\underline{\ddot{r}}_l = \underline{f}_l - \underline{c} - \underline{g} \ . \tag{1-5}$$

By integrating twice we get the position difference

$$\underline{r}_i - \underline{r}_{i-1} = \iint_{i-1}^{i} \underline{\ddot{r}} \, dt \, dt \ . \tag{1-6}$$

In order to evaluate (1-5) we first have to determine the Coriolis acceleration, which requires the instantaneous velocity.

The gravity vector normally is approximated by

$$\underline{g} \approx \begin{bmatrix} 0 \\ 0 \\ \gamma \end{bmatrix} \tag{1-7}$$

where the computation of normal gravity γ again requires the position.

In reality, errors of the instruments, in particular drift effects, and imperfect knowledge of the gravity field have to be taken into account, which we denote by $d\underline{\ddot{\rho}}$. If we add these to eq. (1-5) we obtain

$$\underline{\ddot{r}}_l = \underline{f}_l - d\underline{\ddot{\rho}} - \underline{c} - \underline{g} \tag{1-8}$$

In order to monitor and model these errors, regular stops have to be performed for "zero velocity updates (ZUPT)". At these stops we have

$$\begin{aligned} \underline{\ddot{r}}_l &= \underline{0} \\ \underline{c} &= \underline{0} \end{aligned} \tag{1-9}$$

and therefore eq. (1-8) reduces to

$$\underline{f}_l = d\underline{\ddot{\rho}} + \underline{g} \ . \tag{1-10}$$

Because the hardware IMU normally does not provide direct access to accelerations but only to velocities - after the first integration - the errors are accessible on the velocity level. Because of

$$\underline{\dot{r}}_1 = \underline{0} \tag{1-11}$$

at a ZUPT we obtain

$$d\underline{\dot{\rho}} = \int_{i-1}^{i} \left(\underline{f}_1 - \underline{g} \right) dt \tag{1-12}$$

which, if integrated again, gives us the coordinate error $d\underline{\rho}$. A certain problem remains the interpolating function of the error velocity $d\underline{\dot{\rho}}$ for the purpose of integration. After the second integration we have

$$d\underline{\rho} = \iint_{i-1}^{i} \left(\underline{f}_1 - \underline{g} \right) dt\, dt\,, \tag{1-13}$$

the coordinate residual, which can be controlled at some stations with known coordinate (-differences).

$d\underline{\dot{\rho}}$, $d\underline{\rho}$ can be regarded as residuals, some norm of which is to be minimized in an adjustment process. Actually, the conventional way is to utilize (1-12) and (1-13) in two consecutive steps. In the next section numerical results are presented on the basis of this two-step method.

2. RESULTS IN THE TEST NET UPPER BAVARIA

In 1983 the "Bayerische Kommission für die Internationale Erdmessung" carried out observations with Ferranti FILS MKII of the Belgian Institut Géographique National on two long traverses and a test network (c.f. fig. 1).

In this case the two step method was employed. In a first step $d\underline{\dot{\rho}}$ velocities at the ZUPT stations were approximated by cubic smoothing spline functions

$$d\tilde{\dot{\rho}}(t) = a_i + b_i(t-t_i) + c_i(t-t_i)^2 + d_i(t-t_i)^3 \tag{2-1}$$

where the smoothing is controlled by a parameter s such that

$$s \geq \sum \frac{\left(d\dot{\rho}(t_i) - d\tilde{\dot{\rho}}(t_i) \right)^2}{d^2} \tag{2-2}$$

with

a_i, b_i, c_i, d_i	spline coefficients for interval i
t	time instant
t_i	time instant at the beginning of an interval
$d\tilde{\rho}$	approximate error velocity
d	weight factor
s	smoothing parameter; if s = 0, the spline passes through $d\dot{\rho}$.

In the case of a ZUPT with FILS, 32 consecutive values for the instantaneous error velocity at time spacing of 0.64 s are recorded. These are approximated by a square function through a least squares fit. The adjusted mean $d\dot{\rho}$ thus obtained are then represented by the spline function, example c.f. fig. 2. The resulting coordinate correction can easily by found through integration of the spline function, namely

$$d\rho_i = \sum_{j=1}^{i} a_j (t_{j+1}-t_j) + \frac{1}{2} b_j (t_{j+1}-t_j)^2 + \frac{1}{3} c_j (t_{j+1}-t_j)^3 + \frac{1}{4} (t_{j+1}-t_j)^4 \qquad (i = 2, \ldots, k) \qquad (2\text{-}3)$$

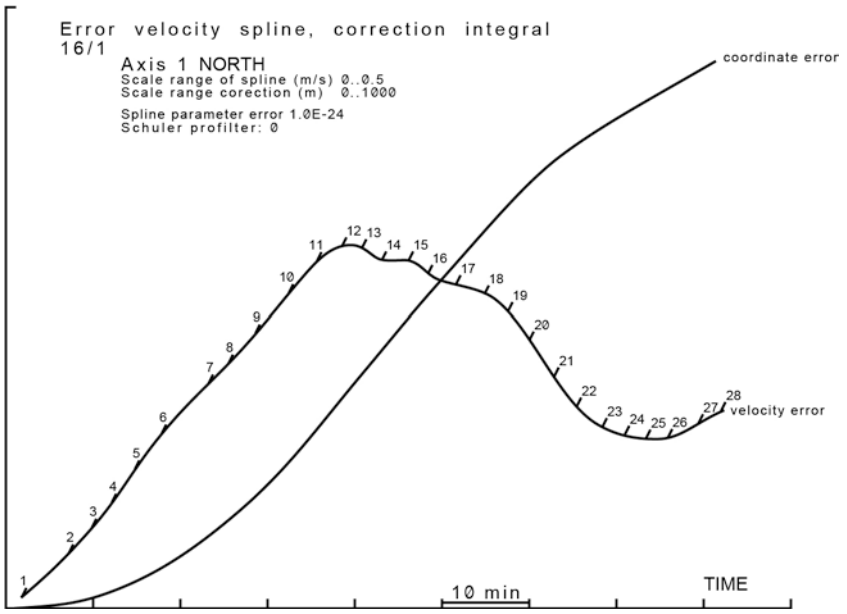

Figure 2: Error velocity spline

In a second step the resulting coordinates were then introduced into a least squares adjustment together with a few (in the example: 5 black triangles in fig. 1) out of the existing control stations. The set of observation equation employed reads

$$\begin{aligned} \varphi^o + v_\varphi &= \varphi \\ \lambda^o + v_\lambda &= \lambda \\ H^o + v_H &= H \end{aligned} \qquad (2\text{-}4a)$$

for the control station values φ^o, λ^o, H^o observed and

$$\begin{aligned} \varphi^i + v_\varphi &= \varphi + \varphi_0 + a_1(\varphi_i^o - \varphi_1^o) + a_2(\lambda_i^o - \lambda_1^o) + a_3(t_i - t_1)^2 \\ \lambda^i + v_\lambda &= \lambda + \lambda_0 + b_1(\varphi_i^o - \varphi_1^o) + b_2(\lambda_i^o - \lambda_1^o) + b_3(t_i - t_1)^2 \\ H^i + v_H &= H + H_0 + c_1(\varphi_i^o - \varphi_1^o) + c_2(\lambda_i^o - \lambda_1^o) + c_3(t_i - t_1)^2 + \\ &\quad + c_4(H_i - H_1) \end{aligned} \qquad (2\text{-}4b)$$

for the preprocessed inertial observations φ^i, λ^i, H^i

with

$a_1, \ldots, c_4$ parameters

φ^o, λ^o, H^o approximate coordinates.

Without going into further details, the results are shown in the form of error vectors for the individual traverses in fig. 3. The mean square deviation in the 40 stations/10 traverses net, computed from the control stations not used in the adjustment, are 30 cm in latitude, 40 cm in longitude and 25 cm in height. These values can be reduced considerably by improved field operation and refined adjustment model.

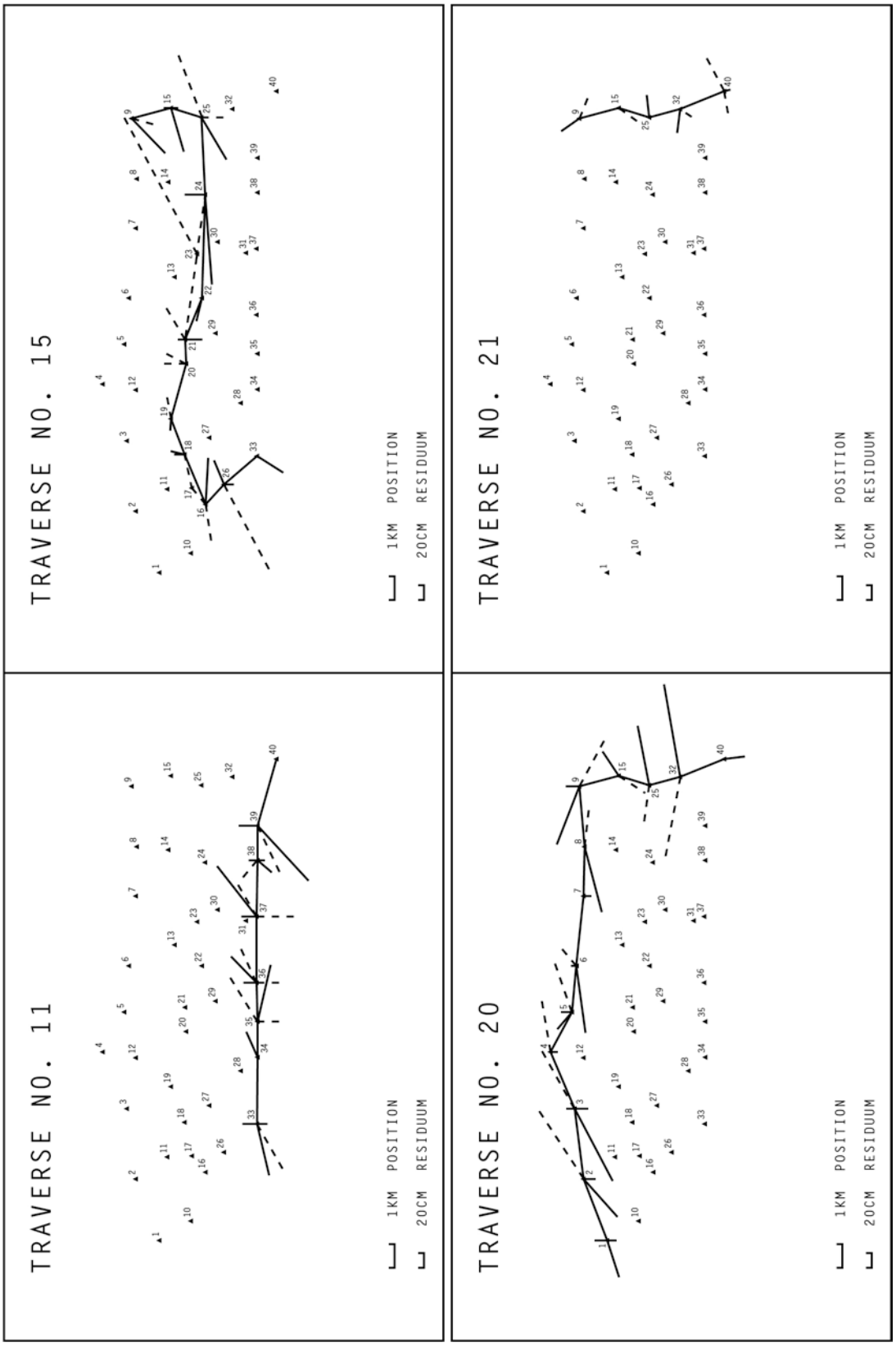

Figure 3: Results from geometric net adjustment: 4 out of a total of 10 traverses back and forth residuals

3. INERTIAL GRAVIMETRY

In this case we shall restrict ourselves to the vertical channel of the local level type Ferranti FILS MKII. Similar developments hold for the two horizontal channels, except that for the vertical channel we need not deal with Schuler frequency because the maximum tilt of the platform keeps sufficiently small not to change the reading of the vertical channel. Furthermore at this stage it is not our aim to recover gravity during motion of the IMU but only at the stops either for point positioning or just for a ZUPT. In this case eq. (1-10) can be applied and we have to separate gravity from instrumental errors in the specific force output.

Because the IMU does not deal with the whole gravity value but just a residual value referred to some reference we have to introduce that reference model (c.f. eq. (1-7)). During alignment a back-off current for the accelerometer is adjusted in order to fit the remaining "gravity residue" (c.f. fig. 4)

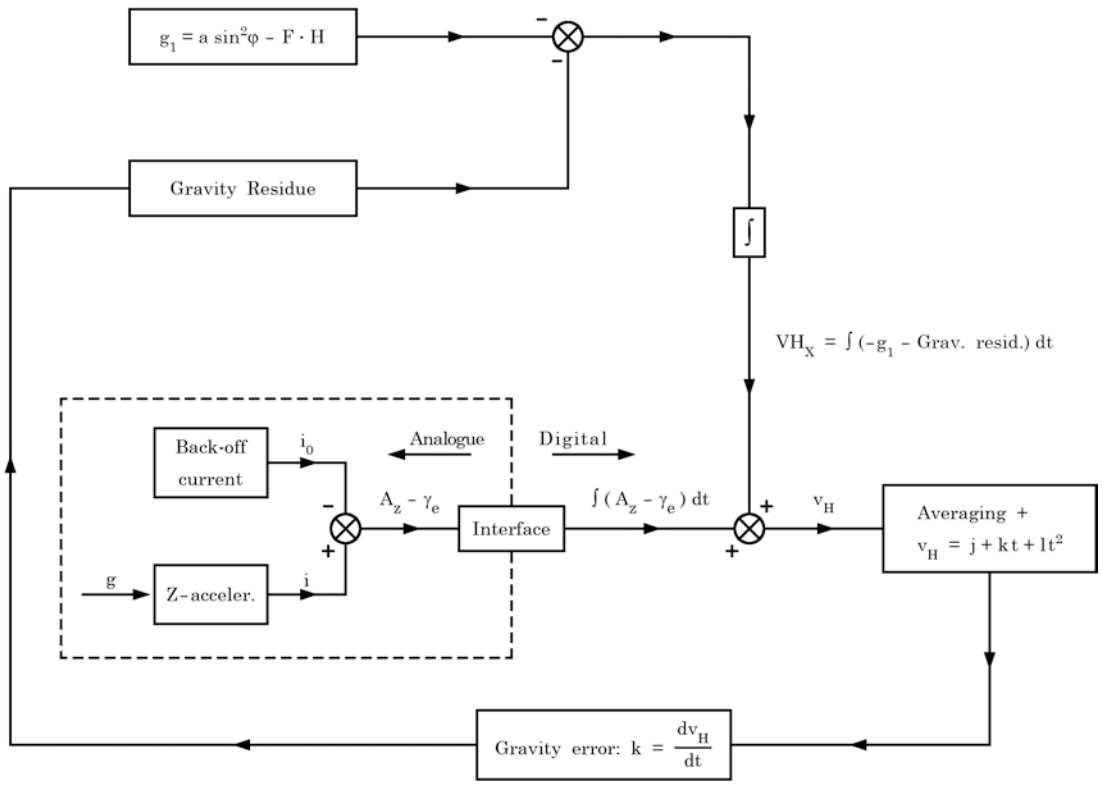

Figure 4: Vertical accelerometer back-off current alignment (***HERREWEGEN, 1981***)

to some reference value given through

$$g_1 = a \sin^2\varphi - F \cdot H \qquad (3\text{-}1)$$

with

- φ latitude
- H height value as predicted by the IMU
- a coefficient taken from some gravity reference model as e.g. the "gravity formula 1980"
- F gravity change with height

The value for F is

$$F = -\frac{d\gamma}{dH} - 2\pi G\rho \approx 0.2 \cdot 10^{-5}\, s^{-2} \qquad (3\text{-}2)$$

where the first term denotes the free air gradient $\left(\sim -0.3 \cdot 10^{-5}\, s^{-2}\right)$ and the second term the infinite Bouguer plate

with

- G gravitational constant
- ρ density of the Bouguer plate.

As indicated above, the specific force or acceleration can only be accessed after the first integration, i.e. as velocity. During ZUPT's 32 consecutive values of the instantaneous velocities with sampling intervals of 0.32 s are recorded. In our program those are approximated by a square function, the linear parameter giving the acceleration, which has the character of a relative Bouguer anomaly as pointed out above.

Figure 5 presents the data of one ZUPT. The square term could give us the linear drift of the "gravity meter". According to own experience these drift values, however, deviate from the overall traverse drift and can therefore not be used for the traverse evaluation.

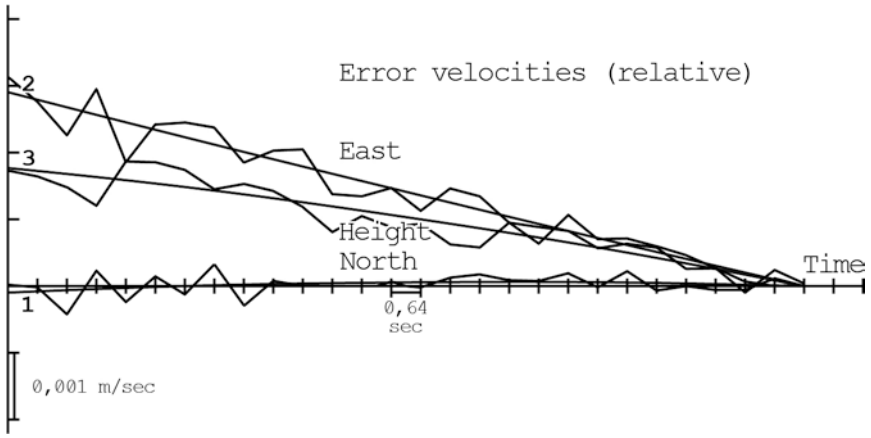

Figure 5: ZUPT instantaneous velocities

Instead, a least squares drift fit has been carried out for the whole traverse including drift terms. We employed the observation equations

$$f_i + v_i = o + g_j + d_1 t + d_2 t^2 \qquad (3\text{-}4a)$$

adding

$$g_j^o + v_j = g_j \qquad (3\text{-}4b)$$

for one or two stations in order to provide the reference level

with

o	zero order parameter
d_1, d_2	drift parameters
t	time
v	residual
g^o	control station gravity value

In this case not the relative Bouguer anomaly observations f' are used in (3-4a) but they are first converted to relative gravity observations f by means of (3-1), (3-2).

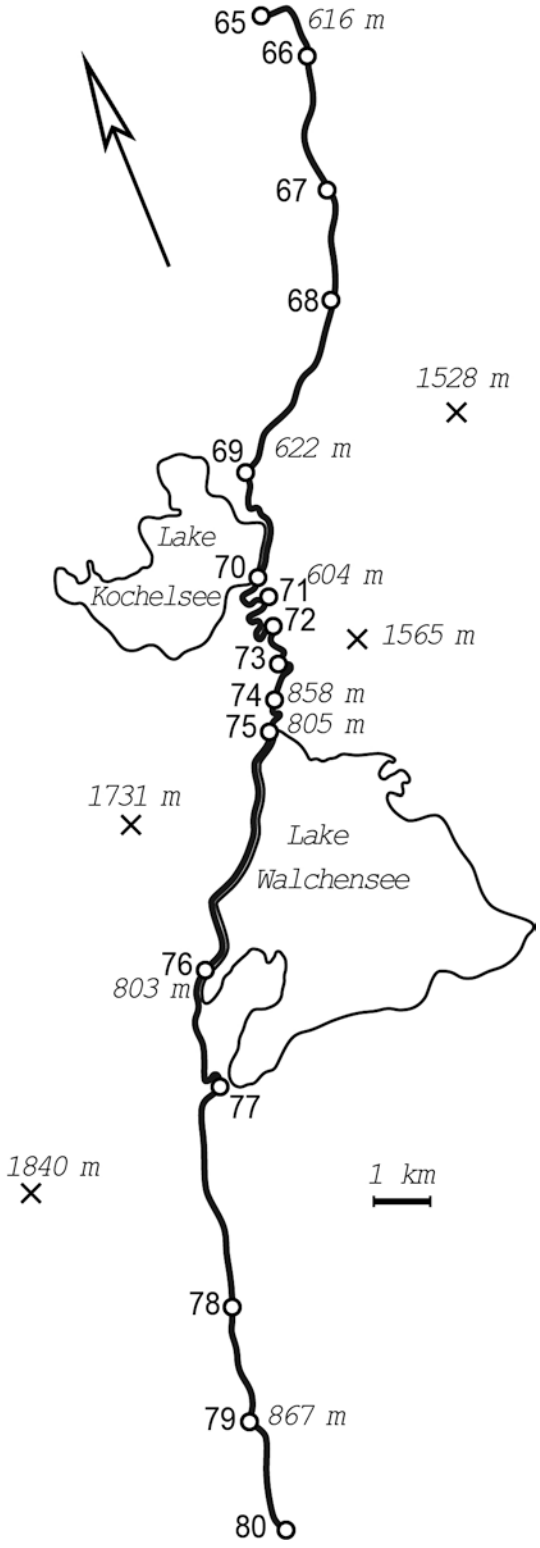

Fig. 6: Inertial gravity traverse into the steps

station	true grav. value mGal 981,	inertial gravity value, traverse 1 mGal 981,	2 mGal 981,	3 mGal 981,
65	631	632	631	632
66	628	624	629	630
67	625	622	619	624
68	617	615	612	614
69	622	620	617	613
70	623	617	617	612
71	612	603	608	603
72	596	589	590	588
73	588		579	585
74	578		577	573
75	589	588	589	588
76	585	587	580	575
77	581		579	
78	568	565	572	
79	557	550	554	
80	551	542	552	

Figure 7: Results of inertial gravity survey

The results for three runs on a rather rugged part of the traverse into the Alps are depicted in figure 6, 7. The deviations from the true values are mainly of systematic nature, their root mean square values being 6 mGal. After further refinement this should be reduced to very few mGal.

4. REFERENCES

BOEDECKER, G.: ***Inertial Gravimetry.*** BGI - Bull. d'Inf. no. 53 (1983), 173-177

BOEDECKER, G.: ***Inertialvermessung.*** Proc. IX. Internat. Kurs f. Ingenieurvermessung, Graz 1984

HERREWEGEN, M. van den: ***Which information can you get out of an inertial system and what can you do with it?*** Proc. Int. Symp. Geodetic Networks and Computations 1981. Pub. DGK, R. B, H. 258 IV. München 1982

AZIMUTH DETERMINATION WITH INERTIAL SYSTEMS

by

Wolfgang LECHNER

Institut für Geodäsie
Universität der Bundeswehr München
Werner-Heisenberg-Weg 39
8014 Neubiberg
Federal Republic of Germany

ABSTRACT

In course of the "Joint Project of Inertial Geodesy" of the Geodetic Institute and the Institute of Astronomical and Physical Geodesy at the University FAF Munich (***CASPARY, HEIN, SCHÖDLBAUER, 1985***) the inertial measuring systems Ferranti Inertial-Land-Surveyor II (FILS II), Honeywell Geo-Spin II and Litton Auto-Surveyor-System II (LASS II) were examined. Besides position and gravity observations azimuth determinations were carried out. The achieved results are comparable with those of meridian gyroscopes of medium precision.

1. INTRODUCTION

Inertial measuring systems have more and more been applied in various domains. The reason for this increased application is found in the accuracies which have been obtained, the complete independence from outside information during the measurements, sighting conditions and atmospheric influence, and the nearly universal utilization. Besides positioning determination for coordinate differences in position and height the direction and amount of gravity vector can be measured.

A further possibility, up to now rarely applied, to take use of the information contents of the orientated platform for geodetic purpose, is given by the possibility of azimuth determination.

2. FUNDAMENTS OF INERTIAL SURVEYING SYSTEMS

The fundament of Inertial Surveying Systems is based on the dynamics of rigid solids in an inertial space *(**e.g. HEITZ 1980**).* To define an inertial coordinate system we use NEWTON's 2nd law of motion

$$\underline{f} = m \cdot \underline{a}$$

(force = mass × acceleration)

Based on the equation of motion of a mass point in this inertial system

$$\underline{r}(t+dt) = \underline{r}(t) + \frac{d\underline{r}(t)}{dt}\,dt + \frac{d^2\underline{r}(t)}{dt^2}\,dt^2$$

$\underline{r}(t)$ = position vector at the time t

$\frac{d\underline{r}(t)}{dt}$ = speed vector at the time t

$\frac{d^2\underline{r}(t)}{dt^2}$ = acceleration vector at the time t

it is possible to determine the variation of the position vector by double integration of the measured accelerations. Realizing this principle the accelerations will be derived from the forces working on the examined masses.

The differential time dt will be realized with the integration interval Δt on condition that

$$\frac{d^2\underline{r}(t)}{dt^2} = \text{const. in } \Delta t$$

The mechanical and mathematical problems to realize this in practice should not be precise in this connection *(**e.g. CASPARY 1983, RINNER 1981**)*.

3. PROCEDURES OF AZIMUTH DETERMINATION

For azimuth determination it is necessary to know the orientation of the inertial system relative to the earth rotation axis. There are generally three methods which are used for the alignment of the platform. Those are realized in

- space stabilized,
- local level and
- strap down

platforms. On grounds of these different procedures there are different ways for the internal calculation of the azimuth but at all events the gyroscopes of the system are used, either to stabilize the orientation in the inertial space in a mechanical way or to register it in short intervals and to take it into consideration at every integration period *(**e.g. CASPARY** 1983, **RINNER** 1981, **SCHÖDLBAUER 1985**)*. The inertial systems we investigated in our project used a space-stabilized platform (Honeywell) or a local level platform (Ferranti, Litton). Strap down systems are not yet in use for geodetic purpose.

To transfer the orientated direction there are different possibilities. The most applied procedure, which is realized, with some modifications, by all producers, uses an autocollimation mirror or a Porro prism. These instruments are fixed connected with the IMU and therefore there is a well-defined orientation for the direction transfer.

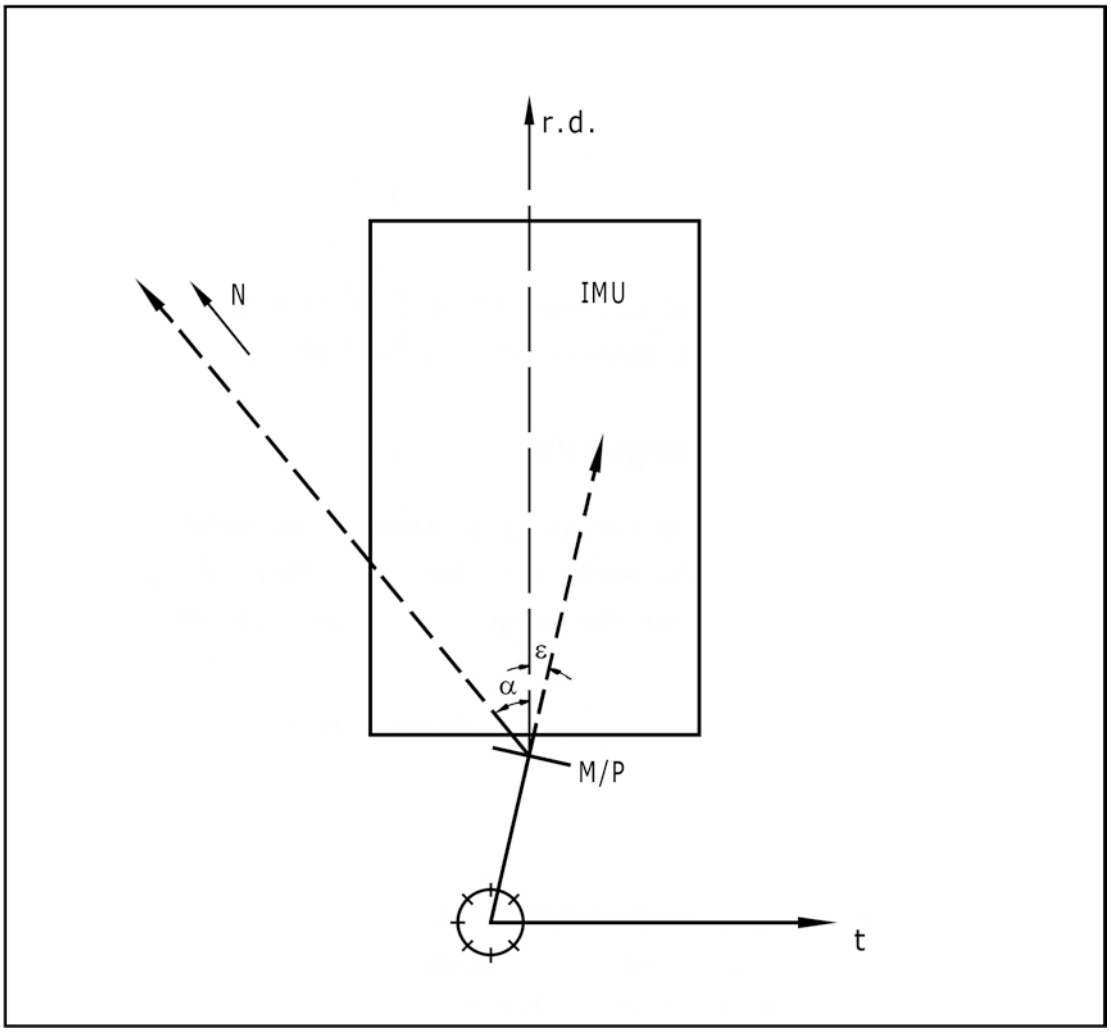

IMU : Inertial Measurement Unit
α : azimuth (internal calculated)
ε : calibration constant
M : autocollimation mirror
P : Porro-prism
r.d.: reference direction of the IMU
t : target

Fig. 1: direction transfer IMU → target

The angle α will be detached or calculated in an internal procedure and so it is only necessary to determine the calibration constant ε to transfer the orientation of the platform to a qualified optical instrument, may be a theodolite (s. Fig. 1).

A further possibility is given with the help of a range finder and a telescopic sight, fitted on the box of the IMU. In combination with a revolving IMU around the vertical axis it is possible to center the calculated azimuth from the platform to a marked line (s. Fig. 2).

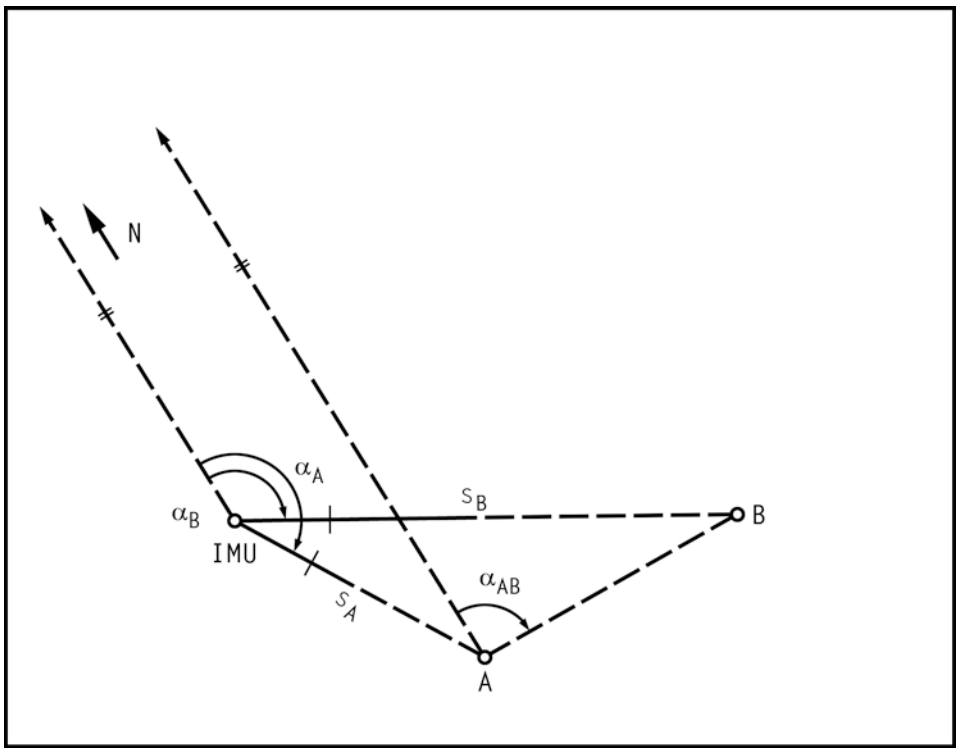

Fig. 2: Centering of azimuths

With the help of plane trigonometry it is possible to calculate the unknown azimuth α_{AB} directly

$$\alpha_{AB} = \alpha_A \pm 200\,\text{gon} + \arcsin\left(\frac{s_B \cdot \sin(\alpha_A - \alpha_B)}{\sqrt{s_A^2 + s_B^2 - 2 \cdot s_A \cdot s_B \cdot \cos(\alpha_A - \alpha_B)}}\right)$$

Because the sighting line of the telescope is not exact parallel with the reference direction of the IMU, it is also necessary to consider a calibration constant in this case.

Other procedures are thinkable but not realized up to now.

4. FIELD TEST

The measurements which were necessary to test the accuracy of azimuth determination were carried out at the test-network "Ebersberger Forst", located in the east of Munich (s. Fig. 3).

The positional accuracy less than 1 cm at the points along our reference lines allows the comparison of determined azimuths and reference values with a standard variation less than 1 mgon (***e.g . CASPARY, HEIN, SCHÖDLBAUER 1985***).

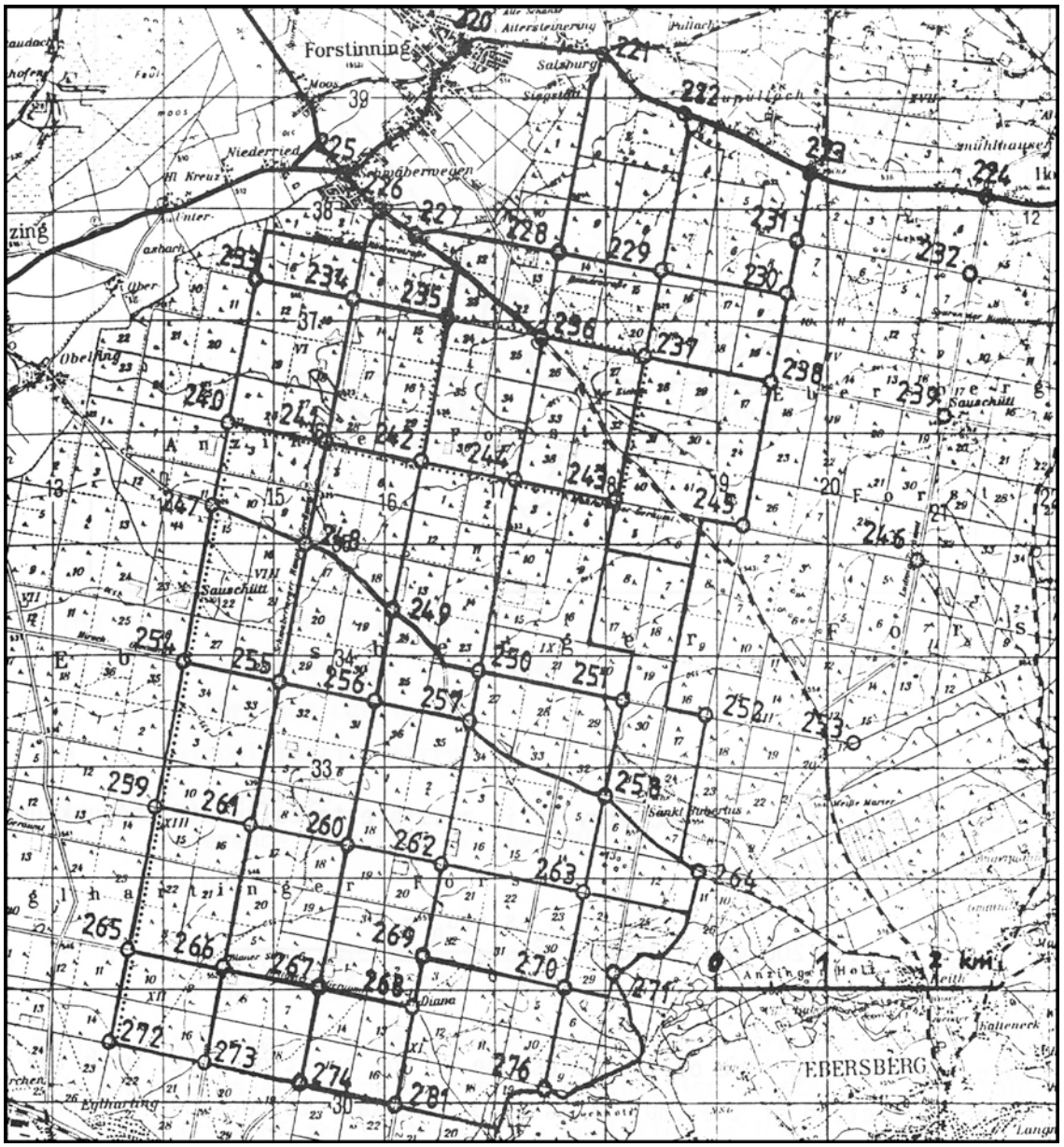

Fig. 3: Test-network "Ebersberger Forst" and reference lines (....)

5. COMPUTATION

The geodetic user of azimuth values is interested in two fundamental questions:

- Which accuracy could be achieved with real-time results?
  (on-line determination)
- Which accuracy could be achieved with smoothing-operations?
  (off-line evaluation)

Under this viewpoint the results of the three inertial systems were analized.

Because there was no calibration constant given by the producer it was necessary to consider an appropriate value as a trend-function. In the stochastic model the observations were regarded as normal distributed, physical uncorrelated and they all have the same weight.

In addition to this it was necessary to consider the different hardware and software conceptions of the inertial systems, especially in the off-line evaluation.

The computations are based on the following results (Fig. 4, 5, 6):

Nr.	Station	Target	Observed Azimuth [gon]	Reference Azimuth [gon]	Difference [gon]	Time [h.m.]
1	272 Ex	265 Ex	14.3416	14.5086	- 0.1670	9.43
2	272 Ex	265 Ex	14.3355	14.5086	- 0.1731	9.51
3	272 Ex	265 Ex	14.3283	14.5086	- 0.1853	10.04
4	272 Ex	265 Ex	14.3111	14.5086	- 0.1975	10.13
5	272 Ex	265 Ex	14.3050	14.5086	- 0.2036	10.19
6	272 Ex	265 Ex	14.2989	14.5086	- 0.2097	10.25
7	272 Ex	265 Ex	14.2806	14.5086	- 0.2280	10.43
8	272 Ex	265 Ex	14.3111	14.5086	- 0.1975	11.41
9	265 Ex	272 Ex	214.3107	214.5108	- 0.2001	11.59
10	265 Ex	272 Ex	214.3168	214.5108	- 0.1940	12.09
11	259 Ex	247 Ex	14.2032	14.3756	- 0.1724	12.32
12	259 Ex	247 Ex	14.2154	14.3756	- 0.1602	12.43
13	259 Ex	247 Ex	14.2337	14.3756	- 0.1419	12.51
14	247 Ex	240 Ex	13.9610	14.1317	- 0.1707	13.39
15	240 Ex	247 Ex	214.0201	214.1335	- 0.1134	14.03
16	240 Ex	247 Ex	214.0323	214.1335	- 0.1012	14.13
17	242 Ex	240 Ex	314.4452	314.8550	- 0.4098	14.37
18	242 Ex	240 Ex	314.4635	314.8550	- 0.3915	14.49
19	243 Ex	242 Ex	314.6895	314.8549	- 0.1654	16.20
20	237 Ex	235 Ex	314.6294	314.8202	- 0.1908	16.29
21	237 Ex	235 Ex	314.6234	314.8202	- 0.1968	16.36
22	235 Ex	235	203.7463	203.9621	- 0.2158	16.59
23	235 Ex	235	203.7402	203.9621	- 0.2219	17.15

Fig. 4: Azimuth determination FILS II

Nr.	Station	Target	Observed Azimuth [gon]	Reference Azimuth [gon]	Difference [gon]	Time [h.m.]
1	265 Ex	272 Ex	210.9120	214.5108	- 3.5988	11.02
2	265 Ex	272 Ex	210.9232	214.5108	- 3.5871	11.11
3	265 Ex	272 Ex	210.9299	214.5108	- 3.5809	11.17
4	259 Ex	247 Ex	10.8169	14.3756	- 3.5587	11.26
5	259 Ex	247 Ex	10.8245	14.3756	- 3.5511	11.36
6	259 Ex	247 Ex	10.8330	14.3756	- 3.5426	11.42
7	247 Ex	240 Ex	10.5759	14.1317	- 3.5558	11.52
8	247 Ex	240 Ex	10.5729	14.1317	- 3.5588	12.02
9	247 Ex	240 Ex	10.5770	14.1317	- 3.5547	12.09
10	240 Ex	247 Ex	210.5761	214.1335	- 3.5574	12.20
11	240 Ex	247 Ex	210.5875	214.1335	- 3.5460	12.27
12	240 Ex	247 Ex	210.5865	214.1335	- 3.5470	12.32
13	242 Ex	240 Ex	311.2232	314.8550	- 3.6318	12.45
14	242 Ex	240 Ex	311.2252	314.8550	- 3.6298	13.00
15	242 Ex	240 Ex	311.2288	314.8550	- 3.6262	13.06
16	243 Ex	242 Ex	311.2771	314.8549	- 3.5778	13.16
17	243 Ex	242 Ex	311.2776	314.8549	- 3.5773	13.27
18	243 Ex	242 Ex	311.2777	314.8549	- 3.5772	13.34

Fig. 5: Azimuth determination Geo-Spin II

Nr.	Station	Target	Observed Azimuth [gon]	Reference Azimuth [gon]	Difference [gon]	Time [h.m.]
1	272 Ex	265 Ex	14.1250	14.5086	- 0.3836	9.36
2	272 Ex	265 Ex	14.1269	14.5086	- 0.3817	9.57
3	272 Ex	265 Ex	14.1244	14.5086	- 0.3842	10.05
4	272 Ex	265 Ex	14.1231	14.5086	- 0.3855	10.13
5	272 Ex	265 Ex	14.1253	14.5086	- 0.3833	10.18
6	265 Ex	259 Ex	14.1262	14.5017	- 0.3755	10.46
7	265 Ex	259 Ex	14.1250	14.5017	- 0.3767	10.51
8	265 Ex	259 Ex	14.1247	14.5017	- 0.3770	10.56
9	259 Ex	254 Ex	14.0475	14.4438	- 0.3963	12.58
10	259 Ex	254 Ex	14.0475	14.4438	- 0.3963	13.02
11	259 Ex	254 Ex	14.0487	14.4438	- 0.3951	13.05
12	242 Ex	243 Ex	114.4429	114.8355	- 0.3926	13.47
13	242 Ex	243 Ex	114.4377	114.8355	- 0.3978	13.56
14	242 Ex	243 Ex	114.4398	114.8355	- 0.3957	14.01

Fig. 6: Azimuth determination LASS II

And now details about the three inertial systems and results of the computations:

Using the Ferranti platform for geodetic measurements, it is necessary to repeat a "Fine-Alignment" about every 90 minutes. On this occasion the orientation of the platform is to be corrected and different system parameters are to be estimated.

To consider a calibration constant in the real-time results and to analyze the accuracy we used least squares adjustment. With the condition that

$$E\{Az_o + C - Az_r\} = E\{OE\} = 0$$

$E\{\ \}$ ... expected value
Az_o ... observed azimuth
Az_r ... reference value of the azimuth
C ... calibration constant (trend parameter)
OE ... orientation error

there is the equation of observations

$$\underline{Az_o} + \underline{v} = \underline{Az_r} - \underline{C}$$

$\underline{v}$ ... vector of residuals

Based on this there are the following results:

$C = \pm 0.1768$ gon
$s_0 = \pm 0.0210$ gon

s_0 ... standard error of the unit weight

Besides this the observations no. 17 and 18 were detected as gross errors and pushed out by a hypothesis test with a type one error less than 0.1 %.

For the post-mission analysis the functional model was expanded. Considering the correction of orientation at every "Fine-Alignment" and the idea of linear gyro-drift fitting straight lines were computed.

The following graphic (Fig. 7) shows the results.

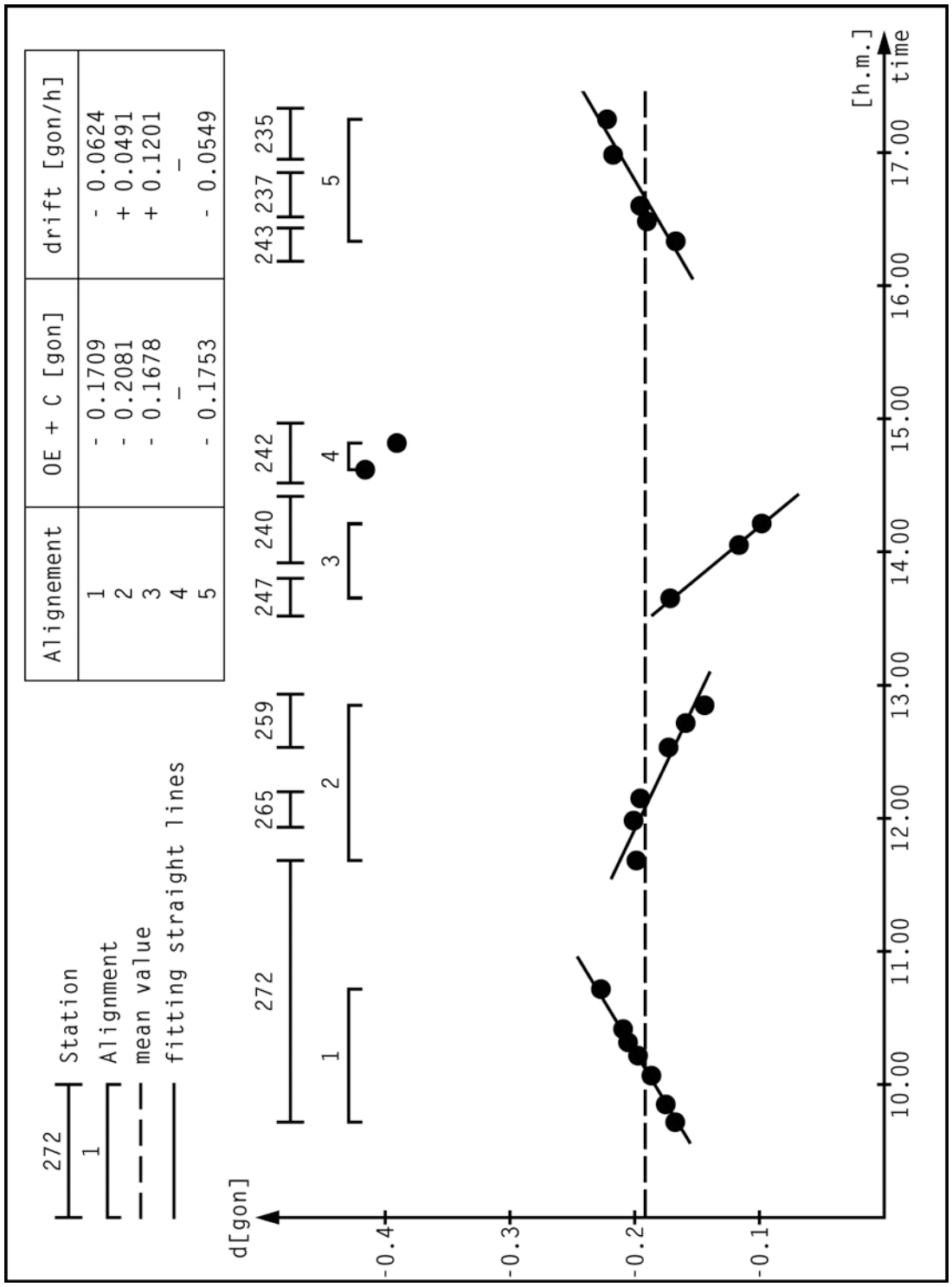

Fig. 7: Results of azimuth determination with the Ferranti Inertial-Land-Surveyor II

The second system which was tested was the Honeywell-platform Geo-Spin II. In contrast to the Ferranti system it is only necessary to practice one alignment at the beginning of the daily survey program, because system parameters are estimated with the use of a Kalman-Filtering procedure and some checkpoints.

For the computation of these results the same mathematic model was applied as for the Ferranti data. Least squares adjustment gives the estimated values (Fig. 8).

$$C = -3.5755 \text{ gon}$$
$$s_0 = \pm 0.0152 \text{ gon}$$

A post mission adjustment seems not to be advisable, because the results do not show systematic effects which allow to determine a physical founded smoothing function. The reason for this unsatisfactory situation is that we are unaware of the exact procedure of parameter-estimation with the implemented Kalman-Filter. Especially the missing information about start values and the estimated process-noise do not allow founded off-line calculations.

And now, last not least, the results of azimuth determination with the Litton Auto-Surveyor-System. Normally there is also needed only one alignment with the Litton platform but because of a breakdown in the energy supply it was necessary to repeat the procedure after two hours and so it is also possible to compare these two phases.

The mathematic model for the computation of the accuracy of the real-time results was the same as for the other systems and the results were

$$C = -0.3877 \text{ gon}$$
$$s_0 = \pm 0.0042 \text{ gon}$$

For post-processing computation there are comparable problems explained for the Honeywell platform, unknown Kalman-Filtering procedure. So it is only possible to realize the estimation of two constant values as a trend function, one for each alignment (Fig. 9).

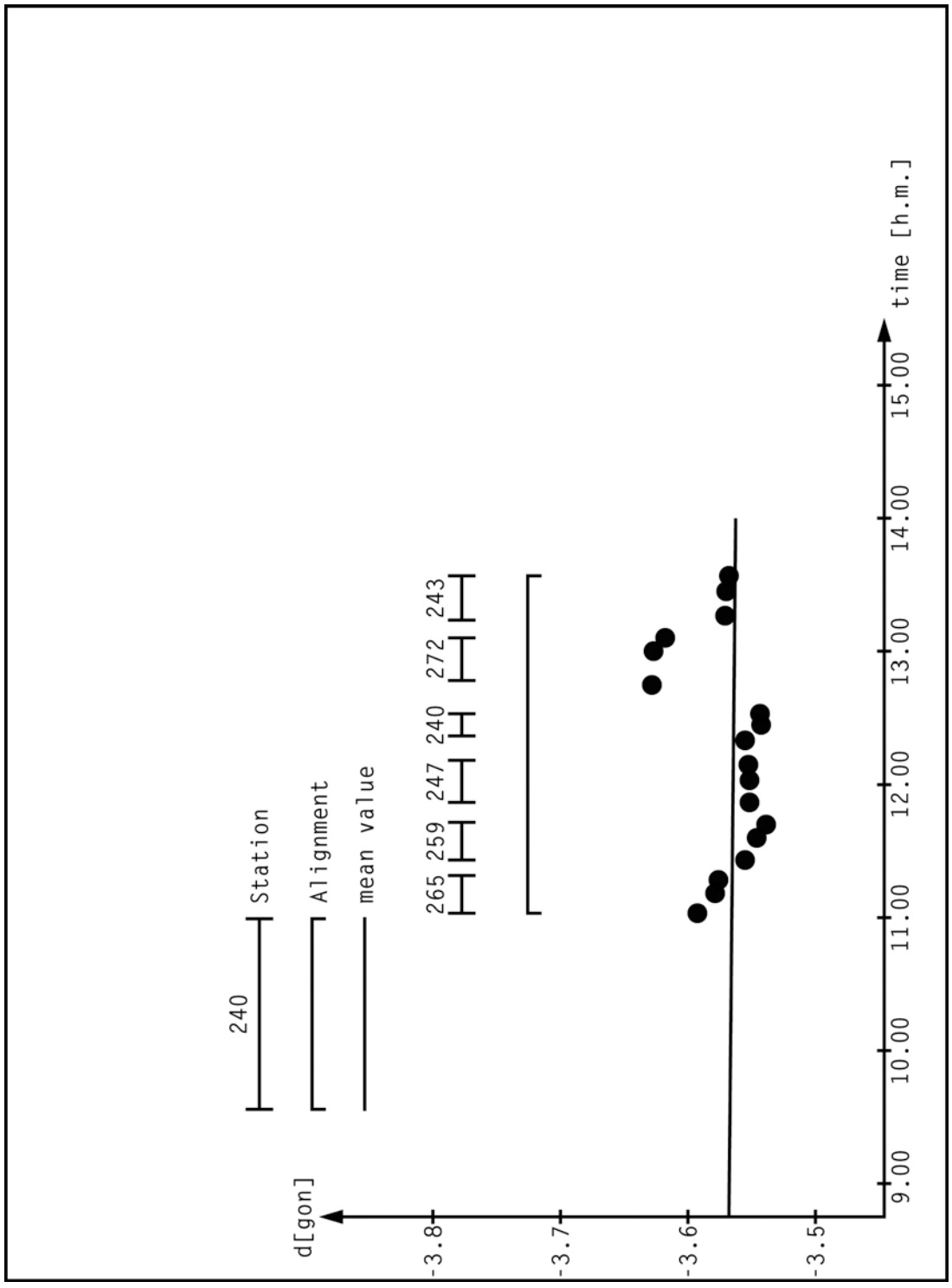

Fig. 8: Results of azimuth determination with the Honeywell Geo-Spin II

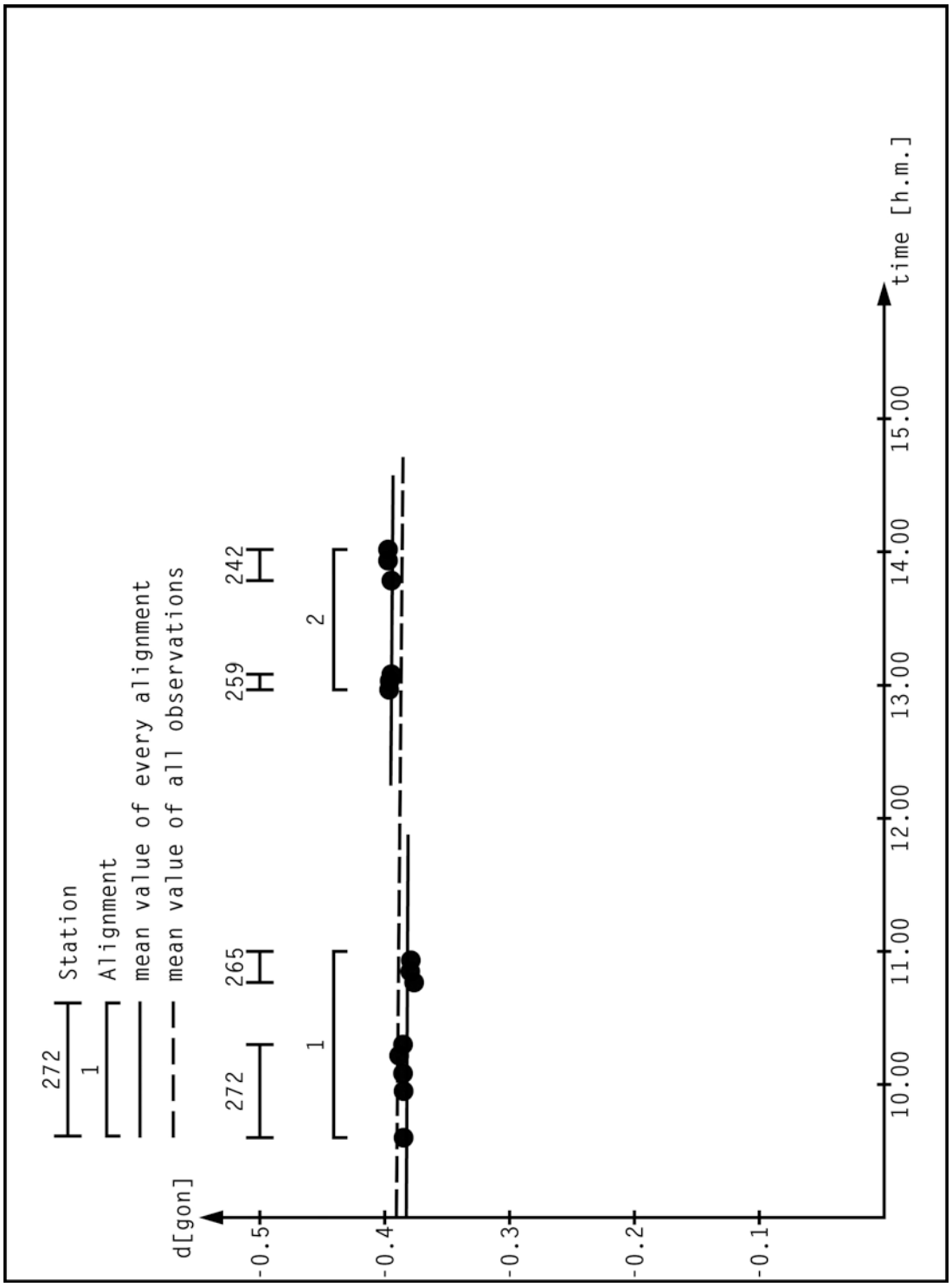

Fig. 9: Results of azimuth determination with Litton Auto-Surveyor-System II

6. COMPARISON AND VALUATION

To compare the three tested inertial systems, it is advantageous to oppose the standard errors of the unit weight which were the results of the evaluation of the time sequences.

unit (ISS)	standard variation real-time results [gon]	standard variations post-mission results [gon]
FILS II	± 0.0210	± 0.0055
Geo-Spin II	± 0.0152	-
LASS II	± 0.0042	± 0.0019

These standard variations are estimators for the accuracy of one observed azimuth with the respective inertial system.

The comparison shows at the first sight that the observations with the Litton system are those with the highest accuracy. That is valid for the real-time results as well as for the smoothed values.

In addition to this the space of time needed for one observation, including building up and dismantling of theodolite, was the shortest with the Litton instrument, too; only 10 minutes in comparison with 15 to 20 minutes with Ferranti and Honeywell platforms. The difference is established in the more simple use of the Porro prism in contrast to the autocollimation mirror.

Finally must be said that the accuracy of azimuths you can observe with inertial systems is comparable with those could be achieved with meridian gyroscopes of medium precision and it only seems to be economic to use inertial survey systems for azimuth determination in addition to other geodetic purpose.

7. REFERENCES

CASPARY, W.: ***Inertiale Vermessungssysteme.*** Vermessungswesen und Raumordnung 4/1983, S. 169ff.

CASPARY, W., HEIN, G., SCHÖDLBAUER, A.: ***Bericht über die Arbeiten am Gemeinschaftsprojekt Inertialgeodäsie, Teil I bis V.*** 1985

HEITZ, S.: ***Mechanik fester Körper, Band 1: Grundlagen, Dynamik starrer Körper.*** Dümmlers Verlag, Bonn 1980, S. 57ff.

RINNER, K.: ***Über geodätische Kreisel und Verfahren der Inertialvermessung.*** Internationale geodätische Woche in Obergurgel 1981, Institutsbericht der Universität Innsbruck

SCHÖDLBAUER, A.: ***Inertial Survey Platforms and their Geodetic Relevant Coordinate Systems.*** In: Proceedings Joint Meeting FIG - Study Groups 5B and 5C on Inertial, Doppler and GPS Measurements for National and Engineering Surveys, July 1-3, 1985. Schriftenreihe des Studiengangs Vermessungswesen der Universität der Bundeswehr München, Heft 20-1, Neubiberg 1985, 89-111

WILKINSON, G.A., WONG, R.V.C.: ***The use of azimuth control in inertial surveying to improve accuracy on an L-shaped traverse.*** In: Proceedings of the Second International Symposium of Inertial Technology for Surveying and Geodesy, Banff 1981

DRIFT EFFECTS IN INERTIAL MEASUREMENT SYSTEMS (RESULTING FROM NONLINEAR TERMS IN THE EQUATIONS OF MOTIONS)

by

Wolfgang MÖHLENBRINK

Institut für Anwendungen der Geodäsie im Bauwesen

Universität Stuttgart
Keplerstraße 10
7000 Stuttgart 1
Federal Republic of Germany

ABSTRACT

Today the adjustment of inertial data is based upon pure kinematic approaches. The IMS is treated as a "black box" and timedependent linear or quadratic drift terms are identified by adjustment.
With kinetic approaches dependent on the dynamic character of the IMS, nonlinear terms within the kinetic Euler equations lead to position errors with n-times the Schuler frequency. These effects as a result of rotations around spin- and output axis are discussed.

ZUSAMMENFASSUNG

Die Auswertung von Inertialdaten erfolgt heutzutage mit rein kinematischen Ansätzen.
Das IMS wird hierbei als "black box" behandelt, dessen zeitabhängige lineare oder quadratische Driftanteile durch Ausgleichungsrechnung identifiziert werden.
Bei kinetischen Ansätzen, abhängig vom dynamischen Charakter des IMS, führen nichtlineare Terme innerhalb der kinetischen Eulergleichungen zu Positionsfehlern mit der n-fachen Schulerfrequenz.
Diese Effekte werden für Rotationen um die Spin- und Outputachse dargestellt.

1. Introduction

Inertial measurement systems (IMS) were developed for the use in air and ship's navigation. Online computations and global missions with accuracies of several hundred meters are main aspects of interest. They led to fast online navigation algorithms based upon linearized equations of motion of the sensors and simplified global gravity models. Today the hardware used in inertial geodesy is developed directly from these instrumentations. Specially selected sensors, high precision calibration methods and linearized dynamic sensor models are characteristics of these instruments. Post mission adjustment techniques in geodesy (Hannah, Schwarz) are used to eliminate drift effects, scale factors and some more deterministic errors. All these approaches are based on pure kinematical models. However, the dynamic character of the inertial sensors accelerometer and mechanical gyro is neglected. Also the dynamics of the stabilized platform is not found in geodetic inertial dataprocessing. But IMS are pure dynamic measurement instruments.

As a source of the accuracy limit of one or more decimeters the unknown gravity field is often discussed. Besides this the dynamic properties will be an important error source. Residuals of inertial data of Ferranti FILS II System calculated by Vassiliou contain harmonics up to six-fold Schuler frequency. What may be the source of this obviously deterministic errors? One important influence may be the dynamic character of the instrumentation. Besides the improvement of gravity field models for inertial positioning it seems to be necessary to develop dynamic approaches for the post mission adjustment techniques of inertial data. This will be demonstrated with the dynamic model of the single-degree-of-freedom mechanical gyro (SDF Gyro). In geodetic publications this type of gyro is often described as a rotational sensor, which measures angular velocities around the input axis. But this is only valid in first approximation. This gyro has also responses to cross axes as spin axis and rotation axis. This means that the spatial movement of the gyro superposes the angular velocity around the input axis. In the following simulation it is shown that different rotational vibrations lead to error torques of the gyro element. Ausmann has shown that orientation errors resulting from the gyros are followed by position errors with Schuler frequency. So quadratic and other nonlinear terms lead to twofold or manifold times Schuler frequency errors

respectively. Today the dynamic models used in IMS (not accessible, installed in the navigational preprocessor) are linear approaches. The following simulation will show that this neglect of nonlinear terms leads to error drift dependent on the movement of the vehicle carrying the IMS. The magnitude of this signal distortion is so large that it will be an important source of the present accuracy limit in inertial geodesy.

2. Single-degree-of-freedom gyro dynamics

Most of the geodetic IMS use mechanical gyros. The stabilisation of the platform keeps spin and input axis rotations small. But in gyro dynamics cross coupling errors are well known (Stieler, Winter). Significant influences of these rotations are still existing in the sensor signals. For further analysis of these effects the whole nonlinear equation of movement of the SDF gyro is developed. The dynamic of the stabilized platform will be neglected. In reality this would reduce the magnitude of the error but the error characteristic should be the same. The model of SDF F 125 gyro used in the Ferranti FILS II system is just of this type.

2.1 Gyro Model

Spin axis, input axis and output axis of the gyro element may be defined as shown in picture 1.

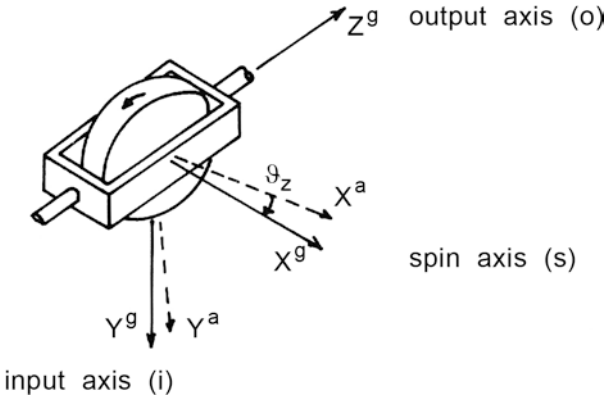

Picture 1: Axes of Gyro Element

In this model the following properties may be valid

1. The rotor spins about an axis of symmetry
2. The rotor spins with constant speed
3. The center of mass of the rotor and of the gyro element coincide
4. The rotor bearings are rigid

The evaluation of the rotational equation of motion of the motor is divided into two steps. First we determine the angular momentum of the gyro including the gimbal rotation, then we compute the time rate of change of the angular momentum vector and equate it to the applied torque.

The resulting angular momentum $\underline{H}_i^g$ is defined as the sum of angular momentums of rotating and non-rotating parts of the gyro.

$$\underline{\underline{H}}_i^g = \underline{\underline{H}}_{ir}^g + \underline{\underline{H}}_{ig}^g = \underline{\underline{I}}_r \cdot \underline{\omega}_{ir}^g + \underline{\underline{I}}_g \cdot \underline{\omega}_{ig}^g \tag{1}$$

$$\begin{aligned} \underline{\underline{H}}_i^g &= \underline{\underline{I}}_r \left(\underline{\omega}_{ig}^g + \underline{\omega}_{gr}^g \right) + \underline{\underline{I}}_g \cdot \underline{\omega}_{ig}^g \\ &= \left(\underline{\underline{I}}_r + \underline{\underline{I}}_g \right) \cdot \underline{\omega}_{ig}^g + \underline{\underline{I}}_r \cdot \underline{\omega}_{gr}^g \\ &= \underline{\underline{I}}_{g+r} \cdot \underline{\omega}_{ig}^g + \underline{\underline{I}}_r \cdot \underline{\omega}_{gr}^g \ . \end{aligned} \tag{2}$$

The inertial tensor is defined as

$$\underline{\underline{I}}_{g+r} = \begin{pmatrix} I_s & 0 & 0 \\ 0 & I_i & 0 \\ 0 & 0 & I_o \end{pmatrix} . \tag{3}$$

From the law of momentum follows

$$\begin{aligned} \frac{(i)_d}{dt} \underline{H}_i &= \underline{M} \\ \frac{(i)_d}{dt} \underline{H}_i^g &= \frac{(g)_d}{dt} \underline{H}_i^g + \underline{\omega}_{ig}^g \times \underline{H}_i^g = \underline{M} \ . \end{aligned} \tag{4}$$

Splitting up in spinning and non-spinning parts yields

$$\frac{(g)_d}{dt}\,\underline{H}^g_{ir} + \frac{(g)_d}{dt}\,\underline{H}^g_{ig} + \underline{\omega}^g_{ig} \times \underline{H}^g_{ir} + \underline{\omega}^g_{ig} \times \underline{H}^g_{ig} = \underline{M} \ . \qquad (5)$$

With the assumption that $\underline{H}^g_{ir}$ is large compared to $\underline{H}^g_{ig}$, the basic equation of motion of the gyro is found:

$$\frac{(g)_d}{dt}\,\underline{H}^g_{ig} + \underline{\omega}^g_{ig} \times \underline{H}^g_{ir} = \underline{M} \ . \qquad (6)$$

For the purpose of inertial navigation it is necessary to describe the motion of the gimbal element in inertial space. The following chain of transformations is provided: The rotor fixed system "r" is rotating against gimbal fixed system "g" with angular velocity ω^g_{gr}. Furthermore the gimbal system "g" is rotating against the case system of the gyro "c" with $\underline{\vartheta} = (\vartheta_x, \vartheta_y, \vartheta_z)^T$ and with angular velocity $\underline{\dot{\vartheta}} = (\dot{\vartheta}_x, \dot{\vartheta}_y, \dot{\vartheta}_z)^T$.

This case system "c" is defined in the platform system "p" (the platform is carrying the sensor elements). Because of mounting uncertainties it is necessary to define misalignment angles $\underline{\alpha}$ between the axis of "p"- and "c"-system, $\underline{\alpha} = (\alpha_x, \alpha_y, \alpha_z)^T$.

The described platform is rotating against inertial space with the angles $\underline{\varphi} = (\varphi_x, \varphi_y, \varphi_z)^T$ and the angular velocity $\underline{\dot{\varphi}} = (\dot{\varphi}_x, \dot{\varphi}_y, \dot{\varphi}_z)^T$.

The rotation matrix $\underline{\underline{C}}^{\alpha}$ for the misalignment of the sensor against the platform is defined by Bryant-(= Cardan-)angles as follows:

$$\underline{\underline{C}}^{\alpha} = \begin{pmatrix} 1 & \alpha_z & -\alpha_y \\ -\alpha_z & 1 & \alpha_x \\ \alpha_y & -\alpha_x & 1 \end{pmatrix} . \qquad (7)$$

The movement of the gyro element against the case system is also defined by Bryant angles and the rotation matrix of the output angle of the sensor is

$$\underline{\underline{C}}^{\vartheta_z} = \begin{pmatrix} \cos\vartheta_z & \sin\vartheta_z & 0 \\ -\sin\vartheta_z & \cos\vartheta_z & 0 \\ 0 & 0 & 1 \end{pmatrix} . \qquad (8)$$

$$\underline{\underline{C}}_c^{\vartheta_g} = \begin{pmatrix} \cos\vartheta_y \cos\vartheta_z & -\cos\vartheta_x \sin\vartheta_z + \sin\vartheta_x \sin\vartheta_y \cos\vartheta_z & \sin\vartheta_x \sin\vartheta_z - \cos\vartheta_x \sin\vartheta_y \cos\vartheta_z \\ -\cos\vartheta_y \sin\vartheta_z & \cos\vartheta_x \cos\vartheta_z - \sin\vartheta_x \sin\vartheta_y \sin\vartheta_z & \sin\vartheta_x \cos\vartheta_z + \cos\vartheta_x \sin\vartheta_y \sin\vartheta_z \\ \sin\vartheta_y & -\sin\vartheta_x \cos\vartheta_y & \cos\vartheta_x \cos\vartheta_y \end{pmatrix} \tag{9}$$

With these definitions the angular velocity of the gimbal system against the inertial space is

$$\underline{\omega}_{ig}^{g} = \underline{\omega}_{ip}^{g} + \underline{\omega}_{pc}^{g} + \underline{\omega}_{cg}^{g} \quad . \tag{10}$$

The resulting angular velocity of the rotor element in inertial space is

$$\underline{\omega}_{ir}^{g} = \underline{\underline{C}}_c^{\vartheta_g} \left(\underline{\underline{C}}_p^{\alpha_c} \underline{\omega}_{ip}^{p} + \underline{\omega}_{cg}^{c} \right) + \underline{\omega}_{gr}^{g} \quad . \tag{11}$$

Introducing this angular velocity into the equation of angular momentum (1) yields

$$\underline{H}_i^g = \underline{\underline{I}}_r \underline{\omega}_{gr}^{g} + \underline{\underline{I}}_{g+r} \left(\underline{\underline{C}}_c^{\vartheta_g} \underline{\underline{C}}_p^{\alpha_c} \underline{\omega}_{ip}^{p} + \underline{\underline{C}}_c^{\vartheta_g} \underline{\omega}_{cg}^{c} \right) \quad . \tag{12}$$

2.2 Rotational Equations of Motion

The use of the law of conservation of momentum and the Coriolis theorem leads to the following nonlinear equation of motion of the mechanical gyro in inertial space. In case of the rate gyro, the gyro element is forced to the case by a spring. Furthermore a damping element reduces the influence of vibrations. With spring constant K and damping factor D the equation of motion may be written as

$$\underline{M}_i^i = \frac{d}{dt}\left(\underline{\underline{I}}_r\,\underline{\omega}_{gr}^g + \underline{\underline{I}}_{g+r}\,\underline{\underline{C}}^{\vartheta}\left(\underline{\underline{C}}^{\alpha}\,\underline{\dot{\varphi}} + \underline{\dot{\vartheta}}\right)\right) + \tag{13}$$

$$+\,\underline{\underline{C}}^{\vartheta}\left(\underline{\underline{C}}^{\alpha}\,\underline{\dot{\varphi}} + \underline{\dot{\vartheta}}\right) \times \left(\underline{\underline{I}}_r\,\underline{\omega}_{gr}^g + \underline{\underline{I}}_{g+r}\,\underline{\underline{C}}^{\vartheta}\left(\underline{\underline{C}}^{\alpha}\,\underline{\dot{\varphi}} + \underline{\dot{\vartheta}}\right)\right)$$

$$\underline{\underline{I}}_{g+r}\,\underline{\underline{C}}^{\vartheta}\,\underline{\ddot{\vartheta}} + D\,\underline{\dot{\vartheta}} + K\,\underline{\vartheta}$$

$$\textcircled{1} \qquad + \underline{\underline{I}}_{g+r}\,\underline{\underline{C}}^{\dot{\vartheta}}\,\underline{\dot{\vartheta}} + \qquad \textcircled{2}$$

$$+ \underline{\underline{I}}_{g+r}\,\underline{\underline{C}}^{\vartheta}\,\underline{\underline{C}}^{\alpha}\,\underline{\dot{\varphi}} + \qquad \textcircled{3}$$

$$+ \underline{\underline{C}}^{\vartheta}\,\underline{\dot{\vartheta}} \times \underline{\underline{I}}_r\,\underline{\omega}_{gr}^g + \qquad \textcircled{4}$$

$$+ \underline{\underline{C}}^{\vartheta}\,\underline{\dot{\vartheta}} \times \underline{\underline{I}}_{g+r}\,\underline{\underline{C}}^{\vartheta}\,\underline{\underline{C}}^{\alpha}\,\underline{\dot{\varphi}} + \qquad \textcircled{5}$$

$$+ \underline{\underline{C}}^{\vartheta}\,\underline{\underline{C}}^{\alpha}\,\underline{\dot{\varphi}} \times \underline{\underline{I}}_{g+r}\,\underline{\underline{C}}^{\vartheta}\,\underline{\dot{\vartheta}} + \qquad \textcircled{6}$$

$$+ \underline{\underline{C}}^{\vartheta}\,\underline{\dot{\vartheta}} \times \underline{\underline{I}}_{g+r}\,\underline{\underline{C}}^{\vartheta}\,\underline{\dot{\vartheta}} \qquad \textcircled{7}$$

$$= -\,\underline{\underline{I}}_{g+r}\,\underline{\underline{C}}^{\vartheta}\,\underline{\underline{C}}^{\alpha}\,\underline{\ddot{\varphi}} - \qquad \textcircled{8}$$

$$-\,\underline{\underline{C}}^{\vartheta}\,\underline{\underline{C}}^{\alpha}\,\underline{\dot{\varphi}} \times \underline{\underline{I}}_{g+r}\,\underline{\underline{C}}^{\vartheta}\,\underline{\underline{C}}^{\alpha}\,\underline{\dot{\varphi}} - \qquad \textcircled{9}$$

$$-\,\underline{\underline{C}}^{\vartheta}\,\underline{\underline{C}}^{\alpha}\,\underline{\dot{\varphi}} \times \underline{\underline{I}}_r\,\underline{\omega}_{gr}^g \qquad \textcircled{10}$$

(14)

The ordering of the different terms shows some nonlinear damping coefficients ② - ⑦ and the input ⑧ - ⑩.

Term ⑧ shows the influence of output axis acceleration. This means that rotational accelerations around all three axes cause error torques of the gyro element.

Term ⑩ contains the input signal and the cross coupling errors. In the linearized navigation equations of preprocessors in IMS usually only the cross coupling between input and output axis is corrected. All the other terms are neglected. It should be proved, how large this influence is in connection with the misalignment errors and whether it is important for inertial geodetic problems. The same problem arises with the anisoinertia torques described in term ⑨. Usually even the largest terms of aniso-

inertia errors resulting from asymmetric torques of the rotor and gimbal element are neglected during the preprocessing of inertial data in the IMS. It will be shown, that these nonlinear terms are of second and higher order. The manifold Schuler frequencies with residuals of Ferranti data calculated by Vassiliou may be a result of these deterministic dynamic model errors.

3 Simulation of SDF gyro signals

In case of the SDF rate gyro the response of the sensor to an arbitrary input can be calculated by convolution of the input signal with the weighting function of the sensor. This way is valid in strength only for linear differential equations with constant coefficients. This solution of the differential equation

$$y'' + c_1 y' + c_0 y = f(t) \tag{15}$$

with arbitrary input $f(t)$ is given by

$$y(t) = \int_0^t g(t-\tau)\, f(\tau)\, d\tau \ . \tag{16}$$

$g(t)$ is the weighting function and contains the sensor dynamic properties. For numeric computations weighting coefficients $g^*(k \cdot T)$, $k = 0, 1, \ldots, n$ can be calculated from the weighting function. With a sufficient number of coefficients and a sufficiently small intervall the sum of convolution will be a good approximation for the integral of convolution.

$$y(n \cdot T) = T \cdot \sum_{y=0}^{n} f(\nu \cdot T) \cdot g^*((n-\nu) \cdot T) \ . \tag{17}$$

This is the linear differential equation of an ideal rate gyro if only rotations around the input axis occur and nonlinear terms are neglected:

$$I_z \cdot \ddot{\theta} + D \cdot \dot{\theta} + K \cdot \theta = H_{ir}^g \cdot \omega_i = H_r \cdot \omega_i \tag{18}$$

H_r is the angular momentum, ω_i the input angular velocity, I_z is the moment of inertia, D a damping coefficient and K the spring constant.

Laplace transformation

$$\left(I_z \cdot s^2 + D \cdot s + K\right) \cdot \mathcal{L}\{\theta\} = H_r \cdot \mathcal{L}\{\omega_i\} \tag{19}$$

leads to the Laplace transfer function

$$G(s) = \frac{H_r}{I_z \cdot s^2 + D \cdot s + K} = \frac{H_r}{I_z} \cdot \frac{1}{s^2 + \frac{D}{I_z} \cdot s + \frac{K}{I_z}} \tag{20}$$

$$\frac{D}{I_z} = 2\xi\omega_0 \quad , \quad \frac{K}{I_z} = \omega_0^2$$

√

with

$$\xi = \frac{D}{2\sqrt{K \cdot I_z}} \tag{21}$$

$$\omega_0 = \sqrt{\frac{K}{I_z}} \quad . \tag{22}$$

The weighting function in case $\xi > 1$ is given by

$$g(t) = \frac{H_r}{I_z} \cdot \frac{1}{\omega_0\sqrt{\xi^2 - 1}} \cdot e^{-\xi\omega_0 \cdot t} \cdot \sinh\left(\omega_0\sqrt{\xi^2 - 1} \cdot t\right) \tag{23}$$

and with a large spring constant K($\xi > 1$) the weighting function g(t) is

$$g(t) = \frac{H_r}{I_z} \cdot \frac{1}{\omega_0\sqrt{1 - \xi^2}} \cdot e^{-\xi\omega_0 \cdot t} \cdot \sinh\left(\omega_0\sqrt{1 - \xi^2} \cdot t\right) \tag{24}$$

For the numeric calculation the sensor parameters are chosen as applicated by Baumann /8/ and Stieler and Winter /6/.

Angular momentum of rotor	$H_r = 4.4 \cdot 10^5$ g·cm²/sec
Damping coefficient	$D = 8.8 \cdot 10^4$ g·cm²/sec
Moment of inertia	$I_z = 176$ g·cm²

To achieve a finite impulse response time of the gyro the spring constant K is defined to $K = 1.1 \cdot 10^7$ g·cm².

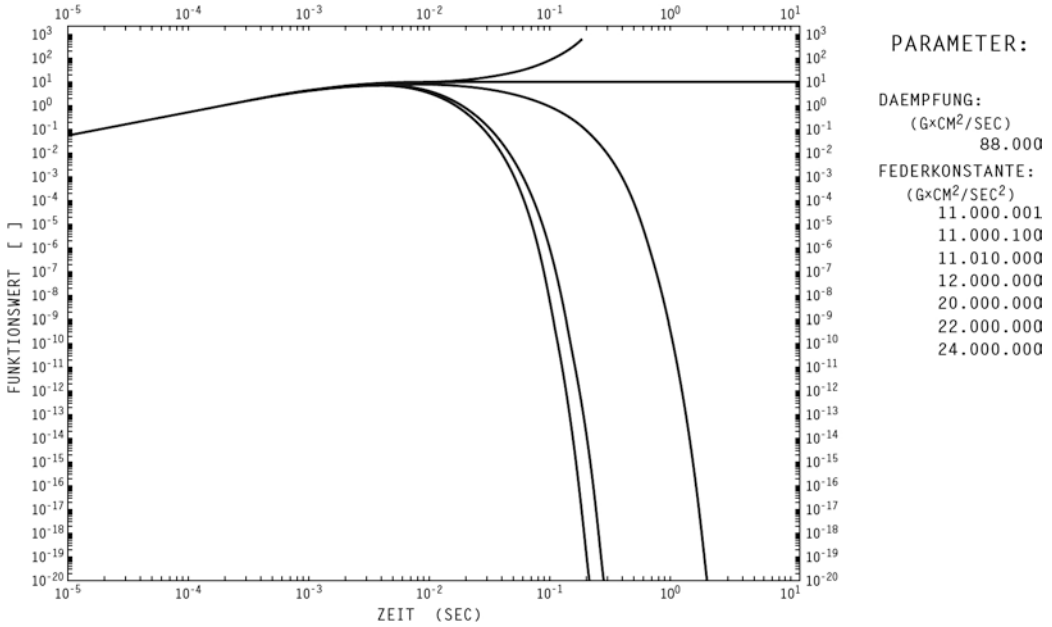

Picture 2: Weighting function of rate gyro

It is the goal of the following simulation of motion to show the influence of the nonlinear terms of the differential equation (14). This is possible with stepwise iteration and introducing nonlinear damping coefficients (pseudo damping) in every step. This can be done for rotation around one axis or around all three axes simultaneously. So it becomes practicable to calculate the gyro response of a signal with arbitrary frequency, amplitude and phase in all three axes. Now it is possible to extract the signal distortion caused by nonlinear terms in the equation of motion. With the deterministic input:

$$\underline{\varphi}(t) = \begin{pmatrix} A_x \cdot \sin(\omega_x \cdot t + \varphi_{xo}) \\ A_y \cdot \sin(\omega_y \cdot t) \\ A_z \cdot \sin(\omega_z \cdot t + \varphi_{zo}) \end{pmatrix} \qquad (25)$$

the angular velocity input is

$$\underline{\dot{\varphi}}(t) = \begin{pmatrix} A_x \cdot \omega_x \cdot \cos(\omega_x \cdot t + \varphi_{xo}) \\ A_y \cdot \omega_y \cdot \cos(\omega_y \cdot t) \\ A_z \cdot \omega_z \cdot \cos(\omega_z \cdot t + \varphi_{zo}) \end{pmatrix} . \qquad (26)$$

The response of the gyro is computed as described in picture 3.

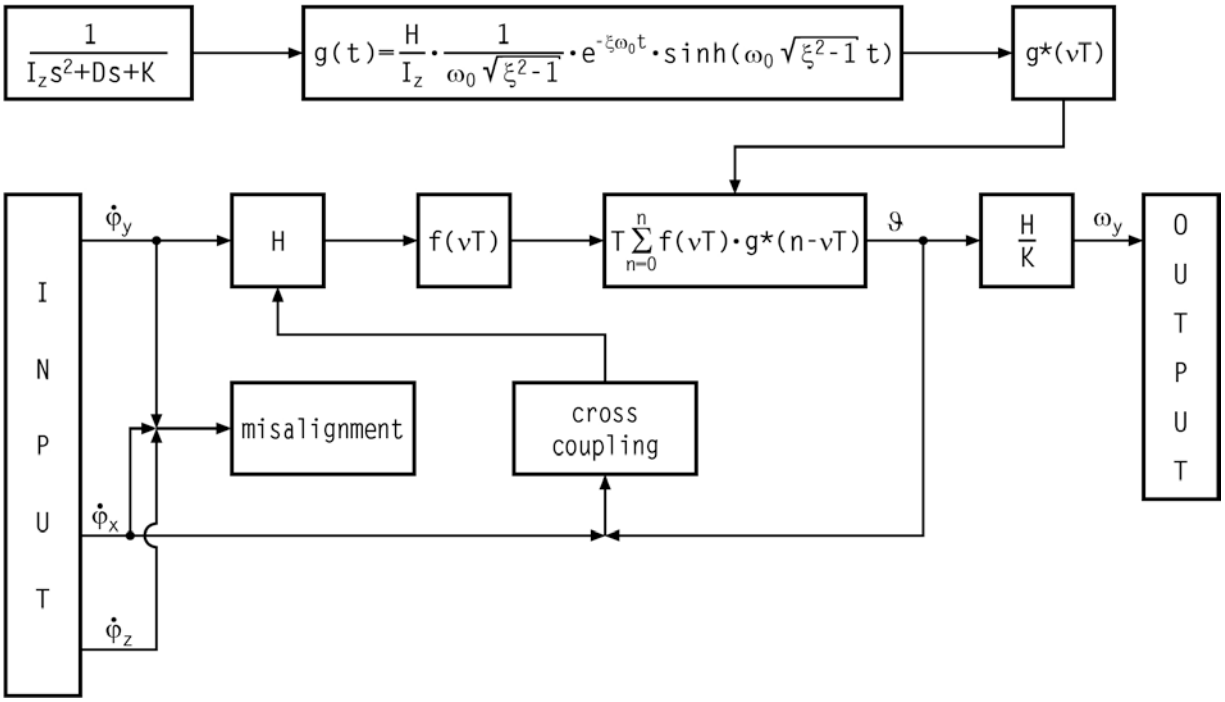

Picture 3: Simulation of SDF gyro response in case of cross coupling error

The influence of the main error terms

- cross coupling error
- anisoinertia error
- output axis acceleration error
- misalignment errors

will now be discussed in detail.

4 Dynamic Gyro Errors

The third row if this equation of motion in matrix form (14) is called output axis equation. For SDF gyros only this axis has a pick-off; spin axis bearings and output axis bearings are supposed to be fixed and there are no pick-offs at these axes. The total equation of motion is given for all three axes. This may be helpful if the dynamic model of accelerometers and two-degree-of-freedom gyros are of interest. This case is not discussed in this paper.

The output axis components of the terms ② to ⑦ are zero in this case. Terms ⑧ to ⑩ contain the main input signal and nonlinear gyro effects.

4.1 Cross Coupling Error

Term ⑩ contains the main input signal and the cross coupling caused by rotations of the sensor around the spin axis correlated with the movement of the gimbal element against the case. The cross coupling effect is normally kept small by means of a strong spring, a servomotor and the use of stabilized platforms. Furthermore it is seen, that additional error torques are produced by the cross axis misalignment and also small cross coupling errors due to misalignment.

$$⑩ = \underbrace{+ H_r \dot{\varphi}_y}_{\text{input}} \underbrace{- H_r \alpha_z \dot{\varphi}_x + H_r \alpha_x \dot{\varphi}_z}_{\text{cross axis misalignment}} \underbrace{- H_r \vartheta_z \dot{\varphi}_x}_{\text{cross coupling}}$$

$$\left.\begin{aligned} &-H_r \alpha_z \vartheta_z \dot{\varphi}_y \\ &+H_r \alpha_y \vartheta_z \dot{\varphi}_z \end{aligned}\right\} \text{cross coupling consequent misalignment}$$

The hardware error compensation of these effects is normally done by linear error correcting terms due to the necessity of online navigation. One important fact may be pointed out: The mechanical gyro is not the sensor delivering a signal that is proportional to the input axis angular rate.

Due to dynamic properties of the sensor the output signal contains influences as a result of the spatial movement of the sensor. In the case of simultaneous movement about spin and output axis the parts of the cross coupling error which are not compensated lead to quadratic position errors.

4.1.1 Simulation of Cross Coupling Error

Neglecting misalignments the response of cross coupling error is calculated with a harmonic input of frequency 0.2 Hz in x,y and z axis and with the maximum of 1.6 degrees for the rotation of the sensor element against

the case. Pic. 4 shows an oscillating and constant part resulting from the cross coupling term. The magnitude of the error in this case is larger than 1. percent. The large drift effect due to the simulated cross coupling is shown in pic. 5.

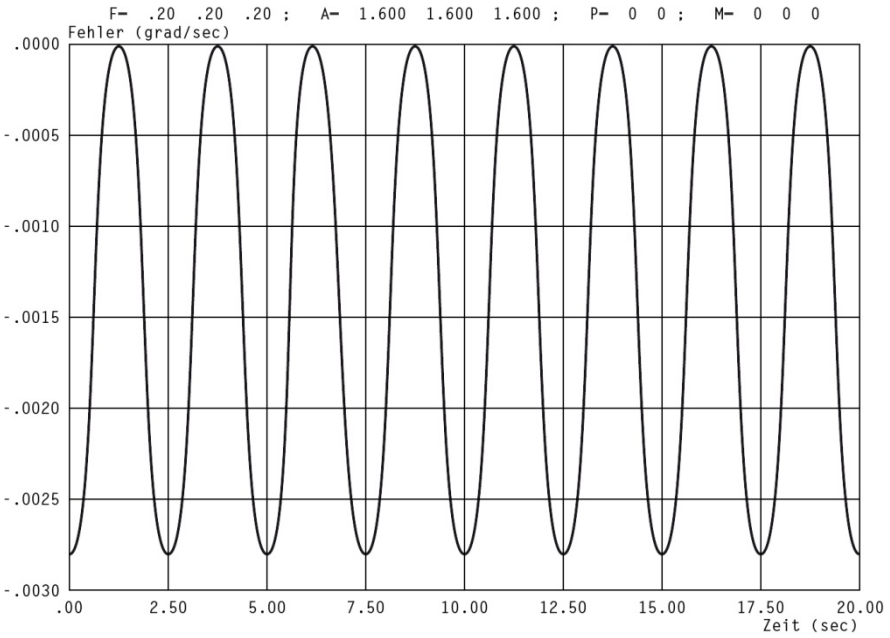

Picture 4: Cross Coupling Error

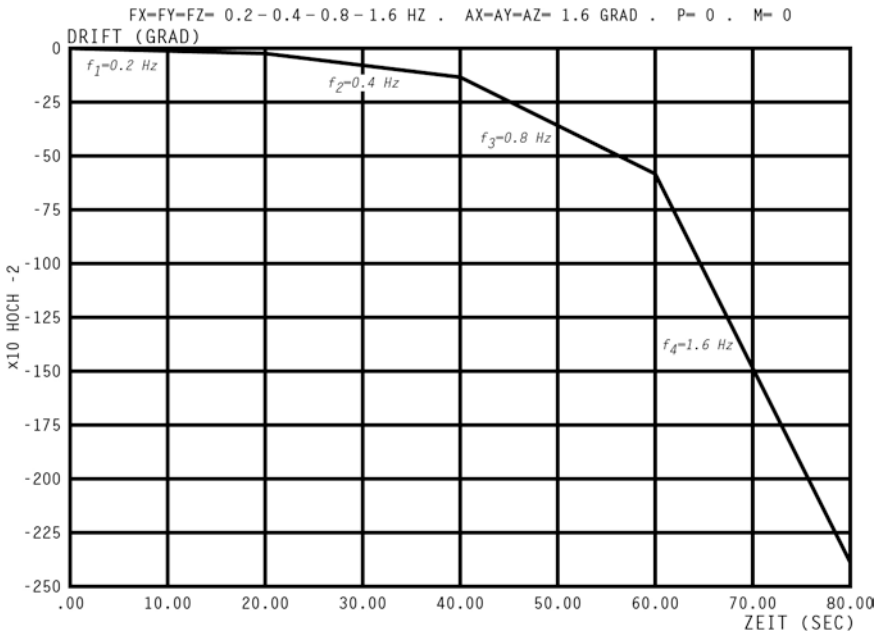

Picture 5: Drift Due to Cross Coupling

4.2 Anisoinertia Error

Resulting from different moments of inertia of the gyro element (rotor and gimbal) an error torque is produced by a simultaneous movement around both axes. As the cross coupling effect as the anisoinertia term leads to a drift of the gyro. The anisoinertia term ⑨ in the equation of motion is a highly nonlinear term dependent on the spatial motion around all three axes and the motion of the gyro element itself against the case.

$$⑨ = - \underline{\underline{C}}^{\vartheta}\,\underline{\underline{C}}^{\alpha}\,\underline{\dot{\varphi}} \times \underline{\underline{I}}_{g+r}\,C^{\vartheta}\,C^{\alpha}\,\dot{\varphi} =$$

$$= \begin{pmatrix} (I_i - I_o)\cdot\left(-\sin\vartheta\cdot\left(\dot{\varphi}_x+\alpha_z\cdot\dot{\varphi}_y-\alpha_y\cdot\dot{\varphi}_z\right)+\cos\vartheta\cdot\left(-\alpha_z\cdot\dot{\varphi}_x+\dot{\varphi}_y+\alpha_x\cdot\dot{\varphi}_z\right)\right)\cdot \\ \cdot\left(\alpha_y\cdot\dot{\varphi}_x-\alpha_x\cdot\dot{\varphi}_y+\dot{\varphi}_z\right) \\ (I_o - I_r)\cdot\left(\cos\vartheta\cdot\left(\dot{\varphi}_x+\alpha_x\cdot\dot{\varphi}_y-\alpha_y\cdot\dot{\varphi}_z\right)+\sin\vartheta\cdot\left(-\alpha_z\cdot\dot{\varphi}_x+\dot{\varphi}_y+\alpha_x\cdot\dot{\varphi}_z\right)\right)\cdot \\ \cdot\left(\alpha_y\cdot\dot{\varphi}_x-\alpha_x\cdot\dot{\varphi}_y+\dot{\varphi}_z\right) \\ -\Delta I\cdot\left(\cos\vartheta\cdot\left(\dot{\varphi}_x+\alpha_x\cdot\dot{\varphi}_y-\alpha_y\cdot\dot{\varphi}_z\right)+\sin\vartheta\cdot\left(-\alpha_z\cdot\dot{\varphi}_x+\dot{\varphi}_y+\alpha_x\cdot\dot{\varphi}_z\right)\right)\cdot \\ \cdot\left(-\sin\vartheta\cdot\left(\dot{\varphi}_x+\alpha_z\cdot\dot{\varphi}_y-\alpha_y\cdot\dot{\varphi}_z\right)+\cos\vartheta\cdot\left(-\alpha_z\cdot\dot{\varphi}_x+\dot{\varphi}_y+\alpha_x\cdot\dot{\varphi}_z\right)\right) \end{pmatrix}$$

The whole anisoinertia term of the output axis as a function of the misalignments, spatial motion and gyro element motion will be:

Anisoinertia - Formeln

Zusammenfassung für SDF mit $\vartheta_x = \vartheta_y = 0$

$$\Delta I_{yx} \cdot \Big[\big(\dot{\varphi}_x^2 - \dot{\varphi}_y^2 \big) \cdot \big(1 - \alpha_z^2 \big) \cdot \vartheta_z -$$ anisoinertia coupling torque

$$- \dot{\varphi}_x \cdot \dot{\varphi}_y \cdot \big(1 - \alpha_z^2 \big) +$$ anisoinertia torque

$$+ \dot{\varphi}_x \cdot \dot{\varphi}_y \cdot \big(1 - \alpha_z^2 \big) \cdot \vartheta_z^2 +$$ quadratic anisoinertia coupling torque

$$+ \big(\alpha_y^2 - \alpha_x^2 \big) \cdot \dot{\varphi}_z^2 \cdot \vartheta_z +$$ anisoinertia coupling torque due to misalignment

$$+ 4 \alpha_z \cdot \dot{\varphi}_x \cdot \dot{\varphi}_y \cdot \vartheta_z +$$

$$+ 2 \cdot \big(\alpha_y - \alpha_x \cdot \alpha_z \big) \cdot \dot{\varphi}_x \cdot \dot{\varphi}_y \cdot \vartheta_z \cdot$$

$$\cdot 2 \cdot \big(\alpha_x + \alpha_y \cdot \alpha_z \big) \cdot \dot{\varphi}_y \cdot \dot{\varphi}_z \cdot \vartheta_z +$$

$$\left. \begin{array}{l} + \alpha_z \cdot \dot{\varphi}_x^2 \\ - \alpha_z \cdot \dot{\varphi}_y^2 \end{array} \right\} \alpha_z \cdot \big(\dot{\varphi}_x^2 - \dot{\varphi}_y^2 \big) -$$ anisoinertia torque due to misalignment

$$- \alpha_x \cdot \alpha_y \cdot \dot{\varphi}_z^2 -$$

$$- \big(\alpha_x + \alpha_y \cdot \alpha_z \big) \cdot \dot{\varphi}_x \cdot \dot{\varphi}_z +$$

$$+ \big(\alpha_y - \alpha_x \cdot \alpha_z \big) \cdot \dot{\varphi}_y \cdot \dot{\varphi}_z -$$

$$- \alpha_z \cdot \big(\dot{\varphi}_x^2 + \dot{\varphi}_y^2 \big) \cdot \vartheta_z^2 -$$ quadratic anisoinertia coupling torque due to misalignment

$$- \alpha_x \cdot \alpha_y \cdot \dot{\varphi}_z^2 \cdot \vartheta_z^2 +$$

$$+ \big(\alpha_x + \alpha_y \cdot \alpha_z \big) \cdot \dot{\varphi}_x \cdot \dot{\varphi}_z \cdot \vartheta_z^2 -$$

$$- \big(\alpha_y - \alpha_x \cdot \alpha_z \big) \cdot \dot{\varphi}_y \cdot \dot{\varphi}_z \cdot \vartheta_z^2 \Big]$$

Anisoinertia coupling torques and anisoinertia torque as described in gyro dynamics are not the only anisoinertia effects in the dynamic model. They are the main terms but misalignment effects of the sensors lead to non-linear effects up to the 4. order. It is evident that these effects are small compared with the main effects. The linear compensation in IMS dynamic models may be sufficient for navigation purposes but it should be proved whether these effects lead to significant parameters in post mission adjustment. Anisoinertia drift has the same character as the cross coupling error drift approximation but it is not so large. The influence of misalignment on the anisoinertia error is shown in picture 6,

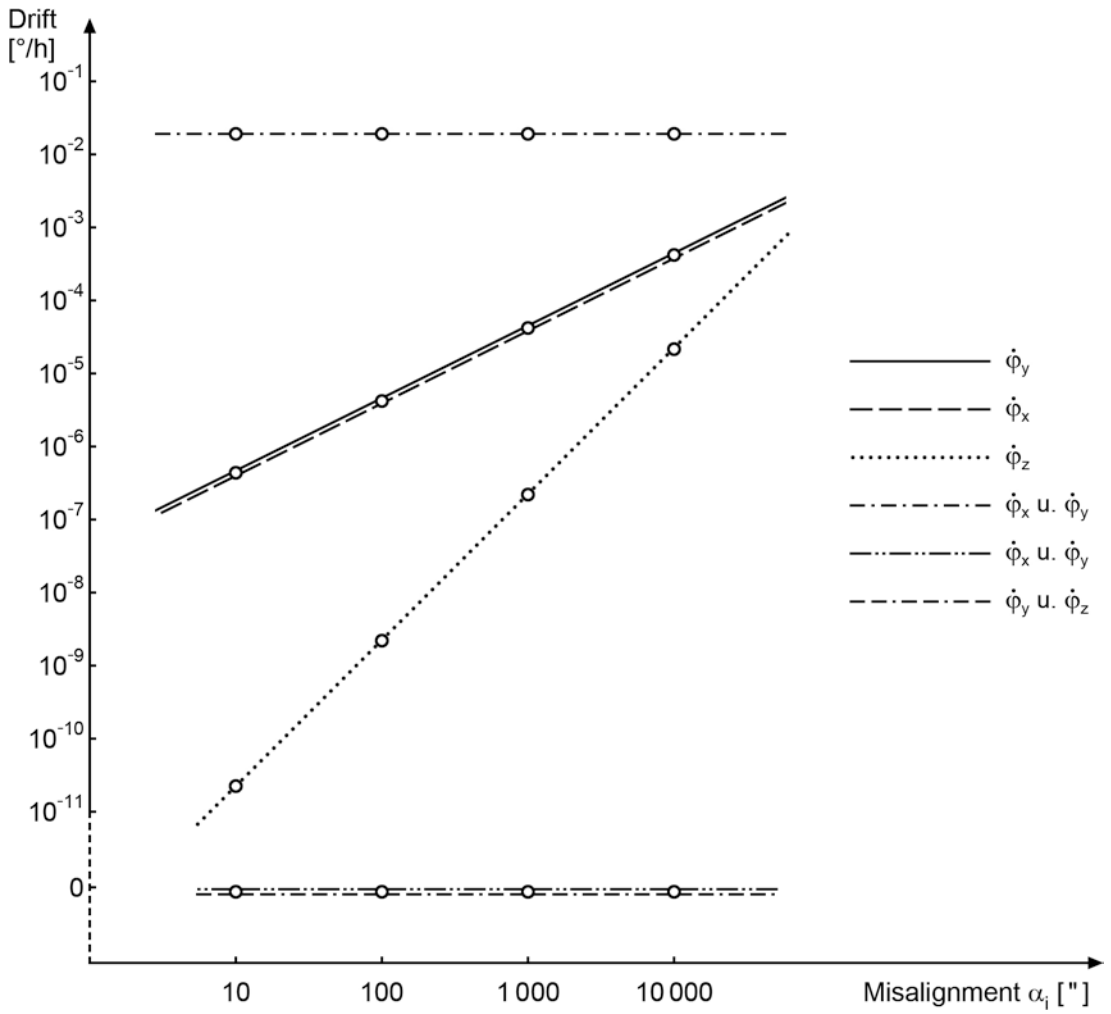

Picture 6: Drift due to anisoinertia and misalignment

Picture 6 shows the anisoinertia error computed with the $\Delta I = 150\,g \cdot cm^2$ as a function of rotation of all three axes of the sensor. A main part is resulting from the simultaneous input around spin and input axis. This leads to a constant drift independent of the misalignment of the sensor. The drift rates are very small and may be of no interest for practical problems. But this should be proved by real data.

4.3 Output axis acceleration

The model of output axis acceleration is found in term ⑧.

$$⑧ \quad -I_o \left(\alpha_y \cdot \ddot{\varphi}_x - \alpha_x \cdot \ddot{\varphi}_y + \ddot{\varphi}_z \right)$$

This error does not lead to a drift in the sense of the word, but to a time drift directly proportional to the rotational acceleration around the output axis. Error and drift due to output axis acceleration neglecting misalignments are shown in picture 7 and 8.

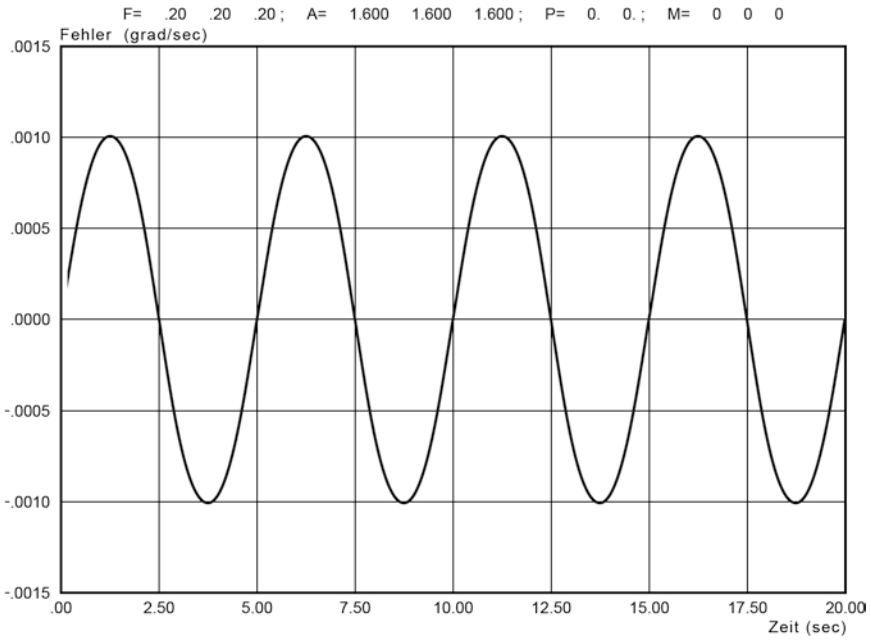

Picture 7: Output axis acceleration error

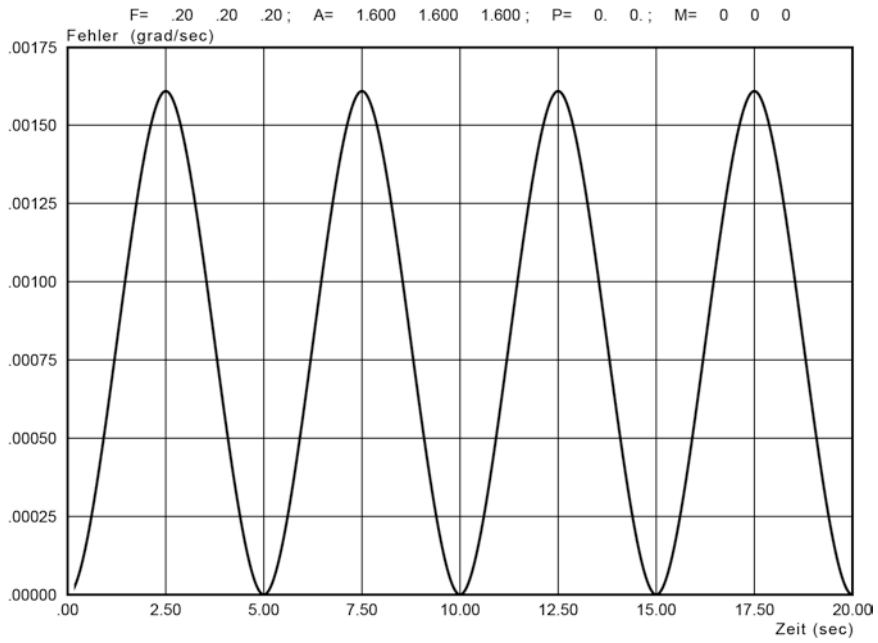

Picture 8: Output axis acceleration drift

So this error leads to a misorientation in inertial space that is proportional to the output axis acceleration. The significant response of this error type follows from the gyro dynamics. The magnitude is much smaller than that of the two other errors described in this paper.

5. Conclusion

The dynamic model of the single-degree-of-freedom gyro in practice will not be sufficient. The assumption of rigid bearings, rigid sensor axes and the neglect of linear acceleration effects on the gyro element lead to other error effects. The goal of this presentation was to show up the possibly large influence of neglected terms in the equation of motion. Based on this model the dynamic behaviour of accelerometers may be described, too. Geodetic post mission adjustment techniques are based on zero velocity update points. The information of spatial movement of IMS between the ZUPT-points is not introduced into the adjustment. But if this information will be applied to the adjustment, it could lead to longer time intervalls between ZUPT-points and to accuracy improvements.

6. Literature

/1/ Britting, K.: Inertial Navigation Systems Analysis. New York, John Wiley & Sons, 1971.

/2/ Pitman, R.: Inertial Guidance. University of California, Engineering and Physical Sciences Extension Series, New York, John Wiley & Sons, 1962.

/3/ Savet, P.: Gyroscopes: Theory and Design. New York, 1961.

/4/ Ziegler, IUTAM: Kreiselprobleme, Gyrodynamics. Symposium Celerina, 1962.

/5/ Klein, Sommerfeld: Die Theorie des Kreisels. Leipzig, 1897/1910.

/6/ Stieler, B., Winter, H.: Gyroscopic Instruments and their Application to Flight Testing. Agardograph, No. 160, Vol. 15, 1983.

/7/ v. Fabeck, W.: Kreiselgeräte. Würzburg, Vogel, 1980.

/8/ Baumann, H.: Fehleranalyse und Simulation eines Trägheitsnavigationssystems mit fahrzeugfesten Sensoren. Dissertation, Technische Universität Braunschweig, 1976.

/9/ Sauer, R., Szabo, I.: Mathematische Hilfsmittel des Ingenieurs, Teil I. Berlin, Springer, 1967.

/10/ Oppelt, W.: Kleines Handbuch technischer Regelvorgänge. Weinheim, Verlag Chemie GmbH, 1972.

/11/ Wiegner, S.: Fehleranalyse und Simulation eines Proportional-Wendekreisels für die Strapdown-Anwendung in einem Inertialnavigationssystem. Selbständige Geodätische Arbeit am Institut für Anwendungen der Geodäsie im Bauwesen, Stuttgart, 1985.

/12/ Vassiliou, A.: Processing of Unfiltered Inertial Data. The University of Calgary, March 1984.

/13/ Hannah, J.: The Development of Comprehensive Error Models and Network Adjustment Techniques for Inertial Systems. Ohio State University, Reports of the Department of Geodetic Science and Surveying, Report No. 330, 1982.

/14/ Schwarz, K.P. and Gonthier, M.: Adjustment Problems in Inertial Positioning. Proceedings of the International Symposium on Geodetic Networks and Computations of the IAG, Volume IV, 1982.

/15/ Wong, R.V.C.: A Kalman Filter-Smoother for an Inertial Survey System of a Local Level Type. The University of Calgary, Division of Surveying Engineering, Publication 20001, 1982.

/16/ Wetzig, V. and Zhuge, H.: Simulations of Strapdown-System Errors and Error Compensation Methods. Mitteilung der Deutschen Forschungs- und Versuchsanstalt für Luft- und Raumfahrt (DFVLR-Mitt. 84-22), 1984.

INERTIAL MEASUREMENTS FOR NATIONAL CONTROL

by

Cyril R. PENTON

Geodetic Survey of Canada
615 Booth Street
Ottawa, Ontario
CANADA
K1A OE9

ABSTRACT

The Canadian Geodetic Survey (CGS), a division of the Surveys and Mapping Branch, Department of Energy, Mines and Resources, acquired its first inertial system, a Litton Auto Surveyor System, in late 1975. For the past ten years, CGS has been using inertial equipment to establish some 8000 multi-purpose control stations in Canada. This control serves as secondary densification to the Canadian primary framework, as control for national mapping programs, and as control for cadastral, legal and a variety of other surveys. This paper reviews the resources and activities involved to the establishment of this control. In addition, problems related to the inclusion of these surveys into the new national datum are considered, and preliminary results are presented of tests of the new Litton DASH II system.

1. INTRODUCTION

The Canadian Geodetic Survey (CGS) has been actively involved in inertial surveying since the purchase of its first Litton Auto Surveyor System (TM) in late 1975. Eight full field seasons have been completed and a ninth campaign is underway. The details of these efforts have been well described in ***Carrière et al.*** (***1977***) and ***Webb and Penney*** (***1981***) and will not be repeated here.

The Inertial Survey System (ISS), as it is referred to at CGS, has been a difficult tool to master. The early promises of a "magic black box" and "the total solution to the geodetic problem" have not been realized. While the ISS has been a cost beneficial tool and has contributed significantly to the extension of national control in Canada, it has not fulfilled the expectations of this "space age technology". With very careful attention to the design and implementation of inertial projects, and with judicial analysis and quality control of data, the ISS has proven to be a provider of reliable control. That is, on traverses of 80 to 100 kilometres, positional repeatability and r.m.s. accuracy with respect to known values have both been demonstrated convincingly to be at the 30 centimetres level. This, of course, presupposes that reliable and consistent external control is employed, since the ISS is strictly an interpolator. There have repeatedly been suggestions of 10 centimetre positional accuracy achievable, but this has not been realized at CGS. Inertially determined elevations have been found to be somewhat better than positions, with r.m.s. accuracies in the 20 to 30 centimetre range routinely achieved. This superiority of vertical results is undoubtedly due to the use of the A1000 accelerometer in the vertical channel of the ISS, as compared to the less precise A200 accelerometers in the horizontal channels. All the systems used by CGS over the years have had this configuration. This decision was influenced by the primary reason for acquiring inertial technology; the mandate to provide fast, accurate, vertical control to support the national mapping program. The other geodetic information, namely the components of the deflection of the vertical and the gravity anomaly, have not been successfully measured in a production environment. We have been referring to the "potential" of the ISS to provide reliable estimates of the relative gravity vector, as a

by-product of the positional information, for some nine-years now. However, we have yet to produce a single ISS determined gravity station. Some limited research has been carried out at CGS to study the possibility of extracting gravity information from the huge mass of inertial data accumulated to date. Tests have shown that r.m.s. accuracies for anomalies determined from a truck-bourne system are at the one milligal level, while for the helicopter mode it is about 2 milligals. In both cases, the existence of systematic trends indicates some improvements may be possible. Recovery of deflection components as a by-product of positional data was first investigated by ***Greggerson and Carrière*** (***1976***) and later by ***Schwarz*** (***1978***). They concluded that repeatability of about one arc-second was possible, but that biases of up to two arc-seconds were noted in comparison to known values. ***Schwarz*** attributed this to an "over-shooting" of the kalman error prediction routines at gradient changes.

The ISS continues to be a complex piece of technology with a rather poor record of downtime due to system failures. This is mainly due to the fact that field maintenance is limited to isolation of faulty modules and replacement with spares. Very little actual repair can be carried out outside of the Litton plant. On the other side of the ledger, the inertial equipment has been flown for many thousands of hours in helicopters, and subjected to a variety of adverse vibrational and climatic conditions. Yet the end products represent a cost savings of 2 to 4 times the cost of establishing the same control by conventional means. A significant additional savings has resulted from the approximately five times production rate of the ISS over conventional means, assuming the same level of resource expenditures.

2. PRODUCTION WITH THE ISS

Approximately 50 ISS projects have been fielded since its beginnings in 1975. These projects range from a handful of stations to support research to several hundred station networks of multi-purpose control. Some 10,000 stations have been surveyed to the end of the 1984 field season with ISS, and an additional 1,302 are planned this current season. This includes the establishment of about 314 stations which will be contracted out to

private industry. Figure 1 shows the distribution of inertial surveys carried out by CGS in Canada. Surveys have been labelled as "area surveys" or "line surveys". Area surveys consist of North-South traverses of 80 to 120 km in length, with stations spaced at 10 km intervals. These traverses are 20 km apart, and are connected by East-West check traverses at about 40 km spacing. All traverses are double run (forward and back), with coordinate updates at the terminal points. Traverses which are to control subsequent traverses are quadruple run. The basic traverse control consists of primary triangulation or doppler satellite stations. The area survey is, therefore, a rigid and well controlled grid of fairly straight interconnecting traverses.

Line surveys consist of a number of individual traverses not laid out in a grid pattern, and not necessarily following a cardinal direction. However, each traverse will be at least doubly run, and will contain at least one checkpoint. This will be either a common station with a cross traverse or an additional intermediate control point.

Of the 10,000 stations surveyed to date, about 2,000 of these are unmarked sites intended primarily for vertical control for mapping. The Canadian National Geodetic Data Bank currently lists coordinate and related information for 8,181 monumented stations. Table 1 lists the distribution of these stations throughout the ten Canadian provinces and two territories and provides some information on their quality. Some clarification of this table is in order. The classifications are the result of an area adjustment and a subsequent consideration of the size of the semi-major axis of the 95% relative error ellipse, as per the 1978 Canadian specifications for classification of control surveys. The adjustment is carried out on the national datum - NAD27, using the Clarke 1866 ellipsoid. These are recognized to be some rather large distortions in this system, and the first-time connection of widely separated chains of triangulation by ISS has unearthed many of these problems. However, until the continental redefinition is carried out, ISS surveys will continue to be integrated into the national networks using a fully constrained adjustment - that is, considering the NAD27 coordinate values of the control as errorless and constraining the inertial surveys to these values. In an attempt to minimize the effect of these distortions, the

MAY '76 system was created. This is essentially a distortion free readjustment of the Canadian primary network on the NAD27 datum. Classification of ISS stations in the MAY '76 system has shown a marked improvement over the published classifications referred to in Table 1.

Prov./Terr.	Secondary Stas.	Lower Order Stas.	Other	Total
Newfoundland	-	-	-	-
Prince Ed. Is.	-	-	-	-
Nova Scotia	122	11	-	133
New Brunswick	68	4	-	73
Quebec	91	8	290	389
Ontario	313	9	-	322
Manitoba	480	21	220	721
Saskatchewan	2065	39	-	2104
Alberta	3330	158	804	4292
British Col.	3	1	-	4
North West T.	35	1	79	115
Yukon Terr.	-	-	28	28
Totals:	6508	252	1421	8181
	(80%)	(3%)	(17%)	

TABLE 1 Distribution of Monumented ISS Stations in Canada

The label "secondary stations" refers to stations classed as second- or third-order (about 60% are second-order). The label "lower order" refers to stations classed as fourth-order or unclassifiable. The latter implies a relative accuracy at the 95% confidence interval of less than 300 parts per million. It should be pointed out that the majority of these classifications involve ISS stations very close to existing primary stations. For example, an ISS station located 1 km from a first-order station would require an accuracy, relative to the primary station, of

better than 12 cm, at the one sigma level, to be classed as a fourth-order station. We have yet to achieve such accuracy in inertial positioning at the Canadian Geodetic Survey. The column labelled "other" represents stations which have not yet been classified, for one reason or another.

The term multi-purpose control has been coined to describe ISS surveys. As noted earlier, the primary reason for CGS to acquire and field inertial equipment was in support of the national mapping program - i.e. mapping control. However, a number of provincial survey agencies (notably Alberta, Saskatchewan, and Manitoba) have entered into cost-sharing programs with the federal Surveys and Mapping Branch (of which CGS is one division). The objective is to provide control at regular intervals to satisfy the province's requirements for secondary densification of the primary network. This densification falls under the provincial jurisdiction. The provincial support consists of station location, marker installation, site preparation and clearing, station description, and photo identification. In addition, the province will provide vertical control by spirit levelling. The federal contribution consists of the provision of equipment and personnel to execute the survey and the data processing, analysis, adjustment, classification and publication of final results. Additional control is provided where necessary, usually in the form of doppler satellite stations. Thus, the provinces bear the cost of station installation and the federal government bears the cost of measurement and computation. This arrangement has worked very well, and has resulted in a high density of reliable control, mainly in western Canada, which can serve a multitude of uses.

The reasons for the lack of inertial control in eastern Canada are largely related to the lower requirements for mapping control, the existence of adequate, conventional, secondary control, the absence of similar cost-sharing arrangements, and the terrain characteristics. The ISS has proven to be an effective tool in the prairie regions of Canada. Minimum site clearing requirements and the availability of an extensive road system allowing an economical placement of fuel for the ISS helicopter has resulted in maximum economy.

3. ISS DATA PROCESSING

The data collected over the past nine years has been processed and stored in a variety of ways. The original system software, designated AUTO 21, produced filtered and on-line, smoothed coordinates. However, the parameters used in the smoothing could not be recorded, nor could the corrections to eccentric points be included. Therefore, an off-line resmoothing, using the Litton smoothing algorithm, is not possible. This software was in use until the spring of 1978, when it was replaced with the AUTO 23 package. Similar to AUTO 21, this package has enhancements which allows the recording of all 79 parameters at each survey point, and allows direct input and application of eccentric or offset measurements in the field. Smoothing was no longer required as soon as a traverse was completed, but could be done at a more convenient time at the field headquarters. This software was used until the end of the 1984 season. Beginning in 1984, CGS began collecting data with the new Litton LASS DASH II system. This consists of basically the same hardware, with the exception of an improved computer and data recording system, and an enhanced software package, including off-line smoothing. Early this year, CGS took delivery of a DASH II system, as did the Mapping and Charting Establishment (MCE) of the Canadian Department of Defence. It is perhaps indicative of the peculiarities of inertial hardware that the MCE system has yet to operate properly, while the CGS system, after some initial problems, appears to be functioning, but with degraded performance.

Data processing is carried out in the field and in the office. In the field, processing is aimed at providing a quality analysis of each day's work so that unacceptable data can be quickly identified and traverses rerun while it is still relatively inexpensive to do so. Off-line smoothing with AUTO 23 was done on an HP9830A desktop computer. With the DASH II, an HP87 is used and data is transferred directly to magnetic tape in the field. In the office, the filtered data is run through program ISSDAT. This software allows correction of identified errors (wrong station ID's, incorrect update coordinates, etc.) and smoothing of the traverses using the Litton algorithm. Traverses are smoothed to either field entered update coordinates or to input table values. A number of attempts have been made over the years to find a better smoother. The

algorithm developed by Dr. K.P. Schwarz and others at the University of Calgary (***Schwarz, 1980***) has been extensively tested (***Penton, 1985***). However, improvements over the Litton smoother on relatively straight traverses are marginal, and it was not considered economical to revise the processing software. Some improvement was found on non-linear traverses, but since residual errors on these traverses after employing the Schwarz smoother are still significant, then the practice of running fairly straight line traverses will continue.

Traverses are individually smoothed with ISSDAT, and are than input to MEASNM and lately, ISSCHECK programs. These basically compare repeated observations of a station, and allow identification of problem traverses. The edited, smoothed traverses are input to the ISSPOS/GANET area adjustment. This adjustment procedure was first described by ***Kouba*** (***1977***) and has remained virtually unchanged. Program ISSPOS takes the smoothed traverses and forms position equations, along with an estimated covariance matrix, for input to the least squares adjustment program, GANET. The first step is to perform a free adjustment for the inertially observed positions. This is used to analyse the internal repeatability and consistency of the data. Problem traverses are identified through a residual analysis. The free adjustment may be iterated a number of times with revised or edited data. It is noteworthy that the adjustment variance factor usually varies between 1 and 2, and consistently fails the F test. However, since there have never been satisfactory reasons to alter the relative weighting scheme, which results from the ISSPOS program, this large variance factor is not considered a problem. Once the free adjustment results are satisfactory, a constrained adjustment is run using coordinates from the MAY '76 system. Existing control values are fixed. The adjusted ISS values are classified using the error ellipse output. Again, the variance factor typically ranges from 1 to 3. For this reason, the error ellipses are appropriately scaled to reflect the actual estimate of the variance factor. In this way, a conservative estimate of the classifications is made. A second constrained adjustment is run, this time using published NAD27 coordinates for the existing control. Classifications computed on the MAY '76 system are downgraded, based on a distortion analysis of the NAD27 based adjustment.

4. CONTINENTAL READJUSTMENT AND ISS SURVEYS

A redefinition of the North American datum and a subsequent continental readjustment will take place at the end of this calendar year. In Canada, this will result in a new set of adjusted coordinates and associated covariance matrix for a framework of stations. The new datum is designated NAD83. The framework will consist of about 7,000 primary triangulation stations and about 1,000 doppler satellite stations augmented by some secondary surveys. However, the bulk of the secondary and lower order surveys will be integrated into NAD83 after the readjustment. Guidelines have been proposed for the integration process, and are described in ***Steeves and Penton*** (***1985***). A scenario for the ongoing maintenance of the geodetic network in the post-readjustment period is detailed in ***Chamberlain et al.*** (***1985***).

Integration of the ISS surveys continues to be a problem. Much work has gone into examining the adjustment alternatives to optimize the contribution of ISS to NAD83. A recently concluded research contract with the University of Calgary (***Schwarz, 1985***) recommended the approach of an adjustment of filtered data. This approach was found to be somewhat better than the CGS approach of smoothing the traverses individually, followed by a network adjustment. However, the decision as to be route which will be followed was based strictly on the problem of limited resources. Consequently, the smoothed traverses will be input to program ISSPOS, and position difference equations and a relative covariance matrix will be generated. This will be fed into the new adjustment program GHOST, which has the capability to handle the position difference equations. It will also allow auxiliary parameters in the form of a scale and a rotation for each traverse to be estimated. This should take care of any problem of datum change - namely position differences based on MAY '76 coordinates adjusted on the NAD83 datum. A Helmert blocking strategy will be used, and the weighted station adjustment approach (***Steeves and Penton, 1985***) will be employed. This will permit some movement in the framework values, and publication of NAD83 values will await the results of this integration. It is recognized that this approach is not the ideal, from the theoretical point of view, but we feel it is the most effective compromise between the ideal and reality.

5. QUALITY OF THE ISS NETWORKS

The feedback from the many users of the ISS networks has generally been very good. Most of the few problems which have been reported have been the result of the misidentification of stations. This is not surprising, considering the practice of establishing the stations one year and measuring them the next year.

A recent example of an external check on the quality of inertial surveys is the Gimli, Manitoba project. This project was executed at the request of the province of Manitoba. It differs from the usual CGS ISS network in that stations were placed every 10 kilometres North-South and East-West. Control for the ISS included 1959 and 1960 primary triangulation stations in the southern edge, doppler stations established by two different agencies on three different projects, a second-order Aerodist station, and previously adjusted ISS stations. The new ISS stations were constrained to these existing control points. A number of these control stations were recently observed using the GPS MACROMETER. Figure 2 shows the differences between the conventional/ISS coordinates and the GPS coordinates. The latter resulted from a minimally constrained adjustment of the MACROMETER data, holding fixed the MAY '76 coordinates of the most easterly triangulation station shown in Figure 2. A number of points about this figure are of interest. There are obvious datum problems between the conventional and GPS coordinates, with a large inconsistency in any scale/rotation relationship evident in the southwest corner. The large discrepancy between the most westerly doppler and triangulation stations is indicative of the type of problem that evolves when the ISS is constrained. The four adjacent ISS stations in the north central part of the network which were also observed by MACROMETER show a surprisingly good agreement with the GPS coordinates. That is, when we consider position differences resulting from each method. Table 2 compares the ISS and "shifted" GPS coordinates for these four stations.

Station	ISS Positions	GPS Positions	Diff. (m)
82R338	50°46'22".890	22".890	-
	97°27'41".155	41".155	-
82R339	50°41'02".350	02".351	-0.03
	97°28'23".380	23".389	-0.18
82R352	50°41'01".441	01".445	-0.12
	97°36'43".990	43".975	0.29
82R353	50°46'45".778	45".784	-0.18
	97°36'07".917	07".905	0.24

NOTE: The GPS positions were shifted by an amount necessary to make the GPS and ISS values of 82R338 identical.

TABLE 2 Comparison of ISS and GPS Positions

An in-depth analysis of the quality of the ISS positions can be found in *Schwarz* (*1985*).

6. FIRST RESULTS WITH THE LITTON DASH-II

The new Litton system acquired in 1984 was extensively tested in May of this year on the Victoriaville test net. Figure 3 is a sketch of this network. The tests were a joint effort of the province of Quebec, MCE and CGS. The province was interested in results on short lines and their usefulness as control for 1:20,000 mapping. MCE was interested in overall system performance and the deterioration of results over very irregular traverses. CGS war primarily interested in an overall evaluation, as well

as looking at results on L-shaped lines, and on long lines with coordinate updates performed at the initial point only. Full details of these tests will be reported at the Third International Symposium on Inertial Technology for Geodesy and Surveying, to be held at Banff, Canada, September, 1985.

The results of the tests were somewhat disappointing, and indicated a longitude bias in the equipment. This problem is more pronounced on lines in the 80 to 100 km range. Figures 4 and 5 present the results of the 10 runs over the fairly straight, 85 kilometre line between stations 7458 and 77KO545. The latitude residuals show some problems on the south-going run, but the mean smoothed data compares favourably with the known values. Figure 5, however, shows a very large longitude bias, with residuals up to 1.8 metres - a far cry from the expected level of less than 50 centimetres. Both forward and reverse runs show this problem, with residuals more pronounced on the southward heading forward run. This problem was also noted in production work, and a decision was made to limit North-South traverses to a maximum of about 60 kilometres in length for the remainder of this field season. The East-West traverses do not appear to be affected.

7. INERTIAL SURVEYING PROSPECTS AT CGS

As was noted earlier, the ISS is a difficult tool to master. The new system has yet to prove to be an improvement over the previous version. In spite of the many problems, the inertial equipment continues to be economically advantageous compared to conventional tellurometer/transit methods or doppler satellite methods. However, the advent of the precise positioning capabilities of GPS equipment, coupled with high production rates and low operating costs will result in the end of inertial positioning activities at GPS in another 3 or 4 years. It is seen that ISS will not be able to compete effectively with GPS in this area. However, the potential of the ISS to provide reliable estimates of the gravity vector is still of very high interest at CGS. To this end, we are eagerly awaiting the development of the new RGSS-7 gravity software package. This package is being developed by Litton Industries for the U.S. Army Engineering Topographic Laboratory and CGS hopes to have access

to this software. Gravity surveys, assuming this software proves to provide reliable and sufficiently accurate information, are considered to be the future of inertial surveying efforts at CGS.

8. REFERENCES

CARRIÈRE, R.J., KOUBA, J., and PENNEY, R.C.: ***Experiences with the Inertial Survey System at Geodetic Survey of Canada.*** Proceedings of the 1st International Symposium on Inertial Technology for Surveying and Geodesy, Ottawa, Canada, October 12-14, pp. 146-161, 1977

CHAMBERLAIN, C.A., STEEVES, R.R., and PENTON, C.R.: ***A Scenario or the Maintenance of the Canadian Geodetic Network.*** To appear in the autumn 1985 edition of the Canadian Surveyor, 1985

GREGGERSON, L.T., and CARRIÈRE, R.J.: ***Inertial Surveying System Experiments in Canada.*** Presented to the International Association of Geodesy at the XVI General Meeting, Grenoble, France, 1975

KOUBA, J.: Geodetic Adjustment of Inertial Surveys. Proceedings of the 1st International Symposium on Inertial Technology for Surveying and Geodesy, Ottawa, Canada, October 12-14, pp. 162-187, 1977

PENTON, C.R.: ***Evaluation of Smoothing Routines or the Inertial Survey System.*** Geodetic Survey of Canada Technical Report No. 4, July, 1985

SCHWARZ, K.P.: ***Accuracy of Vertical Deflection Determination by Present-Day Inertial Instrumentation.*** Presented at the Ninth Geodesy/Solid Earth and Ocean Physics Research Conference, Columbus, Ohio, October 2-5, 1978

SCHWARZ, K.P.: ***Analysis of Inertial Survey Systems.*** Final Report, Contract 07SU.23244-9-4323 between the University of Calgary and the Canadian Geodetic Survey, May, 1982

SCHWARZ, K.P.: ***Comparison of Adjustment and Smoothing Methods for Inertial Networks.*** Final revised report, Contract 01SU.23244-4380, Geodetic Survey Contractors Report Series 85-002, April, 1985

STEEVES, R.R., and PENTON, C.R.: ***Guidelines for the Integration of Geodetic Networks in Canada.*** To appear in the autumn 1985 edition of The Canadian Surveyor.

WEBB, J.D., and PENNEY, R.C.: ***Six Years of Inertial Surveying at Geodetic Survey of Canada.*** Proceedings of the 2nd International Symposium on Inertial Technology for Surveying and Geodesy, Banff, Canada, June 1-5, pp. 325-341, 1981

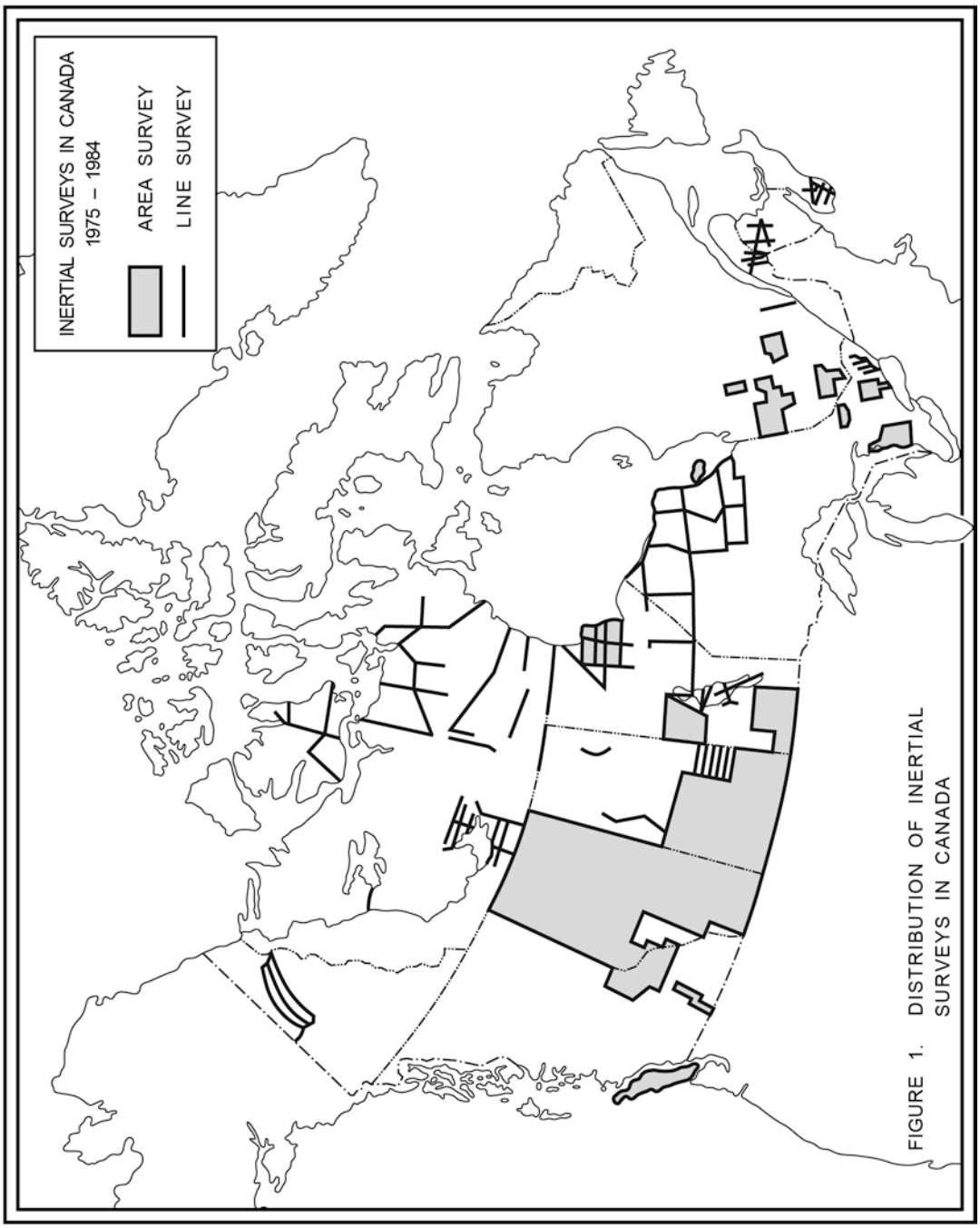

FIGURE 1. DISTRIBUTION OF INERTIAL SURVEYS IN CANADA

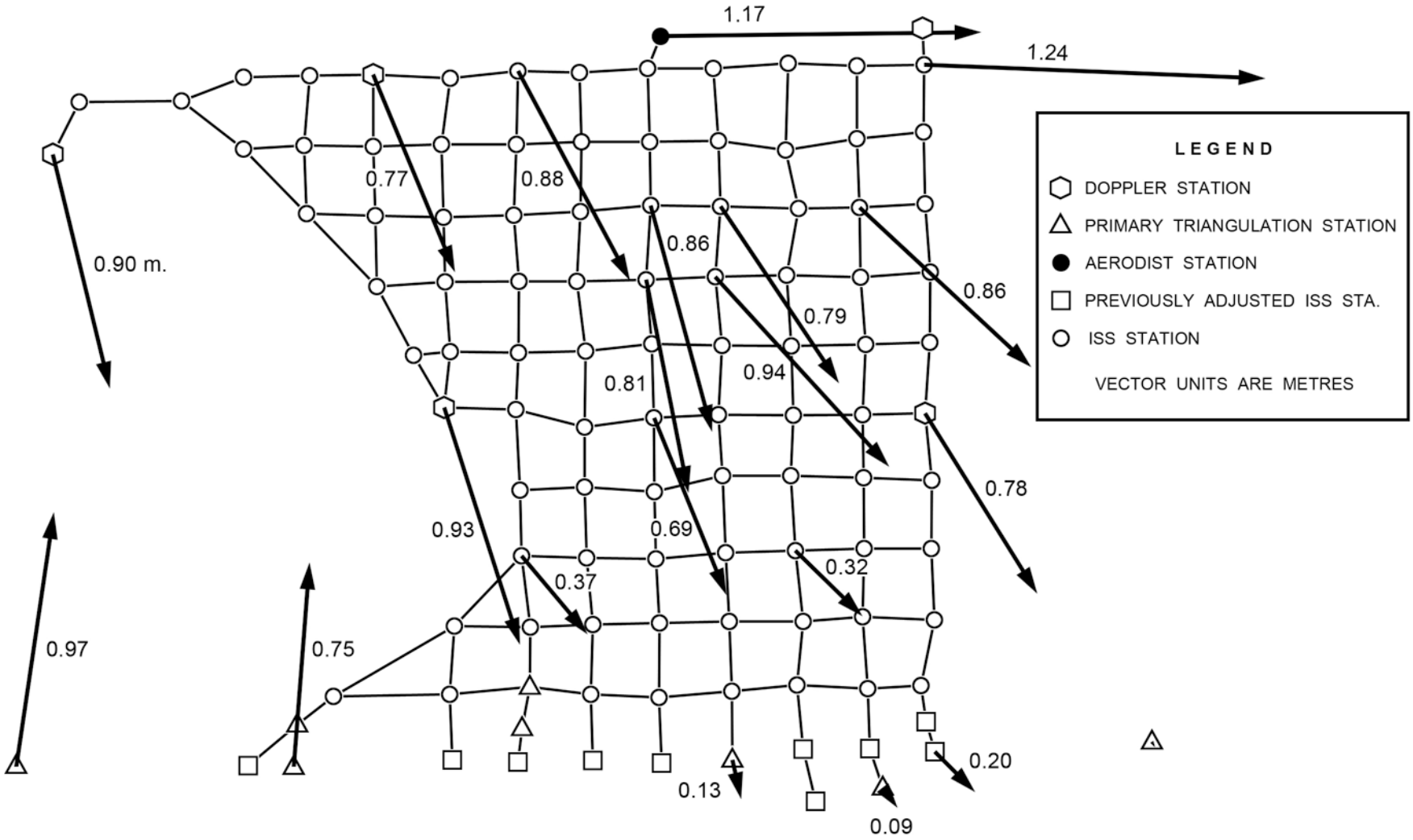

FIGURE 2: GPS TO CONVENTIONAL , POSITION DIFFERENCES

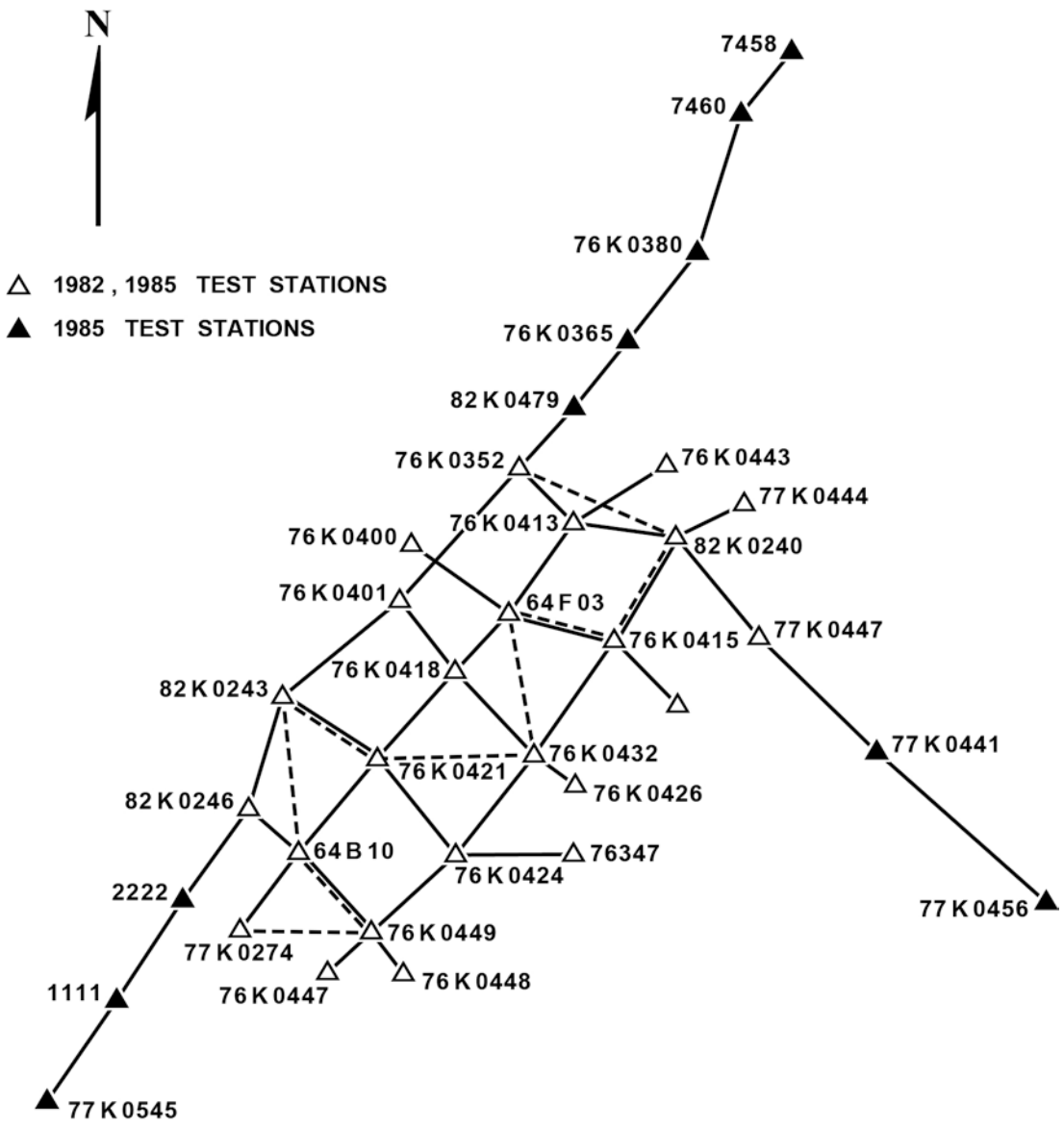

FIGURE 3. VICTORIAVILLE INERTIAL TEST NET

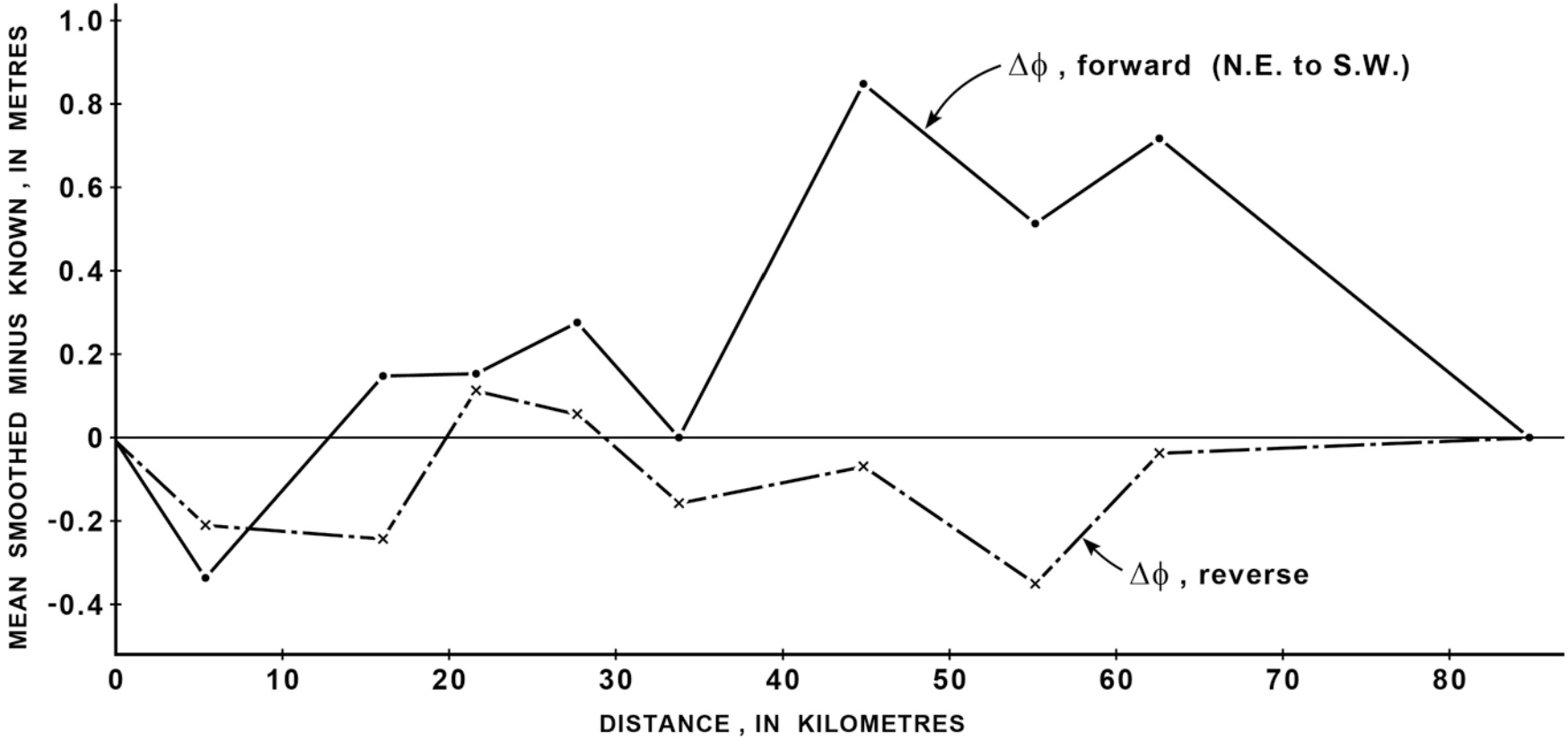

FIGURE 4. RESIDUAL LATITUDE ERRORS AFTER SMOOTHING

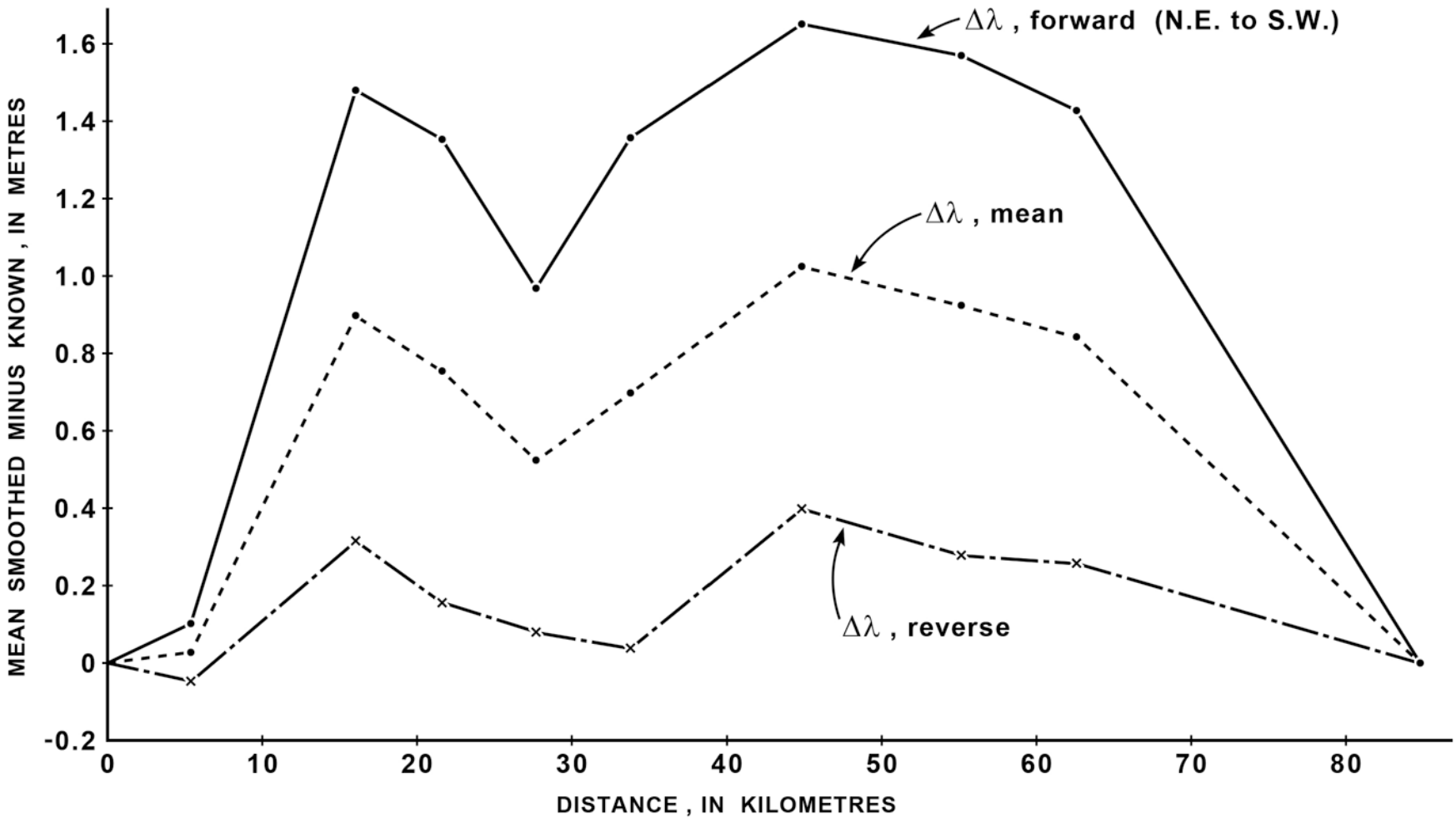

FIGURE 5. RESIDUAL LONGITUDE ERRORS AFTER SMOOTHING

INERTIAL SURVEY PLATFORMS AND THEIR GEODETIC RELEVANT COORDINATE SYSTEMS

by

Albert SCHÖDLBAUER

Universität der Bundeswehr München
Werner-Heisenberg-Weg 39
D-8014 Neubiberg
Bundesrepublik Deutschland

ABSTRACT

Three different inertial platform systems are of interest for geodetic application: local-level, north-orientated systems, space stable systems and strap down systems. The systems can be distinguished by the specific orientation of the accelerometer triads and the corresponding coordinate systems.

This paper treats the transformations being necessary to convert measured acceleration vectors into geodetic coordinates.

ZUSAMMENFASSUNG

Ellipsoidnormal-nordorientierte, raumorientierte und fahrzeugorientierte Trägheitsplattformen unterscheiden sich durch die spezifische Führung der Beschleunigungsmesser und der ihnen zugeordneten Koordinatensysteme.

Im folgenden werden die Transformationen dargelegt, die in den einzelnen Systemen zur Überführung gemessener Beschleunigungsvektoren in räumliche ellipsoidische Koordinaten notwendig sind.

1. INTRODUCTION

Inertial navigation and survey systems are devices that implement Newton's laws of motion to solve geodetic point positioning problems. The fundamental formula of the second law

$$\underline{f}_I = m \cdot \underline{a}_I \tag{1}$$

describes the relationship between an acceleration $\underline{a}_I$, a mass element m and a force $\underline{f}_I$ acting upon m. (The change of motion is proportional to the motive force impressed, and is made in the direction of the straight line in which that force is impressed.) This law enables us to determine accelerations by measuring forces. Acceleration vectors $\underline{a}_I$ continuously observed along a path yield the instantaneous velocity vector $\underline{v}_I$

$$\underline{v}_I = \int_{t_0}^{t} \underline{a}_I \cdot dt \tag{2}$$

and the instantaneous position vector $\underline{x}_I$

$$\underline{x}_I = \int_{t_0}^{t} \underline{v}_I \cdot dt \tag{3}$$

by integration of $\underline{a}_I$ resp. $\underline{v}_I$ from time t_0 to time t.

The force vector $\underline{f}_I$ can be measured in any Cartesian coordinate system with three dynamometers mounted perpendicularly on a platform and, taking into account the reacting mass m, it can be transferred into an acceleration vector $\underline{a}_I$ of the same direction. Thus, dynamometers are accelerometers as well.

Reference systems underlying (1) - (3) have to be free from inertial forces. That means they are considered to be in a straight and uniform motion and not to be uninfluenced by gravitational forces ("inertial systems"). This is a presupposition sufficiently approximated for a coordinate system which has its origin in the center of a reference ellipsoid and which is not participating in the rotation of the earth (e.g. the right ascension system whose z-axis is parallel to the earth's spin axis, whereas the x-axis is defined by the direction to the vernal point). Coordinate systems, however, which are either tied to the surface of the rotating earth or are moving at a platform in its vicinity ("platform coordinate systems") are subject to acceleration of the reference system itself and are, moreover, influenced

by gravitational forces generated by the earth with respect to any masses in its neighbourhood. Thus, forces $\underline{f}_a$ caused by accelerations $\underline{a}$ of such reference systems relative to the surface of the earth and, therefore, relative to a reference ellipsoid are superposed by forces $\underline{f}_s + \underline{f}_g$ (ficticious forces plus gravitational force) arising from this configuration due to kinematic laws of transformation and due to the law of gravitation (see chapter 3).

Concluding we can state that the force $\underline{f}_I$ effective in an inertial reference system, is given by the sum of the partial forces $\underline{f}_a$, $\underline{f}$, $\underline{f}_g$

$$\underline{f}_I = \underline{f}_a + \underline{f}_s + \underline{f}_g \tag{4}$$

The corresponding acceleration vectors ((4)/m) read

$$\underline{a}_I = \underline{a} + \underline{s} + \underline{g} \tag{5}$$

By measurement we get access to the resulting force $\underline{f}_I$ or the resulting acceleration $\underline{a}_I$ respectively. However, what we need for point positioning purposes is the acceleration $\underline{a}$ of the platform coordinate system relative to an earth fixed (geodetic) coordinate system. To obtain this vector by means of (5), we have to provide the ficticious acceleration $\underline{s}$ and the gravitational acceleration $\underline{g}$. This can easily be done with $\underline{s}$ as it proves to be a function $\underline{a}$. However, as far as $\underline{g}$ is concerned, we have generally to compromise ourselves in providing modelled values, e.g. by means of a normal-gravity formula.

2. REFERENCE SYSTEMS OF INERTIAL NAVIGATION AND INERTIAL LAND SURVEY METHODS

As stated before, if accelerations are to be measured in space three accelerometers have to be applied. The most simple construction in doing so is to mount the accelerometers perpendicularly to each other on a platform. The axes of the accelerometers define a platform-related coordinate system. This system follows all translatoric movements of the platform. Depending on the intended alignment of the platform we distinguish

- ellipsoid-normal, north-orientated
- space stable and
- strap down

platform systems.

Essential system components of all systems are gyroscopes which control the orientation of the platform with respect to an inertial reference frame.

Ellipsoid-normal, north-orientated platforms and the related coordinate systems $\underline{x} = (x,y,h)^T$ are kept aligned in a way that the h-axis always points into the direction of the normal and the x-axis into the direction of the meridian of the reference ellipsoid. To maintain this orientation in spite of the rotation of the earth and of the movements of the platform on the earth the platform (and the set of gyroscopes) have to be torqued continuously; see figure 1.

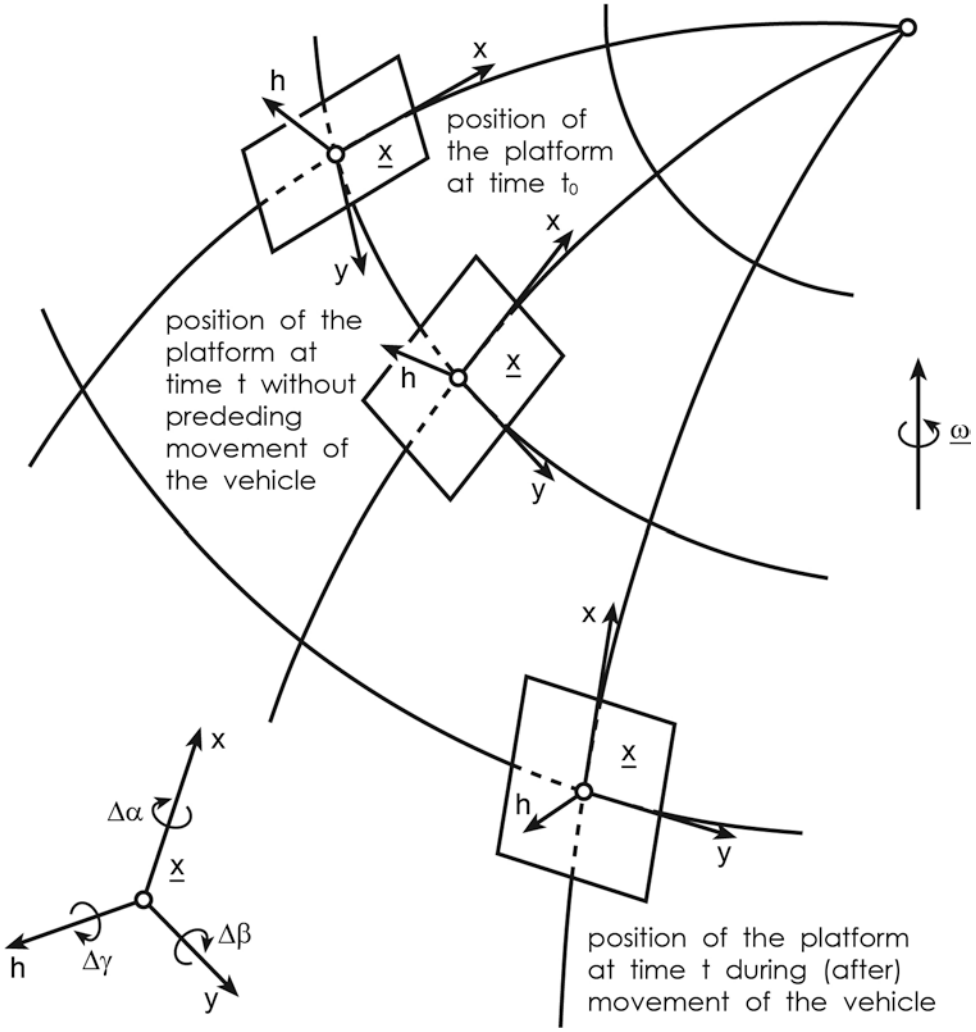

Figure 1: Orientation of an ellipsoid-normal, north-orientated inertial platform

Space stable platforms and the related coordinate systems $\underline{x}^* = (x^*, y^*, z^*)^T$ remain in an initially aligned orientation relative to the inertial space. The rotation of the earth and the platform movements do not disturb this orientation; see figure 2.

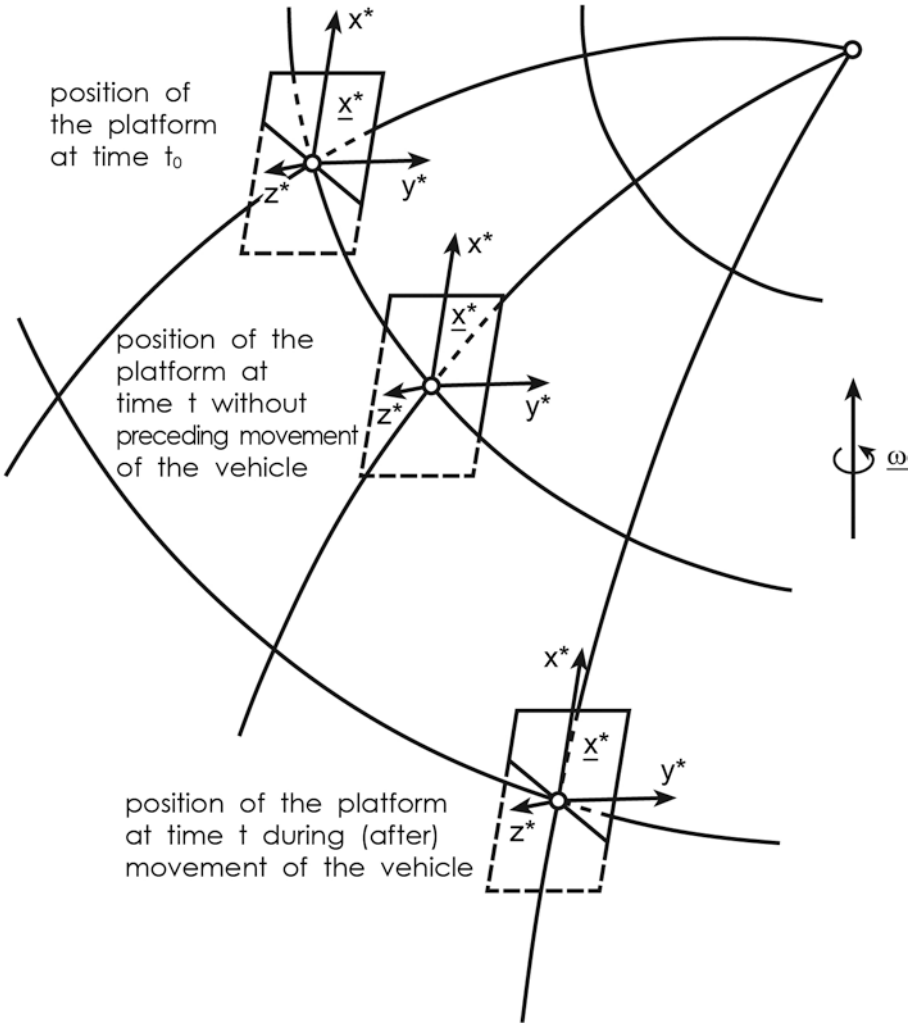

Figure 2: Orientation of space stable platforms

Strap down platforms and the related coordinate systems $\underline{x}^{\sim} = (x^{\sim}, y^{\sim}, z^{\sim})^T$ are taking over their orientation from the carrier (vehicle) in which the platform is installed; see figure 3. The Instantaneous orientation relative to the inertial space (and to the set of gyros) has to be monitored by angular sensors.

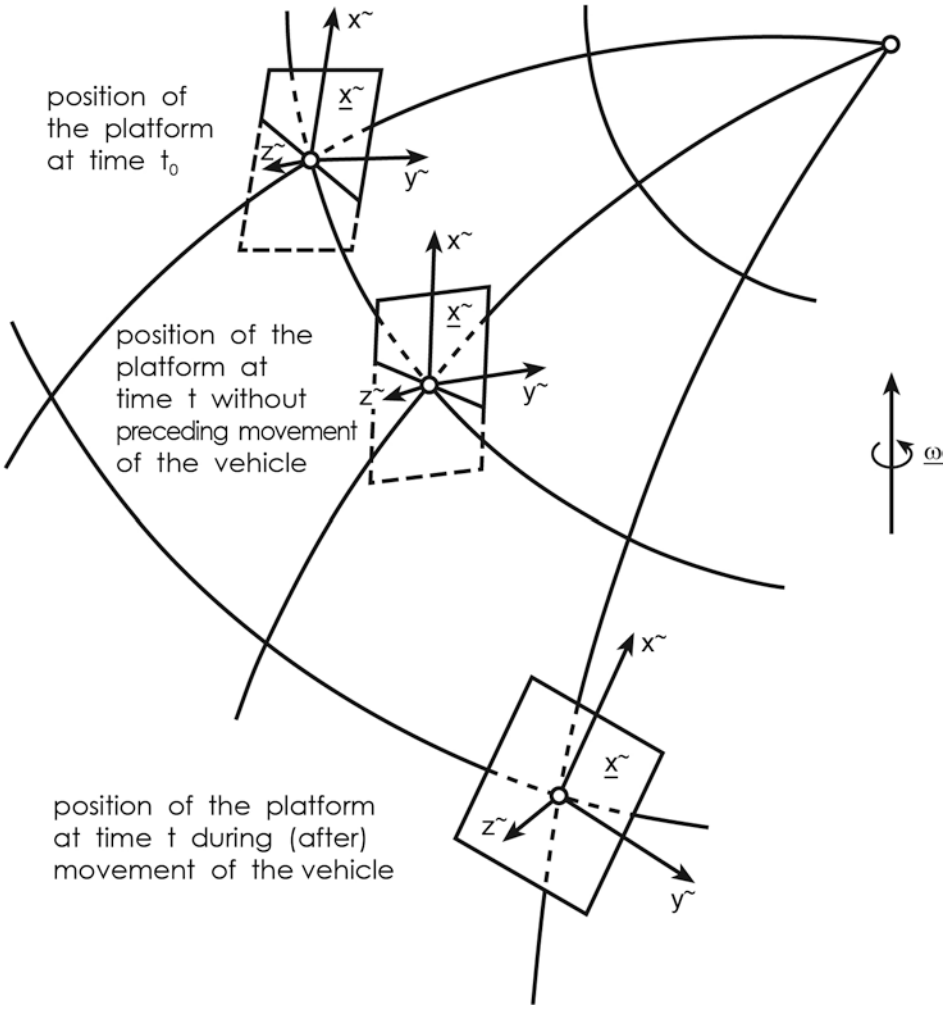

Figure 3: Orientation of strap down platforms

See chapter 4 for more details.

3. THE ACCELERATION VECTOR AND ITS COMPONENTS IN A PLATFORM COORDINATE SYSTEM

Let us now examine the acceleration vector (5) some more detailed and with regard to its effective kinematic elements:

$$\underline{a}_I = \ddot{\underline{x}} + 2\cdot\underline{\rho}*\dot{\underline{x}} + \dot{\underline{\rho}}*\underline{x} + \underline{\rho}*\left(\underline{\rho}*\underline{x}\right) + \underline{k} \qquad (6)$$

(c.f. RAVEN, 1962, p. 22-5; BRITTING, 1979, p. 63; SCHRÖPL, 1979, p. 219; ADAM, 1979, p. 29; HEITZ, 1980, p. 37; GRAFAREND, 1981, p. 39).

In this equation is denoting

$\underline{x}$	=	position vector from the origin of the inertial system to the origin of the applied platform reference system (considering the limited accuracy of inertial platforms this vector can be substituted by a vector which has its origin in the center of the used reference ellipsoid)
$\dot{\underline{x}} = d\underline{x}/dt$	=	derivative of the position vector with respect to time
$\ddot{\underline{x}} = d\dot{\underline{x}}/dt$	=	derivative of the velocity vector with respect to time
$\underline{\rho}$	=	angular velocity of the origin of the platform system with regard to an inertial reference system
$\dot{\underline{\rho}} = d\underline{\rho}/dt$	=	angular acceleration of the origin of the platform system with regard to an inertial reference system
$\underline{k}$	=	gravitational acceleration (without centrifugal acceleration)
$2 \cdot \underline{\rho} * \dot{\underline{x}} = \underline{c}$	=	Coriolis acceleration
$\dot{\underline{\rho}} * \underline{x} = \underline{t}$	=	tangential acceleration
$\underline{\rho} * (\underline{\rho} * \underline{x}) = z$	=	centrifugal acceleration.

Among all the platform coordinate systems which are suitable as reference systems for inertial navigation and point positioning methods (see chapter 2 and 4), the ellipsoid-normal, north-orientated system $\underline{x} = (x,y,h)^T$ plays a central part because of the close geometric relation between this system on the one hand and current geodetic coordinate systems, in particular the system of ellipsoidal geodetic (geographic) coordinates and heights (φ,λ,h), on the other hand. Introducing coordinate differentials we have

$$d\varphi = \frac{1}{M+h} \cdot dx \tag{7}$$

$$d\lambda = \frac{1}{(N+h) \cdot \cos\varphi} \cdot dy \tag{8}$$

$$dh = dh \ , \tag{9}$$

where

φ = geodetic (geographic) latitude)
λ = geodetic (geographic) longitude) relating to a reference ellipsoid
h = ellipsoidal height) (c, e'^2)

$M = c \cdot (1 + e'^2 \cdot \cos^2\varphi)^{-3/2}$ = meridian radius of curvature) of the reference ellipsoid.

$N = c \cdot (1 + e'^2 \cdot \cos^2\varphi)^{-1/2}$ = prime vertical radius of curvature) of the reference ellipsoid.

$R = c \cdot (1 + e'^2 \cdot \cos^2\varphi)^{-1}$ = Gaussian radius of curvature) of the reference ellipsoid.

c = polar radius of curvature) of the ellipsoid.

e'^2 = "second" eccentricity) of the ellipsoid.

Using a restricted compressed formulation by quoting spherical terms only - c.f. the ellipsoidal developments e.g. in ADAMS (1979, p. 33-37) - the vectors in (6) can be described in the ellipsoid-normal, north-orientated coordinate system as follows:

$$\underline{x} = \begin{bmatrix} 0 \\ 0 \\ R+h \end{bmatrix} \tag{10}$$

$$\dot{\underline{x}} = \begin{bmatrix} 0 \\ 0 \\ \dot{h} \end{bmatrix} = \begin{bmatrix} 0 \\ 0 \\ v_h \end{bmatrix} \tag{11}$$

$$\ddot{\underline{x}} = \begin{bmatrix} 0 \\ 0 \\ \ddot{h} \end{bmatrix} = \begin{bmatrix} 0 \\ 0 \\ \dot{v}_h \end{bmatrix} = \begin{bmatrix} 0 \\ 0 \\ a_h \end{bmatrix} \tag{12}$$

$$\underline{v} = \begin{bmatrix} v_x \\ v_y \\ v_h \end{bmatrix} = \begin{bmatrix} (R+h) \cdot \dot{\varphi} \\ (R+h) \cdot \dot{\lambda} \cdot \cos\varphi \\ \dot{h} \end{bmatrix} \tag{13}$$

$$\dot{\underline{v}} = \underline{a} = \begin{bmatrix} a_x \\ a_y \\ a_h \end{bmatrix} = \begin{bmatrix} (R+h)\cdot\ddot{\varphi} \\ (R+h)\cdot\ddot{\lambda}\cdot\cos\varphi \\ \ddot{h} \end{bmatrix} + \begin{bmatrix} \dot{\varphi}\cdot\dot{h} \\ \dot{\lambda}\cdot\dot{h}\cdot\cos\varphi - (R+h)\cdot\dot{\varphi}\cdot\dot{h}\cdot\sin\varphi \\ 0 \end{bmatrix} =$$

$$= \begin{bmatrix} (R+h)\cdot\ddot{\varphi} \\ (R+h)\cdot\ddot{\lambda}\cdot\cos\varphi \\ \ddot{h} \end{bmatrix} + \begin{bmatrix} \frac{v_x\cdot v_h}{R+h} \\ \frac{v_y\cdot v_h}{R+h} - \frac{v_x\cdot v_y}{R+h}\cdot\tan\varphi \\ 0 \end{bmatrix} \qquad (14)$$

$$\underline{\rho} = \begin{bmatrix} -(\omega+\dot{\lambda})\cdot\cos\varphi \\ \dot{\varphi} \\ -(\omega+\dot{\lambda})\cdot\sin\varphi \end{bmatrix} \qquad (15)$$

$$\dot{\underline{\rho}} = \begin{bmatrix} -\ddot{\lambda}\cdot\cos\varphi + (\omega+\dot{\lambda})\cdot\dot{\varphi}\cdot\sin\varphi \\ \ddot{\varphi} \\ -\ddot{\lambda}\cdot\sin\varphi + (\omega+\dot{\lambda})\cdot\dot{\varphi}\cdot\cos\varphi \end{bmatrix} \qquad (16)$$

$$\underline{k} = \begin{bmatrix} k_x \\ k_y \\ k_h \end{bmatrix} \qquad (17)$$

$$\underline{c} = 2\cdot\underline{\rho}*\dot{\underline{x}} = \begin{bmatrix} 2\cdot\dot{\varphi}\cdot\dot{h} \\ 2\cdot(\omega+\dot{\lambda})\cdot\dot{h}\cdot\cos\varphi \\ 0 \end{bmatrix} = \begin{bmatrix} \frac{2\cdot v_x\cdot v_h}{R+h} \\ 2\cdot\left(\omega+\frac{v_y}{(R+h)\cdot\cos\varphi}\right)\cdot v_h\cdot\cos\varphi \\ 0 \end{bmatrix} \qquad (18)$$

$$\underline{t} = \dot{\underline{\rho}} * \underline{x} = (R+h) \cdot \begin{bmatrix} \ddot{\varphi} \\ \ddot{\lambda} \cdot \cos\varphi - (\omega+\dot{\lambda}) \cdot \dot{\varphi} \cdot \sin\varphi \\ 0 \end{bmatrix} =$$

$$= \begin{bmatrix} a_x \\ a_y \\ 0 \end{bmatrix} - \begin{bmatrix} \frac{v_x \cdot v_h}{R+h} \\ \frac{v_y \cdot v_h}{R+h} + \left(\omega + \frac{v_y}{(R+h)\cdot\cos\varphi}\right) \cdot v_x \cdot \sin\varphi \\ 0 \end{bmatrix} \qquad (19)$$

(after substitution of (14)

$$\underline{z} = \rho * (\rho * \underline{x}) = (R+h) \cdot \begin{bmatrix} (\omega+\dot{\lambda})^2 \cdot \cos\varphi \cdot \sin\varphi \\ -(\omega+\dot{\lambda}) \cdot \dot{\varphi} \cdot \sin\varphi \\ -(\omega+\dot{\lambda})^2 \cdot \cos^2\varphi - \dot{\varphi}^2 \end{bmatrix} =$$

$$= \begin{bmatrix} (R+h) \cdot \omega^2 \cdot \cos\varphi \cdot \sin\varphi \\ 0 \\ -(R+h) \cdot \omega^2 \cdot \cos^2\varphi \end{bmatrix} + \begin{bmatrix} (R+h) \cdot (2\cdot\omega\cdot\dot{\lambda} + \dot{\lambda}^2) \cdot \cos\varphi \cdot \sin\varphi \\ -(R+h) \cdot (\omega+\dot{\lambda}) \cdot \dot{\varphi} \cdot \sin\varphi \\ -(R+h) \cdot \left((2\cdot\omega\cdot\dot{\lambda} + \dot{\lambda}^2) \cdot \cos^2\varphi + \dot{\varphi}^2\right) \end{bmatrix} =$$

$$= \begin{bmatrix} (R+h) \cdot \omega^2 \cdot \cos\varphi \cdot \sin\varphi \\ 0 \\ -(R+h) \cdot \omega^2 \cdot \cos^2\varphi \end{bmatrix} + \begin{bmatrix} 2\cdot\omega \cdot v_y \cdot \sin\varphi + \frac{v_y^2}{R+h} \cdot \tan\varphi \\ -\omega \cdot v_x \cdot \sin\varphi - \frac{v_x \cdot v_y}{R+h} \cdot \tan\varphi \\ -2 \cdot \omega \cdot v_y \cdot \cos\varphi - \frac{v_x^2}{R+h} - \frac{v_y^2}{R+h} \end{bmatrix} \qquad (20)$$

where ω is the angular velocity of the earth.

The transition from (6) to (5) is found by gathering

- the elements of the vector $\underline{a} = (a_x, a_y, a_h)^T$ from (12) and (19)

$$\underline{a} = \begin{bmatrix} 0 \\ 0 \\ a_h \end{bmatrix} + \begin{bmatrix} a_x \\ a_y \\ 0 \end{bmatrix} = \begin{bmatrix} a_x \\ a_y \\ a_h \end{bmatrix} \tag{21}$$

- the vector of gravitational acceleration $\underline{k}$ (17) and the component of centrifugal acceleration $\underline{z}$ (20) depending on the angular velocity $\omega(\omega^2)$ of the earth only yielding the vector of gravity acceleration $\underline{g}$

$$\underline{g} = \begin{bmatrix} k_x \\ k_y \\ k_h \end{bmatrix} + \begin{bmatrix} (R+h)\cdot\omega^2\cdot\cos\varphi\cdot\sin\varphi \\ 0 \\ -(R+h)\cdot\omega^2\cdot\cos^2\varphi \end{bmatrix} = \begin{bmatrix} k_x+(R+h)\cdot\omega^2\cdot\cos\varphi\cdot\sin\varphi \\ k_y \\ k_h-(R+h)\cdot\omega^2\cdot\cos^2\varphi \end{bmatrix}$$

$$\begin{bmatrix} g_x \\ g_y \\ g_h \end{bmatrix} = \begin{bmatrix} \xi\cdot g \\ \eta\cdot g \\ g \end{bmatrix} = \begin{bmatrix} \xi\cdot g \\ \eta\cdot g \\ \gamma+dg \end{bmatrix} \approx \begin{bmatrix} 0 \\ 0 \\ \gamma \end{bmatrix} \tag{22}$$

with

$\xi = \phi - \varphi$ = relative deflection of the vertical in latitude

$\eta = (\Lambda - \lambda)\cdot\cos\varphi$ = relative deflection of the vertical in prime vertical

ϕ = astronomical latitude

Λ = astronomical longitude

$\gamma = \gamma_0 + \gamma_2\cdot\sin^2\varphi + \gamma_4\cdot\sin^4\varphi + \left(\gamma_{h_0} + \gamma_{h_2}\cdot\sin^2\varphi\right)\cdot h$
= normal gravity, c.f. SCHWARZ (1981, p. 69)

$dg = g - \gamma = g_h - \gamma$ = gravity anomaly,

- and, finally, after the extractions performed as above, all remaining terms of (6) yielding the vector of the disturbing acceleration $\underline{s}$

$$\underline{s} = \begin{bmatrix} 2\cdot(R+h)\cdot\omega\cdot\dot\lambda\cdot\cos\varphi\cdot\sin\varphi + \dot\varphi\cdot\dot h + (R+h)\cdot\dot\lambda^2\cdot\cos\varphi\cdot\sin\varphi \\ -2\cdot(R+h)\cdot\omega\cdot\dot\varphi\cdot\sin\varphi + 2\cdot\omega\cdot\dot h\cdot\cos\varphi + \dot\lambda\cdot\dot h\cdot\cos\varphi - (R+h)\cdot\dot\varphi\cdot\dot\lambda\cdot\sin\varphi \\ -2\cdot(R+h)\cdot\omega\cdot\dot\lambda\cdot\cos^2\varphi - (R+h)\cdot\left(\dot\lambda^2\cdot\cos^2\varphi + \dot\varphi^2\right) \end{bmatrix} \tag{23}$$

or, if we express $\dot{\varphi}$, $\dot{\lambda}$ and $\dot{h}$ according to (13) through the vector of relative velocity $\underline{v}$

$$\underline{s} = \begin{bmatrix} 2\cdot\omega\cdot v_y\cdot\sin\varphi + \frac{v_x\cdot v_h}{R+h} + \frac{v_y^2}{R+h}\cdot\tan\varphi \\ -2\cdot\omega\cdot v_x\cdot\sin\varphi + 2\cdot\omega\cdot v_h\cdot\cos\varphi + \frac{v_y\cdot v_h}{R+h} - \frac{v_x\cdot v_y}{R+h}\cdot\tan\varphi \\ -2\cdot\omega\cdot v_y\cdot\cos\varphi - \frac{v_x^2}{R+h} - \frac{v_y^2}{R+h} \end{bmatrix} = \begin{bmatrix} s_x \\ s_y \\ s_h \end{bmatrix} \tag{24}$$

The coordinate differentials dx, dy, dh at the right side of (7), (8) and (9) follow from vector $\underline{a}$ (21) by integration with respect to time

$$\underline{dx} = \begin{bmatrix} dx \\ dy \\ dh \end{bmatrix} = \underline{v}\cdot dt = \begin{bmatrix} v_x\cdot dt \\ v_y\cdot dt \\ v_h\cdot dt \end{bmatrix} = \left(\int_{t_0}^{t} \underline{a}\cdot dt\right)\cdot dt = \begin{bmatrix} \left(\int_{t_0}^{t} a_x\cdot dt\right)\cdot dt \\ \left(\int_{t_0}^{t} a_y\cdot dt\right)\cdot dt \\ \left(\int_{t_0}^{t} a_h\cdot dt\right)\cdot dt \end{bmatrix} \tag{25}$$

and, putting (25) into (7), (8) and (9) we obtain

$$d\varphi = \dot{\varphi}\cdot dt = \frac{1}{M+h}\cdot\left(\int_{t_0}^{t} a_x\cdot dt\right)\cdot dt \tag{26}$$

$$d\lambda = \dot{\lambda}\cdot dt = \frac{1}{(N+h)\cdot\cos\varphi}\cdot\left(\int_{t_0}^{t} a_y\cdot dt\right)\cdot dt \tag{27}$$

$$dh = \dot{h}\cdot dt = \left(\int_{t_0}^{t} a_h\cdot dt\right)\cdot dt\ . \tag{28}$$

A further integration with respect to time yields the desired geodetic coordinates (coordinate differences):

$$\Delta\varphi = \varphi - \varphi_0 = \int_{t_0}^{t} \dot{\varphi} \cdot dt = \int_{t_0}^{t} \frac{v_x}{M+h} \cdot dt = \int_{t_0}^{t} \frac{1}{M+h} \cdot \left(\int_{t_0}^{t} a_x \cdot dt \right) \cdot dt \qquad (29)$$

$$\Delta\lambda = \lambda - \lambda_0 = \int_{t_0}^{t} \dot{\lambda} \cdot dt = \int_{t_0}^{t} \frac{v_y}{(N+h) \cdot \cos\varphi} \cdot dt = \int_{t_0}^{t} \frac{1}{(N+h) \cdot \cos\varphi} \cdot \left(\int_{t_0}^{t} a_y \cdot dt \right) \cdot dt \qquad (30)$$

$$\Delta h = h - h_0 = \int_{t_0}^{t} \dot{h} \cdot dt = \int_{t_0}^{t} v_h \cdot dt = \int_{t_0}^{t} \left(\int_{t_0}^{t} a_x \cdot dt \right) \cdot dt \; . \qquad (31)$$

Since the integrands in (20), (30), (31), first of all the "reduced" accelerations a_x, a_y, a_h, are dependent on results of both the first and the second step of integration (see (5), (22), (23), (24)).

$$\frac{1}{M+h} = r_x(\varphi, h) \qquad (32)$$

$$\frac{1}{(N+h) \cdot \cos\varphi} = r_y(\varphi, h) \qquad (33)$$

$$\begin{aligned} a_x = a_{Ix} - g_x - s_x &= a_{Ix} - g_x(\varphi, (\lambda), h) - s_x(\varphi, h, \dot{\varphi}, \dot{\lambda}, \dot{h}) = \\ &= a_x(a_{Ix}, \varphi, (\lambda), h, \dot{\varphi}, \dot{\lambda}, \dot{h}) = \\ &= a_x(a_{Ix}, \varphi, (\lambda), h, v_x, v_y, v_h) \end{aligned} \qquad (34)$$

$$\begin{aligned} a_y = a_{Iy} - g_y - s_y &= a_{Iy} - g_y(\varphi, (\lambda), h) - s_y(\varphi, h, \dot{\varphi}, \dot{\lambda}, \dot{h}) = \\ &= a_y(a_{Iy}, \varphi, (\lambda), h, \dot{\varphi}, \dot{\lambda}, \dot{h}) = \\ &= a_y(a_{Iy}, \varphi, (\lambda), h, v_x, v_y, v_h) \end{aligned} \qquad (35)$$

$$\begin{aligned} a_h = a_{Ih} - g_h - s_h &= a_{Ih} - g_h(\varphi, (\lambda), h) - s_h(\varphi, h, \dot{\varphi}, \dot{\lambda}, \dot{h}) = \\ &= a_h(a_{Ih}, \varphi, (\lambda), h, \dot{\varphi}, \dot{\lambda}) = \\ &= a_h(a_{Ih}, \varphi, (\lambda), h, v_x, v_y) \quad , \end{aligned} \qquad (36)$$

the integration procedure has to be performed by solving a system of differential equations of the second order.

The mathematical model depicted by (29), (30), (31) reflects the function of an ellipsoid-normal, north-orientated platform only in its main deterministic features. Beyond that, it is necessary to take into account instrumental error sources with respect to their deterministic and stochastic components, c.f. JOOS (1975), SEEBER (1979), ADAMS (1979), SCHWARZ (1979, 1981), HUDDLE (1981) and CASPARY (1983) a.o.

For evaluating (29), (30), (31), analogous and digital types of procedures are to discuss. Modern inertial systems are based on digital computers generally.

The pattern of an error free operating ellipsoid-normal, north-orientated platform is outlined in figure 4. The diagram shows the data flow within the computer unit according to (29), (30), (31) ("Nav." = "navigation computer") and the interaction between the platform ("Gyr.", "Acc."), the navigation computer and a control unit, controlling the alignment of the platform.

The navigation computer is a control part of all platform systems. In order to compare the different systems in chapter 4, figure 4 was generalized into figure 5.

4. INERTIAL PLATFORM SYSTEMS FOR GEODETIC APPLICATION AND THE RELATIONS BETWEEN THE RELEVANT COORDINATE SYSTEMS

The characteristical and distinguishing features of geodetic platform systems have already been presented in chapter 2. Now a more detailed description of the systems and the relations between them follows.

4.1 Ellipsoid-Normal, North-Orientated Platform System

Coordinate System $\underline{x} = (x,y,h)^T$

Figures 4 and 5 depict the functional scheme of an ellipsoid-normal, north-orientated platform. The systems of the gyros ("Gyr.") and of the accelerometers ("Acc.") are coupled together and both systems are kept in their defined orientation by a platform control unit. It makes the platform con-

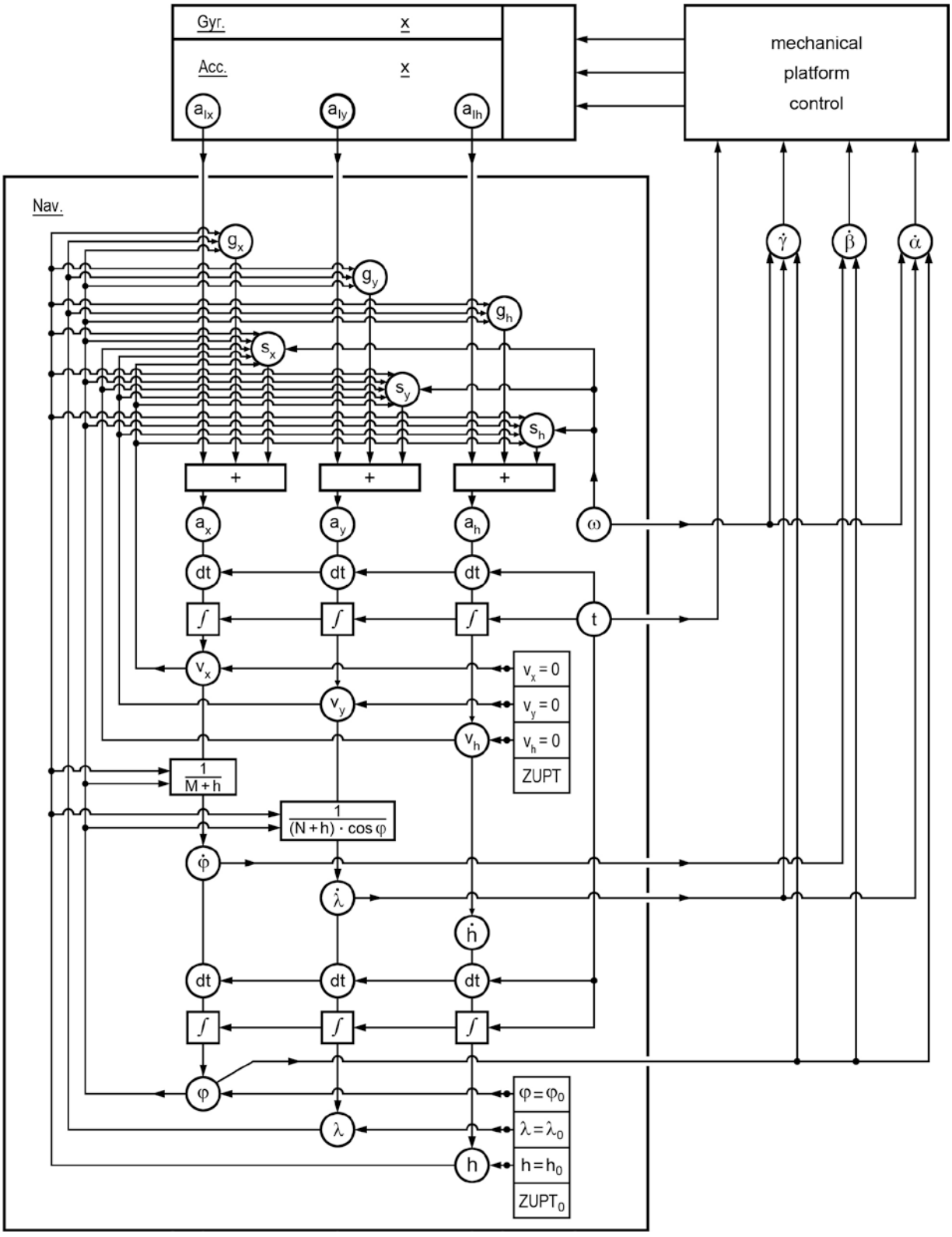

Fig. 4: Functional diagram of an ellipsoid-normal, north-orientated inertial platform system

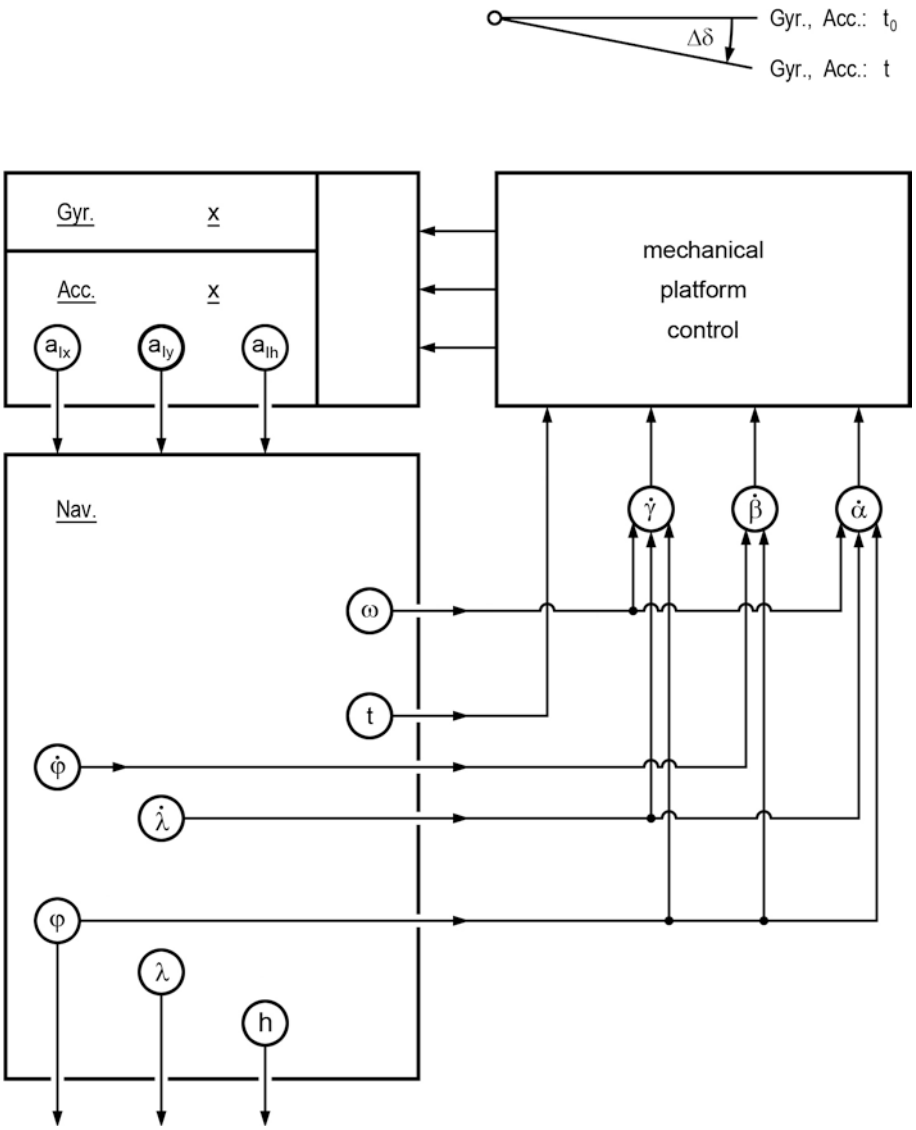

Fig. 5: Functional diagram of an ellipsoid-normal, north-orientated inertial platform system (generalized)

tinuously torque in order to keep the accelerometers aligned properly to the north, to the east and perpendicular to the reference ellipsoid.

The controlling procedure is dependent on the angular velocity ω of the earth and the instantaneous platform (vehicle-)velocity v_x and v_y (components of vector $\underline{v}$ in x- and y-direction) and it obeys the equations

$$\Delta\alpha = \int_{t_0}^{t} \dot{\alpha} \cdot dt = -\int_{t_0}^{t} \sin\varphi \cdot \left(\omega + \frac{v_y}{(N+h)\cdot\cos\varphi}\right) \cdot dt \ , \tag{37}$$

$$\Delta\beta = \int_{t_0}^{t} \dot{\beta} \cdot dt = \int_{t_0}^{t} \frac{v_x}{M+h} \cdot dt \ , \tag{38}$$

$$\Delta\gamma = \int_{t_0}^{t} \dot{\gamma} \cdot dt = -\int_{t_0}^{t} \cos\varphi \cdot \left(\omega + \frac{v_y}{(N+h)\cdot\cos\varphi}\right) \cdot dt \ , \tag{39}$$

where $\Delta\alpha$, $\Delta\beta$ and $\Delta\gamma$ are torquing angles referring to the h-, y- and x-axis of the platform.

Proceeding from the sensed accelerations a_{Ix}, a_{Iy} and a_{Ih}, the navigation computer processes the described geodetic coordinates φ, λ and h and, moreover, provides the torquing parameters $\Delta\alpha$, $\Delta\beta$ and $\Delta\gamma$ mentioned above.

Two firms produce inertial systems of this type for geodetic application: Litton (LASS: L. Auto-Surveyor System) and Ferranti (FILS: F. Inertial Land Surveyor and PADS: Position and Azimuth Determining System), c.f. MUELLER (1981) and SCHWARZ (1981).

4.2 Space Stable Platform System

Coordinate System $\underline{x}^* = (x^*, y^*, z^*)^T$

Figure 6 shows the functional diagram and the time dependent orientation of the system of axes. This type of platform links the system of the gyro axes ("Gyr.") and the system of the accelerometers ("Acc.") together, too, but the platform keeps its orientation stable relative to the inertial space. Instead of the mechanic regulating device of system No. 4.1, we are dealing here with an analytical procedure transforming the measured accel-

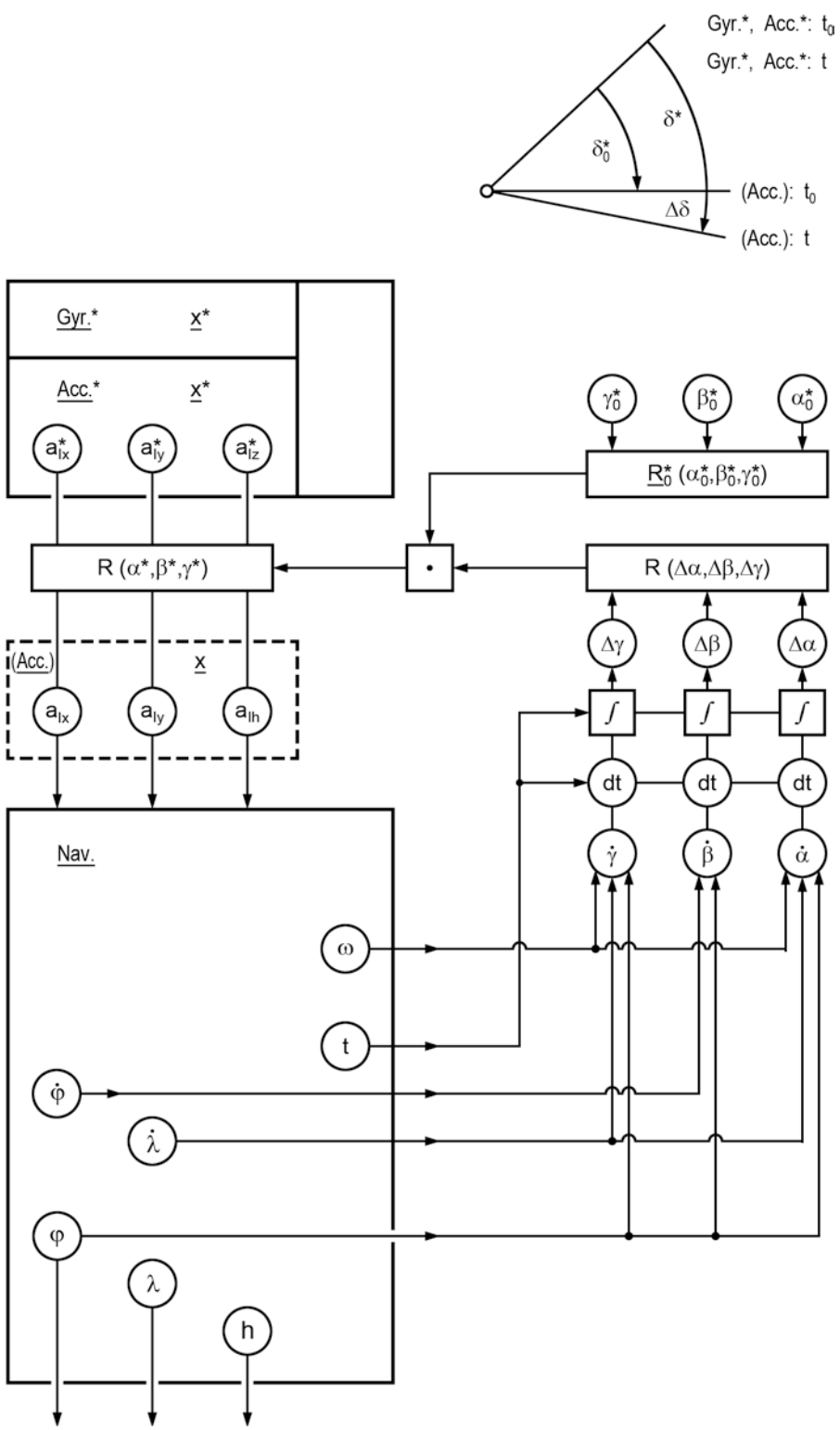

Fig. 6: Functional diagram of a space-stable inertial platform system

erations $\underline{a}_I^* = (a_{Ix}^*, a_{Iy}^*, a_{Iz}^*)^T$ into ficticious accelerations $\underline{a}_I = (a_{Ix}, a_{Iy}, a_{Ih})^T$ that an ellipsoid-normal, north-orientated platform would sense. This transformation concerns a rotation which can be described by a rotating matrix $\underline{R}^* = \underline{R}^*(\alpha^*, \beta^*, \gamma^*)$ relying on three (e.g. cardanic) angles. The matrix is composed of the matrix of the initial orientation of the platform (angles $(\alpha_0^*, \beta_0^*, \gamma_0^*)$) and of a matrix based on position-, velocity- and time-dependent angles $(\Delta\alpha, \Delta\beta, \Delta\gamma)$, c.f. (37), (38), (39).

The following equations (40) describe the necessary transformations specifying the determining parameters.

$$\begin{aligned} \underline{x} &= \underline{R}^* \cdot \underline{x}^* \\ \underline{a}_i &= \underline{R}^* \cdot \underline{a}_i^* \end{aligned} \qquad (40)$$

with

$$\begin{aligned} \underline{R}^* &= \underline{R}^*(\alpha^*, \beta^*, \gamma^*) \\ &= \underline{R}^*(\alpha_0^*, \beta_0^*, \gamma_0^*) \cdot \underline{R}(\Delta\alpha, \Delta\beta, \Delta\gamma) \\ &= \underline{R}^*(\alpha_0^*, \beta_0^*, \gamma_0^*, \Delta\alpha, \Delta\beta, \Delta\gamma) \\ &= \underline{R}^*(\alpha_0^*, \beta_0^*, \gamma_0^*, \dot{\alpha}, \dot{\beta}, \dot{\gamma}, t) \\ &= \underline{R}^*(\alpha_0^*, \beta_0^*, \gamma_0^*, \omega, \varphi, \dot{\varphi}, \dot{\lambda}, t) \\ &= \underline{R}^*(\alpha_0^*, \beta_0^*, \gamma_0^*, \omega, \varphi, h, v_x, v_y, t) \ . \end{aligned}$$

The further calculations, starting from the reduced accelerations $\underline{a}_I = (a_{Ix}, a_{Iy}, a_{Ih})^T$ and leading to the desired coordinates φ, λ and h, are equal to those which have to be executed by the navigation computer in an ellipsoid-normal, north-orientated system (figure 4).

A space-stable platform type is produced by Honeywell (GEO-SPIN), c.f. MUELLER (1981) and SCHWARZ (1981).

4.3 Strap-Down Platform System

Coordinate System $\underline{x}^{\sim} = (x^{\sim}, y^{\sim}, z^{\sim})^T$

A functional diagram of a strap-down type of platform is shown in figure 7. As in the space stable system No. 4.2, the gyros provide an inertial refer-

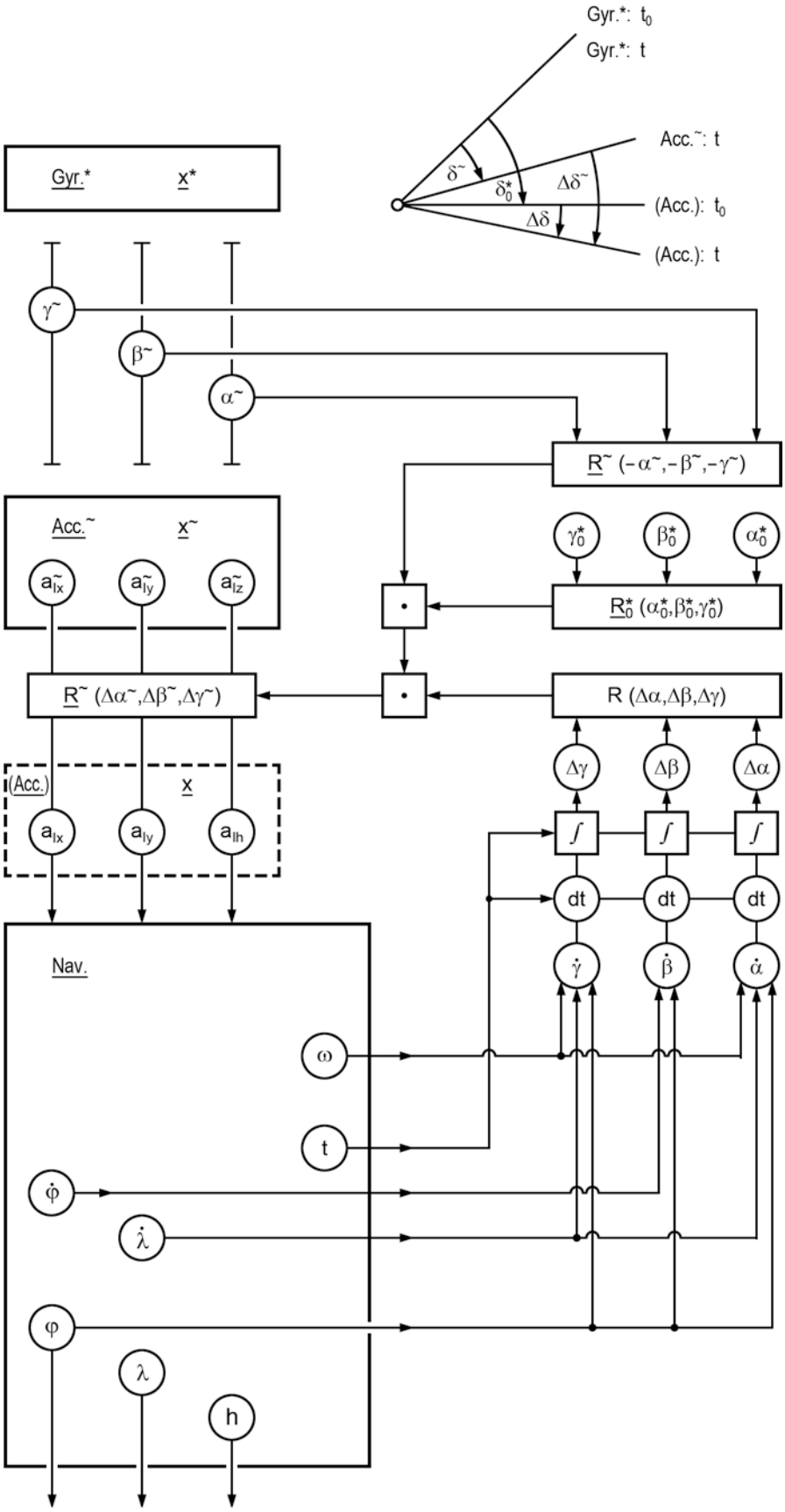

Fig. 7: Functional diagram of a strap-down inertial platform system

ence frame. However, the platform carrying the accelerometers is strapped to the carrier (vehicle). Therefore it follows all the movements of the carrier, both translatoric and rotating motions. The rotations relative to the space stable gyro system are monitored by angular sensors.

In order to transform the measured acceleration vectors $\underline{a}_I^{\sim}$ of the $\underline{x}^{\sim}$-system into those that would be measured by using the ellipsoid-normal, north-orientated system No. 4.1 ($\underline{a}_I$) we have to apply the transformations treated in No. 4.2 and denoted by $\underline{R}^*(\alpha_0^*,\beta_0^*,\gamma_0^*)$ and $\underline{R}(\Delta\alpha,\Delta\beta,\Delta\gamma)$ and, beyond it, we have to take into account the instantaneous orientation of the carrier expressed by a rotation matrix $\underline{R}^{\sim} = \underline{R}^{\sim}(-\alpha^{\sim},-\beta^{\sim},-\gamma^{\sim})$. Thus the complete rotation matrix $\underline{R}^{\sim} = \underline{R}^{\sim}(\Delta\alpha^{\sim},\Delta\beta^{\sim},\Delta\gamma^{\sim})$ is composed of three individual rotation matrices. Summarizing, we can describe the transformation from the $\underline{x}^{\sim}$- into the $\underline{x}$-system, and, thus, from acceleration vectors $\underline{a}_I^{\sim} = (a_{\tilde{I}x},a_{\tilde{I}y},a_{\tilde{I}z})^T$ into $\underline{a}_I = (a_{Ix},a_{Iy},a_{Ih})^T$ as follows.

$$\begin{aligned} \underline{x} &= \underline{R}^{\sim} \cdot \underline{x}^{\sim} \\ \underline{a}_i &= \underline{R}^{\sim} \cdot \underline{a}_i^{\sim} \end{aligned} \qquad (41)$$

with

$$\begin{aligned} \underline{R}^{\sim} &= \underline{R}^{\sim}(\Delta\alpha^{\sim},\Delta\beta^{\sim},\Delta\gamma^{\sim}) \\ &= \underline{R}^{\sim}(-\alpha^{\sim},-\beta^{\sim},-\gamma^{\sim}) \cdot \underline{R}^*(\alpha_0^*,\beta_0^*,\gamma_0^*) \cdot \underline{R}(\Delta\alpha,\Delta\beta,\Delta\gamma) \\ &= \underline{R}^{\sim}(\alpha^{\sim},\beta^{\sim},\gamma^{\sim},\alpha_0^*,\beta_0^*,\gamma_0^*,\Delta\alpha,\Delta\beta,\Delta\gamma) \\ &= \underline{R}^{\sim}(\alpha^{\sim},\beta^{\sim},\gamma^{\sim},\alpha_0^*,\beta_0^*,\gamma_0^*,\dot{\alpha},\dot{\beta},\dot{\gamma},t) \\ &= \underline{R}^{\sim}(\alpha^{\sim},\beta^{\sim},\gamma^{\sim},\alpha_0^*,\beta_0^*,\gamma_0^*,\omega,\varphi,\dot{\varphi},\dot{\lambda},t) \\ &= \underline{R}^{\sim}(\alpha^{\sim},\beta^{\sim},\gamma^{\sim},\alpha_0^*,\beta_0^*,\gamma_0^*,\omega,\varphi,h,v_x,v_y,t) \ . \end{aligned}$$

The essential difference between matrix $\underline{R}^{\sim}$ inherent to the strap-down platform system and matrix $\underline{R}^*$ of the space-stable platform system (No. 4.2) or the corresponding follow-up procedure of the ellipsoid-normal, north-orientated configuration (No. 4.1) has to be seen under a dynamic aspect. Whereas $\underline{R}^*$ following the rotation of the earth and the translatoric motions of the vehicle changes very slowly and almost uniformly, the elements of $\underline{R}^{\sim}$, due to inevitable changes in the direction of the vehicle (yaw-, pitch-, roll-motions) are subject to large angular altera-

tions $\tilde{\alpha}, \tilde{\beta}, \tilde{\gamma}$ in short-time-intervals. Therefore it is necessary to handle a large number of data in a very short time and, thus, to employ a powerful processing computer.

Up to now, strap-down inertial systems are not yet available for survey purposes. Considering the rapid improvement of onboard high-speed computer technology and the opportunity of reducing the number of mechanical components, it is likely that future platform systems will be of this type (MUELLER, 1981).

5. REFERENCES

ADAMS, J.R.: ***Description of the Local Inertial Survey System and its Simulation.*** Technical Report No. 59, Department of Surveying Engineering, University of New Brunswick, Fredericton 1979

BRITTING, K.R.: ***Inertial Navigation System Analysis.*** Wiley-Interscience, New York, London, Sidney, Toronto 1971

CASPARY, W.: ***Inertiale Vermessungssysteme.*** VR – Vermessungswesen und Raumordnung 45, S. 169-188, 1983

GRAFAREND, E.: ***From Kinematical Geodesy to Inertial Positioning.*** In Schwarz, K.P. (Editor): Proceedings of the Second International Symposium on Inertial Technology for Surveying and Geodesy, June 1-5, 1981, S. 35-50, Banff 1981

HEITZ, S.: ***Mechanik fester Körper mit Anwendungen in Geodäsie, Geophysik und Astronomie;*** Band 1: Grundlagen, Dynamik starrer Körper. Dümmlers Verlag, Bonn 1980

HUDDLE, J.R.: ***Theory and Performance of the Litton Inertial Surveyors and Recent Developments.*** Proceedings FIG XVI. International Congress, 512.4, Montreux 1981

JOOS, D.K.: ***Fehlermodell eines Inertialnavigationssystems für integrierte Navigation durch Ausgleichung nach der Methode der kleinsten Quadrate.*** Dissertation, Universität Stuttgart, 1975

MAGNUS, K.: ***Kreisel – Theorie und Anwendungen.*** Springer-Verlag, Berlin, Heidelberg, New York 1971

MUELLER, I.I.: Inertial Survey Systems in the Geodetic Arsenal. In Schwarz, K.P. (Editor): Proceedings of the Second International Symposium on Inertial Technology for Surveying and Geodesy, June 1-5, 1981, S. 11-33, Banff 1981

RAVEN, F.H.: ***Kinematics. In Flügge, W. (Editor): Handbook of Engineering Mechanics,*** S. 22- , McGraw-Hill Book Company, New York, Toronto, London 1962

SEEBER, G.: ***Inertiale Vermessungssysteme und ihre Anwendungen in der Geodäsie.*** Zeitschrift für Vermessungswesen 104, S. 460-471, 1979

SCHÖDLBAUER, A.: ***Bezugssysteme der Landesvermessung unter Berücksichtigung terrestrischer und satellitengeodätischer Meß- und Auswerteverfahren.*** In Schödlbauer, A., Welsch, W. (Herausgeber): Satelliten-Doppler-Messungen, Beiträge zum geodätischen Seminar, 24./25. September 1984, S. 63-153, Schriftenreihe des Wissenschaftlichen Studiengangs Vermessungswesen der Hochschule der Bundeswehr München, Heft 15, Neubiberg 1984

SCHRÖPL, H.: ***Teldix Taschenbuch der Navigation.*** Teldix GmbH, Heidelberg 1979

SCHWARZ, K.P.: ***Grundgleichungen und Fehlermodelle für inertiale Meßsysteme.*** Zeitschrift für Vermessungswesen 104, S. 447-460, 1979

SCHWARZ, K.P.: ***A Composition of Models in Inertial Surveying.*** In Schwarz, K.P. (Editor): Proceedings of the Second International Symposium on Inertial Technology for Surveying and Geodesy, June 1-5, 1981, S. 61-76, Banff 1981

NNSS Doppler Measurements

- The Navy Navigation Satellite System -

- Review Paper -

TRANSIT DOPPLER SATELLITE POSITIONING FOR NATIONAL AND ENGINEERING CONTROL SURVEYS

by

Peter RICHARDUS
Wageningen
The Netherlands

ABSTRACT

A review is given of the Transit Doppler Satellite Positioning modes as to the developments in the seventies, and the latest increase of precision by means of improvements on the satellite techniques and the mathematical models involved. A comparison is made with NAVSTAR-GPS at its present possibilities.

1. INTRODUCTION

With the NAVSTAR-GPS rising fast above the geodetic horizon, it seems to be difficult to conduct a review of the Doppler Satellite observations on the Transit System in another way than in the style of an obituary. The relatively few papers dealing with Doppler Positioning on Transit in this symposium point in that direction. G.P.S. steals the show.

Although the Transit Doppler with the Broadcast- and Precise Ephemerides will remain operative until 1984, such an obituary would be simple, but for a number of recent developments. The trend of an increasing accuracy has not come to an end yet, so that the field of application is still extending. However, at least in the field of national control and engineering surveys Transit Doppler will not win the race against G.P.S., it will at least lose a large part of its importance.

Transit Doppler can be considered as a trainingschool. Much of the experience in observational and computational techniques can in some way or another be applied to G.P.S. and other future geodetic satellites or satellite systems, for instance the POPSAT (an acronym for Precise Orbit Positioning Satellite) which may be launched by ESA in the early nineties, and which systems may yield a precision of positioning and translocation of about three to four times better than Transit Doppler. The fundamental problems concerning the datum, and datum transformation which came to the fore when Doppler coordinates had to be compared with - or incorporated into other systems, pertain to geometry, and are independent of observational techniques be it satellite, terrestrial of otherwise. The experience gained is equally applicable in the future.

With this in mind, it may be worthwhile to relate briefly the fast evolution of Transit Doppler after it was released for civilian use in 1969. Until 1975 a long series of publications mainly from the U.S. and Canada appeared on which the present techniques are based. Without being exhaustive the following papers may be mentioned. By Duane Brown (1970) "Near term prospects for positional accuracies of 0.1 to 1.0 meter from Satellite Geodesy"; by Brown and Trotter "The development of the Geodetic Short Arc Geodetic Adjustment Computation Programmes"; "Doppler Control" the famous Ph.D. thesis by David Wells of the New Brunswick University. The publications by Anderle, Hittel, Krakiwsky and Kouba, which were supported by numerous field experi-

ments. Kouba is well known by this Geodop computation programmes.

In those years it became apparent that Transit Doppler measurements could successfully compete with precise astronomical positioning, and many types of terrestrial surveys. It had the economical advantage to be almost independent of bad weather conditions, it needed only few personnel, and observation stations did not need to be intervisible with multipoint positioning sub-metre precision was reached. In the translocation mode, where Doppler satellite measurements act as indirect distance measurements, accuracies were attained of 1.5 ppm up to 200 km and 1 ppm for distances up to 600 km.

As the instruments became more compact, and the paper-punchtape was replaced by magnetic tape, the Transit Doppler method soars high. As applications may be mentioned - the establishment of 1st and 2nd order control surveys in countries and areas where other control survey stations are scarce or nonexistent.

- Control surveys for the mapping of large riverbasins and irrigation areas. As such can be considered the provision of passpoints for photogrammetrical and remote sensing surveys. Very well known is the early application to the small scale radar mapping of the Amazon riverbasin with the old Geoceiver instruments in 1972.
- Positioning of drilling platforms and oilrigs on the continental shelves.
- The setting out of concession boundaries by sea as well as by land. Also international boundaries have been determined this way.
- The tracing of pipelines; transmission lines; the positioning of microwave communication towers.
- Positioning for geophysical prospecting. Generally not the highest precision is required for this type of surveys. Rough orthometric heights of unknown points in remote areas have actually been determined in the following way. The orthometric heights of some stations being known, the geoidal height can be derived by Doppler positioning, which renders ellipsoidal heights. These stations then act as reference stations to determine the geoidal height of an unknown point by interpolation. Doppler positioning at that point leads to its orthometric height.

The high relative accuracy at remote distances provided the possibility to check the scale and orientation of existing continental and national control

surveys. The method can also lead to a "zero order" network as datum points, and transformation parameters for the junction of networks into the Transit reference system and reversed. There are actually two reference systems: one for the B.E. - and the other for the P.E., which is rotated about the Z-axis by an angle of 0'8 sec of arc, and has a slight scale difference. To my knowledge in the literature no mention has been made of the corresponding covariance transformations for the comparison of precision.

Transit Doppler did not get into full swing in Europe until 1975/1976, after combined efforts of Boucher, Paquet, Seeger and (last not least) Peter Wilson started in the years 1973/1974. They found great support all over the continent. Since then a long series of international and national Doppler Campaigns have been organized. Of these only the EDOC 2 (European Doppler Campaign) in 1975 comprising 32 stations should be mentioned. It was aimed at the connection of Doppler coordinates with the ED 50 European Triangulation Datum. These ED 50 coordinates - though not being the best of geodetic quality - form the basis for the mineral legislation of the countries concerned, and are therefore of great legal and commercial significance.

In October 1976 a large symposium was organized in Las Cruzas (New Mexico), where the experience of approximately 50 countries was brought together. Transit Doppler was called the most important development in the history of geodesy ever. Two more symposia followed in January 1979 (Austin) and again in Las Cruzas 1982. The proceedings of these three meetings give the best record of this type of satellite positioning.

G.P.S., however, was throwing its shadow ahead more and more, virtually since its conception in 1973.

2. LATEST IMPROVEMENTS ON TRANSIT DOPPLER OBSERVATIONS

Since 1982/83 new technical developments and mathematical model studies of the atmospheric disturbances and of the modes of positioning and translocation have given a second chance to Transit Doppler positioning attaining a higher precision.

2.1 Improvement of the orbital data

The limited accuracy of the orbital data is a major source of errors on the

position coordinates of observation stations. The availability of the P.E. for some of the Transit Satellites signified a major improvement in this respect, although under certain circumstances of processing of an increased number of observations with the B.E. could yield an equivalent result.

Through the launching of the NOVA satellite in the Transit System, which is equipped with a drag compensation device, the precision of positioning has improved with a factor 2. Paquet reports from the results of investigations at the Brussels' Tranet Station that the NOVA satellite with the P.E. increases the orbital accuracy by about 60 %. This is only a first approximation, as the NOVA orbital parameters so far are processed with the data of the Earth's gravity field obtained from the non-drag free satellites in the system. The P.E. of NOVA leads to a standard deviation of the single point positioning of approx. 30 cm. This is about half the standard deviation of the result obtained with the P.E. of the old 30190 Transit satellite. When the NOVA orbit will be computed with an improved gravity model, the standard deviation will be reduced further to 20 cm.

2.2 Atmospheric refraction

The tropospheric and ionospheric refraction have always exercised a limiting influence on the positional accuracy.

Leaving observations below an elevation of 10° out of consideration it is easily calculated that the wet component of the tropospheric refraction shows errors amounting to 2 % of the wet and dry components collectively (approx. 25 cm for an elevation of 10°). With a positional precision of 20 to 30 cm the model of this component should be improved to reduce the errors to less than 2 cm. Water vapour microwave radiometry to derive the water vapour distribution along a vertical profile gives encouraging results. The dry component model seems quite satisfactory.

The influence of the ionospheric refraction is largely - but not sufficiently in many cases - eliminated by the application of two frequencies (400 and 150 MHz) in the well known way. The residual errors mainly of the station heights have been analysed (Anderle, Dehant, Paquet, Schlüter, Strange). These heights show time dependent variations with various characteristic periods. ***TSCHERNING and GOAD (1983)*** studied the correlation with the sunspot numbers at 800 points in North America, known in height above mean sea-

level, and where the geoidal heights could be independently computed, so that the ellipsoidal height could be derived. The relationship found to estimate the error in the Doppler ellipsoidal heights for the individual points caused a decrease of the standard deviation from 55 cm to 20 cm of the yearly means of the differences between the two ellipsoidal heights.

2.3 Mathematical model studies

From the early seventies many investigations concerning the mathematical model have been carried out in a search for a mode where rank deficiencies due to a lack of a proper definition of a coordinate system, or to a critical configuration could be avoided. This means that all unknowns in the problem should be expressed as functions of observations only, without making use of given coordinates and orbital parameters. Only a sufficient number of simultaneous observations can lead to such a model. Aardom (1971) and Molenaar in his graduate thesis in 1972 indicated solutions in that direction. Then it is relatively quiet on this front until 1978. Recently solutions have been given amongst others by ***GRAFAREND et al. (1982)*** with practical applications to part of the German-Austrian Doppler campaigns. This part of research does not seem completed as yet.

The improvement of the Geodop computation programme - Geodop V has shown remarkable results. The main features consist of 1) the possibility to select a gravity model for the processing of the transmitted orbital parameters (e.g. the GEM 9 model) and 2) the facility to solve for all 6 Kepler parameters in a multistation adjustment, incorporating the full short arc mode. Also higher order ionospheric corrections can be processed. There are more improvements.

There are many promising practical results. Comparisons of Doppler with terrestrial coordinates and heights show discrepancies between 10 and 20 cm. Ellipsoidal height differences show discrepancies even of 10 - 15 cm. A recent translocation experiments in the Netherlands showed actual discrepancies of

Doppler - terrestrial (in the national datum) of 4 cm
Doppler - terrestrial (in the ED 50 datum) of 1 cm
Doppler - terrestrial (in the ED 79 datum) of 4 cm

at a distance of 99.85 km.

3. SO WHAT ? OR WHAT NOW ?

What does the comparison mean of the latest Transit Doppler results with those of the G.P.S.? The satellites of G.P.S. have a considerable higher altitude, so that the non-gravitational forces and the short wavelength parts of the gravity field of the Earth have almost no influence on the orbit; higher frequencies for the two channels have been selected for a more effective elimination of the ionospheric refraction; the oscillator stability is better and the data acquisition is continuous. However, the signal is not as strong, and the Doppler shift is smaller (lower). Experiments show that where Transit Doppler is applicable in positioning the same results are obtained with the G.P.S. Doppler mode, but about two to three times faster. For baselines from 200 km to 2000 km Transit Doppler is better in current use thanks to the NOVA satellites.

The facilities of G.P.S. to measure phases and phase differences of the carrier wave allow for the very high precision of 1 ppm in the measurement of distances ranging from 1 to a few hundred km. It opens the possibility even to use G.P.S. for tacheometric surveys provided the receivers are adapted. G.P.S. thus fills a gap between the generally expensive terrestrial techniques on the one side and Doppler Transit on the other. The application of G.P.S. measurements of national and engineering surveys seems to be unlimited.

It seems, however, at present that practical and economical considerations will hamper the general application.

At first there still is the uncertainty about the availability of the codes. Both the Precise and the C/A code can be used at present, but what will happen after the complete constellation of the 18 satellites becomes operational in 1988? Campbell already proposed to use the L_2 channel of G.P.S. only and determine the ionospheric influence with simultaneous Transit Doppler observations.

Secondly the cost of the equipment is high, although improvement in this respect will not fail to come. Pooling of instruments will be necessary certainly for many universities. Referred is to the already existing University Navstar Consortium.

Should or could the Transit system be abandoned after the transitional period, or updated with more NOVA type satellites? After all in 1984 alone about 16000 Transit Doppler receivers have been sold, admittedly 90 % for navigational purposes, but still. However, the future with respect to Transit looks gloomy. If it comes to the worst may the Transit system die with the dignity and honour it deserves.

No wonder from the point of view of surveying and geodesy proposals have been put forward for the establishment of a third system, independent of constraints on the code, like Popsat and Navsat.

Many other questions have and will come up. We will hear more of them and possibly the answers during the sessions of this symposium.

4. REFERENCES (by no means exhaustive)

PROCEEDINGS of the Doppler Satellite Positioning symposia in Las Cruzas 1976; Austin 1979 and Las Cruzas 1982

EGGE, D., SCHENKE, H.W., SEEBER, G.: ***The Niedoc '81 Doppler Campaign - Geodop V short arc results.*** Paper presented at the XVIII. IUGG General Assembly, Hamburg 1983

GRAFAREND, E. et al.: ***The processing of Satellite Doppler Observations in the free network mode.*** Allgemeine Vermessungsnachrichten 7/1982

HUSTI, G.J.: ***On the absolute and relative accuracy of Doppler Satellite Positioning.*** Geodesia, March 1985

PAQUET, P.: ***Past and future of space radioelectric measurement.*** Geodesia, March 1985

TSCHERNING, C.C., GOAD, C.C.: ***Correlation between Time-dependent Variations of Doppler-determined heights and sunspot numbers.*** Paper presented at the Journées Luxembourgoises de Géodynamique, Nov. 1983

ON THE CONSISTENCY OF THE STATION COORDINATES DERIVED FROM SATELLITE DOPPLER OBSERVATIONS

József ÁDÁM⊗

Department of Geodetic Science
Stuttgart University, Keplerstr. 11,
D-7000 Stuttgart 1, FRG

ABSTRACT

The reliability of the satellite Doppler technique for accurate positioning has been proved in many national and international Doppler observation campaigns. Experiences with Doppler satellite geodetic techniques show that, with different models and softwares, slight differences in station coordinates do occur. Very small differences in chord lengths give a good impression of the internal consistency of the Doppler satellite networks. Observations at identical points during several campaigns result in coordinate variations from campaign to campaign using both Broadcast Ephemeris /BE/ and Precise Ephemeris /PE/. Time series analysis of the coordinates derived from long series of Doppler observation data at different sites indicates systematic variations on the station coordinates.

Since the availability of the PE is restrictive, for some countries and campaigns only the BE can be used for geodetic applications. Hence it is necessary to know what are the internal consistency, long-term stability and external errors of the station coordinates evaluated from the BE, what are the coordinate differences between the results of BE and PE solutions, etc. It is very important for us therefore to know what the resulting positions mean.

In this paper the results of some observation campaigns /Hungarian Doppler Observation Campaigns; HDOC80 and HDOC82 in particular/ from the viewpoint of internal consistency are outlined. The results of the least squares spectral analysis of Doppler station height coordinates at station Penc, Hungary as well as a multiple time series analysis of the height series of stations Bruxelles /Belgium/, Graz-Lustbühel /Austria/, Wettzell /FRG/ and Penc /Hungary/ are shortly summarized. The paper further deals with the precision and accuracy of both BE and PE coordinate systems obtained through Doppler surveys and also their interrelationship.

⊗On leave from the Institute of Geodesy and Cartography, Satellite Geodetic Observatory H-1373 Budapest, Pf. 546, Hungary

1. INTRODUCTION

The Navy Navigation Satellite System /NNSS/, also known as the TRANSIT, is being used worldwide for geodetic positioning. Widespread acceptance by the geodetic community has been primarily due to its economy, portability, reliability and operational ease. Doppler positioning has provided itself as a fast, all weather and powerful geodetic observation system. It leads to a set of 3D geocentric Cartesian coordinate solution, which can be used not only to provide scale, orientation and shape control for national or continental geodetic networks, but also to positioning a given geodetic datum with respect to the geocentre of the earth. Satellite Doppler methods have also been found very useful in geodynamical studies /continuous polar motion monitoring, plate motion, etc./, see e.g. Anderle /1976/, Anderle and Malyevac /1983/, Kouba /1981, 1983/.

Continuous Doppler observations to the TRANSIT satellites are carried out by about 20 stations operated by the Defense Mapping Agency /TRANET = Tracking Network stations/, the Naval Astronautics Group /OPNET = Operational Network stations/ and cooperating international stations. The Defense Mapping Agency /DMA/ uses the observations made by the entire station network to determine the Precise Ephemeris /PE/ used in non-real-time calculations of geodetic positions. These ephemeris are also used to determine the positions of the base stations from their own Doppler observations in order to monitor the stability of the coordinate system established by the PE. The PE is a set of values for earth-fixed positions and velocities at one-minute intervals computed by fitting 48-hour orbital arcs to Doppler data. Since these data are from the worldwide TRANET network and no extrapolations are involved, the PE is consistent at the 2-m level.

The Naval Astronautics Group uses the observations made by its four OPNET stations to compzte the Broadcast Ephemeris /BE/ which is injected in the satellite memory, transmitted in real time, and used for navigation and geodetic applications. The BE are fitted to a 30-hour Doppler data span every 12 hours, and

resulting orbits are then extrapolated for up to 30 hours into the future and finally uploaded into the satellite memory every 12 hours. The BE is received at an observing station in the form of coded parameters from which earth-fixed satellite positions can be calculated. These parameters are divided into 14 fixed orbit parameters whose values change only twice a day and four sets of variable orbit parameters whose values change every two minutes. Because of a limited word length the variable parameters are rounded off to the nearest 10 m, which results in positioning errors due to rounding-off errors of up to 6 m. Accuracy of the BE was investigated by e.g. Wells /1974/, Arur /1979/, Jenkins and Leroy /1979/ and Ziegler /1979/. According to the investigations made by Jenkins and Leroy /1979/, the errors can still approach 100 m, mainly due to uncertainty in orbit predictions. The largest prediction errors are in the along-track direction and are caused by unpredictable changes in the air drag. Further error sources are due to predicted pole positions, changes in UT1-UTC during the prediction span, initial orbital parameters, etc. It is estimated by Arur /1979/ that the positional uncertainty of BE may vary between 19 to 26 m in-track, 15 to 20 m cross-track and 9 to 10 m in radial directions depending on the incidence of the epoch of observations in the interinjection period.

The accuracy of Doppler mpoint positioning depends upon a lot of factors, including the accuracy of the ephemeris data used, the accuracy of the meteorological data used, the capabilities and operating conditions of the Doppler receiver, the number and distribution of satellite passes used, the capabilities of the data reduction program, the quality of the measured data, etc. Current estimation of internal consistency of Doppler derived geocentric positions in point positioning is about 0.5 m by using the PE and within the range 2 to 5 meters by using the BE. However, by using the BE in “short arc” method, the Doppler satellite system can reach accuracies ranging from 0.1 m to 0.5 m in relative positioning. Clearly, this mode of operation, which requires only the BE, is particularly suitable for strengthening the scale and orientation of national geodetic control networks and for engineering control purposes.

Since the availability of the PE is restrictive, for some countries, cf. e.g. Chen /1982/, Colič et al. /1984/, Joó et al. /1985/, Pachelski /1982/ and Stomma /1982/, and for some campaigns, e.g. WEDOC; cf. Rinner and Pesec /1982/ and Pesec and Mihály /1984/, only the BE can be used for geodetic applications. Hence it is very important and necessary to know what are the internal consistency, long-term stability and external errors of the station coordinates evaluated from the BE, what are the coordinate differences between the results of the BE and PE solutions, what is the most appropriate transformation between coordinate systems of the PE and BE, etc. It is very important for us therefore to know what the resulting positions by using the BE mean, see e.g. Alpár et al. /1984/, Ádám /1982, 1984/.

2. INTERNAL CONSISTENCY OF THE STATION COORDINATES EVALUATED FROM THE BE

Differences normally result in Doppler derived position solutions when either different data sets or different computer programs are used in data reduction. Differences also occur when different assumptions are made regarding constraints to be applied in data processing. Often these constraints are necessarily different due to computer program concept and design differences or because of analyst preferences even when the same computer program is used, see e.g. Boucher et al. /1981/, Pesec and Schlüter /1982/.

According to the experiences in Doppler satellite geodesy, see e.g. Baldi et al. /1984/, Boucher et al. /1981/, Ehlert et al. /1982/, Heister and Glasmacher /1984/, Jenkins and Leroy /1979/, Pachelski /1982/, Pesec and Schlüter /1982/, Rutscheidt /1982/, Schlüter and Wilson /1981/, Stomma /1982/, the internal consistency of the BE solutions can never be as good as that of PE solutions. In spite of this fact, some Doppler solutions with BE fit very well with the terrestrial networks, se e.g. Frevel et al. /1984/, Joó et al. /1985/. In the following the experiences obtained on the internal consistency of the BE solutions of the Hungarian Doppler Observation Campaigns /HDOC80

and HDOC82/ will be summarized.

The Doppler satellite networks established during the Hungarian Doppler Observation Campaigns in 1980 /HDOC80/ and 1982 /HDOC82/ are shown on Fig. 1. The measurements were carried out with a CMA-751 and a JMR-1 receiver by translocation in 1980 and with three JMR-1A and one JMR-4A receivers by multilocation in 1982. The observations collected during these campaigns are processed on a Honeywell Bull computer using GEODOP Version III, SPPENC

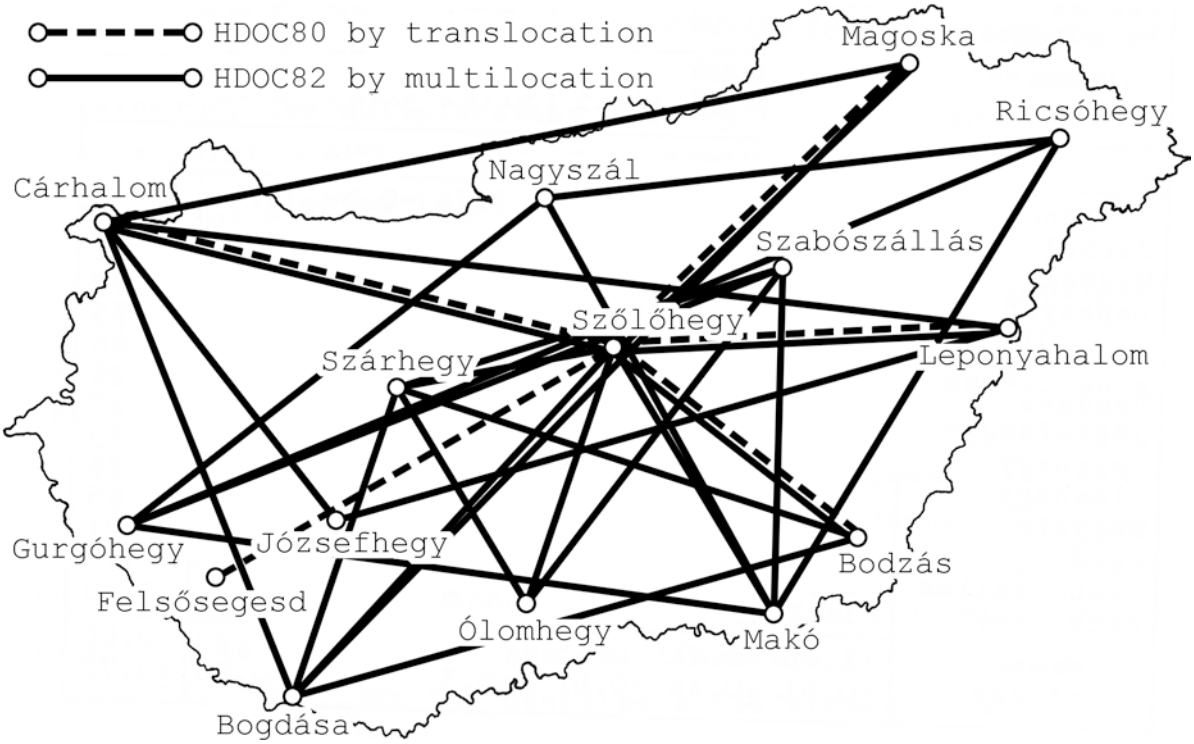

FIGURE 1 Doppler stations – HDOC80 and HDOC82 networks

and SADOSA programs, cf. Czobor /1982/, Joó et al. /1985/, Mihály /1982, 1984/. The computations were only performed with the aid of the BE. Different solutions have been computed using the data from the all available TRANSIT satellites:

a/ Single Point /SP/ Positioning by SPPENC and GEODOP

b/ Translocation /TL/ and Multi Point /MP/ adjustment using semi short arc techniques by GEODOP and SADOSA.

The different coordinate sets obtained are abbreviated in the following by SPPENC, GEODOP/SP/, SADOSA, GEODOP/TL/ and

Site	Coordinate differences in meters						dr in [m]
	Geocentric system			Local system			
	dX	dY	dZ	dN	dE	dh	
HDOC80:	GEODOP/TL/		minus		SADOSA		
Szőlőhegy	0.64	-1.12	3.21	2.01	-1.27	2.51	3.46
Cárlahom	-0.34	0.27	2.09	1.59	0.37	1.38	2.13
Magoska	2.53	-1.25	3.03	0.59	-2.08	3.53	4.14
Leponyahalom	1.95	0.00	1.79	-0.12	-0.73	2.53	2.65
Bodzás	1.88	1.27	2.93	0.41	0.51	3.65	3.71
Felsősegesd	3.95	-0.16	0.14	-2.54	-1.56	2.60	3.96
mean	1.77	-0.16	2.20	0.32	-0.79	2.70	3.34
st. dev.	±1.49	±0.93	±1.15	±1.61	±1.05	±0.83	±0.79
HDOC82:	GEODOP/MP/		minus		SADOSA		
Szőlőhegy	1.42	-0.13	2.50	0.74	-0.60	2.71	2.88
Cárlahom	1.06	-0.13	2.35	0.86	-0.43	2.40	2.58
Magoska	0.78	-0.44	2.56	1.28	-0.69	2.29	2.71
Leponyahalom	1.76	-0.42	2.32	0.49	-1.05	2.71	2.94
Bodzás	2.26	0.65	2.66	0.13	-0.20	3.54	3.55
Gurgóhegy	-0.15	-0.23	0.82	0.72	-0.18	0.45	0.86
Bogdása	2.19	-0.69	2.31	0.26	-1.33	2.96	3.26
Józsefhegy	1.11	-0.55	1.84	0.62	-0.87	1.95	2.22
Szárhegy	0.79	-0.70	0.99	0.29	-0.91	1.09	1.45
Ólomhegy	1.64	-0.29	2.67	0.79	-0.81	2.94	3.15
Nagyszál	1.09	0.81	2.28	0.57	0.41	2.56	2.65
Makó	1.07	-0.46	2.67	1.24	-0.81	2.51	2.91
Szabószállás	1.38	0.16	2.77	0.87	-0.33	2.95	3.10
Ricsóhegy	1.11	-0.55	2.71	1.20	-0.93	2.56	2.98
mean	1.25	-0.21	2.25	0.72	-0.62	2.40	2.66
st. dev.	±0.61	±0.46	±0.62	±0.36	±0.76	±0.80	±0.72

TABLE 1 Coordinate differences between results of the two campaigns, HDOC80 and HDOC82, using GEODOP and SADOSA program solutions

GEODOP/MP/. Due to differences in the procedure of data handling, the results obtained by different programs differ from each other. Table 1 shows the coordinate differences dX, dY, dZ between the GEODOP and SADOSA coordinate sets for both campaigns /in translocation and multilocation, respectively/ and their transformed values into the northings /dN/, eastings /dE/ and heights /dh/ whit the linear deviations $dr = /dX^2+dY^2+dZ^2/^{1/2}$.

A comparison of geodetic height differences at all sites shows that the SADOSA derived heights are consistently below those derived with the GEODOP program. Generally, the coordinate differences between the GEODP/MP/ and SADOSA solutions of the HDOC82 are slightly smaller than similar variations of the HDOC80. Average values of the differences in positions dr are 3.34 m /±0.79/ and 2.66 m /±0.72/, respectively. This feature is well represented in Table 2 which is a summary of average values of the coordinate differences and linear deviations evaluated from different program solutions of both campaigns. Mean values of the average differences in positions dr are 3.40 m /±0.75/ and 2.80 m /±0.55/, respectively. In sum, Table 1 and 2 show a slightly higher internal consistence of the results obtained by the multilocation than by the translocation /or single point positioning/. It is partly due to the higher quality data collected in 1982.

Observations at five identical points during both campaigns, HDOC80 and HDOC82 /see on Fig. 1/ allow us to study the so-called “campaign-related datum”-problem in the case of using BE. Table 3 is a summary of coordinate differences between results of the two campaigns for different program solutions and the linear deviations dr in positions. This comparison shows considerable discrepancies between both campaigns. For the multi point solutions /GEODOP/MP/,SADOSA/, the discrepancies are mainly in the heights. These solutions are horizontally more stable. Furthermore, the coordinate differences evaluated from the results of SADOSA and GEODOP/MP/ solutions agree very well, despite the different network adjustment constraints. Average values of the linear deviations dr in positions for the four program solutions even for the single point positioning solutions /GEODOP/SP/,SPPENC/ again agree well. Mean of the average values is 5.26 m /±0.22/.

Considering the coordinate differences in Table 1-3, one should state that the internal agreements within the campaigns are better. The surprisingly large systematic differences between HDOC80 and HDOC82 might be due to certain biases of BE as, for example, possible small changes of the reference system /or

HDOC	Coordinate differences between	Average values of the coordinate differences in meters						dr in [m]
		Geocentric system			Local system			
		$\overline{dX}$	$\overline{dY}$	$\overline{dZ}$	$\overline{dN}$	$\overline{dE}$	$\overline{dh}$	
1982	SADOSA GEODOP/MP/	-1.25	0.21	-2.25	-0,72	0.62	-2.40	2.66
	SADOSA GEODOP/SP/	0.08	0.87	-2.75	-2.14	0.79	-1.77	3.30
	SADOSA SPPENC	-1.69	-1.25	-1.60	0.38	-0.60	-2.54	3.09
	GEODOP/MP/ GEODOP/SP/	1.33	0.66	-0.50	-1.42	0.17	0.63	2.02
	GEODOP/MP/ SPPENC	-0.44	-1.46	0.65	1.10	-1.23	-0.14	2.33
	GEODOP/SP/ SPPENC	-1.76	-2.12	1.15	2.51	-1.39	-0.77	3.37
	mean value standard deviation							2.80 ±0.55
1980	SADOSA GEODOP/TL/	-1.77	0.16	-2.20	-0,32	0.79	-2.70	3.34
	SADOSA GEODOP/SP/	-0.07	0.95	-0.50	-0.54	0.93	-0.18	1.93
	SADOSA SPPENC	0.14	-0.19	-3.20	-2.25	-0.27	-2.28	3.90
	GEODOP/TL/ GEODOP/SP/	1.70	0.79	1.70	-0.22	0.17	2.53	3.71
	GEODOP/TL/ SPPENC	1.91	-0.35	-1.01	-1.94	-1.03	0.43	3.68
	GEODOP/SP/ SPPENC	0.22	-1.14	-2.70	-1.72	-1.20	-2.10	3.85
	mean value standard deviation							3.40 ±0.75

TABLE 2 Summary of average values of the coordinate differencies and linear deviations evaluated from different program solutions for the two campaigns, HDOC80 and HDOC82

computational procedure of BE, appearing of the air drag compensated NOVA satellite, etc./ in the period 1980-1982.

Note that much more agreement was found on the results of the West European Doppler observation campaigns with the use of PE, see Schlüter and Wilson /1981/, Ehlert et al. /1982/. Careful comparisons show that the average consistency of the West

Site	Coordinate differences in meters						dr in [m]
	Geocentric system			Local system			
	dX	dY	dZ	dN	dE	dh	
Solution:	SADOSA		1982	minus		1980	
Szőlőhegy	-4.71	-0.75	-1.73	-2.24	-0.87	-4.46	5.07
Cárlahom	-4.68	-0.91	-2.50	-1.83	-0.47	-5.04	5.38
Magoska	-5.31	-0.31	-2.31	-2.25	-1.67	-5.08	5.80
Leponyahalom	-4.68	-1.34	-1.42	-2.59	-0.50	-4.33	5.07
Bodzás	-5.27	-1.06	-1.83	-2.59	-0.88	-4.98	5.68
mean	-4.93	-0.87	-1.96	-2.30	-0.88	-4.78	5.40
st. dev.	±0.33	±0.38	±0.44	±0.31	±0.48	±0.35	±0.34
Solution:	GEODOP/MP/		1982	minus		1980	
Szőlőhegy	-3.93	0.24	-2.44	-1.01	-1.54	-4.25	4.63
Cárlahom	-3.28	-1.31	-2.24	-1.08	0.32	-4.03	4.18
Magoska	-7.06	0.50	-2.78	-2.90	-3.04	-6.33	7.60
Leponyahalom	-4.87	-1.76	-0.89	-3.19	-0.18	-4.16	5.25
Bodzás	-4.89	-1.68	-2.10	-2.10	-0.18	-5.08	5.58
mean	-4.81	-0.80	-2.09	-2.06	-0.92	-4.77	5.45
st. dev.	±1.43	±1.09	±0.72	±1.01	±1.37	±0.96	±1.32
Solution:	GEODOP/SP/		1982	minus		1980	
Szőlőhegy	-7.62	-0.24	0.37	-5.60	-2.33	-4.65	7.63
Cárlahom	-3.90	-0.86	-1.01	-2.28	-0.29	-3.43	4.12
Magoska	-5.73	2.37	0.64	-3.78	-4.34	-2.49	6.23
Leponyahalom	-2.32	-1.24	0.15	-2.03	-0.29	-1.66	2.63
Bodzás	-5.26	0.38	1.75	-4.69	-2.21	-2.01	5.56
mean	-4.97	0.08	0.38	-3.68	-1.89	-2.85	5.23
st. dev.	±1.99	±1.42	±0.99	±1.53	±1.69	±1.21	±1.93
Solution:	SPPENC		1982	minus		1980	
Szőlőhegy	-2.40	0.39	-2.64	-0.23	-1.17	-3.39	3.59
Cárlahom	-4.86	-2.03	-3.18	-1.72	0.56	-5.88	6.15
Magoska	-1.63	4.53	-4.23	-2.88	-4.86	-3.08	6.41
Leponyahalom	-0.35	-1.77	-3.40	-1.59	-1.51	-3.16	3.85
Bodzás	-0.61	3.28	-3.48	-2.85	-3.24	-2.11	4.82
mean	-1.97	0.88	-3.39	-1.85	-2.04	-3.52	4.96
st. dev.	±1.81	±2.95	±0.57	±1.09	±2.07	±1.41	±1.29

TABLE 3 Coordinate differences between results of the two campaigns /HDOC 80 and HDOC82/ for different program solu- solutions and the linear deviations dr in positions

European Doppler networks is better than 0.5 m and the relative accuracy is better than 1 ppm.

Chord lengths between	Differences /in m/ in Chord lengths			
	GEODOP 1982 minus 1980	SADOSA 1982 minus 1980	SADOSA minus GEODOP 1980	SADOSA minus GEODOP 1982
Szőlőhegy - Cárlahom	1.65	0.06	1.67	0.08
Szőlőhegy - Magoska	2.25	0.39	1.52	-0.33
Szőlőhegy - Leponyahalom	-1.52	-0.56	-0.56	0.39
Szőlőhegy - Bodzás	-2.01	-0.32	-2.44	-0.76
Cárlahom - Magoska	3.26	0.84	2.53	0.11
Cárlahom - Leponyahalom	-0.13	-0.49	0.82	0.45
Cárlahom - Bodzás	-0.31	-0.28	-0.65	-0.62
Magoska - Leponyahalom	-1.39	-0.84	-1.21	-0.67
Magoska - Bodzás	0.77	-0.41	0.01	-1.17
Leponyahalom - Bodzás	0.60	-0.33	1.13	0.20
mean value standard deviation	0.32 ±1.72	-0.19 ±0.49	0.28 ±1.52	-0.23 ±0.55
Mean values and errors of differences between n(n-1)/2 chord lengths of the Doppler networks, HDOC80 /n=6/ and HDOC82 /n=14/		mean st. dev.	-0.55 ±1.78	-0.10 ±0.59

TABLE 4 Summary of differences between chord lengths evaluated from the results of the campaigns HDOC80 and HDOC82 in different program /MP/ solutions

Chord lengths between identical points of both campaigns within program systems, and chord lengths betwenn all points evaluated from different program solutions within campaigns have been compared. The results are given in Table 4. They demonstrate a remarkable consistency, despite the large coordinate differences in the two years between HDOC80 and HDOC82. Solutions of SADOSA program system for both campaigns agree very well.

3. LONG TERM CONSISTENCY OF THE STATION COORDINATES

The Satellite Geodetic Observatory /SGO/ in Hungary routinely computes the positions of the station Penc using the TRANSIT satellites in order to monitor the stability of the coordinate system established by the BE, cf. Ádám /1984/. The resulting Doppler station coordinate time series are analyzed for long-term repeatability and periodic behaviour for different time intervals. The least squares sepctral analysis as developed by Vaníček, see Vaníček /1971/, Wells and Vaníček /1978/, indicates clearly periodic terms especially in the height components. However, time variation of the coordinate time series is lately modified. This feature is clearly visible on Fig. 2 which shows the power spectral functions s/ω/ of the height coordinate time series of different time intervals for the station Penc. The periods detected on the height coordinates are summarized in Table 5. Time variation of both parts /1978-1980 and

Time interval	Periods in days
1978-1980	373, 252, 198, 121, 99, 72, 59, 48, 29
1981-1984	296, 153, 126, 76, 45
1978-1984	1432, 448, 320, 198, 124, 45, 22

TABLE 5 Periods detected on the height coordinate time series of different time intervals

1981-1984/ of the ehight coordinates differs from each other. This analysis also indicates that some changes might be on certain part of the BE Doppler satellite system.

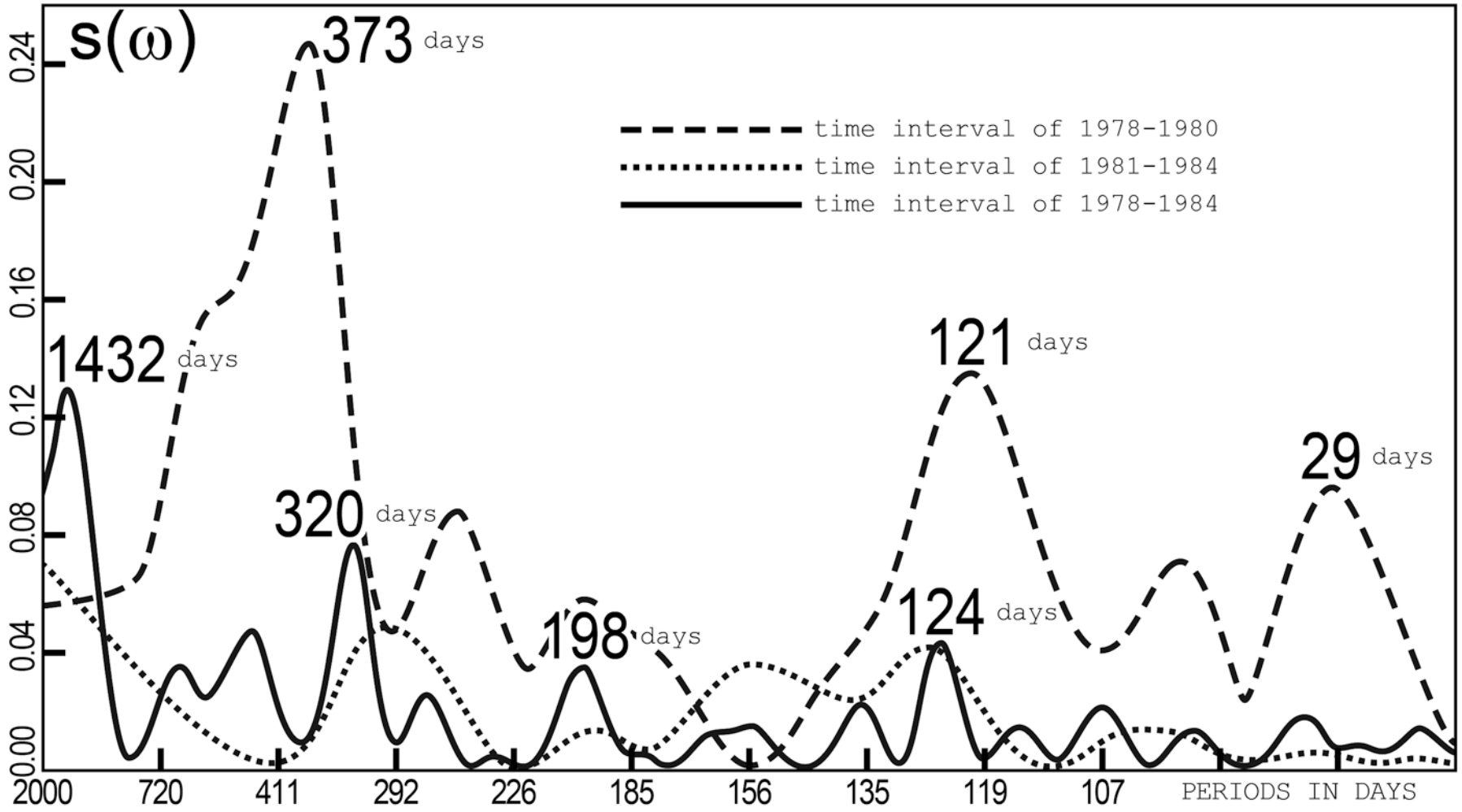

FIGURE 2 Power spectrum functions of the height coordinate time series covering different time intervals

In order to compare and to study the time-dependence features of our Doppler station coordinates at Penc with those derived at other stations close to Penc, a multiple time series analysis of coordinate sets of the stations Bruxelles /Belgium/, Graz-Lustbühel /Austria/, Wettzell /FRG/ and Penc /Hungary/ has been carried out, cf. Ádám /1985/. Since the most significant periodicities are detected in the height coordinate time series at all stations, we used only the height coordinates. A collection of height coordinates derived at the stations shown on Figure 3 is a multiple or vector-valued time series. Each height coordinate time series contains 100 values with 10-day equidistant time interval. The height coordinates plotted on Figure 3 cover the time from early of April, 1978 to end of December, 1980. The coordinates of Bruxelles and Graz-Lustbühel were derived from the PE with the program systems ORB and GEODOP, respectively, cf. Dehant and Paquet /1983/, Rinner and Pesec /1979/. The height coordinates of station Wettzell and Penc presented on Figure 3 were deduced by using the BE with the program systems GEODOP and SADOSA, respectively, cf. Schlüter et al. /1982/, Ádám /1984/.

An inspection of the Figure 3 suggests that the time changes of individual height series differ from each other, and at the same time, the individual height series are quite strongly interrelated. These features are well represented by the autocorrelation and cross correlation functions of the height series plotted on Figure 4 with the abbreviations of B=Bruxelles, G= Graz-Lustbühel, W=Wettzell and P=Penc. Each height series was analyzed by least squares spectral analysis. The corresponding power spectrum functions are displayed on Figure 5 against periods of time in days. Each height series displays smallish linear trend. The different time changes of the individual height series are clearly visible on this Figure. The periods detected on the individual height coordinate series are summarized in Table 6, where values in brackets are most significant. Considering the height coordinate series of PE solutions, on the height series of station Bruxelles, with high peak only one-year period appears, and at the same time, on the height coordinates of station Graz-Lustbühel two main peaks appeared. The

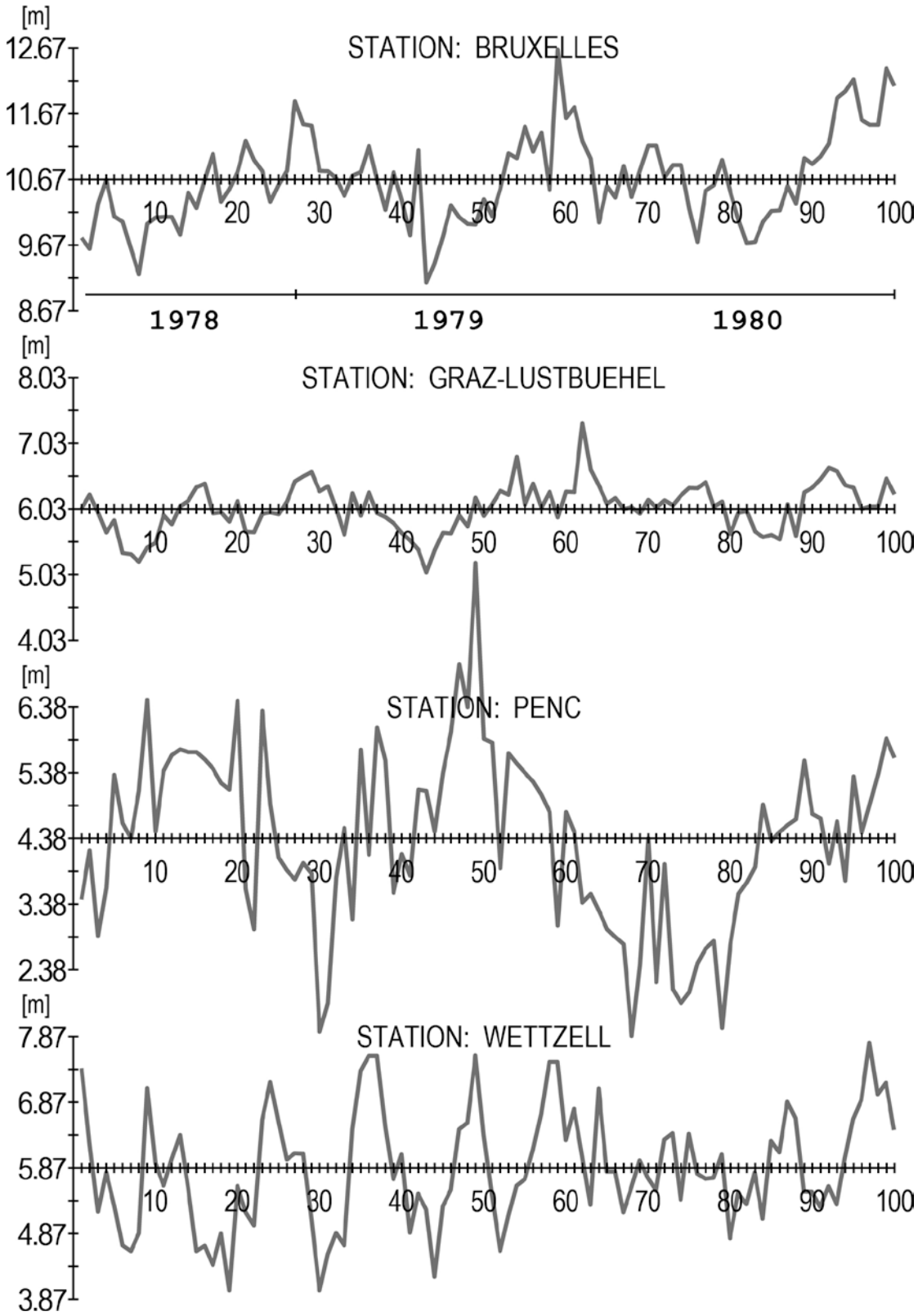

FIGURE 3 Height coordinate time series of the stations. Mean values are as follows: Bruxelles: 150.67 m /±0.70/, Graz-Lustbühel: 496.03 m /±0.37/, Wettzell: 665.87 m /±0.88/ and Penc: 294.38 m /±1.34/.

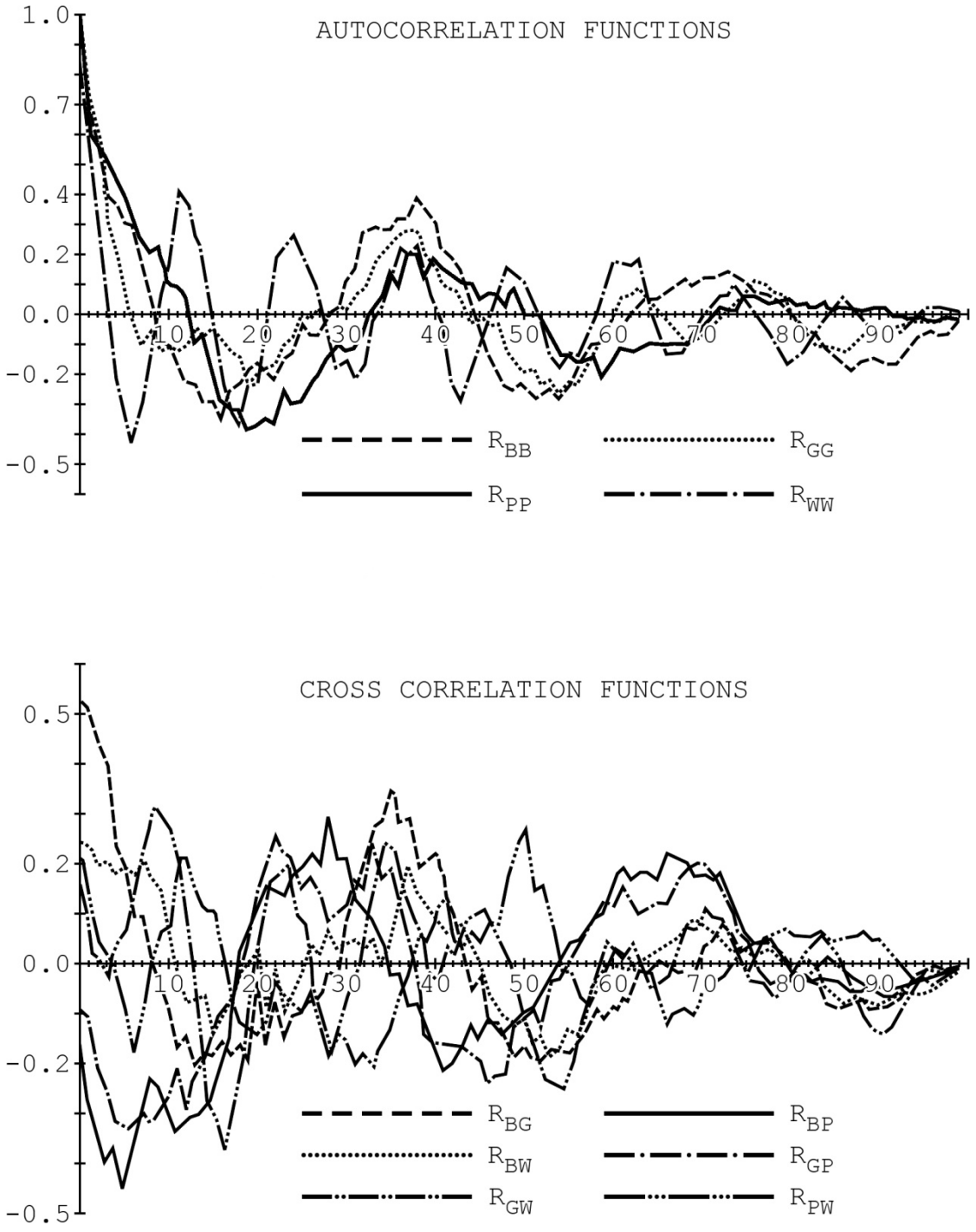

FIGURE 4 Autocorrelation and cross correlation functions of the height series.

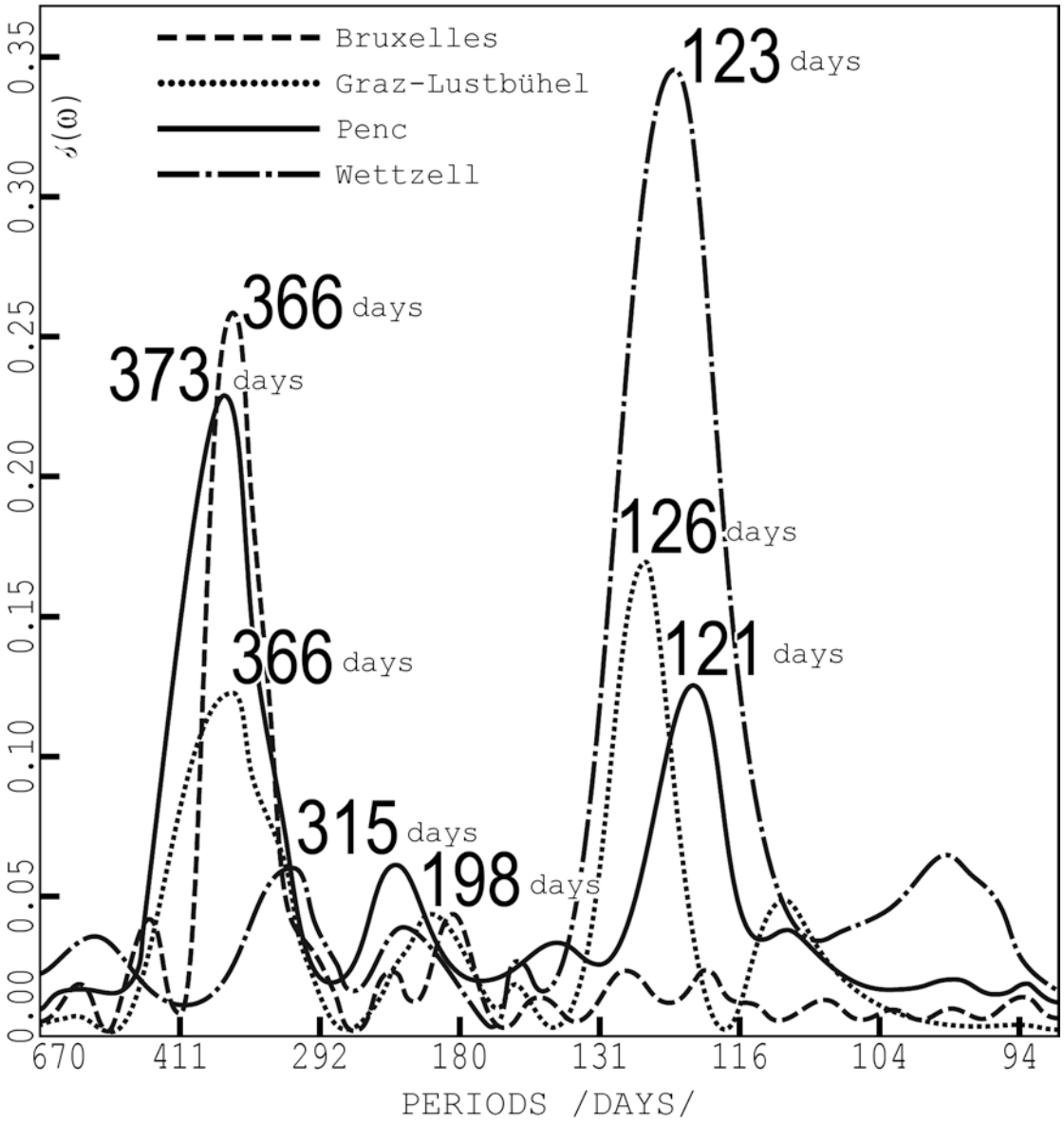

FIGURE 5 Power spectrum functions of the height series

Station	periods in days
Bruxelles	/366/,198,107,82,64,52,35,21
Graz-Lustb.	/366/,187,159,/126/,112
Wettzell	529,315,194,145,/123/,99,77
Penc	/373/,252,198,/121/,98,72,59,48,/29/

TABLE 6 Periods detected on the height coordinates of the stations /values in brackets are most significant/

time changes of height series of BE solutions also differ from each other. The different time change features shown on Figure 4 and 5 might partly be due to the different statistical data handling procedure of the individual program systems.

Note that the time variation of the Doppler coordinates is well known, see e.g. Anderle /1975/, Ádám /1984/, Dehant and Paquet /1983/, Rinner and Pesec /1979/, Schlüter et al. /1982/. Basically three characteristic periods were detected during independent investigations of the individual station coordinate series by spectral analysis: four months, one year and twelve years. It is noted by Dehant and Paquet /1983/ that the physical origin of the height variations is mainly related to the ionospheric refraction which perturbs the radio signals. A strong correlation between time dependent variations of Doppler height and sunspot numbers has been found by Tscherning and Goad /1985/. A possible explanation of the four-month periodicity is given by Borza and Varga /1982/ claiming that the fluctuation is a virtual effect due to a non adequate use of long period harmonics of the geopotential in the orbital model. This effect may be also a consequence of an error in the atmospheric model used in the BE computations, as noted by Almár and Ádám /1982/, because the perigee of any TRANSIT satellite is crossing the diurnal atmospheric bulge also with a four months period. Hence the problem of the time dependent variations of Doppler station coordinates seems much more complex, because on the coordinate series all physical and model effects are superimposed. Therefore, it would be extremely interesting to perform a multiple time series analysis on the TRANET station coordinate set covering nearly a 20-year time interval as suggested by Ádám /1985/.

4. EXTERNAL ERRORS OF THE DOPPLER SATELLITE SYSTEMS

Internal consistency excludes most of the external errors of Doppler satellite system itself. The estimation of the system error is usually based on external comparisons between Doppler derived coordinates and those obtained from the external standards. The serious source of the external consistency is the

error of ephemeris systems.

The origin, scale and orientation of the PE Doppler system are defined by the adopted coordinates of the TRANET stations. The current adopted coordinates define the NSWC 9Z-2 coordinate system /gravity model used is NSWC 10E-2/. The NSWC 9Z-2 system and its predecessor NWL 9D were extensively compared to other independent satellite and astronomical systems, see e.g. Hothem /1979, 1983/, Hothem et al. /1982/. It was shown that the NWL 9D /and NSWC 9Z-2/ requires corrections of about +4 m in the Z coordinate, -0.4 ppm in scale, and +0.8″ in longitude east in order to be consistent with international conventions for scale /the speed of light/, pole and longitude orientations.

Coordinate system of the BE is NWL 10D /gravity model used is WGS 72/. According to the investigations made by Jenkins and Leroy /1979/, this coordinate system is rather close to the NSWC 9Z-2. The BE and PE coordinate systems defined by globally distributed tracking stations differ by only two or three metres. However, results of some national and international West European Doppler Observation Campaigns, se e.g. Ashkenazi /1979/, Boucher et al. /1981/, Schlüter and Pesec /1982/, Seeger et al. /1979/, show considerable differences in the transformation parameters obtained between estimated coordinate systems of the BE and PE solutions. One of the major unresolved questions at present is to find an appropriate transformation between coordinate systems of BE and PE.

5. SUMMARY

Considering the results of the Hungarian Doppler Observation Campaigns, HDOC80 and HDOC82, with the use of BE there is a slightly higher internal consistence of the results obtained by the multilocation than by the translocation. The internal agreements within campaigns are better. The systematic differences between HDOC80 and HDOC82 Doppler solution results are

much more higher than expected. However, the chord lengths comparisons show considerable internal consistency.

Time variation of Doppler station coordinate time series at station Penc, Hungary, is lately modified. Time changes of different station coordinate time series differ from each other. In this field further investigations are also needed.

For the transformation of the BE system into a system which is most consistent with the conventional system, we should have twofold transformation: one of them is a transformation between systems of the BE and PE, and the other is a transformation from the PE. This latter transformation is quite clear because of the well known transformation parameters. A more difficult problem is to find an appropriate transformation between systems of the BE and PE.

ACKNOWLEDGEMENTS

I thank Dr. Wolfgang Schlüter /Satellite Observation Station, Wettzell, FRG/, Professor Paul Paquet /Observatoire Royal de Belgique, Bruxelles, Belgium/ and Dr. Peter Pesec /Observatorium Graz-Lustbühel, Austria/ to have provided me with the Doppler coordinates.

This work has been partly prepared during the author’s visit at the Department of Geodetic Science, Stuttgart University, FRG, as an Alexander von Humboldt fellow with Professor Dr. E. W. Grafarend as his host and has been presented to the Joint Meeting FIG Study Groups 5B and 5C on “Inertial, Doppler and GPS Measurements for National and Engineering Surveys”, Munich, July 1-3, 1985.

The financial support of the author’s participation in the Joint Meeting of the FIG Study Groups 5B and 5C by the Alexander von Humboldt-Foundation is also gratefully acknowledged.

REFERENCES

ALMÁR,I.-ÁDÁM,J.: The role of a geodynamic observatory in the geodetic nat. Paper presented at the Intercosmos Scientific Conference, Suzdal, USSR, 1982.

ALPÁR, GY.-BÖLCSVÖLGYINÉ BÁN,M.-GAZSÓ,M.: Comparison of astro-gravimetric spherical harmonic and satellite Doppler geoidal heights in Hungary. Proceedings of the ISSTG Symposium Vol. 1, pp. 32-46, Sopron, Hungary, 1984.

ANDERLE,R.J.: Long term consistency in positions of sites determined from Doppler satellite observations. NSWC Report, TR-3433, November 1975.

ANDERLE,R.J.: Polar Motion Determined by Doppler Satellite Observations. Bull.Géod. 50/1976/, pp. 377-390.

ANDERLE,R.J.-MALYEVAC,C.A.: Current plate motions based on Doppler Satellite observations. Geophysical Research Letters, Vol. 10, No. 1, pp. 67-70, January, 1983.

ARUR,M.G.: Experiments for Improved Positioning by means of Integrated Doppler Satellite Observations and the NNSS Broadcast Ephemeris. Paper presented at the 2nd Int.Geod.Symp. on Satellite Doppler Positioning, Austin, USA, 1979.

ASHKENAZI,V.: Recent Doppler Campaigns in the United Kingdom. Paper presented at the 2nd Int.Geod.Symp. on Satellite Doppler Positioning, Austin, USA, 1979.

ÁDÁM,J.: Investigation of the similarity transformation between Doppler and terrestrial geodetic networks in Hungary /in Hungarian/. Geodézia és Kartográfia, 34/1982/, 2/89-97/.

ÁDÁM,J.: Investigation of Hungary’s geodetic control network based on coordinates got by Doppler Satellite Observations /in Hungarian/. Geodézia és Kartográfia, 36/1984/, 5/328-339/.

ÁDÁM,J.: A Least Squares Spectral Analysis of the Doppler Coordinate Time Series Obtained at the Satellite Geodetic Observatory, Station Penc, Hungary. Proceedings of the ISSTG Symposium, Vol. 2, pp. 131-140, Sopron, Hungary, 1984.

ÁDÁM,J.: Empirical Multiple Time Series Analysis of Station Coordinates Derived from Doppler Satellite Observations. Paper presented at the 1st Hotine-Marussi Symposium on Mathematical Geodesy, Roma, Accademia dei Lincei, 3-6 June, 1985.

BALDI,P.-ZERBRINI,S.-LOHMAR,F.J.-MARCHESINI,C.: Doppler Measurements for the Strengthening of the Italian Geodetic Network. Bolletino di Geodesia e Scienze Affini, Anno XLIII, No. 1, pp. 13-24, 1983.

BORZA,T.-VARGA,M.: An attempt for explanation of the four-month period in Doppler position fix data. Paper presented at the Intercosmos Scientific Conference, Suzdal, USSR, 1982.

BOUCHER,C.-PAQUET,P.-WILSON,P.: Final report on the observations and computations carried out in the Second European Doppler Observation Campaign /EDOC-2/. DGK, Reihe B, No. 255, 1981.

CHEN,J.Y.: Geodetic Datum and Doppler Positioning. Dissertation, Mitteilungen des Geod.Inst.Techn.Univ. Graz, Folge 39, Graz, 1982.

COLIČ,K.-LOHMAR,F.J.-SOLARIČ,M.: An indirect way to determine the geocentric coordinates of the Hvar Doppler station in PE-system starting from two new MPBE-solutions for the project IDOC-82. Observations of Artificial Earth Satellites, No. 23, pp. 477-486, Praha, 1984.

CZOBOR,Á.: Satellite Doppler measurements for the Hungarian geodetic network /in Hungarian/. Geodézia és Kartográfia, 34/1982/, 2/81-84/.

DEHANT,V.-PAQUET,P.: Modeling of the apparent height variations of a TRANET station. Bull.Géod., 57/1983/, pp. 354-364.

EHLERT,D.-SCHLÜTER,W.-WILSON,P.: Combining the results of simultaneous Doppler observation campaigns – Demonstrated on the basis of the results of European measurements. Paper presented at the 3rd Int.Geod.Symp. on Satellite Doppler Positioning, Las Cruces, New Mexico, 1982.

FREVEL,H.-HASCH,B.-LOHMAR,F.J.: Die Rheinland-Pfälzische Dopplerkampagne RPDOC’83. ZfV 8/1984, pp. 397-406.

HEISTER,H.-GLASMACHER,H.: Satelliten-Dopplermessungen im Testnetz Inntal. In Schödlbauer,A. and Welsch,W. /Eds./: Satelliten-Doppler.Messungen, Schriftenreihe HSBw, Heft 15, pp. 307-326, München, 1984.

HOTHEM,L.D.: Determination of accuracy, orientation and scale of satellite Doppler point-positioning coordinates. Paper presented at the 2nd Int.Geod.Symp. on Satellite Doppler Positioning, Austin, Texas, USA, 1979.

HOTHEM, L.D.-VINCENTY,T.-MOOSE,R.E.: Relationship between Doppler and other advanced geodetic system measurements based on global data. Paper presented at the 3rd Int.Geod.Symp. on Satellite Doppler Positioning, Las Cruces, New Mexico, 1982.

HOTHEM,L.D.: Analysis of Doppler, Satellite Laser, VLBI and Terrestrial Coordinate Systems. Unpublished Paper, presented at the IUGG XVIII General Assembly, Hamburg, FRG, 1983.

JENKINS,R.E.-LEROY,C.F.: “Nroadcast” versus “Precise” Ephemeris Apples and Oranges? Paper presented at the 2nd Int.Geod. Symp. on Satellite Doppler Positioning, Austin, USA, 1979.

JOÓ,I.-ÁDÁM,J.-CZOBOR,Á.-MIHÁLY,SZ.: Improvement of the Hungarian National Geodetic Control Network by Satellite Doppler Positioning. Paper presented at the Joint Meeting FIG Study Groups 5B and 5C on “Inertial, Doppler and GPS Measurements for National and Engineering Surveys”, München, July 1985.

KOUBA,J.: Satellite Doppler positioning for geodynamics. Ann. Géophys., t. 37, fasc. 1, 1981, pp. 205-212.

KOUBA,J.: A Review of Geodetic and Geodynamic Satellite Doppler Positioning. Rev. Geophys. Space Phys., 21/1983/, pp. 27-40.

MIHÁLY,SZ.: Results of satellite Doppler positioning in Hungary’s geodetic network computed by SALOSA /in Hungarian/. Geodézia és Kartográfia, 34/1982/, 2/84-88/.

MIHÁLY,SZ.: Hungarian geodetic network computation using Doppler observations performed in 1982 /in Hungarian/. Geodézia és Kartográfia, 36/1984/, 5/319-328/.

PACHELSKY,W.: Position of the Station Borowiec in the Doppler Observation Campaign WEDOC80. Artificial Satellites, Vol. 17, Nos. 2-3, pp. 11-21, 1982.

PESEC,P.-MIHÁLY,SZ.: West-East European Doppler Observation Campaign WEDOC-2; Preliminary Results. Proceedings of the ISSTG Symposium, Vol. 2, pp. 141-150, Sopron, 1984.

PESEC,P.-SCHLÜTER,W.: Deutsch-Österreichische Dopplerkampagne, Auswertung und Ergebnisse. DGK, Reihe B, No. 260, 1982.

RINNER,K.-PESEC,P.: Doppler activities in Austria. Paper presented at the XVII. IUGG General Assembly, Canberra, 1979.

RINNER,K.-PESEC.P.: West-East European Doppler Observation Campaign: Final Results. Manuscripta Geodaetica, Vol. 7/1982/, pp. 117-132.

RUTSCHEIDT,E.H.: A Review of Some Aspects of Doppler Satellite Geodesy. CSTG Bulletin, No. 4, pp. 167-185, Columbus, 1982.

SCHLÜTER,W.-WILSON,P.: Combining the results of European Doppler Observation Campaigns computed at the IFAG/SFB78. Paper presented at the Int.Symp. on Geodetic Networks and Computations, München, FRG, 1981.

SCHLÜTER,W.-BLENSKI,G.-HERZBERGER,K.-MÜLLER,W.-STÖGER,R.: Results from permanent Doppler observations at Wettzell using broadcast and precise ephemeris. Paper presented at the 3rd Int.Geod.Symp. on Satellite Doppler Positioning, Las Cruces, New Mexico, USA, 1982.

SEEGER,H.-SCHLÜTER,W.-HERZBERGER,K.-KRAMER,F.-SOLTAU,G.: The German-Austrian/German Part/ and the EROS Doppler Observation Campaigns /DÖDOC and EROS-DOC/. Paper presented at the 2nd Int.Geod.Symp. on Satellite Doppler Positioning, Austin, 1979.

STOMMA,A.: Internal Inconsistence of Reference System Determined by On-board Ephemerides of NNSS Satellites. Artificial Satellites, Vol. 17, Nos. 2-3, pp. 23-32, 1982.

TSCHERNING,C.C.-GOAD,C.C.: Correlation Between Time Dependent Variations of Doppler-Determined Height and Sunspot Numbers. J.Geophys.Res., Vol. 90, No. B6, pp. 4589-4596, 1985.

VANIČEK,P.: Further Development and Properties of the Spectral Analysis by Least Squares. Astrophysics and Space Science, 12/1971/, pp. 10-33.

WELLS,D.E.: Doppler Satellite Control. Techn.Rep. No. 29, Dep. of Surv.Eng., Univ. of New Brunswick, Canada, 1974.

WELLS, D.E.-VANIČEK,P.: Least Squares Spectral Analysis. Techn. Rep. No. 84, Dep. of Surv.Eng., Univ. of New Brunswick, Fredericton, Canada, 1978.

ZIEGLER,R.E.: Ephemeris Comparisons. Paper presented at the 2nd Int. Geod. Symp. on Satellite Doppler Positioning, Austin, Texas, USA, 1979.

IMPROVEMENT OF THE HUNGARIAN NATIONAL GEODETIC CONTROL NETWORK BY SATELLITE DOPPLER POSITIONING

István JOÓ
National Office of Lands and Mapping
H-1860 Budapest, Kossuth Lajos tér 11.

and

József ÁDÁM, Árpád CZOBOR, Szabolcs MIHÁLY
Institute of Geodesy and Cartography
Satellite Geodetiv Observatory
H-1373 Budapest, Pf.546
Hungary

ABSTRACT

In the course of the establishment of the new and advanced geodetic control systems in Hungary, a new geodetic datum identified here as the Hungarian Datum 1972 /HS72/ was introduced. An independent readjustment of our astrogeodetic network was performed in 1972 by using the rotation ellipsoid of the Geodetic Reference System 1967. The HD72 refers to a reference coordinate system located and oriented relatively at the initial terrestrial point Szőlőhegy.

In early of 1980's the Satellite Geodetic Observatory has developed plans to carry out satellite Doppler observations at our primary control network. In a modernization frame of the National Office of Lands and Mapping, in 1980 and 1982 Hungarian Doppler Observation Campaigns /HDOC80 and HDOC82/ were carried out in order to check scale and orientation of the terrestrial network as well as to determine an appropriate set of transformation parameters between HD72 system and both the HDOC80 and HDOC82 Doppler systems. Satellite Doppler observations of both campaigns HDOC80 and HDOC82 were processed by using the home developed SADOSA and the GEODOP-III program systems.

The paper involves an outline of the structure, main characteristics and some results on the accuracy investigations of our primary control and satellite Doppler networks. A short outline is given about our plans for development of the Hungarian geodetic controls to fulfil the requirements of the integrated geodesy.

1. INTRODUCTION

It has been known for a long time, that for any scientific and practical activity, even including most cartographic works, up-to-date execution depends on the availability of a contiguous, homogeneous geodetic network of adequate reliability for the area in question /country, region, continent/.

In Hungary this has been the prevailing standpoint for a long time. Thus, for the planning of scientific investigations and geodetic-cartographic works, for the allocation of financial and technical resources, establishing, maintaining and developing the horizontal control network have always been given high priority to.

During the 10-15 years following the end of World War II, in Hungary completely new horizontal control network has been set up. Later on greatly increased users' demand as well as realized scientific programs /geoid-determination, geodetic confirmation of geodynamic experiments/ have presented much greater requirements for the geodetic networks. Considering these facts, beginning with the end of the 1960s, further development of the existing horizontal and vertical control networks were started in our country.

In our paper the Hungarian fundamental horizontal geodetic control network is presented. Results from the Hungarian Doppler Observation Campaigns HDOC80 and HDOC82 are compared with the Hungarian Datum 1972 /HD72/ values. A short outline is given about our those works – now are in progress – whose aim is to improve the updating of geodetic control networks using the latest equipments and methods of geodesy.

2. THE HORIZONTAL GEODETIC CONTROL NETWORK

2.1. Review of the network

Principal features of the first-order triangulation network of Hungary shown on Fig. 1. are the following:

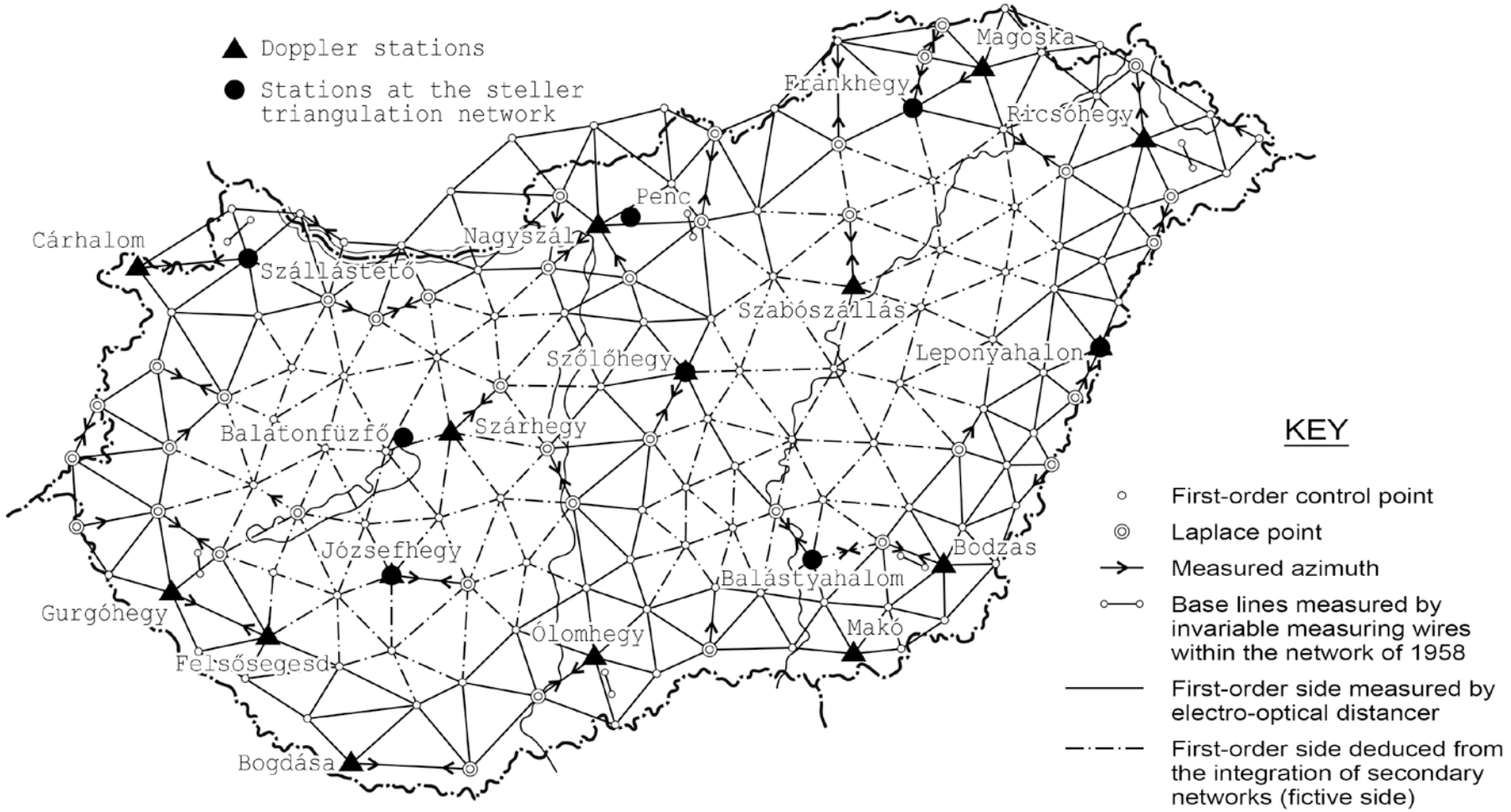

FIGURE 1 The Astrogeodetic Network of Hungary

- average side length: 25-27 km
- number of first-order points: 150
- number of first-order triangles: 250
- number of first-order directions: 798
- number of Laplace-points: 59
- number of measured lengts: 27.

The length of seven sides were determined by the classical method, but all 27 sides were measured by electro-optical distance meter with a mean square error of

$$\mu_D = \pm 3{,}6 \text{ mm},$$

which means a relative error of 1:7 000 000 with

$$D_{average} = 25\text{-}27 \text{ km}.$$

Astronomical positionings are characterized by the mean square errors of

$$\mu_{\varphi,\lambda} = \pm 0{,}08'' \quad \text{and}$$

$$\mu_{\alpha} = \pm /0{,}12 - 0{,}15/''.$$

The reliability of angular measurements are characterized by

$$\mu_{Ferrero} = \pm 0{,}403'' \quad \text{and}$$

$$\mu_{o\text{-}direction} = \pm 0{,}434''$$

obtained from the adjustment, and which equals to ±63 mm with lengths of 27 km, corresponding to a relative error of 1:475 000. Further details are presented by JOÓ /1978a, 1983a,b/.

No second-order network has been established in Hungary.

Principal features of the third-order network are the following: 7-8 km average side length, 2126 third-order points, μ_{angle} = ±0,46", linear mean square error obtained by the adjustment is ±/1,5-2,5/ cm, corresponding to a relative error of 1:300 000.

Based on the primary network, establishment of the fourth-order network is at present under progress in Hungary. Its point density is 1 point/2-3 km^2. Linear reliability of the points is ±/2-3/ cm, corresponding to a relative error of

1:50 000 – 1:60 000.

The fourth-order network was complete for 72% of Hungary's area at the end of 1984.

From the viewpoint of the survival of the first-order network, construction of reinforced concrete towers on 100 first-order points is important, see JOÓ /1978b/. Measurements from these towers can be performed at any time and thus, these towers offer a fair chance for repeated measurements needed for geo-dynamical analyses. Average heights of the towers is 20,8 m, the highest of them is 30 m.

2.2. Development of the horizontal control network

Shortly after finishing the establishment of the fundamental network, its checking was subsequently started which consists of the following works:

- detailed critical examination of the measurements
- performance of complementary measurements /angular and distance measurements, astronomical positioning/.

On the basis of the critical examination of the triangulation network and complementary measurements, the independent national readjustment of the astrogeodetic network was performed in 1972 using new ellipsoid /IUGG /1967//, and establishing a new geodetic Hungarian Datum /HD72/.

Later investigations to the comparison between the old and new primary horizontal control networks of Hungary have been taken place, especially focussing on the azimuthal values and the scale of these networks, see JOÓ /1979a,b/.

These investigations resulted in the homogeneity and great reliability of the established fundamental network. Despite all these, a plan has been worked out for the refinement of the network by space techniques. It involves satellite Doppler observations and application of the stellar triangulation.

2.3. Concept to updating and further developing of the primary control networks

Recognizing the fact that the increasing requirements of the accuracy can not be achieved without integration of the net-

works, we have initiated a concept of the integrated 3D network. According to this concept.

- A trilateration program has been started. For the uniform scale of the network, a comparison baseline compatible to the features of EDM instruments was established. The scale of it was determined by the Finnish Geodetic Institute, Helsinki, using the scale of the Nummela International Baseline /CZOBOR and KONTTINEN, 1981/.
- A program to establish a geometrically uniform, combined horizontal and vertical network has been worked out. All stations of astrogeodetic network will get precise-levelled heights and all of the basic bench-marks will be tied to the horizontal network /VINCENTY, 1979/.
- Satellite Doppler observations on the 15 first-order stations in the frame of HDEC80 and HDOV82 were carried out to determine the geocentric location of the HD72 network as well as to check the scale and orientation of it /Fig. 2./.

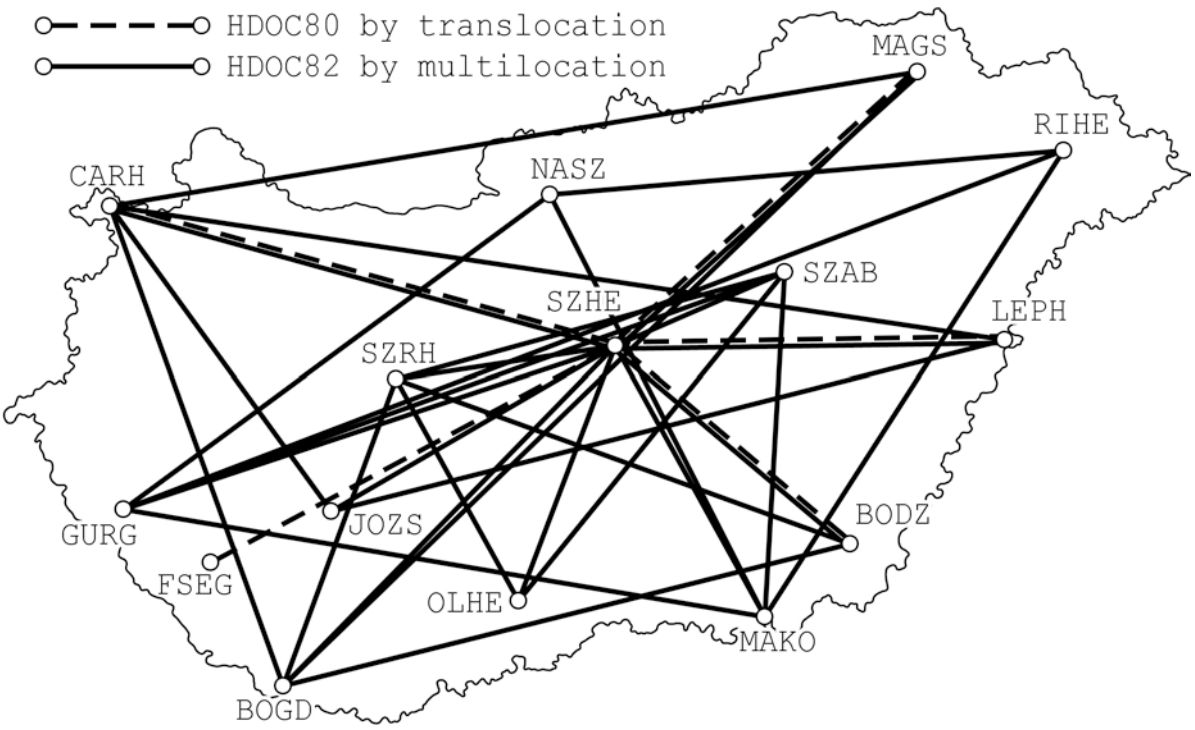

FIGURE 2. Doppler stations in the triangulation network of Hungary

- For the independent network orientation the measurements of a stellar triangulation network containing 7 stations are in progress. Up to the end of 1984, two closed triangles with the average side length of 150 km has been completed /Fig. 3./. Accuracy of the single azimuth is 0.3-0.5 sec of arc.

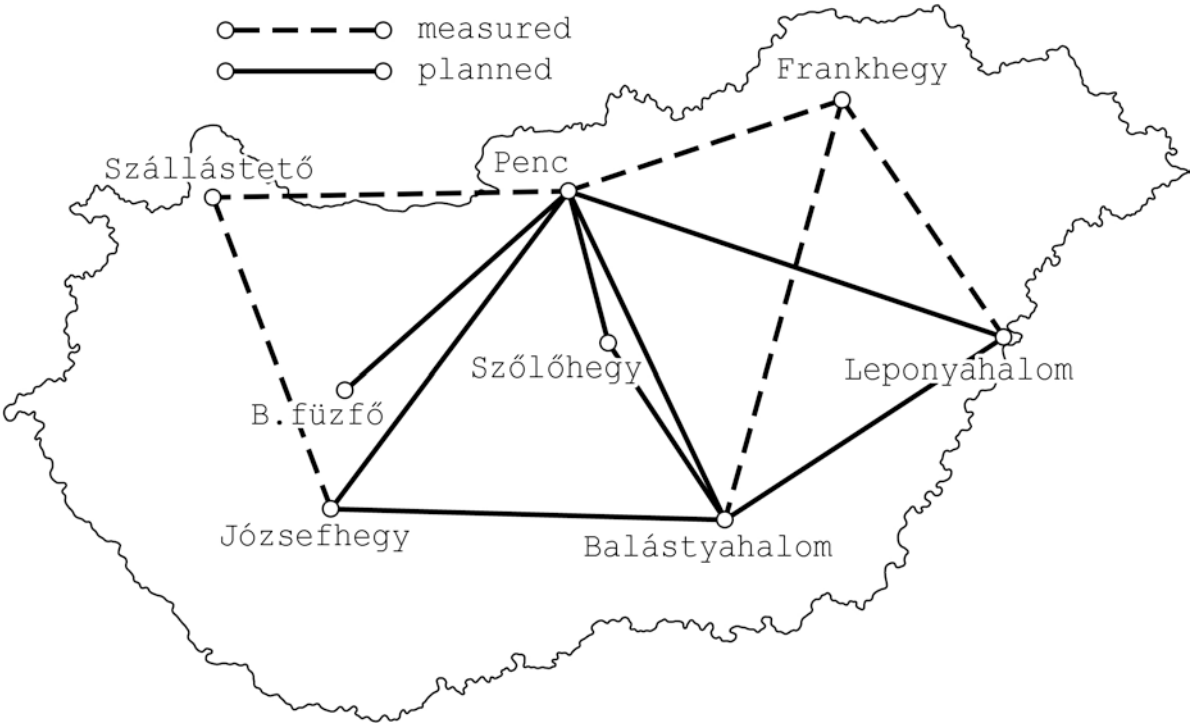

FIGURE 3. Hungarian Stellar Triangulation Network

- To build up of a 3D network it is necessary to include physical parameters. The instrumental coordinate system is tied to the local vertical, e.g. to the normales of the local potential surface. Determination of the local vertical basically depends on the effect of the “internal-zone”. In this decade we intend to finish the program of the detailed gravimetric measurements around 92 points within a radius of 7 km.
- All available measured data in the astrogeodetic network will be arranged into databasis. Beyond the archivation task the databasis software will be able to compile an input

deck for the 3D adjustment, too. The adjustment program package under development has the ability to handle seven parameters per points which are three geometric and four physical ones.

Applying the state of art mathematical solutions it will be possible dynamically to maintenance the network. It means that the newest observations can be included without complete readjustment. In such a way the “scientific network” will be contained the whole measured data and from this up-to-date coordinates we can compute coordinates in any kind of projection system.

3. SATELLITE DOPPLER POSITIONING IN THE HUNGARIAN NETWORK

In a modernization frame mentioned in the previous paragraph, in 1980 and 1982 satellite Doppler positioning campaigns have been carried out on selected points of the Hungarian primary control network.

These Doppler observation campaigns were designed
- to determine geocentrical coordinates of selected points of the HD72 network,
- to compute transformation parameters between the satellite Doppler and the terrestrial geodetic networks,
- to check scaling and orientation of the HD72 network, to investigate the over-all stability and accuracy of the first-order network,
- to detect local distortions in the HD72 network,
- to provide independent source of space orientated geodetic observations for strengthening and readjustment of the primary control network of Hungary,
- to examine the levelling network and the geoid in Hungarian area.

3.1. Doppler observations

The first Hungarian Doppler Observation Campaign in 1980 /HDOC80/ was an experimental and comprised six points translocated by two receivers /JMR-1 and CMA-751/. Details and

results of this campaign are discussed by CZOBOR /1982/ and MIHÁLY /1982/.

The second Hungarian Doppler Observation Campaign 1982 /HDOC82/ has been carried out partly on the experiences obtained in the previous one. In HDOC82 altogether 14 points have been measured, five points common with those of HDOC80. Simultaneously four Doppler receivers were observing: three JMR-1A and a JMR-4A receivers. The Brown's method of interlocking quadrilaterals and the Kouba's multistation method was combined in the observational strategy /BROWN, 1976 and KOUBA, 1976/. The Zentralinstitut für Physik der Erde, GDR, took part in HDOC82 in the frame of a bilateral cooperation. Realization and experiments of the HDOC82 are presented by ÁDÁM and HÖRCSÖKI /1983/ and ÁDÁM et al. /1983/.

The points and their interconnection are shown on Fig. 1. and Fig. 2., respectively. In HDOC80 and HDOC82 all the available satellites of NNSS have been observed.

3.2. Processing and the results

The network adjustment has been carried out using two different program systems. One of them was the SADOSA program developed by Satellite Geodetic Observatory in a cooperation frame with JMR Instruments Inc., USA. The other was the GEODOP program version III developed by Kouba /KOUBA and BOAL, 1975/. Here the SADOSA results are presented. Detailed description of the program is given by BRUNELL et al. /1982/ and MIHÁLY /1983/.

Observations of both the HDOC80 and the HDOC82 have been processed separately in short arc multilocation mode of SADOSA using the Broadcast Ephemerides. The observables were properly weighted and the unknowns for orbital biases and error model parameters were properly constrained.

Principally the quasi-geocentrical coordinates of antenna phase centres, the relative positions between them and the respective reliability estimations are obtained.

Table 1. presents the following main figures of adjustment: effective passes per point with emphasis on the network initial point Szőlőhegy, mean value of the residual r.n.s. /$\overline{\sigma}_v$/, degree of freedom /f/, a'posteriori standard daviation of unit weight /μ_o/ as well as the standard deviation of ellipsoidal latitude, longitude and height /μ_φ, μ_λ, μ_H/.

On the basis of the results by SADOSA it can be pointed out that geometry of the observed orbits is well balanced, the number of passes is even better than satisfactory. The residual r.m.s. partly shows that the receivers operated properly and the mathematical model was suitable.

	HDOC80	HDOC82
Passes per point	43-131	56-168
Passes at initial point	628	347
$\overline{\sigma}_v$	±0.15 m	±0.10 m
F	21470	37756
μ_o	±0.45	±1.18
μ_φ	±0.37 m	±/0.19-0.22/m
μ_λ	±/0.15-0.24/m	±/0.13-0.19/m
μ_H	±/0.12-0.18/m	±/0.08-0.12/m

TABLE 1. Main figures of adjustment by SADOSA

In either adjustment the coordinate system is defined by complexity of all orbits in an averaged manner. This is the system in which the quasi-geocentrical coordinates of the points are given. The standard deviations of quasi-geocentrical coordinates μ_φ, μ_λ and μ_H in Table 1. are interpreted in the above coordiante system considered as an errorless.

The standard deviations of rectangular relative coordinates and of distances between the points derived by SADOSA are given in upper and lower triangles of Table 2. and Table 3. Experiences have proven that these standard deviations are reasonable or a little optimistic. Detailed description of processing and results is presented by MIHÁLY /1982, 1984/.

Stations	SZHE	CARH	MAGS	LEPH	BODZ	FSEG
SZHE		16 17 13	9 11 8	10 12 9	9 12 8	14 19 12
CARH	18		18 20 15	19 21 15	18 21 15	21 25 17
MAGS	10	21		13 16 12	13 16 11	16 22 14
LEPH	12	22	13		14 17 12	17 22 15
BODZ	11	21	11	14		17 22 14
FSEG	17	19	19	22	23	

TABLE 2. Standard deviations of relative X,Y,Z and distances in cm from the HDOC80.

3.3. Comparison of the results from both the campaigns HDOC80 and HDOV82 with HD72

Comparisons of both the Doppler-solutions HDOC80 and HDOC82 with the terrestrial reference coordinates of HD72 have been performed by transforming the three-dimensional terrestrial coordinates to the Doppler results. Transformation equation of the Bursa-Wolf model was used in a least-squares adjustment ÁDÁM /1982b/ and ÁDÁM et al. /1982/ to determine the appropriate set of the transformation parameters.

The different investigational results presented by ÁDÁM /1982a, 1984/ indicate that the coordinate systems of the Doppler /HDOC80 and HDOC82/ and the HD72 terrestrial geodetic networks are translated and rotated with respect to each other. Results of the transformations together with the corresponding residuals are listed in Table 4. and 5. A first investigation of the results leads to the conclusion that significant values have been obtained for the seven parameters by the coordinate set derived from the HDOC82.

Station	SZHE	CARH	MAGS	LEPH	BODZ	GURG	BOGD	JOZS	SZRH	OLHE	NASZ	MAKO	SZAB	RIHE
SZHE		5 9 5	8 12 7	8 13 7	8 13 7	8 12 7	6 10 5	8 12 7	6 10 5	7 11 7	11 17 9	8 12 7	6 9 5	11 17 9
CARH	9		9 14 8	8 13 8	9 15 8	9 15 8	7 12 6	8 12 7	8 13 7	9 14 8	12 19 11	9 15 8	8 13 7	12 19 11
MAGS	10	14		11 17 10	11 17 9	11 17 10	9 14 8	10 16 9	10 16 9	11 17 10	14 21 12	11 17 10	10 15 9	13 21 12
LEPH	13	14	10		11 18 10	11 17 10	10 15 9	9 14 8	10 16 9	11 17 10	14 21 12	11 17 10	10 16 9	13 21 12
BODZ	11	15	8	13		10 17 9	9 14 8	11 17 9	8 14 7	10 16 9	13 21 11	11 17 9	9 15 9	13 21 11
GURG	12	7	16	18	18		9 15 8	11 17 9	9 15 8	10 16 9	10 15 8	7 12 6	7 12 7	9 15 9
BOGD	7	7	11	15	14	12		9 15 8	8 13 7	9 15 8	12 19 11	10 15 8	8 13 7	12 19 11
JOZS	11	9	14	14	18	17	7		10 15 8	11 16 9	13 20 11	11 17 9	9 15 8	13 21 12
SZRH	10	12	14	17	14	14	7	9		8 13 7	12 19 10	9 15 8	7 12 6	12 19 10
OLHE	6	12	12	16	16	16	14	16	9		13 20 11	10 16 9	8 13 7	13 20 11
NASZ	11	20	21	21	17	13	12	14	14	9		10 15 8	11 17 9	11 16 9
MAKO	8	14	9	13	14	12	16	17	14	17	10		7 12 6	9 15 8
SZAB	9	13	10	16	8	12	11	14	12	9	17	6		11 17 9
RIHE	17	20	20	11	13	15	17	20	19	17	17	10	16	

TABLE 3. Standard deviations of relative X,Y,Z and distances in cm from the HDOC82

Transformation	HDOC80 – HD72							HDOC82 – HD72						
translation	ΔX = 40.28 ± 14.10 m ΔY = -88.23 ± 11.19 m ΔZ = - 9.33 ± 14.49 m							ΔX = 58.37 ± 5.59 m ΔY = -81.35 ± 5.72 m ΔZ = -28.93 ± 6.05 m						
scale	K = /2.64 ± 1.32/ ppm							K = /2.12 ± 0.60/ ppm						
rotation	ε_Z = 0.84″ ± 0.29″ ε_Y = 0.47″ ± 0.58″ ε_X = 0.72″ ± 0.37″							ε_Z = 0.77″ ± 0.14″ ε_Y = 0.43″ ± 0.23″ ε_X = 0.36″ ± 0.18″						
	μ_o = ±0.54							μ_o = ±0.35						
Stations	v_X /m/	v_Y /m/	v_Z /m/	v_x /m/	v_y /m/	v_H /m/	v_R /m/	v_X /m/	v_Y /m/	v_Z /m/	v_x /m/	v_y /m/	v_H /m/	v_R /m/
SZHE /Szőlőhegy/	-0.04	-0.18	-0.13	-0.02	-0.16	-0.16	0.23	0.06	-0.21	-0.14	-0.08	-0.22	-0.12	0.26
CARH /Cárhalom/	-0.42	-0.40	0.83	0.94	-0.26	0.26	1.01	-0.22	-0.66	0.29	0.49	-0.57	-0.06	0.75
MAGS /Magoska/	0.35	-0.80	-0.05	-0.06	-0.88	-0.02	0.88	0.15	-0.17	-0.21	-0.20	-0.21	-0.11	0.31
LEPH /Leponyahalom/	-0.22	0.23	-0.30	-0.11	0.29	-0.30	0.44	-0.08	-0.29	-0.01	0.12	-0.24	-0.13	0.30
BODZ /Bodzás/	0.49	0.45	0.14	-0.35	0.24	0.53	0.68	-0.18	0.06	-0.30	-0.10	0.12	-0.32	0.35
FSEG /Felsősegesd/	-0.16	0.71	-0.49	-0.38	0.72	-0.32	0.88	-	-	-	-	-	-	-
GURG /Gurgóhegy/								-0.09	-0.52	-0.35	-0.07	-0.47	-0.42	0.64
BOGD /Bogdása/								0.04	0.39	-0.11	-0.19	0.36	0.03	0.41
JOZS /Józsefhegy/								-0.21	-0.06	0.23	0.32	0.01	0.02	0.32
SZRH /Szárhegy/								0.22	0.93	0.84	0.20	0.81	0.95	1.27
OLHE /Ólomhegy/								-0.26	0.26	-0.40	-0.16	0.33	-0.40	0.54
NASZ /Nagyszál/								-0.25	0.23	-0.03	0.10	0.30	-0.13	0.34
MAKO /Makó/								0.33	0.30	0.32	-0.08	0.16	0.51	0.35
SZAB /Szabószállás/								0.48	0.11	-0.11	-0.43	-0.07	0.25	0.50
RIHE /Ricsóhegy/								0.02	-0.35	0.00	0.09	-0.33	-0.08	0.35
standard deviation	±0.35	±0.56	±0.46	±0.48	±0.55	±0.34	±0.30	±0.23	±0.41	±0.33	±0.24	±0.38	±0.37	±0.27

TABLE 4. Transformation of the Doppler-networks of HDOC80 and HDOC82 to HD72.

The residuals v_X, v_Y and v_Z have been transformed into the more convenient northings $/v_N/$, eastings $/v_E/$ and heights $/v_H/$.

The linear deviation $/v_R/$ computed by $v_R = /v_X^2+v_Y^2+v_Z^2/^{1/2} = /v_N^2+v_E^2+v_H^2/^{1/2}$ is also listed. The residuals of both Doppler results are of the order of a few decimeters; so far the overall conformity between the Doppler and the terrestrial networks turned out to be much higher than it has been expected. From the results of HDOC80 and HDOC82, the average linear deviation $/\overline{v}_R/$ are 0.69 m and 0.49 m, respectively. Both Doppler-solutions with SADOSA and the Broadcast Ephemeris fit very well with the terrestrial network of HD72.

Table 5. includes the correlation matrices of the 7-parameter transformations from both campaigns of HDOC80 and HDOC82. In studying the resulting parameters we have to realize that there exists a strong correlation e.g. between the translation and the rotation parameters.

The chord-lengths derived in all combinations $/n(n-1)/2/$ from the solutions HDOC80 and HDOC82 are compared with the HD72-values. The mean values of the differences in the chord-lengths are 0.65 m and 0.45 m for the relations of HDOC80-HD72 and HDOC82-HD72 with a standard deviation of ±0.68 and ±0.54, respectively. This fact is expressed by the systematic scale difference parameters of 2.60 ppm and 2.12 ppm between both the Doppler and HD72 networks. It is to be noted that according to the investigations presented by JOÓ /1979a,b/, there is a scale difference parameter of similar meaning between the old and the new terrestrial network of Hungary, too.

		ΔX	ΔY	ΔZ	K	ε_Z	ε_Y	ε_X
HDOC80	ΔX	1.00	0.41	-0.65	-0.38	-0.02	0.91	-0.48
	ΔY		1.00	-0.46	-0.17	0.65	0.47	-0.84
	ΔZ			1.00	-0.43	-0.14	-0.89	0.61
	K				1.00	0.00	0.00	0.00
	ε_Z					1.00	0.13	-0.18
	ε_Y						1.00	-0.54
	ε_X							1.00
HDOC82	ΔX	1.00	0.42	-0.55	-0.44	0.06	0.88	-.45
	ΔY		1.00	-0.50	-0.15	0.72	0.51	-0.87
	ΔZ			1.00	-0.46	-0.26	-0.87	0.62
	K				1.00	0.00	0.00	0.00
	ε_Z					1.00	0.26	-0.32
	ε_Y						1.00	-0.54
	ε_X							1.00

TABLE 5. Correlations between the 7 unknowns of the 7 parameter-transformation.

4. REFERENCES

ÁDÁM,J.: Investigation of the similarity transformation between Doppler and terrestrial geodetic networks in Hungary /in Hungarian/. Geodézia és Kartográfia, 34, 2/89-97/, 1982a.

ÁDÁM,J.: On the Determination of Similarity Coordinate Transformation Parameters. Bollettino di Geodesia e Scienze Affini, XLI, 3/283-290/, 1982b.

ÁDÁM,J., HALMOS,F., VARGA,M.: On the concepts of combination of Doppler satellite and terrestrial geodetic networks. Acta Geodaet., Geopphys. et Montanist. Acad. Sci. Hüng. 17/2/, pp. 147-170, 1982.

ÁDÁM,J., CZOBOR,Á., FEJES,I., MIHÁLY,Sz.: Doppler activities at the Satellite Geodetic Observatory, Penc, Hungary. Invited Paper, No. 511.2, FIG XVII. International Congress, Sofia, June 19-28, 1983.

ÁDÁM,J., HÖRCSÖKI,F.: Realization and experiments of the satellite Doppler observations on the terrestrial geodetic network of Hungary in 1982 /in Hungarian/. Geodézia és Kartográfia, 35/1983/, 6/411-417/.

ÁDÁM,J.: Investigation of Hungary's geodetic control network based on coordinates got by Doppler satellite observations /in Hungarian/. Geodézia és Kartográfia, 36/1984/, 5/328-339/.

BROWN,B.C.: Doppler surveying with the JMR-1 receiver. Bull. Géod., 50/1976/, pp. 9-25.

BRUNELL,R.D., MALLA,R., FEJES,I., MIHÁLY,Sz.: Recent Satellite Processing Software Improvements at JMR. The 3rd Int. Geod.Symp. on Satellite Doppler Positioning, Las Cruces, USA, 1982.

CZOBOR,Á., KONTTINEN,R.: Calibration base extension at Penc /in Hungarian/. Geodézia és Kartográfia, 33/1981/, 1/29-33/.

CZOBOR,Á.: Satellite Doppler measurements for the Hungarian geodetic network /in Hungarian/. Geodézia és Kartográfia, 34/1982/, 2/81-82/.

JOÓ,I.: The new horizontal geodetic network of Hungary. Second International Symp. on the Redefinition of North American Geodetic Network, Washington, Apr. 24-28, 1978a.

JOÓ,I.: Die Erhaltung der ungarischen geodätischen Festpunkte. ÖZ, 66. Jahrgang, 1978b.

JOÓ,I.: Comparison between the azimuth values derived from the old and the new high-order control networks of Hungary /in Hungarian/. Geodézia és Kartográfia, 1979a.

JOÓ,I.: A comparison between the scale characteristics of the old and new control networks of Hungary /Hung./, Geodézia és Kartográfia, 1979b.

JOÓ,I.: The Hungarian geodetic horizontal and vertical controls. III. International Symp. on Deformation Measurements by Geodetic Methods, FIG, Aug. 25-27, 1982, Budapest. Akadémiai Kiadó, 1983, Budapest.

JOÓ,I.: Geodetic Control Networks. Hungarian National IAG-Report for the Gen. Assembly of IUGG Hamburg, 1983.

KOUBA,J.: Doppler satellite control in establishing geodetic control networks. Publ. of the Earth Physics Branch, Vol. 45, No. 3, Ottawa, Canada, 1976.

KOUBA,J., BOAL,J.D.: Program GEODOP Documentation. Geodetic Survey of Canada, 1975.

MIHÁLY,Sz.: Results of satellite Doppler positioning in Hungary's geodetic network computed by SADOSA /in Hungarian/. Geodézia és Kartográfia, 34/1982/, 2/84-88/.

MIHÁLY,Sz.: SADOSA Program System /I. Mathematical Description, II. Programming Documentation, III. Operator's Manual/. Hungarian Geodetic Survey /Institute of Geodesy and Cartography/, Satellite Geodetic Observatory, Budapest, 1983.

MIHÁLY,Sz.: Hungarian geodetic network computation using Doppler observations performed in 1982 /in Hungarian/. Geodézia és Kartográfia, 36/1984/, 5/319-328/.

VINCENTY,T.: The HAVAGO Three-Dimensional Adjustment Program. NOAA/NOS NGS 17, Rockville, Md., May 1979.

PRACTICAL RESULTS OF INTERFEROMETRIC PROCESSING OF NNSS DOPPLER OBSERVATIONS

Szabolcs MIHÁLY, Tibor BORZA and István FEJES
Institute of Geodesy and Cartography
Satellite Geodetiv Observatory, Penc
H-1373 Budapest, Po Box 546
Hungary

ABSTRACT

An interferometric approach has been proposed earlier to process Doppler observations of NNSS satellites. To check this approach test network measurements have been carried out on baselines of different lengths and processed by conventional and interferometric methods. The paper gives a short description of the mathematical model and two versions of software developments. The two sets of results have been compared to each other: the distances derived from 4-10 passes agree with distance obtained conventionally from 50 passes within 2-18 cm. Based on 4-10 passes /8-24 hours of observations/ a 10 cm repeatability of interferometric distances has been reliably demonstrated on a N-S oriented 180 km baseline.

1. INTRODUCTION

Earlier an interferometric fringe count processing approach has been proposed to process the Doppler observations of NNSS satellites /FEJES, MIHÁLY 1980 and BRUNELL et al. 1982/. The proposal was followed by software development at the satellite Geodetic Observatory /SGO/, Penc, Hungary in different directions. Some results have already been shown on GPS Symposium in Rockville, USA /MIHÁLY et al. 1985/.

The preliminary investigations and developments have shown the interferometric fringe count processing approach as a promising method to utilize the Doppler observations to ob-

tain high quality results in interstation distance determination. As a consequence three types of test network measurements have been carried out on high precision surveyed baselines of different lengths with purpose to check the method in practice:

- The Penc test on very short baselines /29-210 m/.
- The Finnish-Hungarian Doppler Observation Campaign /FHDOC/ on the High Precision Traverse of Finland on baselines of different lengths /CZOBOR et al. 1984/. The FHDOC has been carried out under the Scientific Agreement between the Finnish Geodetic Institute and the Hungarian Geodetic Survey /20-200 km/.
- The Doppler Baseline Interferometry test measurements /DBLI test/ on relatively long baselines /40-800 km/.

This paper presents a short concept of realization and some practical results obtained with the Penc test and the DBLI test. Interferometric processing of the FHDOC recently is in process, therefor the results will be published only later.

2. THE CONCEPT

2.1. Mathematical model

A detailed description of the mathematical model is given by FEJES and MIHÁLY /1983/. Some main features are described below.
On Fig. 1. let us consider two receivers A and B observing strictly simultaneously the same orbit between points 1 and 2. In this case the N^A and N^B Doppler counts are obtained by receiver A and B, respectively. In the interferometric approach these Doppler counts will be processed in a special way.

The quantities τ_1 and τ_2 on Fig. 1. are the time differences of arrival of the signals from a single source. They are the basic observables of interferometry.
Geometrically their difference can be expressed as follows

$$c\cdot(\tau_2-\tau_1) = \left(|\overline{S}_2-\overline{R}^B| - |\overline{S}_2-\overline{R}^A|\right) - \left(|\overline{S}_1-\overline{R}^B| - |\overline{S}_1-\overline{R}^A|\right) =$$

$$= (\bar{r}_2^B - \bar{r}_2^A) - (\bar{r}_1^B - \bar{r}_1^A) \qquad /1/$$

where c is the light velocity; $\bar{S}$ and $\bar{R}$ are geocentrical vectors and $\bar{r}$ is topocentrical vector with the respective indecis.

The same difference $c \cdot (\tau_2 - \tau_1)$ can be expressed using the results of Doppler observations. In this case after considering the other factors which exist in practice, the expression looks as follows

$$c \cdot (\tau_2 - \tau_1) = \frac{c}{f_s} \cdot \left[N^B \cdot \frac{t^A}{B} - N^A - \Delta f \cdot \Delta t^A \right] -$$

$$- [(r_2^B - r_1^B) - (r_2^A - r_1^A)] -$$

$$- \left[(\dot{r}_2^B - \dot{r}_1^B) - (\dot{r}_2^A - \dot{r}_1^A) \right] \cdot \bar{\tau}_k^B -$$

$$- \left[(\dot{r}_2^A - \dot{r}_1^A) \cdot \Delta\tau_k \right] - \Delta \qquad /2/$$

where
f_s is the satellite frequency,
Δf is the frequency difference of the two receivers,
Δt^A and Δt^B are the time intervals for which the Doppler counts
N^A and N^B were obtained,
r_2^A, r_1^A, r_2^B and r_1^B are the receiver-to-satellite slant ranges at epochs t_2^A and t_1^A, respectively,
$\dot{r}_2^A$, $\dot{r}_1^A$, $\dot{r}_2^B$ and $\dot{r}_1^B$ are the respective slant range rates,
$\bar{\tau}_k^B$ is the receiver time delay at locking-on the k-th orbit for station B,
$\Delta\tau_k$ is the delay difference of the two receivers,
Δ is the sum of different corrections,
t_2^A and t_1^A are the time epochs at satellite associated with the beginning and the end of counting the N^A at receiver A.

Eq.1. and Eq.2. are the basic expressions used in interferometric processing of Doppler observations which we call interferometric fringe count equations.

There are two very important parameters in the model:

the time delay differences $\Delta\tau_k$ and the frequency difference Δf of the two receivers. The accuracy requirements are less than ± 10 μs and ± 0.002 Hz in $\Delta\tau$ and Δf, respectively. A special handling is necessary in the measurements and the processing. The other quantities in the above equations can be approximated well enough.

Summerizing all the error sources, the interferometric fringe counts will be affected generally by an error less than 10 cm.

2.2. Software developments

Two independent versions of software has been developed: an INTERF and a PENCDIP program. In each case the mathematical model is based on the interferometric fringe count processing suggested by FEJES and MIHÁLY (1983/.

2.2.1. INTERF program

The first software version developed by MIHÁLY is called INTERF /Interferometry/. It is an integral part of the SADOSA program system /BRUNELL et al. 1982, MIHÁLY 1983/. The purpose of INTERF is to process synchronously observed NNSS Doppler data for performing percise network adjustment of relative positions and distances between the observing stations /as max. 15 stations/. The INTERF computations are based on auxiliary measurement at the beginning of campaign and on SADOSA computations in a previous stage.

The Δf frequency difference of two receivers necessary for INTERF program /Eq.2./ is obtained pass by pass in SADOSA program of the SADOSA program system with an accuracy of 2 mHz.

The $\Delta\tau_k$ delay difference of the two receivers and the $\bar{\tau}_k^B$ /Eq.2./ is derived for each pass as follows. At the beginning of the observation campaign a $\Delta\tau_0$ delay difference of the two receivers are measured within 1 μs accuracy. At this initial epoch the receiver A is supposed to have a $\bar{\tau}_0^A$ average delay and a $\bar{\tau}_0^B = \bar{\tau}_0^A + \Delta\tau_0$ is computed for the receiver B. It is allowed for $\bar{\tau}_0^A$ to have an error of 50-100 μs or even more. Delays for the receivers A and B at a pass k are computed by the following formulae:

$$\bar{\tau}_k^A = \bar{\tau}_0^A + \sum_{j=1}^{k} \Delta\tau_j^A \ , \qquad /3/$$

$$\bar{\tau}_k^B = \bar{\tau}_0^B + \sum_{j=1}^{k} \Delta\tau_j^B \ , \qquad /4/$$

where $\Delta\tau_j^A$ and $\Delta\tau_j^B$ is the from-pass-to-pass change of the receiver delay at sits A and B, respectively. They are derived using the formula given by LOILER /1980/ with an accuracy better than 1 μs. For proper tracking of these changes all consecutive lock-ons have to be incorporated. Finally, the delay difference is as follows

$$\Delta\tau k = \bar{\tau}_k^B - \bar{\tau}_k^A \qquad /5/$$

with an accuracy 2-10 μs depending on the number of lock-on.

It is of importance to note that the INTERF program uses precise station coordinates and corrected orbits adjusted by the SADOSA program.

The program has been developed and running on a HWB 20 computer, Fortran language, but not fully operating yet.

2.2.2. PENCDIP program

The second software version we call PENCDIP for Penc Doppler Interferometroc Program. The PENCDIP software program package has been developed at the Satellite Geodetic Observatory, Penc, Hungary by Fejes and Borza. The purpose of PENCDIP is to process synchronously observed 2 station NNSS Doppler data for high precision interstation distance determination. An other novel feature in the program is the dynamic integration of the nominal 4.6 s intervalls. Here three to seven, in average five 4.6 s nominal intervalls are integrated depending on the raw data sequence quality. This yealds a more efficient use of raw Doppler data than the conventional rigid 0.5 minute integrations. As a result the processing of a small number of passes /4-10/ gives equivalent or superior accuracy as compared with conventional programs.

In the PENCDIP program structure three main program stage

should be distinguished. The first in which one cassette of a single station is processed. The raw data from the cassette reader is input via the IBM XT RS232 port and stored on magnetic disk. A tape directory is generated which contains all necessary parameters of that particular cassette for further processing.

The second stage selects and handles strictly synchronous station pair data. After dynamic integration the satellite positions are computed using the broadcast ephemerides. The observed fringe counts are also produced. A station pair directory is generated which contains the necessary parameters for the adjustment. This directory may contain the parameters of more than one cassette.

In the third stage the baseline solution is computed by keeping one station fixed /station A/ and computing corrections to the second /station B/. Station A as the reference station should have a well established Doppler point position. This stage is interactive in the sense that the operator may select passes which are to be included in the solution.

The package has been developed and presently running on a standard IBM XT personal computer with DOS 2.0. The programming language is the Microsoft Advanced Basic which is standard for the IBM PC. The program accepts raw JMR data on cassette. Access for other type of data /i.e. MX 1502/ is under consideration. Additional parameters which has to be measured on site /receiver frequency and clock differences as referenced to the UTC and meteorological data/ can be input via the keyboard.

3. PRACTICAL RESULTS

3.1. Penc test

In 1982-1983 a series of Doppler observations has been carried out on the test network of the SGO at Penc. This network is surveyed practically with no error. The distance between the test points varies from 29.77 m to 218.83 m.

The purpose was to prove the fassibility of the interferometric method on very short distances and to analyse the

error budget. The detailed description and some results are given by FEJES and MIHÁLY /1983/.

The error budget investigation showed that a distance accuracy better than 10 cm could be achieved. It was concluded that the distance determination by interferometric method does not depend on the point separation in case of very short distances.

Using the PENCDIP program a revised processing has been carried out on the baseline of 38.56 m length between the PENC6 and PENC1 points. As it is shown in Table 1. altogether 17 passes have been used.

The results are given in Table 2. The deviations from surveyed distance and the repeatibility RMS values show the practical limits of accuracy by the given method.

3.2. DBLI observations and results

The observations were carried out during a four station campaign DBLI in cooperation with the Zentralinstitut für Physik der Erde, Potsdam, GDR. The results of this campaign will be published elsewhere /BORZA et al. 1985/.

Here we report only the observations at station Penc and Baja both in the territory of Hungary. The baseline orientation was dominatly N-S. Approximate distance is 180 km.

The two stations were occupied by JMR-1A type Doppler receivers from 8 to 12 October 1984. As external reference oscillators rubidium standards have been connected to the receivers. During each pass the receiver clock and UTC differences were recorded with an accuracy of 1 μs. Meteorological data were also recorded. The observational set up is demonstrated on Figure 2.

Due to this observational set up the critical parameters for interferometric fringe count processing could be obtained with sufficient accuracy. The differential receiver frequency was known better than 1 mHz at 400 MHz and the differential delay was known better than 2 μs. The absolute receiver delays were computed with respect to the UTC and no satellite clock corrections to the UTC have been taken into account. The point

position of the reference station /Station A: Penc/ has been computed by the SADOSA program system and held fixed in the following PENCDIP processing.

In Table 3. a summary on the BAJA-PENC synchron passes is given. In Table 4. the interstation distance solution results are presented. The data has been divided into independent groups of 4-5 passes and processed by the PENCDIP program. The selection criteria was E-W symmetry of at least 2 pairs of passes within one group. The 90° CA passes were considered either E or W according to the selection requirements.

The average distance from the 7 independent solutions each containing 4-5 passes gave 180102.10 m. The repeatability RMS was ±0.13 m. The average distance from 4 independent solutions each consisting of 8-10 passes gave 180102.08 m. The repeatability RMS was ±0.09 m.

In Table 5. the relative coordinates and the distances obtained by conventional and interferometric methods are presented. Here 50 and 40 passes have been processed by the SADOSA and PENCDIP program, respectively, 38 passes common for both programs. The versions used by SADOSA were: two-station adjustment, two-station synchroneity and rigorous synchroneity of the Doppler counts. The standard deviations derived by SADOSA are demonstrated, too. In Table 5. the distance deviation is surprisedly small, only 2 cm. The deviations in relative coordinates are larger, 34 cm, 41 cm and 32 cm.

3.3. Error analysis of PENCDIP

a/ In case of the Baja-Penc baseline the variance-covariance matrices of different solutions have been analised. Including 4-5 passes into the solution the major axis of the error ellipsoid is oriented eo E-W and about 3 times larger than the minor axis. This means, that the distance error is smallest along the satellite orbit.
Using 8-10 passes in the solution this dependence diminishes. Using 20-25 passes the largest error became N-S oriented probably due to the along track orbit errors.

b/ Up to 180 km distances we have not found any serious unmo-

dellable effect of the atmosphere or the orbit errors. At 600-800 km distances however these factors become significant and the distance error can reach ±1 m when using less than 10 passes.

c/ The accuracy requirement to the initial coordinates for station A is some meters and for station B is 300-500 m.

4. CONCLUSIONS

The concept of interferometric fringe count processing of NNSS data has been demonstrated on a medium long N-S baseline /180 km/ and gave repeatability RMS of ±0.13 m using only 4-5 passes in the adjustment. By including 8 or more passes the repeatability improved to ±0.10 m.

The experiments showed that NNSS Doppler receivers with additional time and frequency reference can be applied to determine distances on 10-20 cm accuracy level depending on the baseline orientation and without requiring interstation visibility from some hundreds m up to 200 km. The necessary observing time is 6-12 hours.

5. REFERENCES

BORZA,T.-FEJES,I.-MIHÁLY,SZ.-DIETRICH,R.-GENDT,G.-LEHMANN,K. 1985: The Doppler Baseline Interferometry Experiment /DBLI/. /Acta Geod. Geoph. et Mont., In preparation/.

BRUNELL,R.D.-MALLA,R.-FEJES,I.-MIHÁLY,SZ. 1982: Recent Satellite Processing Improvements at JMR. Proc. 3rd International Geodetic Symposium on Satellite Doppler Positioning, 8-12 Febr. 1982, Las Cruces, N.M., USA.

CZOBOR,Á.-ÁDÁM,J.-MIHÁLY,SZ.-VASS,T.-PARM,T.-OLLIKAINEN,M. 1984: Preliminary Results of Finnish-Hungarian Doppler Observation Campaign. Paper presented at the Intercosmos Scientific Conference, Section 4, Karlovy-Vary, Czechoslovakia.

FEJES,I.-MIHÁLY,SZ. 1980: A suggestion to use Doppler receiver as VLBI terminals. Paper presented at the Intercosmos Scientific Conference, Sction 6, Albena, Bulgaria.

FEJES,I.-MIHÁLY,SZ. 1983: Interferometric Approach in the NNSS Data Processing. Paper presented at the 34. IAF Congress, Budapest, Hungary, 10-15 October 1983. /Acta Astronautica 1985, in press/.

LOILER,R.D. 1980: JMR-1A Computed Lock-On Time Delay. JMR Memo Number RDL80046, JMR Instruments Inc., Chatsworth, CA, USA.

MIHÁLY,SZ. 1983: SADOSA Program System /I. Mathematical description, II. Operators Manual, III. Programming Documentation/. Institute of Geodesy and Cartography, Satellite Geodetic Observatory, Budapest, Hungary.

MIHÁLY,SZ.-BORZA,T.-FEJES,I. 1985: Interferometric Processing of NNSS Doppler Observations. Proceedings of the 1st International Symposium on Precise Positioning with the GPS, Rockville, Maryland, USA, 15-19 April 1985.

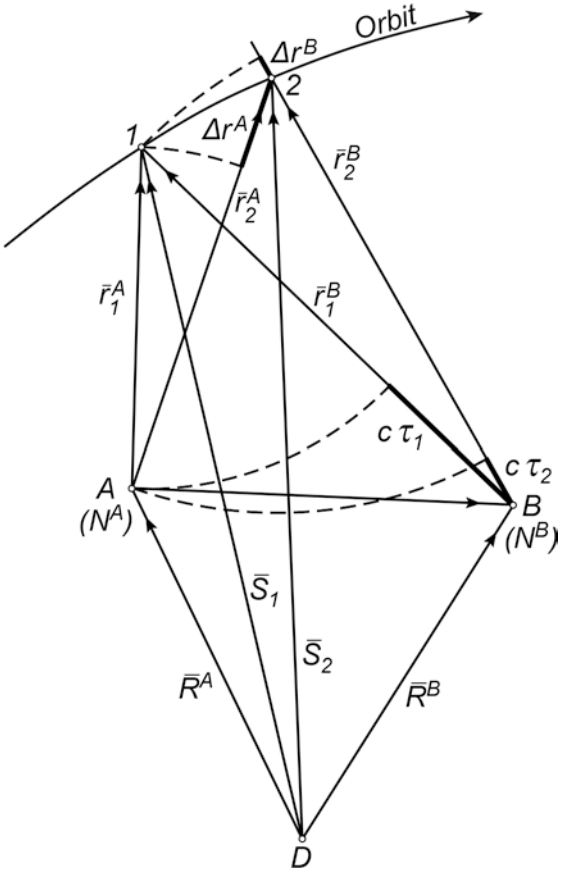

FIGURE 1. Geometry of interferometry from Doppler observations.

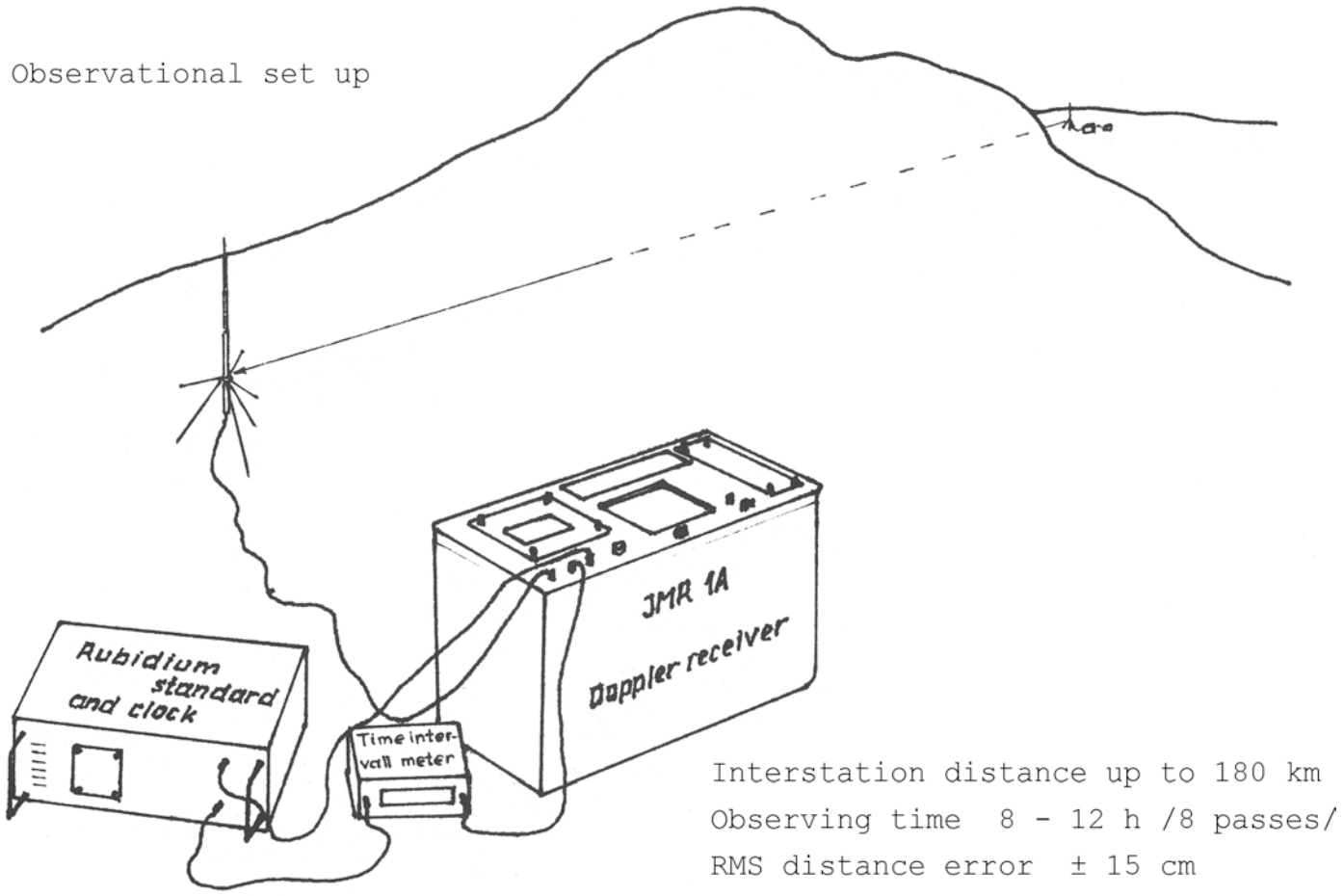

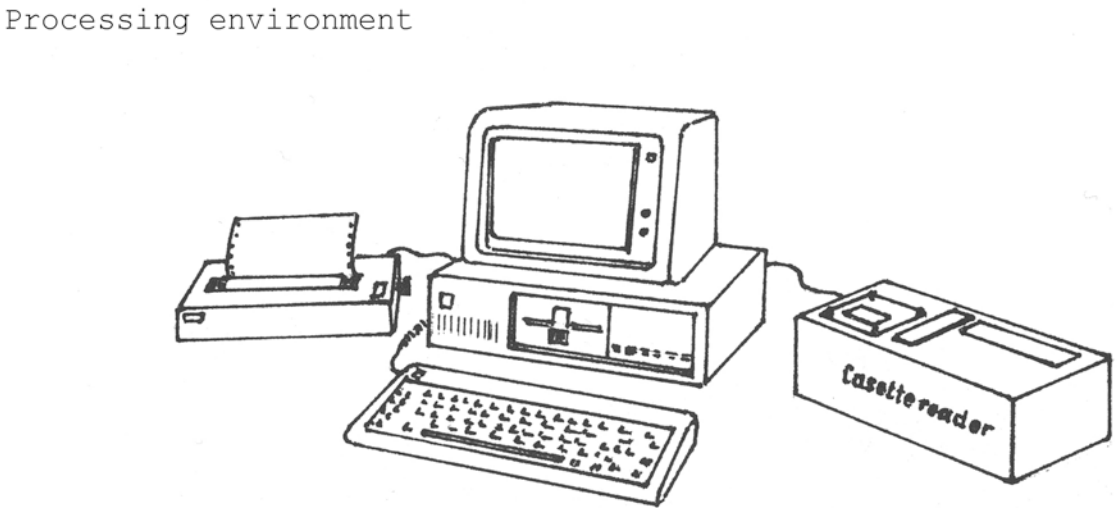

FIGURE 2. Observational set up and processing environment as applied to the PENCDIP program.

No	DATE d h m	SAT	GEOM	CA degree	D DELAY /μs/	D FREQ /mHz/
1	1531808	48	E	32	83	0.0
2	1531924	13	E	55	108	0.0
3	1532112	13	W	41	53	0.0
4	1540022	14	E	23	95	0.0
5	1540360	20	W	67	123	0.0
6	1540626	48	E	45	108	0.0
7	1540814	48	W	58	37	0.0
8	1542022	13	W	81	64	0.0
9	1550014	19	E	53	58	0.0
10	1550202	19	W	50	96	0.0
11	1550604	48	E	33	56	0.0
12	1550752	48	W	76	114	0.0
13	1551316	14	E	63	52	0.0
14	1551446	20	E	45	36	0.0
15	1552328	19	E	24	140	0.0
16	1562028	13	W	70	12	0.0
17	1541358	19	W	50	103	0.0

TABLE 1. Pass summary. Baseline: Penc6-Penc1, 1983.

Passes included in the solution	Interstation distance	Deviation from surveyed value	Standard deviation	Average distance	Repeatability RMS
1 – 17	38.56	0.00	±0.09	-	-
1 - 9 10 - 17	38.55 38.56	0.01 0.00	0.14 0.13	38.56	±0.01
1 - 5 6 - 9 10 – 13 14 – 17	38.50 38.62 38.53 38.57	0.06 -0.06 0.03 -0.01	0.20 0.19 0.22 0.16	38.56	0.05

TABLE 2. Results of processing by PENCDIP program.
Baseline: Penc6-Penc1, 1983. Surveyed distance: 38,56 m.
Receivers with common oscillator.

Pass No	DATE d h m	SAT	GEOM	CA degree	D DELAY /μs/	D FREQ. /mHz/
1	2820816	20	W	45	- 81	0.6
2	2821010	13	E	68	- 69	0.6
3	2822056	20	W	23	- 7	0.6
4	2822112	13	E	27	49	0.6
5	2822300	13	W	78	18	0.6
6	2830550	11	E	34	- 40	0.6
7	2830738	11	W	68	15	0.6
8	2830852	20	W	21	- 8	0.6
9	2831122	48	W	81	- 26	0.6
10	2831842	11	E	68	14	0.6
11	2832030	11	W	25	20	0.6
12	2832150	48	E	40	- 30	0.6
13	2832210	13	E	80	- 37	0.6
14	2832338	48	W	63	- 48	0.6
15	2832356	13	W	28	-205	0.6
16	2840740	20	W	69	- 51	0.6
17	2840910	48	E	21	- 22	0.6
18	2841058	48	W	90	13	0.6
19	2841202	13	W	26	- 15	0.6
20	2841248	48	W	19	- 1	0.6
21	2842120	13	E	31	59	0.6
22	2850558	11	E	46	27	0.6
23	2850632	20	E	58	- 34	0.6
24	2850818	20	W	33	14	0.6
25	2850924	13	E	39	57	0.6
26	2851112	13	W	59	54	0.6
27	2851226	48	W	26	- 15	0.6
28	2851730	20	E	22	26	0.6
29	2851914	20	W	81	24	0.6
30	2852040	11	W	19	103	0.6
31	2852252	48	W	90	42	0.6
32	2860004	13	W	22	60	0.6
33	2860044	48	W	19	33	0.6
34	2841838	20	E	69	- 21	0.6

TABLE 3. Pass summary. Baseline: Penc6-Baja, 1984, DBLI.

Passes included in the solution	Interstation distance	Standard deviation	Average distance	Repeatability RMS
1 – 34	180 102.09	± 0.08	-	-
1 – 17	102.03	0.11	180 102.10	± 0.10
18 – 34	102.17	0.13		
1 - 9	101.97	0.12	102.08	0.09
10 – 17	102.07	0.18		
18 – 25	102.08	0.14		
26 – 34	102.20	0.19		
1 - 4	101.94	0.19	102.10	0.13
6 – 10	102.09	0.16		
12 – 15	102.12	0.16		
20 – 24	102.14	0.18		
25 – 28	102.31	0.19		
29 – 34	101.95	0.25		

TABLE 4. Results of processing by PENCDIP program.
Baseline: Penc6-Baja, 1984, DBLI.

PROGRAM	Passes	Δx /m/	Δy /m/	Δz /m/	Interstation distance
SADOSA /rigor./	50	130253.23 ± 0.15	23458.80 ± 0.27	-122149.70 ± 0.13	180102.11 ± 0.12
PENCDIP	40	130253.57	23458.39	-122149.39	180102.09

TABLE 5. Relative positions and distances by SADOSA /rigorous synchroneity option/ and PENCDIP.
Baseline: Pence6-Baja, 1984, DBLI.

GPS Measurements

- The Global Positioning System -

RECOMMENDED GPS TERMINOLOGY

David E. WELLS
Department of Surveying Engineering
University of New Brunswick
Fredericton, New Brunswick
Canada E3B 5A3

ABSTRACT. A proposal for standardized GPS terminology is presented. The concepts behind the terms are defined, and the reasons for selecting particular terms are given. A Glossary of terms is appended.

INTRODUCTION

It is probable that the Global Positioning System (GPS), and perhaps other similar systems such as GLONASS, GEOSTAR and NAVSAT (McDonald and Greenspan, 1985), will find wide applications in surveying and geodesy over the next several years. The community of users and variety of equipment are both likely to be very heterogeneous. The establishment of standards is necessary to permit communication and cooperation among these users, who may employ various kinds of equipment and software.

Such communication and cooperation (and hence such standards) should exist on at least three levels. A common understanding of the concepts involved in GPS positioning requires standard terminology. The possibility for exchange of observed data requires standard data structures. The combination of results from various GPS campaigns requires consistency among these results, which would ideally be achieved by use of standard processing algorithms. In this paper an attempt is made to deal with only the first of these, a standard terminology.

Many new concepts and terms have begun to appear in the surveying literature as a result of the complexity and flexibility of GPS. This paper recommends a standard terminology for GPS which is specific enough to describe the complexities, but general enough to accomodate the flexibility of GPS and the possible use of other similar systems. A Glossary of terms, both recommended and otherwise, drawn from the recent GPS literature, appears as an Appendix.

A standard terminology is no more than a set of conventions, assigning specific meanings to a set of terms. We have tried to keep these terms as few and as simple as possible, and have included enough discussion to place them in context, and to give reasons why they are preferred over alternatives. The proposed terms are presented under eight headings: applications, satellites, signal, measurements, receivers, differencing, network solutions, and uncertainties.

As GPS continues to evolve, so will the most appropriate terminology used to describe it. This proposal should be considered as only one step in this evolutionary process. Comments and suggestions for future versions are welcome, and should be sent to the author.

A word of acknowledgement. The original version of this paper was prepared by the author and Demitris Paradissis, and presented by the latter at a meeting in Sopron, Hungary in July 1984 of the Subcommission on Standards of the Committee on Space Techniques of Geodynamics. Subsequent comments and corrections were provided by Gerhard Beutler, Nick Christou, Charles Counselman, Mike Eaton, Ron Hatch, Larry Hothem,
Patrick Hui, Hal Janes, Alfred Kleusberg, Richard Langley, Richard Moreau, Ben Remondi, Fred Spiess, Rock Santerre, Tom Stansell, Petr Vanicek, Richard Wong, and Larry Young. The present version was compiled from their comments, and further revised with the help of Yehuda Bock, Claude Boucher, Ron Hatch, Hal Janes, Alfred Kleusberg, and Ben Remondi. Without this extensive help, this proposal would not exist. However, errors and misconceptions which remain are the sole responsibility of the author.

APPLICATIONS

KINEMATIC (or DYNAMIC) POSITIONING refers to applications in which a trajectory (of a ship, ice field, tectonic plate, etc.) is determined.

STATIC POSITIONING refers to applications in which the positions of points are determined, without regard for any trajectory they may or may not have.

Consideration was given to basing these definitions on whether there was significant receiver motion or not, or in terms of the required accuracies. However, in the first case, the existance of receiver motion, *per se*, did not seem to introduce a fundamental difference from static applications, so long as the accuracy obtainable for instantaneous positioning is adequate. In the second case, there are examples of kinematic applications (e.g. marine 3D seismic) which may have higher accuracy requirements than some static applications (e.g. small scale mapping control).

Formally, kinematics is that branch of mechanics which treats motion without regard to its cause, which is the case here. Dynamics relates the motion to its cause. However, the term dynamic positioning has become so firmly rooted in common (mis)usage, that it may be unrealistic to expect a switch to the term kinematic positioning.

RELATIVE POSITIONING refers to the determination of relative positions between two or more receivers which are simultaneously tracking the same radiopositioning signals (e.g. from GPS).

Alternatives to the term "relative" which were considered were "differential" and "interferometric". While both are valid, "differential" may be misconstrued to imply some infinitesimal process, and "interferometric" has specific, as well as general, connotations (see the discussion on this point in the Receivers section below). As well, "interferometric" emphasizes the measurement technique rather than the relative positioning application.

Real time relative positioning implies that signals (containing sufficient information for relative positioning) from all receivers are somehow broadcast in real time for processing at a central site (which may be at one of the receivers).

Because many GPS errors (clock errors, ephemeris errors, propagation errors) are correlated between observations obtained simultaneously at different sites, the relative positions between these sites can be determined to a higher accuracy than the absolute positions of the sites. In its simplest form, relative positioning involves a pair of receivers. For **kinematic relative positioning**, where the trajectory is of interest, one of these will be a monitor receiver at a known stationary location, and the other will be a mobile receiver tracing out the trajectory of interest. **Static relative positioning** involves determination of the difference in coordinates between pairs of points of a network. In this case, there is no restriction that one receiver remain at the same control point throughout the network survey (although that may be one feasible strategy). Usually at present independent baseline vectors between pairs of these points are computed as an intermediate step. When only two receivers are used for relative positioning (one baseline at a time), baselines can be considered independent. In general, using **n** receivers, the number of combinations of receiver pairs (baselines) is **n (n-1) / 2**. However, only **(n-1)** of these are rigorously independent (see the Network Solutions section below for more on relative static positioning).

SATELLITES

One confusing issue concerning GPS terminology is the numbering or identification of the GPS satellites. Several systems are used: the launch sequence number, an orbit position number, a number identifying which week of the 37-week long P-code has been assigned to the satellite (the PRN number), as well as more conventional NASA and international satellite identification numbers. Table 1 lists all these numbers for the

eleven GPS Block I (prototype) satellites. Since the satellite ephemeris message uses the PRN number to identify satellites, that is the one which has gained widest use.

TABLE 1: GPS SATELLITE IDENTIFICATION

LAUNCH SEQUENCE NUMBER	ORBITAL POSITION NUMBER	ASSIGNED VEHICLE PRN CODE	NASA CATALOGUE NUMBER	INTERNATIONAL DESIGNATION	LAUNCH DATE (YY-MM-DD)	STATUS
1	0	4	10684	1978-020A	78-02-22	crystal clock
2	4	7	10893	1978-047A	78-05-13	not operating
3	6	6	11054	1978-093A	78-10-07	operating
4	3	8	11141	1978-112A	78-12-11	operating
5	1	5	11690	1980-011A	80-02-09	not operating
6	5	9	11783	1980-032A	80-04-26	operating
7					81-12-18	launch failed
8	2	11	14189	1983-072A	83-07-14	operating
9	1	13	15039	1984-059A	84-06-13	operating
10	4	12	15271	1984-097A	84-09-08	operating
11					85-08-??	launch plan

SIGNAL

The GPS signal has a number of components, all based on the fundamental frequency F = 10.23 MHz (see Figure 1). Two carries are generated at 154 F (called L1), and 120 F (called L2). Pseudorandom noise codes are added to the carries as binary biphase modulations at F (P-code) and F/10 (S-code), previously called C/A-code). A 1500-bit-long binary message is added to the carriers as binary biphase modulations at 50 bits per second.

PSEUDORANDOM NOISE CODE (PRN code) is any of a group of binary sequences that exhibit noise-like properties, the most important of which is that the sequence has a maximum autocorrelation at zero lag.

BINARY BIPHASE MODULATIONS on a constant frequency carrier are phase changes of either 0° (to represent a binary 0) or 180° (to represent a binary 1). These can be modelled by

$$y = A(t) \cos (\omega t - \phi) \quad (1)$$

where the amplitude function A(t) is a sequence of +1 and -1 values (to represent 0° and 180° phase changes, respectively).

The P-code is a long (about 10^{14} bits) sequence, and the S-code is a short (1023 bit) sequence. The two codes are impressed on separate carriers that are in quadrature (the carriers are 90° apart in phase). For the present prototype (Block I) GPS satellites, and those to be used for the next decade (Block II), the S-code is normally available only on the L1 frequency. It is likely that access of civilian users to the P-code will be restricted, once the present prototype GPS satellites are replaced by production versions. Other similar systems (e.g. GLONASS) will undoubtedly have signal structures different to GPS.

MEASUREMENTS

Either the carrier or the code can be used to obtain GPS observations. In the case of carrier observations, phase is measured. In the case of code observations, usually pseudoranges are measured, but phase of the code can also be measured. Carrier measurements are subject to ionospheric phase advance, and code measurements to ionospheric group delay.

CARRIER BEAT PHASE is the phase of the signal which remains when the incoming Doppler-shifted satellite carrier signal is beat (the difference frequency signal is generated) with the nominally-constant reference frequency generated in the receiver.

This term is preferable to the four alternatives "phase", "carrier phase", "reconstructed carrier phase" and "Doppler phase" for the following reasons. "Phase" does not distinguish between carrier and code measurements, for each of which phase measurements can be made (by very different techniques). "Carrier phase" implies that the phase of the GPS signal carrier itself is observed, which is not the case. "Reconstructed carrier phase" emphasizes the technique by which the signal to be observed is obtained, rather than emphasizing the signal itself. "Doppler phase" implies that the signal to be observed is due solely to the Doppler shift of the satellite carrier signal, which may not be the case (if, for example, the receiver reference frequency is intentionally offset significantly from the unshifted satellite carrier frequency).

Measurements of the carrier beat phase can be either complete instantaneous **phase measurements**, or **fractional instantaneous phase measurements**. The distinction between the two is that the former includes the integer number of cycles of the carrier beat phase since the initial phase measurement, and the latter is a number between zero and one cycles.

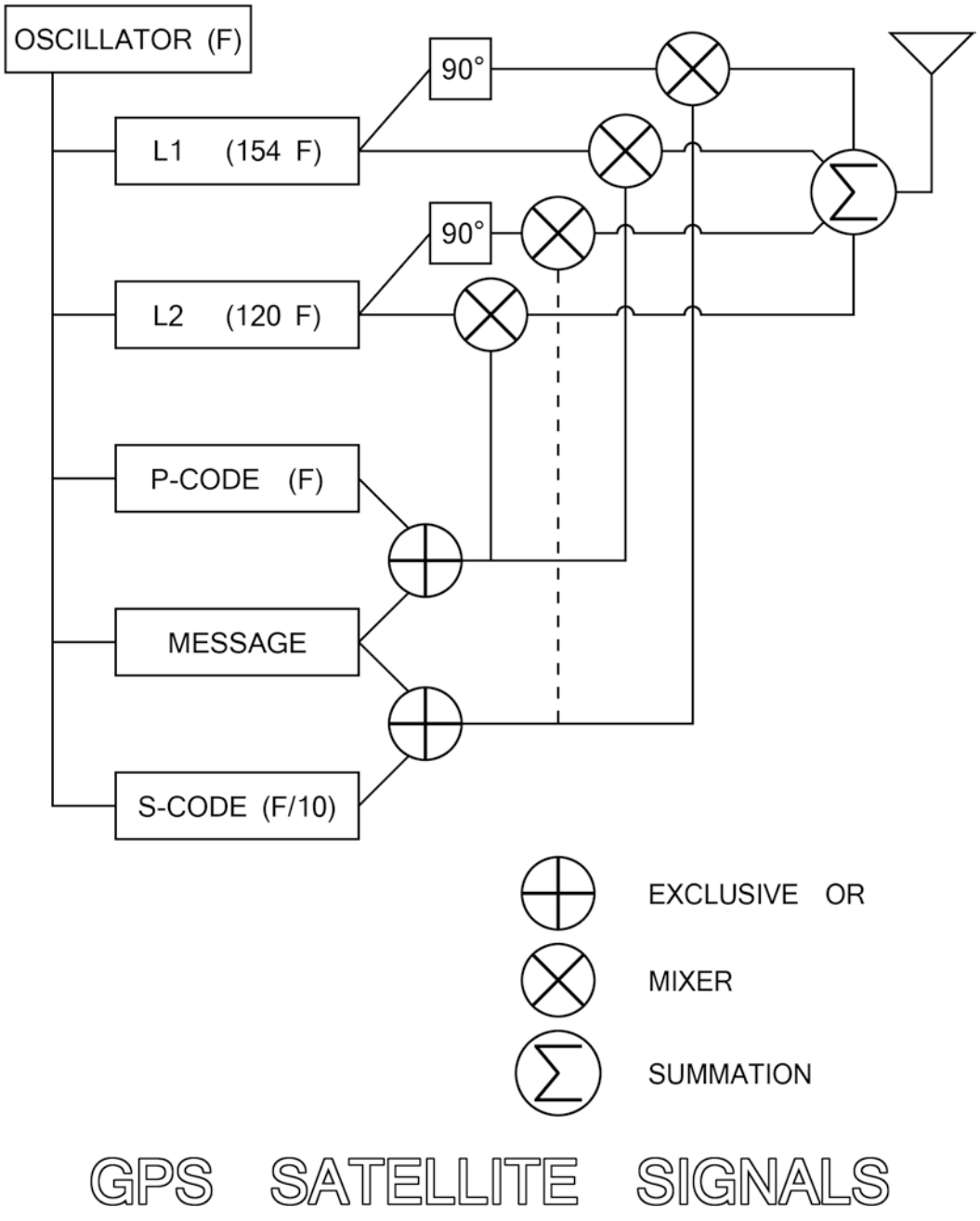
OSCILLATOR (F)
90°
L1 (154 F)
90°
L2 (120 F)
P-CODE (F)
MESSAGE
S-CODE (F/10)
EXCLUSIVE OR
MIXER
SUMMATION
GPS SATELLITE SIGNALS

FIGURE 1

CARRIER BEAT PHASE AMBIGUITY is the uncertainty in the initial measurement, which biases all measurements in an unbrocken sequence. The ambiguity consists of three components

$$\alpha_i + \beta^j + N_i^j \qquad (2)$$

where
α_i is the fractional initial phase in the receiver,
β^j is the fractional initial phase in the satellite (both due to various contributions to phase bias, such as unknown clock phase, circuit delays, etc.), and
N_i^j is an integer cycle bias in the initial measurement.

The carrier beat phase can be related to the satellite-to-receiver range, once the phase ambiguity has been determined. A change in the satellite-to-receiver range of one wavelength of the GPS carrier (19 cm for L1) will result in one cycle change in the phase of the carrier. Carrier beat phase measurement resolutions of a few degrees of phase are possible. Hence the measurements are sensitive to sub-centimetre range changes.

The complete instantaneous phase measurement differs from the more familiar continuously integrated Doppler measurement only because the latter does not include this ambiguity (assumes it to be zero).

Depending on receiver design, the phase samples are made at either epochs of the receiver clock, or at epochs of the satellite clock (as transferred through the modulations imbedded in the received satellite signal). I am not aware of a receiver which uses satellite timing, however.

Delta Pseudorange is a commonly used term which incorrectly implies it is somehow associated with code measurements. In fact Delta Pseudorange is the difference between two carrier beat phase measurements, made coincidently with (code) pseudorange epochs.

PSEUDORANGE is the time shift required to align (correlate) a replica of the GPS code generated in the receiver with the incoming GPS code, scaled into distance by the speed of light. This time shift is the difference between the time of signal reception (measured in the receiver time frame) and the time of emission (measured in the satellite time frame).

Pseudoranges change due to variations in the satellite-to-receiver propagation delay, and are biased by the time offset between satellite and receiver clocks. The resolution of pseudorange measurements depends on the accuracy with which the incoming and replicated codes can be aligned. An alignment accuracy of a few nanoseconds is equivalent to metre-level range resolution.

RECEIVERS

GPS receivers have one or more channels. Two kinds of channels are useful for static positioning using carrier phase measurements: squaring type channels, and correlation type channels.

> A **CHANNEL** of a GPS receiver consists of the radiofrequency and digital hardware, and the software, required to track the signal from one GPS satellite at one of the two GPS carrier frequencies.
>
> A **SQUARING-TYPE CHANNEL** multiplies the received signal by itself to obtain a second harmonic of the carrier, which does not contain the code modulation.

The squaring concept is simply shown by squaring equation (1) to obtain

$$y^2 = A^2 \cos^2(\omega t + \phi) = A^2 [1 + \cos(2\omega t + 2\phi)] / 2 \qquad (3)$$

Since $A(t)$ is the sequence of +1 and -1 values representing the code, $A(t)^2 = A^2$ is always equal to +1 and may be dropped from equation (3). The resulting signal y^2 is then pure carrier, but at twice the original frequency. Note that for a simple squaring loop, any noise on the signal is also squared. In practice as shown in Figure 2, the incoming signal is first differenced with a local reference frequency to obtain the carrier beat phase signal, at an intermediate frequency much lower than the original carrier frequency.

This is a simple conceptual description of the squaring process which, in practice, is implemented by one of several proprietary techniques which have been developed. These proprietary techniques often involve some method of narrowing the GPS signal bandwidth from 20 MHz (due to the P-code "spreading"), to a bandwidth the order of several Hertz. Only the carrier is obtained from a squaring-type channel. Pseudoranges and the message cannot be obtained. An example of such a receiver is the Macrometer™ V-1000, a six channel receiver which does not require any knowledge of the code, capable of continuously tracking the L1 carrier beat phase second harmonic, from six satellites.

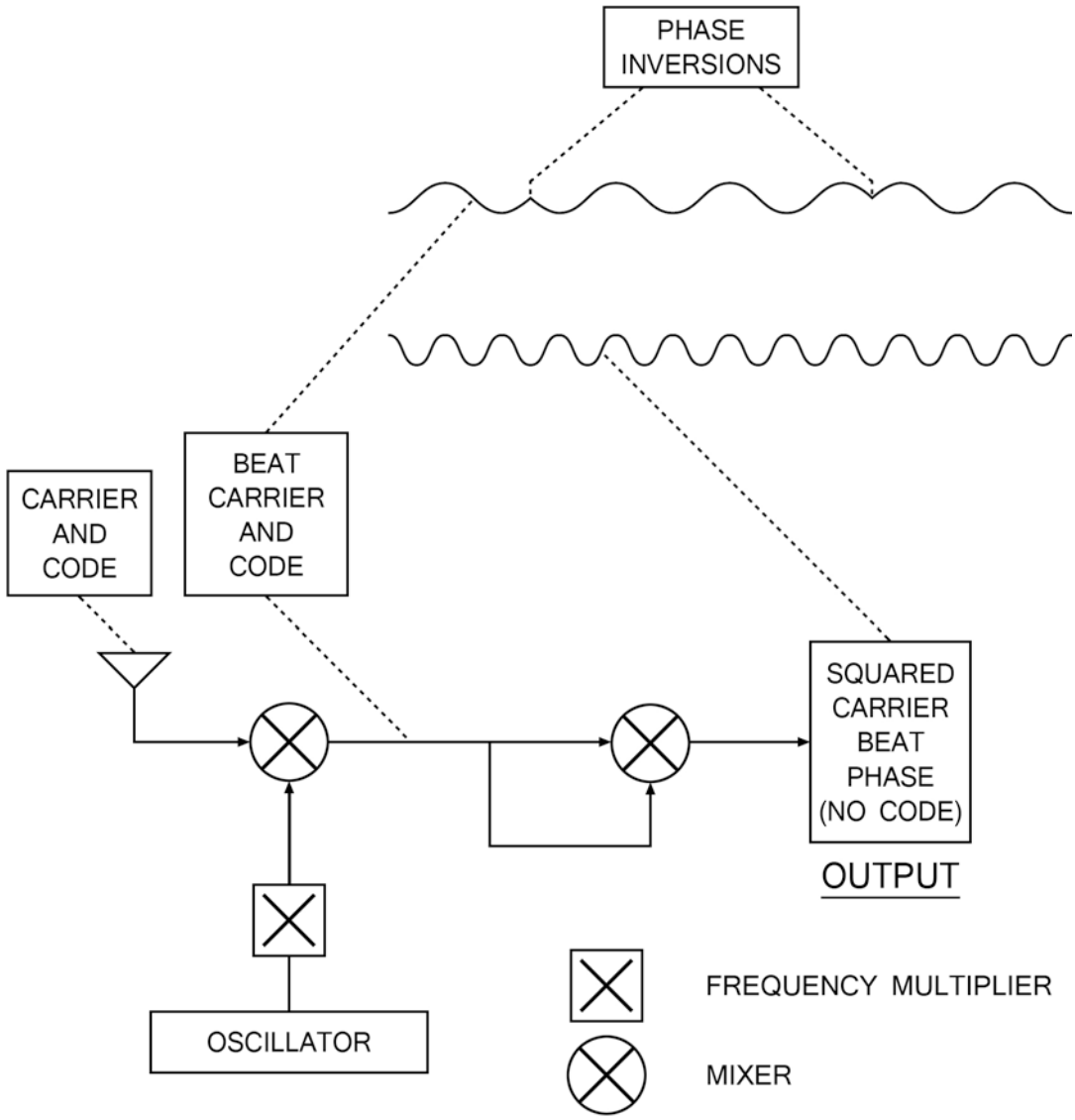
PHASE
INVERSIONS
CARRIER
AND
CODE
BEAT
CARRIER
AND
CODE
SQUARED
CARRIER
BEAT
PHASE
(NO CODE)
OUTPUT
OSCILLATOR
FREQUENCY MULTIPLIER
MIXER
GPS SQUARING-TYPE CHANNEL

FIGURE 2

An alternative to the squaring process, which also does not require detailed knowledge of the code, is the SERIES technique [Buennagel et al., 1984] in which the GPS signal is despread by tracking the Doppler shift of the code modulation transitions, without detailed knowledge or recovery of the actual code sequences or use of the carrier

> A **CORRELATION-TYPE CHANNEL** uses a delay lock loop to maintain an alignment (correlation peak) between the replica of the GPS code generated in the receiver, and the incoming code.

In simple terms, the code correlation concept involves generating a replica of the code sequence [the sequence of +1 and -1 values represented by A(t) in equation (1)] within the receiver, and to align this replica in time (correlate) with the incoming signal. Once aligned, multiplying the two codes together results in only +1 values for the resulting amplitude function. In Figure 3, the incoming signal is first reduced in frequency by differencing with a local carrier (point A). The signal resulting from multiplying this incoming signal by the local code replica (point B) will have the code removed, but only if the two codes are aligned. The correlation peak detector tests for the presence of the code, and corrects the delay (point C) of the locally generated code replica to maintain alignment, completing the delay lock loop. This time delay is the pseudorange measurement (see above). Also, once the receiver code generator is aligned to the incoming code, its output is a reading of the satellite clock at the time of signal transmission. The fourth and final kind of information obtained from a code correlation channel is the 50 bit per second message containing the ephemeris.

This is a simple conceptual description of a correlation-type channel. In practice, details of the correlation process may involve any of a number of advanced techniques (e.g. tau dither, early minus late gating), and may be implemented predominantly in hardware, or predominantly in software, depending on receiver design.

Code correlation channels may be either multiplexing or switching, depending on how the satellite message bits are accumulated.

> A **MULTIPLEXING CHANNEL** is sequenced through a number of satellite signals (each from a specific satellite and at a specific frequency) at a rate which is synchronous with the satellite message bit-rate (50 bits per second, or 20 milliseconds per bit). Thus one complete sequence is completed in a multiple of 20 milliseconds.
>
> A **SWITCHING CHANNEL** is sequented through a number of satellite signals (each from a specific satellite and at a

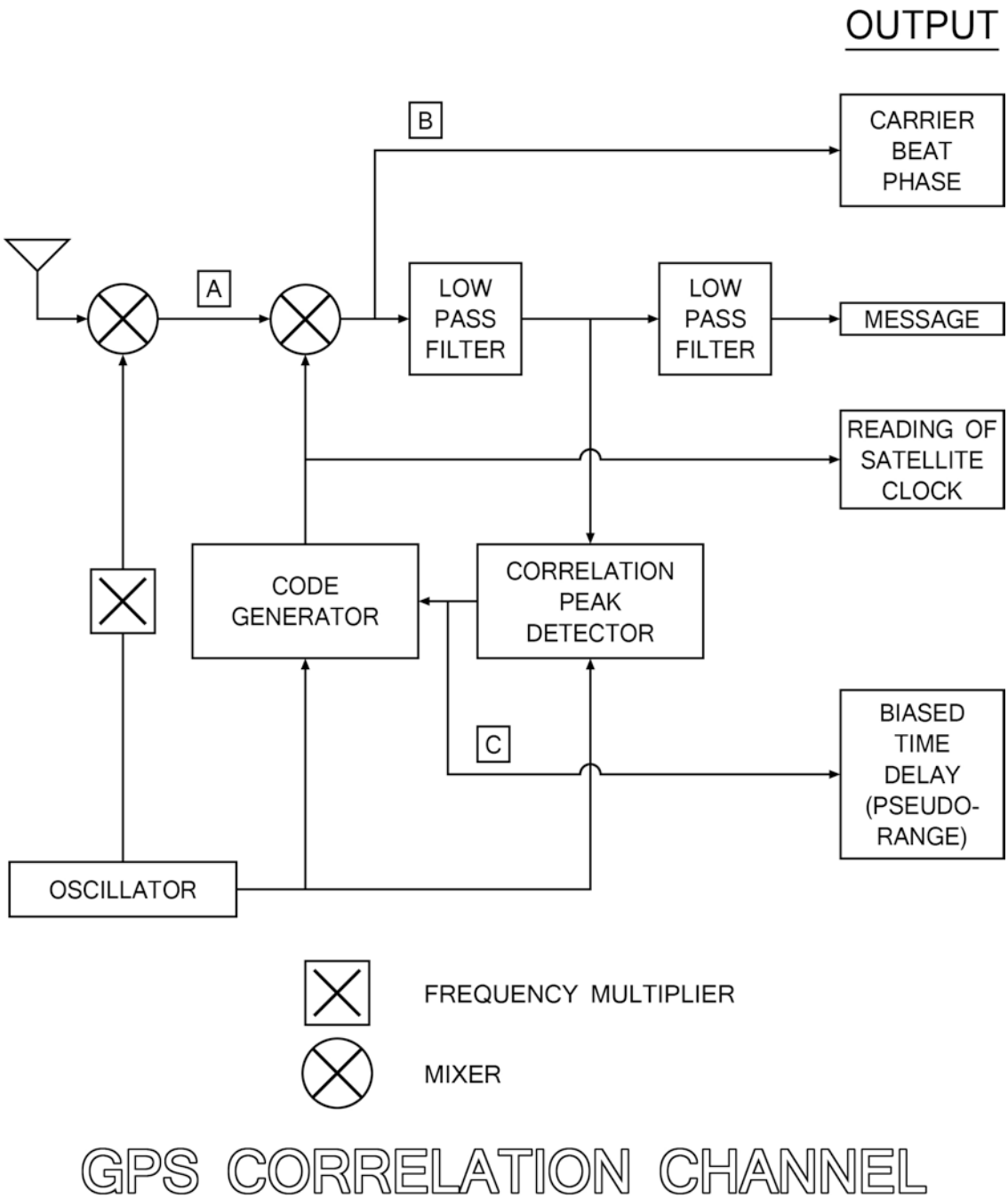
OUTPUT
B
CARRIER BEAT PHASE
A
LOW PASS FILTER
LOW PASS FILTER
MESSAGE
READING OF SATELLITE CLOCK
CODE GENERATOR
CORRELATION PEAK DETECTOR
C
BIASED TIME DELAY (PSEUDO-RANGE)
OSCILLATOR
FREQUENCY MULTIPLIER
MIXER
GPS CORRELATION CHANNEL

FIGURE 3

specific frequency) at a rate which is slower than, and asynchronous with, the message data rate.

A multiplexing channel builds up a map of the message from each satellite one bit (for each satellite) per sequence cycle. An example of a multiplexing receiver is the Texas Instruments 4100, which has one multiplexing channel which tracks both L1 and L2 signals from up to four satellites (a total of eight signals), dwelling on each for five milliseconds, hence taking two bit-periods (40 milliseconds) to complete one sequence. Each satellite is visited once per bit period (on alternating frequencies), in order not to lose any message bits. Software in the receiver tracks all signals in such a way that values for all signals, referred to the same epoch, can be ontained.

Switching channels may dwell on each signal for relatively short (less than a second) or relatively long (tens of seconds to hours) periods. If the sequence time is short enough for the channel to recover (through software prediction) the integer part of the carrier beat phase (in practice no more than several seconds), then the channel is a fast-switching channel. A switching channel builds up a map of the message from each satellite many bits per signal dwell time. In order that all parts of each satellite message are sampled, the dwell times must progress through the message (that is the sequencing must be asynchronous with the message data rate).

A receiver with many channels is a multichannel receiver. It may be that these channels are of the same type (all code correlation, or all squaring), or of different types. For example, since civil access to the P-code is expected to be restricted in the future, and the S-code is not expected to be available on the L2 carrier, a civilian dual frequency receiver must either have squaring channels for both L1 and L2, or code correlation channels for L1 and squaring channels for L2.

A multichannel switching receiver may have more or less flexibility in how the channels are used. For example, three possible scenarios are

- All channels track the same signal continuously (while the satellite is visible). For highly kinematic applications, where the receiver motion over even a fast-switching sequence period is significant, this may be the only feasible strategy.
- All channels fast-sequence through a subset of the signals to be tracked. This reduces the number of channels required (perhaps to one).
- Some channels track one signal continuously, with other channels switching through the signals (perhaps to collect ephemeris data from all visible satellites).

A very different alternative is to simply record the total GPS receives signal as a "noise" signal (although it consists of carries and codes from all visible satellites) at each station in a network, and then to extract between-receiver differences (see below) by correlating the recorded data station-pair by station-pair, and satellite by satellite. This is the interferometric approach. The receiver in this case would be very simple and inexpensive. The lack of real time quality control, however, makes this an

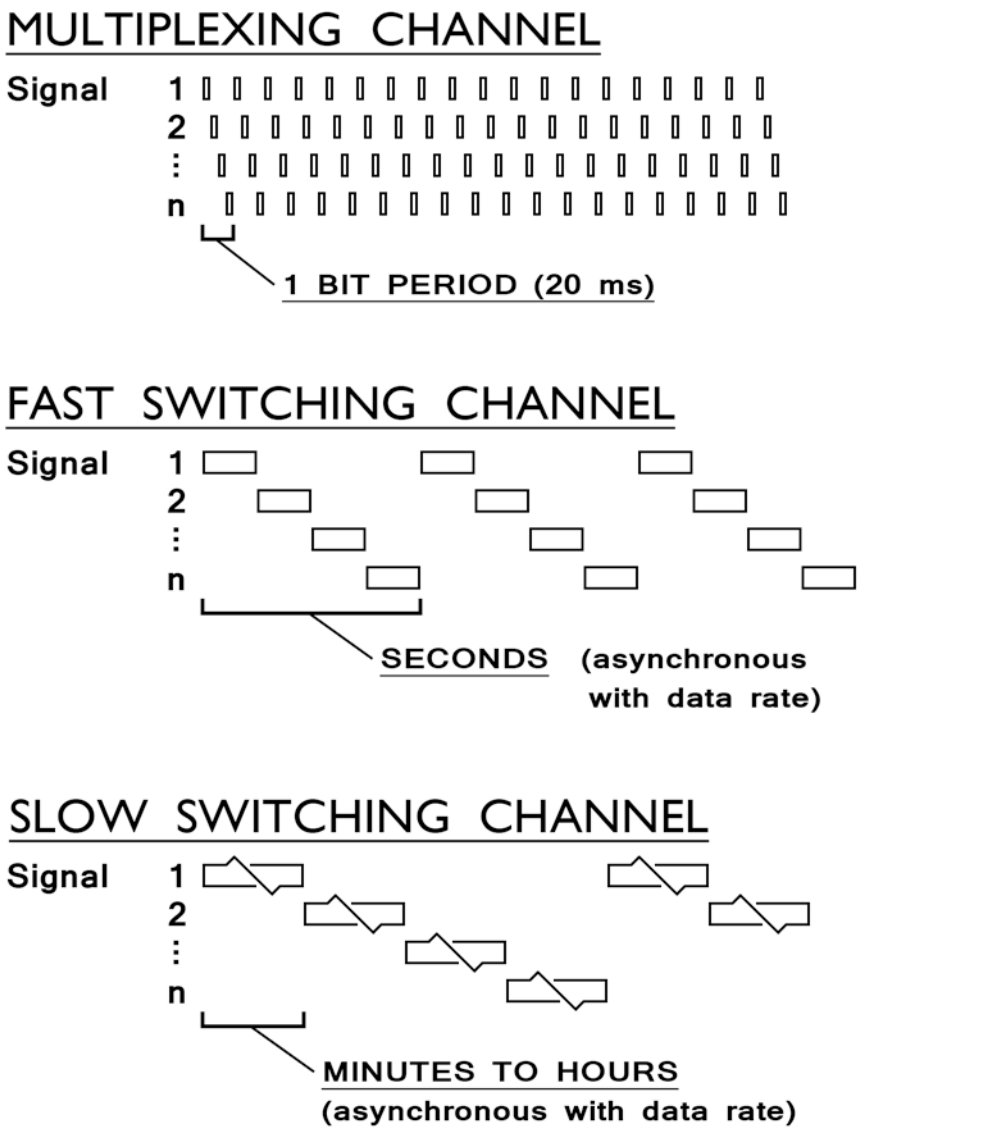

MULTIPLEXING AND SWITCHING CHANNELS

FIGURE 4

impractical option. Note that, in principle, any technique involving comparison of measurements made by two receivers could be called an interferometric technique. We have noted above the preference for using "relative positioning" in place of this more general m,eaning for interferometry.

DIFFERENCING

For relative static positioning, many of the errors are correlated among the various measurements which are made. One approach is to attempt to model this correlation through blas parameter estimation and correlated weighting of the observations. Another commonly used approach for processing carrier measurements involves taking differences between measurements, since this removes or reduces the effect of errors which are common to the measurements being differenced. GPS measurements can be differenced in several ways: between receivers, between satellites, between time epochs, and between L1 and L2 frequencies. Figure 5 illustrates the first three of these. All but between-epoch differences involve the concept of simultaneity.

SIMULTANEOUS MEASUREMENTS are measurements referred to time frame epochs which are either exactly equal, or else so closely spaced in time that the time misalignment can be accomodated by correction terms in the observation equation, rather than by parameter estimation.

A **BETWEEN-RECEIVER** carrier beat phase difference is the instantaneous difference in the complete carrier beat phase measurement made at two receivers simultaneously observing the same received signal (same satellite, same frequency).

A **BETWEEN-SATELLITE** carrier beat phase difference is the instantaneous difference in the complete carrier beat phase measurement made by the same receiver observing two satellite signals simultaneously (same frequency).

A **BETWEEN-EPOCH** carrier beat phase difference is the difference between two complete carrier beat phase measurements made by the same receiver on the same signal (same satellite, same frequency).

A **BETWEEN-FREQUENCY** carrier beat phase difference is the instantaneous difference between (or, more generally, any other linear combination involving) the complete carrier beat phase measurements made by the same receiver observing signals from the same satellite at two (or more) different frequencies.

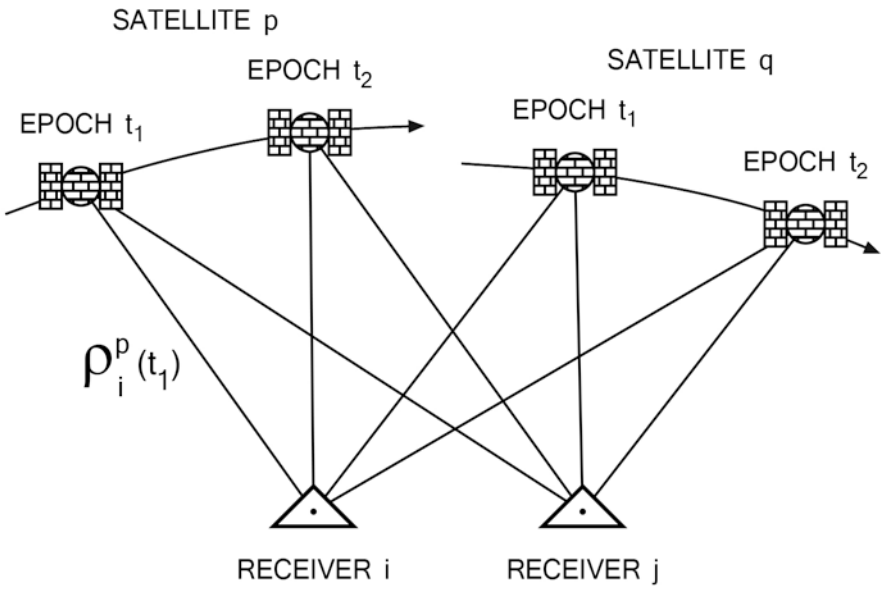

BETWEEN-RECEIVER	BETWEEN-SATELLITE	BETWEEN-EPOCH
$[\rho_i^p(t_1) - \rho_j^p(t_1)]$	$[\rho_i^p(t_1) - \rho_i^q(t_1)]$	$[\rho_i^p(t_2) - \rho_i^p(t_1)]$
$[\rho_i^q(t_1) - \rho_j^q(t_1)]$	$[\rho_j^p(t_1) - \rho_j^q(t_1)]$	$[\rho_j^p(t_2) - \rho_j^p(t_1)]$
$[\rho_i^p(t_2) - \rho_j^p(t_2)]$	$[\rho_i^p(t_2) - \rho_i^q(t_2)]$	$[\rho_i^q(t_2) - \rho_i^q(t_1)]$
$[\rho_i^q(t_2) - \rho_j^q(t_2)]$	$[\rho_j^p(t_2) - \rho_j^q(t_2)]$	$[\rho_j^q(t_2) - \rho_j^q(t_1)]$

GPS PHASE MEASUREMENT DIFFERENCING

FIGURE 5

Between-receiver differences remove or reduce the effect of satellite clock errors (and cancel the β^j term in the ambiguity expression of equation 2, which is common to both measurements). For baselines which are short compared to the 20,000 km GPS satellite height, between-receiver differences also significantly reduce the effect of satellite ephemeris and atmospheric refraction errors. **Between-satellite** differences remove or reduce the effects of receiver clock errors (and cancel the α_i term in the ambiguity expression of equation 2, which is common to both measurements). **Between-epoch** differences are the same as integrated Doppler measurements (and cancel all three terms $\alpha_i + \beta^j + N_i^j$ in the ambiguity expression of equation 2, all of which are common to both measurements). However, clock errors remain in this case. **Between-frequency** differences are not made for the purpose of ionospheric refraction correction, but rather to generate a signal which is a linear combination of L1 and L2, and hence has a coarser (or finer) wavelength (Hatch and Larson, 1985).

Many combinations of these differences are possible. It is important that which differences, and their order, be specified in describing a processing method. For example, **Receiver-Satellite Double Differences** refers to differencing between receivers first and between satellites second; **Receiver-Time Double Differences** refers to differencing between receivers first, then between time epochs; **Receiver-Satellite-Time Triple Differences** refers to differencing between receivers, then satellites, and finally time.

Figure 5 illustrates differences between receivers, satellites and epochs for the simplest possible case (two receivers, two satellites, two epochs, and one frequency). A total of eight carrier beat phase measurements are made. Each of the three possible single differences reduces this to four. Double differencing further reduces this to two measurements. These measurements correspond to only one triple difference measurement. In practice, many more receivers, satellites and epochs are involved. In this case, there are, for example, many ways in which Receiver-Satellite Double Differences can be formed.

NETWORK SOLUTIONS

GPS network processing techniques are still in their infancy, and it is probably too early to fully define the terminology required to describe and distinguish between them. However some of the simple concepts can be stated.

The simplest static relative positioning observation strategy, to survey a network of points, is to use one pair of receivers which occupy, in some sequence, all the baselines desired to determine the network. Most of the work done to date has used this method. In this case, two concepts are well defined:

A **BASELINE** consists of a pair of stations for which simultaneous GPS data has been collected.

A two-receiver **OBSERVING SESSION** is the period of time over which GPS data is collected simultaneously at both ends of one baseline.

When more than two receivers are used simultaneously, the baseline and session concepts must be extended:

An n-receiver **OBSERVING SESSION** is the period of time over which GPS data is collected simultaneously at n stations.

Two **SESSIONS** are **INDEPENDENT** to the extent, that we can ignore any common biases affecting the observations in both cases.

Two **BASELINES** are **INDEPENDENT** if they have been determined from independent sessions.

Once enough GPS satellites are in orbit to provide continuous coverage, the definition of a multi-receiver observing session will become more blurred, since the definite break between sessions now provided by the limited periods of satellite availability will no longer exist.

To obtain a network solution, either the GPS observations can be taken directly into a network adjustment program, or else the baseline solutions can be obtained individually first, and taken as vector pseudo-observations into a simpler three dimensional network adjustment. The advantage of the former approach is that biases and correlations affecting the data can more easily be taken into account. In each case, the network adjustment may use either a batch algorithm (processing the entire set of observations in one run), or a sequential algorithm (in which the data can be processed and results obtained on a session by session, or even observation by observation, basis). The most important practical property of a sequential algorithm is that the data can be processed in a sequence of computer runs, rather than in one large run. Programs having this property are said th have a "restart" capability.

UNCERTAINTIES

Uncertainties in surveying are conventionally expressed in terms of covariance matrices. The uncertainty in a set observations $\boldsymbol{\ell}$ is contained in the covariance matrix $\mathbf{C}_{\boldsymbol{\ell}}$ for those observations. In general this quantity will be the sum of the contributions from many error sources. Each error source will have its own properties, such as

dependence on geometry, correlations in various ways between observations, etc. According for these properties is not a simple task, and to date has not been fully addressed for GPS.

The uncertainty in a solution **X** is contained in the solution covariance matrix $\mathbf{C_x} = \left(\mathbf{P_x} + \mathbf{A^t}\,\mathbf{P_\ell}\,\mathbf{A}\right)^{-1}$ where $\mathbf{P_x}$ = the appriori solution weight matrix, **A** = the design matrix, and $\mathbf{P_\ell} = \mathbf{C}_{\ell^{-1}}$.

For planning and preanalysis, it is often convenient to seperate the geometric factors affecting the solution (contained in **A**) from the measurement uncertainties (contained in $\mathbf{P_\ell}$). One scalar measure of these geometrical factors is the dilution of precision.

The **DILUTION OF PRECISION (DOP)** is given by

$$\mathbf{DOP} = \sqrt{\mathbf{Trace}\left(\mathbf{A^T A}\right)^{-1}}\ .$$

The smaller of DOP, the stronger the geometry.

In the case of kinematic point positioning, several kinds of DOP exist, depending on the parameters of the solution:

- **GDOP** = geometrical DOP (three position coordinates plus clock offset)
- **PDOP** = position DOP (three coordinates)
- **HDOP** = horizontal DOP (two horizontal coordinates)
- **VDOP** = vertical DOP (height only)
- **TDOP** = time DOP (clock offset only)
- **HTDOP** = horizontal-time DOP (two horizontal coordinates and clock offset).

When the DOP factor exceeds a specified maximum value at some location for some period of time, it indicates that the normal equation matrices in those circumstances have become ill-conditioned to some extent. This is sometimes referred to as an "outage" of the GPS system.

For static positioning applications, what is important are the variations in the geometry of the satellite configuration over the entire time span of the data, and over the network of receivers simultaneously tracking the signals. This may not be adequately represented by the geometrical configuration at one instant at a single location. However, it may be impractical to attempt to evaluate a more rigorous DOP.

Standard methods of expressing kinematic application accuracies recently adopted by NATO [1983] are presented here without recommendation, for comment:

- For one dimensional error, the interval in metres containing 95% of the observations.

- For two or three dimensional radial error, the number which represents the radial distance in metres centred on the mean position of a large number of trials of the actual or desired system, which includes 95% of the observations.
- To express performance independent of geometrical factors, a 95% measure in terms of portions of a cycle or of a second.
- Speed accuracy as a dimensioned number (e.g. cm/sec) including 95% of observations from a large number of trials.

REFERENCES

Bauersima, I. (1983). "NAVSTAR/Global Positioning System (GPS) III: Erdvermessung durch radiointerferometrische Satellitenbeobachtungen." Mitteilungen der Satelliten-Beobachtungsstation Zimmerwald Nr. 12, Druckerei der Universität Bern.

Bossler, J.D., C.C. Goad and P.L. Bander (1980). "Using the Global Positioning System (GPS) for geodetic positioning." Bulletin Géodésique, 54, pp. 553-563.

Bowditch, N. (1981). "Useful tables, calculations, glossary of marine navigation." Vol. II of The American Practical Navigator, Publication No. 9, DMAHTC, Washington, D.C.

Buennagal, L.A., P.F. MacDoran, R.E. Neilan, D.J. Spitzmesser and L.E. Young (1984). "Satellite emission range inferred earth survey (SERIES) project: Final report on research and development phase, 1979 to 1983." JPL publication 84-16, March.

Counselman, C. and S. Gourevitch (1981). "Miniature interferometer terminals for earth surveying: Ambiguity and multipath with Global Positioning System." IEEE Transactions on Geoscience and Remote Sensing, Vol. GE-19, No. 4, pp. 244-252.

Davidson, D., D. Delikaraoglou, R. Langley, B. Nickerson, P. Vanicek and D. Wells (1983). "Global Positioning System differential positioning simulations." Department of Surveying Engineering Technical Report 90, University of New Brunswick, Fredericton.

Dixon, R.C. (1975). Spread Spectrum Systems. John Wiley.

Goad, C.C. and B.W. Remondi (1983). "Initial relative positioning results using the Global Positioning System." Paper presented at the XVIII General Assembly of the IUGG, IAG Symposium D, Hamburg, F.R.G., August.

Hatch, R. and K. Larson (1985). "MAGNET-4100 GPS survey program test results." These proceedings.

Johnson, C.R., P.W. Ward, M.D. Turner and S.D. Roermerman (1981). "Applications or a multiplexed GPS user set." In: Global Positioning System. Papers published in Navigation, reprinted by The (U.S.) Institute of Navigation, Vol. II, pp. 61-77.

Jorgensen, P.S. (1980). "NAVSTAR/Global Positioning System 18-satellite constellations." In: Global Positioning System. Papers published in Navigation, reprinted by The (U.S.) Institute of Navigation, Vol. II, pp. 1-12.

Kalafus, R.M. (1984). "RTCM SC-104 progress on differential GPS standards." Presented at the Annual Meeting of the U.S. Institute of Navigation, Cambridge, MA, June.

Martin, E.H. (1980). "GPS user equipment error models." In: Global Positioning System. Papers published in Navigation, reprinted by The (U.S.) Institute of Navigation, pp. 109-118.

McDonald, K.D. and R.L. Greenspan (1985). "A survey of GPS satellite system alternatives and their potential for precise positioning." These proceedings.

Mertikas, S. (1983). "Differential Global Positioning System navigation: A geometrical analysis." M.Sc. thesis, Department of Surveying Engineering, University of New Brunswick, Fredericton, May.

Milliken, R.J. and C.J. Zoller (1980). "Principle of operation of NAVSTAR and system caharacteristics." In: Global Positioning System. Papers published in Navigation, reprinted by The (U.S.) Institute of Navigation, pp. 3-14.

NATO (1983). "Methods of expressing navigation accuracies." North Atlantic Treaty Organization Standardization Agreement 4278.

Remondi, B.W. (1984). "Using the Global Positioning System (GPS) phase observable for relative geodesy: Modelling, processing, and results." Ph.D. dissertation, The University of Texas at Austin, May.

Scott, V.D. and J.G. Peters (1983). "A standardized exchange format for NAVSTAR GPS geodetic data." Applied Research Laboratories, The University of Texas at Austin, March.

Spilker, J.J. (1980). "GPS signal structure and performance characteristics." In: Global Positioning System. Papers published in Navigation, reprinted by The (U.S.) Institute of Navigation, pp. 29-54.

Stiffler, J.J. (1966). "Telecommunications." Vol. V of Space Technology, NASA.

United States Department of Defense/Department of Transportation (1982). Federal Radionavigation Plan. Vols. I-IV, March.

van Dierendock, A.J., S.S. Russell, E.R. Kopitzke and M. Birnbaum (1980). „The GPS navigation message." In: Global Positioning System. Papers published in Navigation, reprinted by The (U.S.) Institute of Navigation, pp. 55-73.

Ward, P. (1981). "An inside view of pseudorange and delta pseudorange measurements in a digital NAVSTAR GPS receiver." Presented at the ITC/USA/'81 International Telemetering Conference, San Diego, October.

Wells, D. (1974). "Doppler satellite control." Department of Surveying Engineering Technical Report 29, University of New Brunswick, Fredericton, N.B.

Wells, D., P. Vanicek and D. Delikaraoglou (1981). "Application of NAVSTAR/GPS to geodesy in Canada: Pilot study." Department of Surveying Engineering Technical Report 76, University of New Brunswick, Fredericton, N.B.

APPENDIX I
GLOSSARY OF GPS TERMINOLOGY

Ambiguity

see Carrier Beat Phase Ambiguity

Bandwidth

A measure of the width of the spectrum of a signal (frequency domain representation of a signal) expressed in Hertz (Stiffler, 1966).

Baseline

A baseline consists of a pair of stations for which simultaneous GPS data has been collected.

Beat frequency

Either of the two additional frequencies obtained when signals of two frequencies are mixed, equal to the sum or difference of the original frequencies, respectively. For example, in die identity,

cos A cos B = (cos(A+B) + cos(A-B))/2,

the original signals are **A** and **B** and the beat signals are **A+B** and **A-B**. The term Carrier Beat Phase refers only to the difference **A-B**, where **A** is the incoming Doppler-shifted satellite carrier signal, and **B** is the nominally-constant reference frequency generated in the receiver.

Between-epoch difference

The difference between two complete carrier beat phase measurements made by the same receiver on the same signal (same satellite, same frequency), but at different time epoch.

Between-frequency difference

The instantaneous difference between (or, more generally, any other linear combination involving) the complete carrier beat phase measurements made by the same receiver observing signals from the same satellite at two (or more) different frequencies.

Between-receiver difference

The instantaneous difference in the complete carrier beat phase measurement made at two receivers simultaneously observing the same received signal (same satellite, same frequency).

Between-satellite difference

The instantaneous difference in the complete carrier beat phase measurement made by the same receiver observing two satellite signals simultaneously (same frequency).

Binary pulse code modulation

Pulse modulation using a string (code) of binary numbers. This coding is usually represented by ones and zeros with definite meanings assigned to them, such as changes in phase or direction of a wave (Dixon, 1975).

Binary biphase modulation

Phase changes on a constant frequency carrier of either 0° or 180° (to represent binary 0 or 1 respectively). These can be modelled by $\mathbf{y = A(t) \cos(\omega t + \phi)}$, where the amplitude function **A(t)** is a sequence of +1 and -1 values (to represent 0! orm180° phase changes respectively) (Dixon, 1975).

Carrier

A radio wave having at least one characteristic (e.g. frequency, amplitude, phase) which may be varied from a known reference value by modulation (Bowditch, 1981, Vol. II).

Carrier frequency

The frequency of the unmodulated fundamental output of a radio transmitter (Bowditch, 1981, Vol. II).

Carrier beat phase

The phase of the signal which remains when the incoming Doppler-shifted satellite carrier signal is beat (the difference frequency signal is generated) with the nominally-constant reference frequency generated in the receiver.

Carrier beat phase ambiguity

The uncertainty in the initial measurement, which biases all measurements in an unbroken sequence. The ambiguity consists of three components

$$\alpha_i + \beta_j + N_i^j$$

where

α_i is the fractional initial phase in the receiver

β_j is the fractional initial phase in the satellite (both due to various contributions to phase bias, such as unknown clock phase, curcuit delays, etc.), and

N_i^j is an integer cycle bias in the initial measurement.

Channel

A channel of a GPS receiver consists of the radiofrequency and digital hardware, and the software, required to track the signal from one GPS satellite at one of the two GPS carrier frequencies.

Chip

The minimum time interval of either a zero or a one in a binary pulse code.

C/A-code

see S-code.

Complete instantaneous phase measurement

A measurement of carrier beat phase which includes the integer number of cycles of carrier beat phase since the initial phase measurement. See fractional instantaneous phase measurement.

Correlation-type channel

A GPS receiver channel which uses a delay lock loop to maintain an alignment (correlation peak) between the replica of the GPS code generated in the receiver and the incoming code.

Delay lock

The technique whereby the received code (generated by the satellite clock) is compared with the internal code (generated by the receiver clock) and the latter shifted in time until the two codes match. Delay lock loops can be implemented in several ways, for example, tau dither and early-minus-late gating (Spilker, 1980).

Delta pseudorange

The difference between two carrier beat phase measurements, made coincidentally with (code) pseudorange epochs.

Differenced measurements

see Between-epoch difference; Between-frequency difference; Between-receiver difference; Between-satellite difference.

Many combinations of differences are possible. Which differences, and their order, should be specified in describing a processing method (for example Receiver-Satellite Double Differences).

Differential positioning

see Relative Positioning.

Dilution of precision (DOP)

A description of the purely geometrical contribution to the uncertainty in a dynamic position fix, given by the expression

$$\mathbf{DOP} = \sqrt{\mathbf{Trace}\left(\mathbf{A}^{\mathbf{T}}\mathbf{A}\right)^{-1}},$$

where A is the design matrix for the solution (dependent on satellite/receiver geometry). The DOP factor depends on the parameters of the position fix solution. Standard terms in the case of kinematic GPS are:

GDOP (three position coordinates plus clock offset in the solution)
PDOP (three coordinates)
HDOP (two horizontal coordinates)
VDOP (height only)
TDOP (clock offset only) and
HTDOP (horizontal position and time).

Doppler shift

The apparent change in frequency of a received signal due to the rate of change of the range between the transmitter and receiver. See carrier beat phase.

Dynamic positioning

see Kinematic positioning

Fast switching channel

A switching channel with a sequence time short enough to recover (through software prediction) the integer part of the carrier beat phase.

Fractional instantaneous phase measurement

A measurement of the carrier beat phase which does not include any integer cycle count. It is a value between zero and one cycle. See complete instantaneous phase measurement.

Frequency band

A range of frequencies in a particular region of the electromagnetic spectrum (Wells, 1974).

Frequency spectrum

The distribution of amplitudes as a function of frequency of the constituent waves in a signal (Wells, 1974).

Handover word

The word in the GPS message that contains time synchronization information for the transfer from the S-code to the P-code (Milliken and Zoller, 1980).

Independent baseline

Baselines determined from independent observing sessions.

Independent observing sessions

Sessions for which any common biases affecting the observations can be ignored.

Ionospheric refraction

A signal travelling through the ionosphere (which is a nonhomogeneous and dispersive medium) experiences a propagation time different from that which would occur in a vacuum. Phase advance depends on electron content and affects carrier signals. Group delay depends on dispersion in the ionosphere as well, and affects signal modulation (codes). The phase and group advance are of the same magnitude but opposite sign (Davidson et al., 1983).

Interferometry

see Relative positioning

Kinematic positioning

Kinematic positioning refers to applications in which a trajectory (of a ship, ice field, tectonic plate, etc.) is determined.

Lane

The area (or volume) enclosed by adjacent lines (or surfaces) of zero phase of either the carrier beat phase signal, or of the difference between two carrier beat phase signals. On the earth's surface a line of zero phase is the locus of all points for which the observed value would have a exact integer value for the complete instantaneous phase measurement. In three dimensions, this locus becomes a surface.

L-band

The radio frequency band extending from 390 MHz to (nominally) 1550 MHz (Bowditch, 1981, Vol. II).

Multipath error

An error resulting from interference between radiowaves which have travelled between the transmitter and the receiver by two paths of different electrical lengths (Bowditch, 1981, Vol. II).

Multichannel receiver

A receiver containing many channels.

Multiplexing channel

A receiver channel which is sequenced through a number of satellite signals (each from a specific satellite and at a specific frequency) at a rate which is synchronous with the satellite message bit-rate (50 bits per second, or 20 milliseconds per bit). Thus one complete sequence is completed in a multiple of 20 milliseconds.

Observing session

The period of time over which GPS data is collected simultaneously by two or more receivers.

Outage

The occurence in time and space of a GPS Dilution of Precision value exceeding a specified maximum.

Phase lock

The technique whereby the phase of an oscillator signal is made to become a smoothed replice of the phase of a reference signal by first comparing the phases of the two signals and then using the resulting phase difference signal to adjust the reference oscillator frequency to eliminate phase difference when the two signals are next compared (Bowditch, 1981, Vol. II). The smoothing time span occurs over approximately the inverse of the bandwidth. Thus a 40 hertz loop bandwidth implies an approximately 25 millisecond smoothing time constant.

Phase observable

See Carrier beta phase.

P-code

The Precise (or Protected) GPS code – a very long (about 1014 bit) sequence of pseudorandom binary biphase modulations on the GPS carrier at a chip rate of 10.23 MHz which does not repeat itself for about 257 days. Each one-week segment of the P-code is unique to one GPS satellite, and is reset each week.

Precise positioning service (PPS)

The highest level of dynamic positioning accuracy that will be provided by GPS, based on the dual frequency P-code (U.S. DoD/DOT, 1982).

Pseudolite

The ground-based differential GPS station which transmits a signal with a structure similar to that of an actual GPS satellite (Kalafus, 1984).

Pseudorandom noise (PRN) code

Any of a group of binary sequences that exhibit noise-like properties, the most important of which is that the sequence has a maximum autocorrelation, at zero lag (Dixon, 1975).

Pseudorange

The time shift required to align (correlate) a replica of the GPS code generated in the receiver with the received GPS code, scaled into distance by the speed of light. This time shift is the difference between the time of signal reception

(measured in the receiver time frame) and the time of emission (measured in the satellite time frame).

Pseudorange difference

See Carrier beat phase.

Receiver channel

See Channel.

Reconstructed carrier phase

See Carrier beat phase.

Relative positioning

The determination of relative positions between two or more receivers which are simultaneously tracking the same radiopositioning signals (e.g. from GPS).

Restart capability

A property of a sequential processing computer program, that data can be processed rigorously in a sequence of computer runs, rather than only in one long run.

S-code

The Standard GPS code (formerly the C/A, Coarse/Aquisition, or Clear/Access code) – a sequence of 1023 pseudorandom binary biphase modulations on the GPS carrier at a chip rate of 1.023 MHz, thus having a code repitition period of one millisecond.

Satellite constellation

The arrangement in space of the complete set of satellites of a system like GPS.

Satellite configuration

The state of the satellite constellation at a specific time, relative to a specific user or set of users.

Simultaneous measurements

Measurements referred to time frame epochs which are either exactly equal, or else so closely spaced in time that the time misalignment can be accomodated by correction terms in the observation equation, rather than by parameter estimation.

Slow switching channel

A switching channel with a sequencing period which is too long to allow recovery of the integer part of the carrier beat phase.

Spread spectrum systems

A system in which the transmittet signal is spread over a frequency band much wider than the minimum bandwidth needed to transmit the information being sent (Dixon, 1975).

Squaring-type channel

A GPS receiver channel which multiplies the received signal by itself to obtain a second harmonic of the carrier, which does not contain the code modulation.

Standard positioning service (SPS)

The level of kinematic positioning accuracy that will be provided by GPS based on the single frequency S-code (U.S. DoD/DOT, 1982).

Static positioning

Positioning applications in which the positions of points are determined, without regard for any trajectory they may or may not have.

Switching channel

A receiver channel which is sequenced through a number of satellite signals (each from a specific satellite and at a specific frequency) at a rate which is slower than, and asynchronous with, the message data rate.

Translocation

See Relative positioning.

User equivalent range error (UERE)

The contribution to the range measurement error from an individual error source, converted into range units, assuming that error source is uncorrelated with all other error sources (Martin, 1980).

Z-count word

The GPS satellite clock time at the leading edge of the next data subframe of the transmitted GPS message (usually expressed as an integer number of 1.5 second periods) (van Dierendock et al., 1980).

REVIEW PAPER
GPS-TECHNOLOGY AND METHODOLOGY FOR GEODETIC APPLICATIONS

Ph. Hartl, W. Schöller, K.-H. Thiel

Institute of Navigation
University of Stuttgart

Keplerstraße 11
7000 Stuttgart 1
Fed. Rep. of Germany

ABSTRACT

Present and final system configuration of the GPS-NAVSTAR and possible applications are reviewed. The pseudo-random noise-sequences (PRN-coding), in combination with Doppler and phase measurements, allow the realization of an extremely precise and flexible system for many kinds of navigation purposes.

The design concept alternatives for GPS-receivers are discussed with respect to the application of

- One and Two-carrier Receiving Systems
- One or Multiple Ranging Receiver channels
- Analog or Digital Circuitry
- Only Code and Carrier Information
- Carrier Phase Extraction.

Actually available GPS-receivers are reviewed.

The various geodetic and geodynamic measurement tasks are shortly discussed in view of applicable measurement configurations.

INTRODUCTION

The NAVSTAR GPS has been under development and test for over one decade First results with the initial space vehicles (SV) brought up high civil interest in the system. Various types of GPS-receivers appeared or were announced for a growing community of potential users. Doubts about the availability of the precise P-code led to the development of codeless and pure C/A-code receivers with doppler and carrier phase measurement for geodetic applications. Much work has been investigated to produce computer algorithms for high accurate position and baseline estimations and especially to solve the problem of phase ambiguity.
In this review the NAVSTAR GPS is described with particular emphasis to points of geodetic interest. First we will discuss satellite orbits and ranging measurements, then show different receiver concepts with a list of some existing receivers and finally come to the measuring methods for geodetic application.

Space segment

The operational NAVSTAR GPS will consist of 18 satellites, deployed in six orbital planes equally spaced 60 degrees in longitude and inclined to the equator at 55 with 3 satellites per plane. The satellites are shifted 40 to north for successive planes, as shown in figure 1 and they are all in

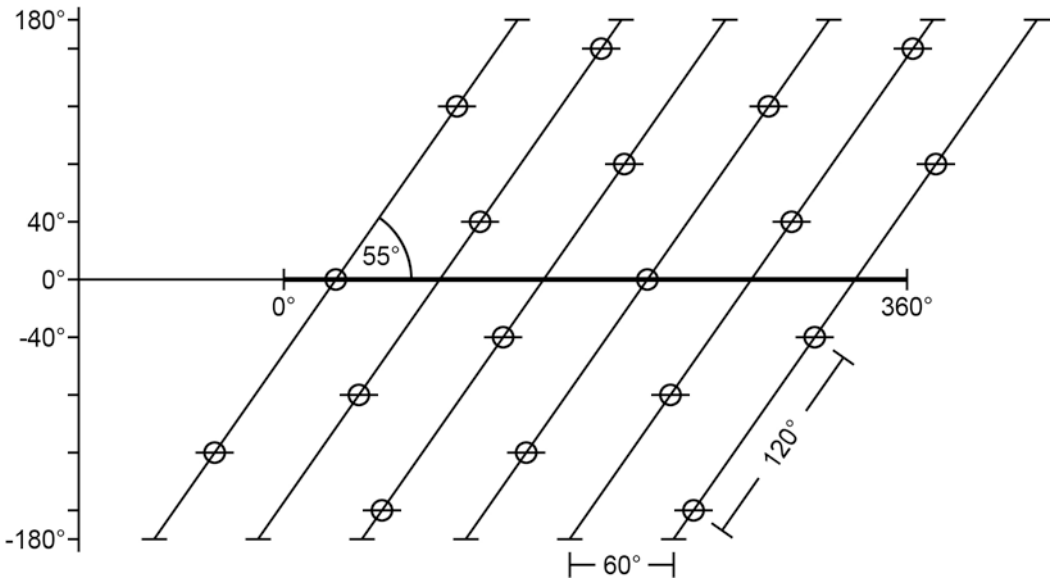

Fig. 1
FUTURE FULL SCALE SATELLITE CONFIGURATION

circular, 12 hour orbits with approximately 20183 km altitude.

The present system is an experimental system in PHASE II for full scale development and system test. Satellites are deployed in two planes, spaced 120° in longitude und inclined about 63°. The satellite configuration is shown in figure 2. Two satellites (number 4 and 7) can’t be used any longer, because of their health situation.

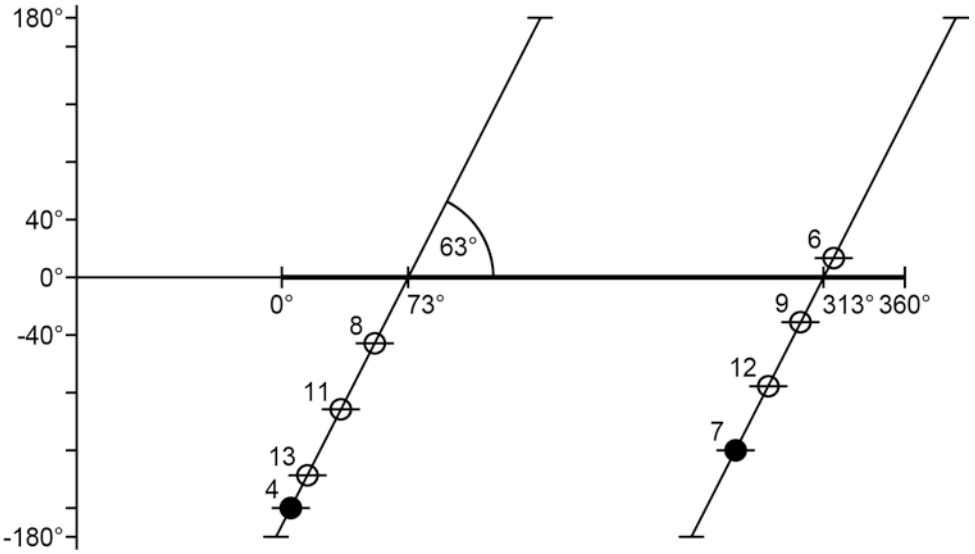

Fig. 2
PRESENT CONFIGURATION OF GPS - SATELLITES

In figure 3 through 6 we show several possibilities of representing the satellite orbits.

Figure 3 shows the orbit configuration. The viewpoint lies over Munich, with a non rotating earth. Figure 4 shows a more sophisticated view on the satellite orbit. The observer rotates with the earth for a whole day. For a better control, the ground tracks are plotted on the globe.

Because of the 12 hour orbit of the satellites the ground traces are fixed from day to day. Therefore a satellite passes over the same points every 23 hr 55 min and 56.6 sec. Most of the difference from 24 hours is due to the difference between the solar and siderial day. Thus a satellite appears 4 min 3.4 sec earlier each day. A computed ground

PRESENT SATELLITE CONFIGURATION

INSTITUT FUER NAVIGATION DER UNI STUTTGART

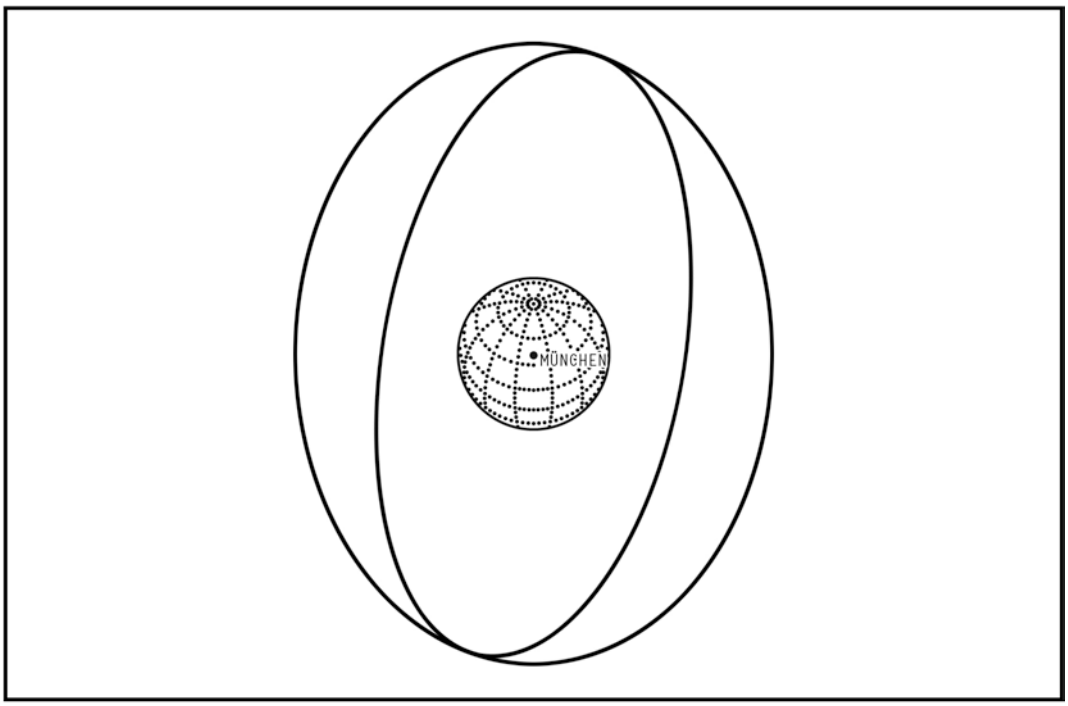

FIG. 3a
POINT OF VIEW ABOVE SPHEROID = 200 000 KM

FUTURE SATELLITE CONFIGURATION

INSTITUT FUER NAVIGATION DER UNI STUTTGART

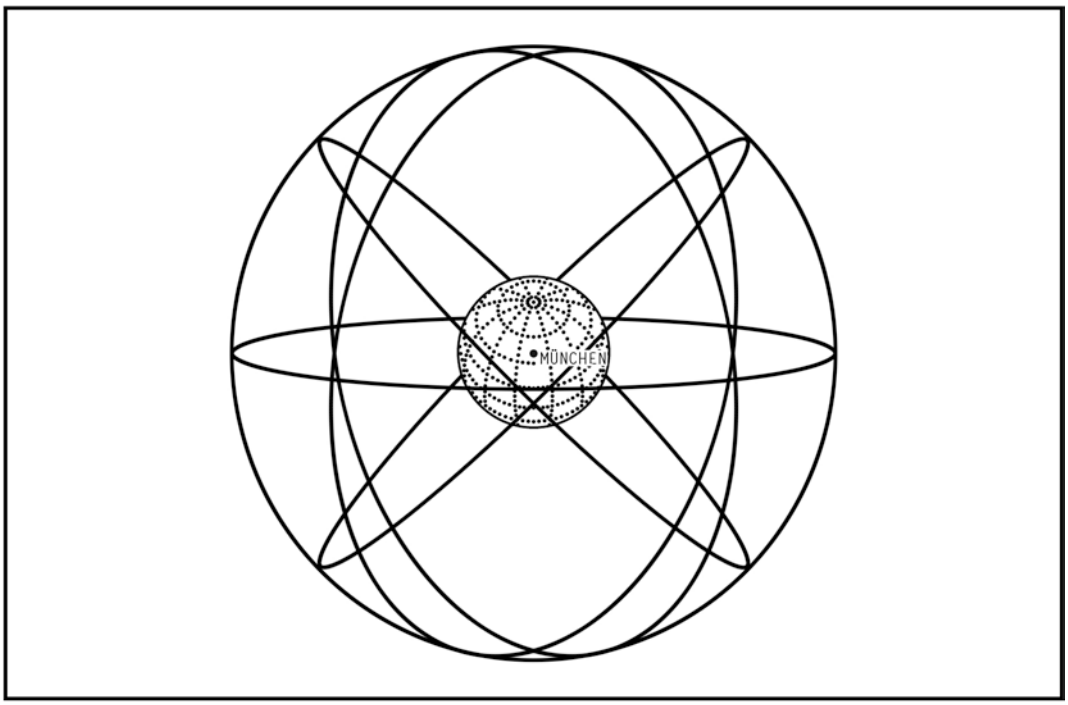

FIG. 3b
ORBITS OF THE GPS-SATELLITES

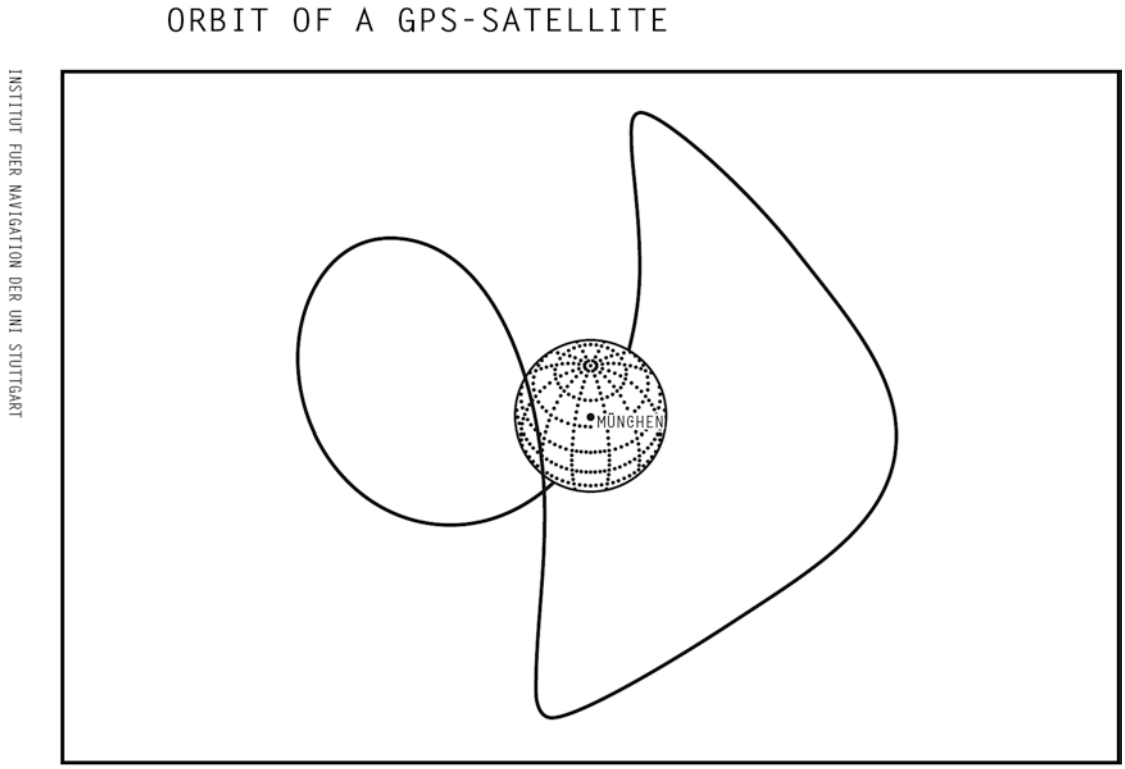

FIG. 4
POINT OF VIEW ABOVE MUNICH = 200 000 KM

track in the Mercator chart in figure 5 can be used for a long time, only regarding n’times the time difference of about 4 min when determing a satellite ground track position.

For various tasks it is necessary to know the satellite’s position in the sky. This information is early achieved from figure 6, where the satellite position is defined by azimuth and elevation. In this representation the surroundings - high buildings, mountains etc. – can be embedded, so that real visibility of a satellite can be demonstrated. Here once more the time shift of 4 min is the only changing factor. This representation – azimuth and elevation – is the basis for calculating satellite alert data. In figure 7 we show an example for Munich. In figure 8 as an example the visibility of the 6 satellites of the present configuration is shown.

A 3D geodetic position fix requires pseudo-range-measurements from four GPS satellites, with time being the fourth unknown variable. So one must assure, that the signals of 4 satellites can be received. The concept of the pseudo-range-measurements is simplified and illustrated in figure 9. All satellites are synchronised to exactly the same – GPS time –

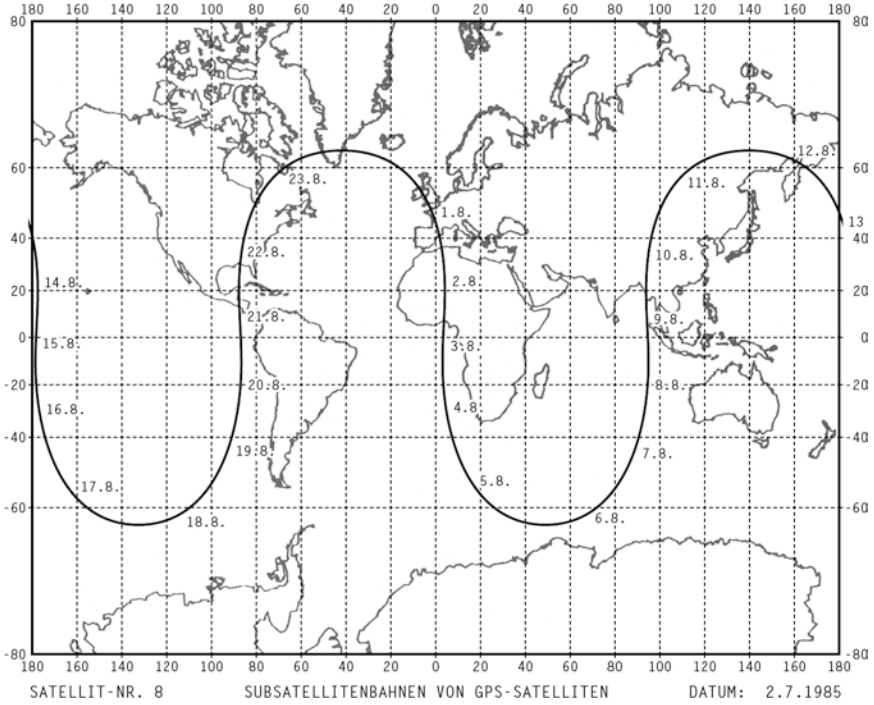

Figure 5

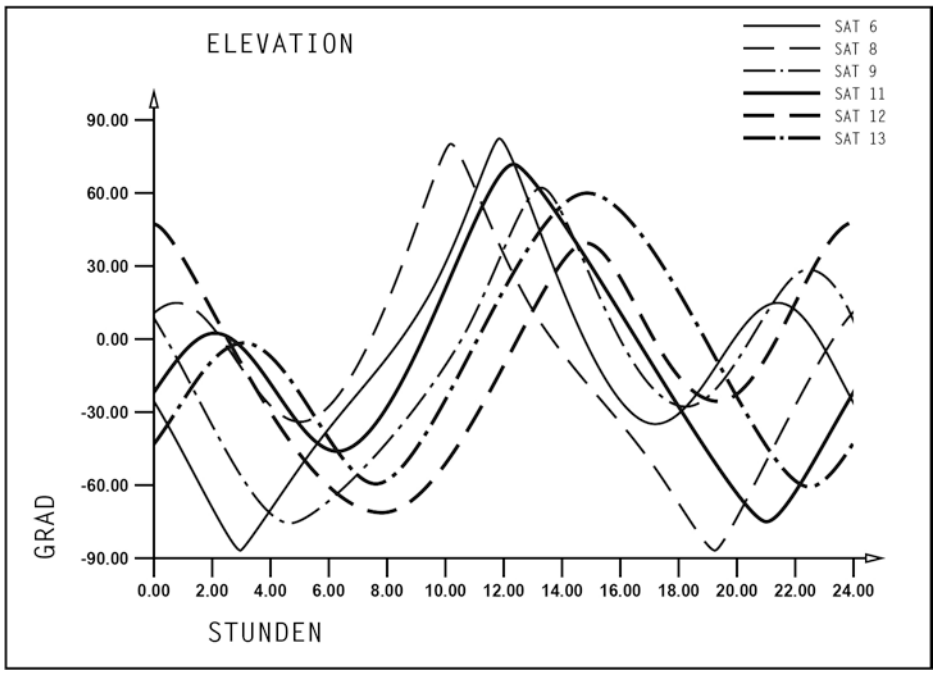

Figure 6a

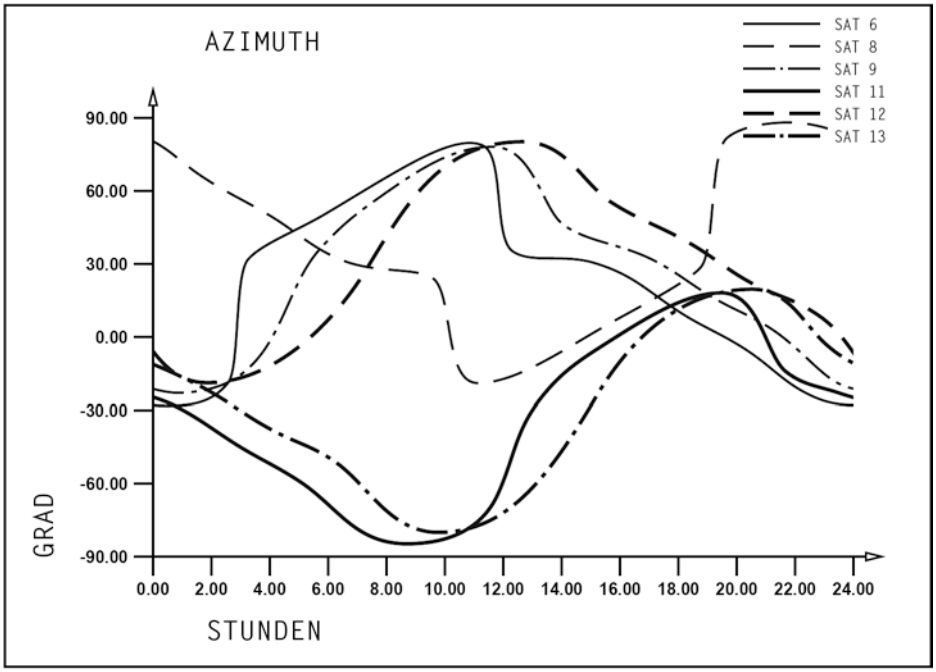

Figure 6b

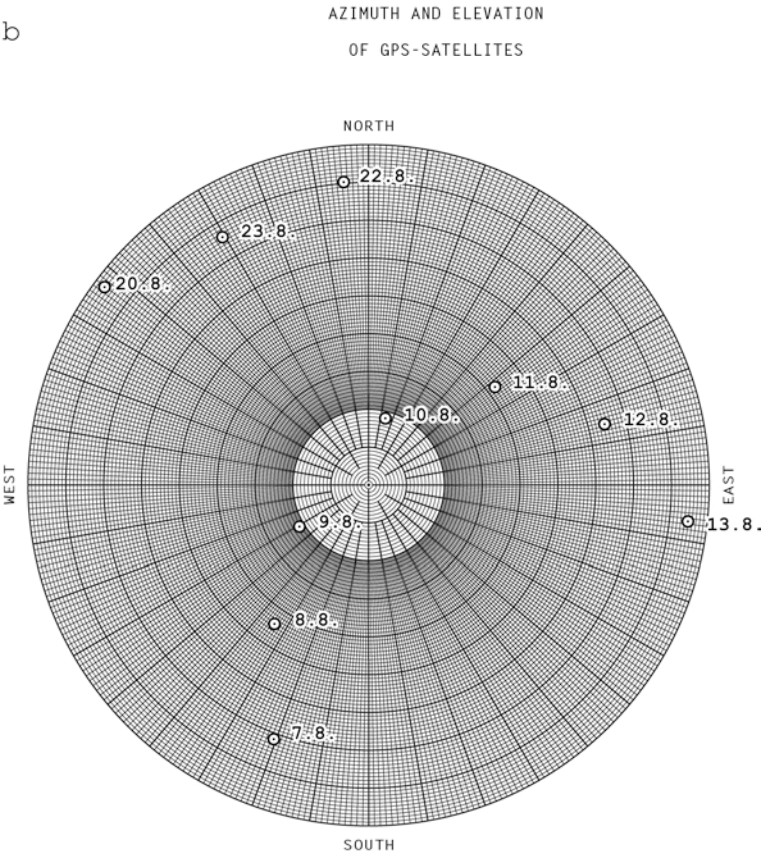

Figure 7

```
SICHTBARKEITSTABELLE FUR DEN TAG:    2   7          1985

SAT.NR

 6                       *  *  *  *  *  *  *                    *  *
 8     *  *  *  *                  *  *  *                       *  *
 9     *                       *  *  *  *  *  *  *
11        *  *  *  *                  *  *  *  *
12        *                           *  *  *  *  *  *
13              *  *  *  *              *  *  *  *  *

ZEIT   0  1  2  3  4  5  6  7  8  9 10 11 12 13 14 15 16 17 18 19 20 21 22 23
```

Figure 8

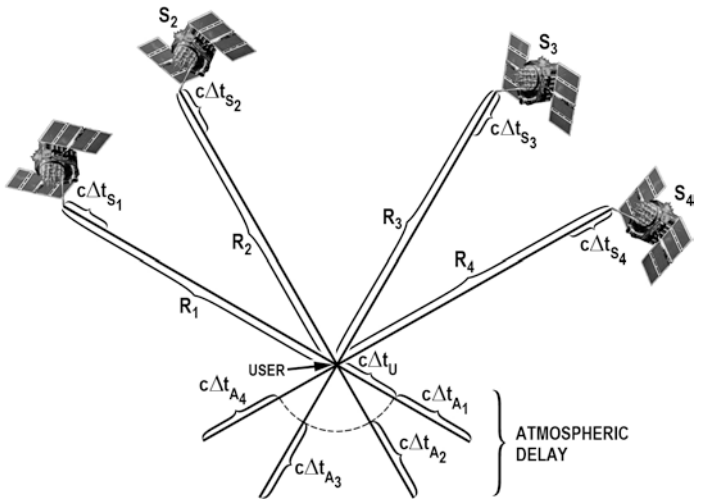

Figure 9

and therefore transmitting the ranging information simultaneous. A range measurement is defined as the transit time from the Space Vehicle (SV) to the observing user (receiver), scaled by the speed of light.

$$R_i = c \cdot (t_R - t_S) - c \cdot \Delta t_{A_i} \qquad (1)$$

R_i true slant range

t_R GPS receive time

t_S GPS transmit time

Δt_{A_i} propagation delays

The receiver time offset Δt_R from GPS time allows only pseudorange measurements and the clock offset must be determined.

$$R_i = R_i + ct_{A_i} + c\Delta t_R + c\Delta t_{S_i} \qquad (2)$$

R_i pseudo range

$c\Delta t_{S_i}$ satellite clock offset from GPS time

The user must solve for four unknowns his position coordinates X, Y, Z (earth fixed and earth centered – WGS 72) and his clock offset Δt_R.

Defining

$$R_i = \sqrt{(X_{S_i} - X_R)^2 + (Y_{S_i} - Y_R)^2 + (Z_{S_i} - Z_R)^2} \qquad (3)$$

we get with equation (2):

$$R_i = \sqrt{\left[(X_{S_i} - X_R)^2 + (Y_{S_i} - Y_R)^2 + (Z_{S_i} - Z_R)^2 + c \cdot \Delta t_{A_i} + c \cdot (\Delta t_R + \Delta t_{S_i})\right]} \qquad (4)$$

The estimation for the unknown also gives a result for the measurement error statistic, represented in the covariance matrix, from which we can derive the definition of the GDOP factors as

$$HDOP = \sqrt{(\sigma_{xx^2} + \sigma_{yy^2})}$$

$$VDOP = \sigma_{zz}$$

$$PDOP = \sqrt{(\sigma_{xx^2} + \sigma_{yy^2} + \sigma_{zz^2})} \qquad (5)$$

$$TDOP = \sigma_{tt}$$

$$PDOP = \sqrt{(\sigma_{xx^2} + \sigma_{yy^2} + \sigma_{zz^2} + \sigma_{tt^2})}$$

We can interpret these factors with the satellite geometrie. In (1) it is shown, that the volume V of a tetrahedron (figure 10) is reciprocal to the value of PDOP.

$$PDOP \approx 1/V$$

In figure 11 GDOP, PDOP and the HDOP from the future 18 satellite configuration are plotted for a latitude of 40°. The quality of position determination depends on time and latitude. Because of the repeatability of the orbits the GDOP also repeats each day. For precise measurements it is necessary to choose the times with lowest GDOP factors.

The present configuration is arranged in such a way, that highest ranging accuracy is attainable in the testing area of Yuma in Arizona. Also promoted by the proximity to the Vandenberg located Monitor Station, Master Control Station

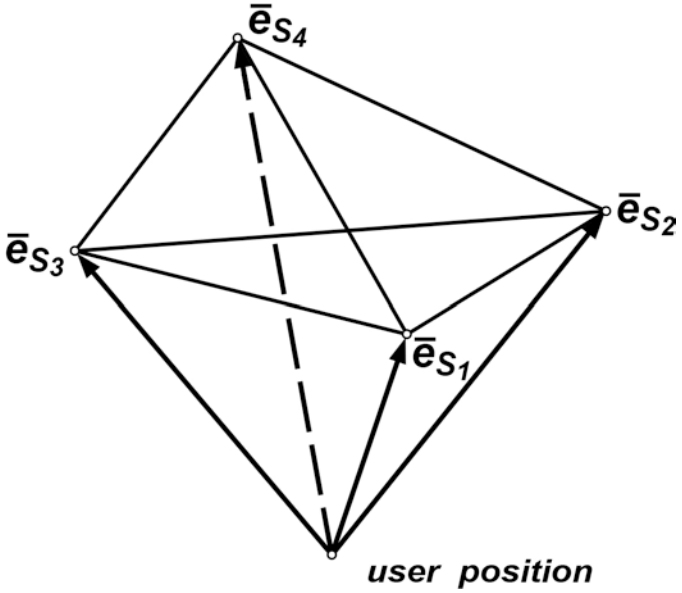

Figure 10

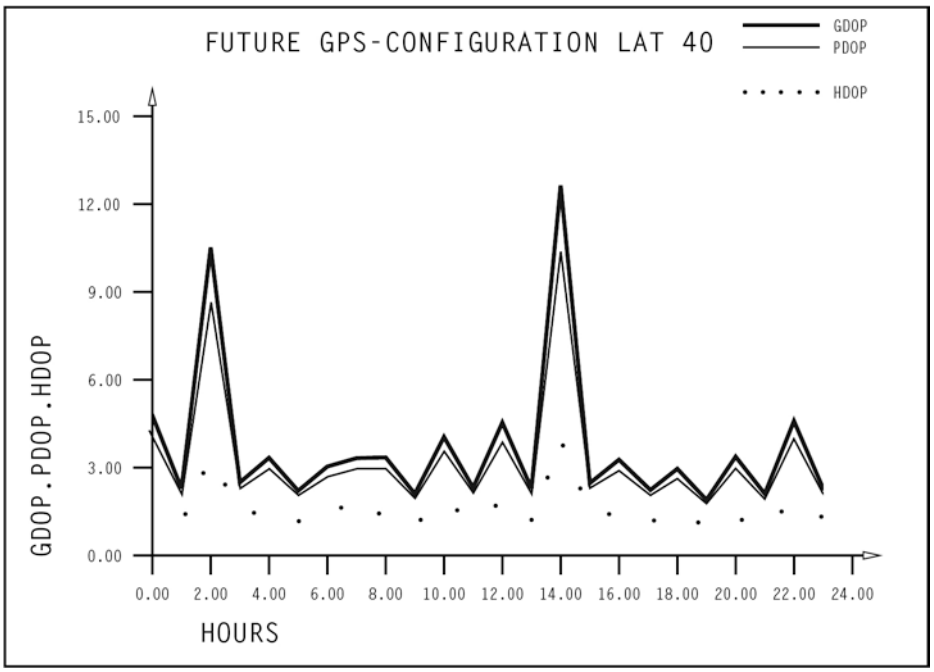

Figure 11

and Upload Station.

These stations belong to the ground control segment of GPS. Successful operation and system accuracy depends on the precise knowledge of satellite parameters, like position and time. Four Monitor Stations (MS) continuously track the SV's and the one-way range measurements were transmitted to the Master Control Station. Finally the computed ephemeris, clock updates for each SV along with almanac, special messages and diagnostics are daily transmitted from the accociated Upload Station to the GPS space vehicles. The Master Control Station will be located in the consolidated Space Operations Center at Colorado Springs.

GPS Signal Structure

For navigation information the satellite transmits two L-band signals with center frequencies L_1 at 1575.42 MHz and L_2 at 1227.6 MHz. These and all other frequencies are coherently derived from the satellite clock frequency (10.23 MHz). L_1 and L_2 are exact multiples of the clock frequency ($L_1 = 142 \cdot 10.23$ MHz, $L_2 = 120 \cdot 10.23$ MHz) and both frequencies are required for ionospheric error compensation. The L_1 carrier is QPSK modulated by two PRN-signals, the P-Code – P(t) – (now "Precise positioning Service") with 10.23 MHz clock rate and the C/A-Code – C(t) – (now "Standard Positioning Service") with 1.023 MHz clock rate.

The navigation message – ephemeris, correction terms, almanac etc. _ is modulated on both signals by modulo 2 multiplication with a data rate of 50 bit per second.

The L2 carrier is normally BPSK modulated with the P-Code. In Phase II an alternative modulation with the C/A-Code for special testing facilities can be achieved. The transmitted signals are

$$s_{L_1} = A_P \cdot P(t) \cdot D(t) \cdot \cos(w_1 t + \Phi) + A_C \cdot C(t) \cdot D(t) \cdot \sin(w_2 + \Phi) \qquad (7)$$

$$s_{L_2} = B_P \cdot P(t) \cdot D(t) \cdot \cos(w_1 t + \Phi) \qquad (8)$$

where A_P, A_C and B_P are constant amplitudes of the codes.

The ranging information, that can be derived from these signals are concentrated in table 1.

	frequency	Length of one element time/range	Resolution within one element	possible range resolution
C/A-code	1 kHz	1 msec = 300 km	1 chip	300 m
P -code	1/7·86400 Hz	1 week	1 chip	30 m
C/A-chip	1.023 MHz	1/1.023 µs = 293.3 m	< 1/50	< 6 m
P -chip	10.23 MHz	1/10.23 µs = 29.3 m	< 1/50	< 0.6 m
L_1-carrier	1575.42 MHz	1/1.57542 µs = 19.05 m	< 6° = 1/60	< 0.3 m
L_2-carrier	1227.6 MHz	1/1.2276 µs = 24.43 m	< 6° = 1/60	< 0.4 m

Table 1: Ranging information from GPS-signals

With the C/A-Code we have a range ambiguity of 300 km, therefore a rough information about the receiver position is useful. For better range measurement one should assure, that no ambiguous resolution is chosen. This could be achieved by the following range measurement with overlapping resolution.

C/A-code	300 km	300 m
C/A-chip	300 m	3 m (30 cm)
P-chip	30 m	30 cm (3 cm)
L_2	24 cm	2.4 mm
L_1	19 cm	1.9 mm

Another possibility is the integrated Doppler measurement, as it is done with TRANSIT. In figure 12 some Doppler shifts

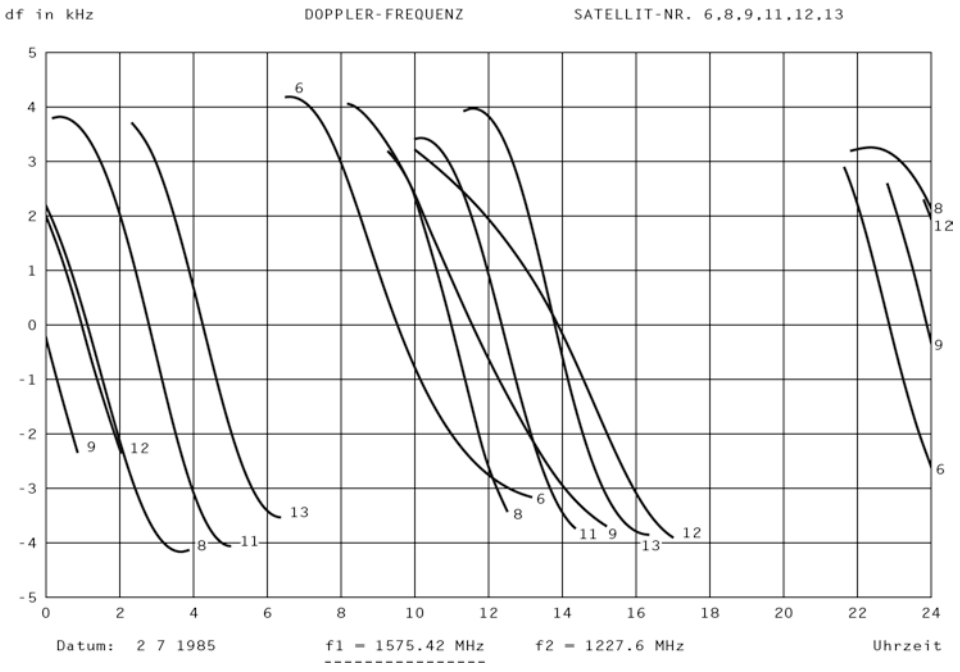

Figure 12

are plotted. The greatest Doppler offset will be about +4.8 kHz.

Receiver concepts

Regarding the different measurements we may compose several types of geodetic receivers with different accuracies and complexity

- C/A-code range measurement 3 m
- C/A+P_{L1}-code 0.3 m
- C/A+P_{L1}+P_{L2}-code with ionosphere compensation 0.3 m
- C/A-code+clock P_{L1}+clock P_{L2} 0.6 m
- C/A-code+clock P_{L1}+clock P_{L2}+Doppler (clock C/A) 0.6 m and velocity
- C/A-code+clock P_{L1}+clock P_{L2}+Φ_{L1}+Φ_{L2}+Doppler (clock C/A)

Integrated Doppler observations are assumed to be independent from range measurements. Beside these combinations the technical realisation can be based on the

- sequential
- multiplex, or
- multichannel

concept and on

- analog
- digital
- hybrid

techniques therefore many different receivers can be developed, leading to different performances.

A single channel sequencing GPS receiver offers the lowest price, simplicity and can provide rather high accuracy for stationary tasks. Conversely a multichannel receiver provides a maximum of accuracy under dynamics, continuous tracking of four satellites with integrated Doppler, high data collection and maximum antijam performance. These both types can be realized as analog, digital or hybrid instrument, whereas a single receiver multiplex set should be a digital one. A multiplex receiver can provide almost all benefits of a multichannel set, except a loss of 6 dB in SNR, because not all the signal power of a SV can be used continuously.

This fact can be of interest in a hostile environment.

Figure 13 shows a typical hardware concept of a GPS receiver. There are three parts, the front end with 1st IF, the decision loops and the microprocessor with I/0 unit and data recording unit. Most difference we find in various loop implementations. Table 2 contains a list of several reveivers and their characteristics.

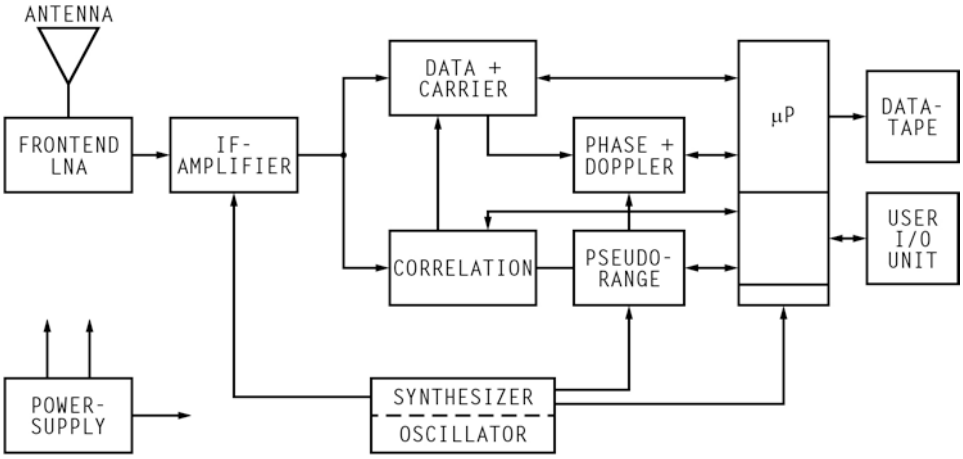

BLOCK DIAGRAM OF A GPS-RECEIVER

Figure 13

RECEIVER	DESIGNATION	MEAS.	CODES	CH.	FREQU.	REMARK
JPL SERIES/SERIES X	geod./geoph.	PH , R	CR + P	6	L1,L2	hybrid
STANFORD TELEC. INC.	time/civil	PH , R	C + P	1	L1,L2	analog
COLLINS	milit.	R	C + P	4	L1,L2	an/dig
TEXAS INSTR. TI4100	civil/geod.	PH , R	C + P	4	L1,L2	dig/MX
TRIMBLE 4000A	civil	R , ΔR	C	1	L1	dig/MX
5000A	time/frequ.	R	C	1	L1	
MAGNAVOX X-SET	milit.	R	C + P	4	L1,L2	
Y-SET				1		
MACROMETER V1000	civil/geod.	PH	-	6	L1	
AFGL				6	L1,L2	
SERCEL TR5S	civil	PH , R	C	5	L1	analog
ALLEN OSBORNE TTR-5	time/pos.	R	C	1	L1	
POLYTECHNIC XR1	time/geod.	R	C	1	L1	
WILD/MAGNAVOX WM-101	geod.	R , PH	C	4	L1,L2	an/dig
JAPANES RADIO Co	civil	R	C	1	L1	dig/MX
SONY	time/nav.	R	C		L1	
S E L	prototype	R	C	1	L1	dig/MX
PRAKLA SEISMOS	prototype	R	C	1	L1	dig/MX

L1 = 1.515426 GHz, L2 = 1.2276 GHz
MX = Multiplex

Table 2

Measuring methods

The maximum accuracy for absolute point positioning with GPS is not good enough for geodetic applications. Table 3 gives a example for PPS measurements. For better results differential measurement – like Translocation mode with TRANSIT - should be used. Within a limited area all bias terms can be removed, and the attainable accuracy is better than 1 meter. The principles of differential measurements is shown in figure 14.

ERROR BUDGET

ERROR SOURCE	ABS. BIAS	GPS RAND.	TOTAL	DIFF. BIAS	GPS RAND.	TOTAL
- CLOCK AND NAVIGATION SUBSYSTEM STABILITY	0	2.7	2.7	0	2.7	2.7
- PREDICTABILITY OF SATELLITE PERTURBATIONS	1	0	1	0	0	0
- OTHER	0	0.9	0.9	0	0.9	0.9
- EPHEMERIS AND CLOCK PREDICTION	2.5	0	2.5	0	0	0
- IONOSPHERIC DELAY COMPENSATION	2.3	0	2.3	0	0	0
- TROPOSPHERIC DELAY COMPENSATION	0	2.0	2.0	0	0	0
- RECEIVER NOISE AND RESOLUTION	0	1.5	1.5	0	2.0	2.0
- MULTIPATH	0	1.2	1.2	0	1.2	1.2
1 SYSTEM USER EQUIVALENT RANGE ERROR (UERE)	3.54	3.97	5.3	0	3.97	3.97

Table 3

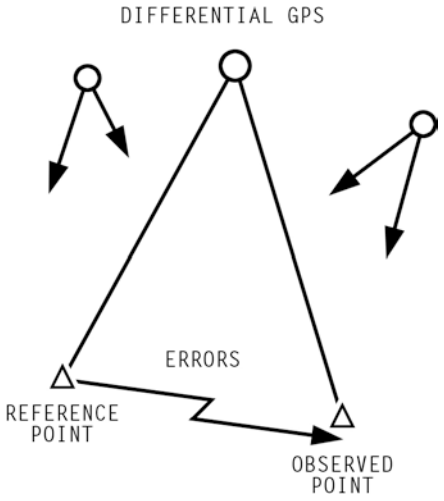

Figure 14

Differential GPS offers best results for exact navigation - landing on small airports, ship navigation in harbour regions etc. – and good assumptions for geodetic users.

For geodetic application one can use some special measurement methods

- Differential range

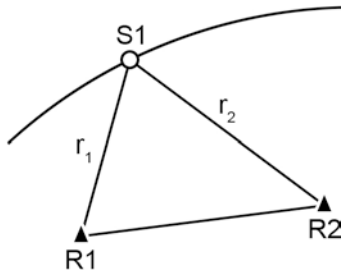

* eliminates bias of satellite and for short distance the propagation delay, for long distances the use of both frequencies is necessary

- Range difference (integrated Doppler)

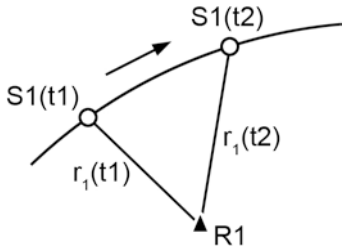

- Differential range difference (double difference)

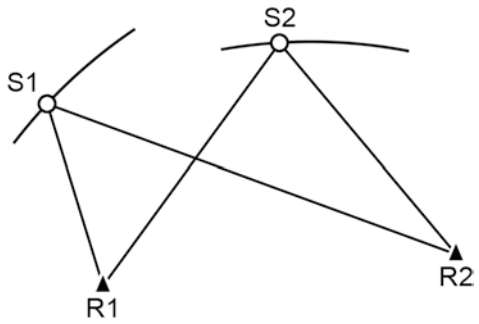

* satellite bias and relative receiver bias can be eliminated

- Differenced range difference (triple difference)

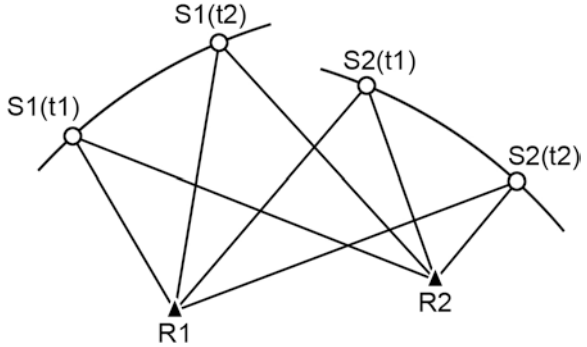

* satellite bias and relative receiver bias and unknown phase shift

The more effort in measurement will be investigated, the more error sources can be excluded. These measurement will achieve high geodetic positioning, but one will always need two receivers as a minimum.

Conclusion

GPS offers many ways of measurement techniques important for geodetic applications. They will be used more in the future, as they can meet the practical needs. It is true that the instrumentation is still too expensive. But one can except considerable cost reductions for the future, because of the continuing technological progress in microelectronics.

REFERENCES

1. Masahiko Kihara, Tsuyoshi Okada, “A Satellite Selection Method and Accuracy for the Global Positioning System”, NAVIGATION, Vol. 31, No. 1, Spring 1984.

- Review Paper -

SATELLITE AND INERTIAL SURVEYING:

TRENDS AND PROSPECTS

by

Edward J. Krakiwsky
Division of Surveying Engineering
The University of Calgary
Calgary, Alberta, Canada
T2N 1N4

ABSTRACT

The NAVSTAR Global Satellite Positioning System (GPS), along with Inertial Surveying Systems (ISS) and Inertial Navigation Systems (INS) have revolutionized position determination. The use of these systems is identified within the context of user applications. Present obstacles hindering full implementation of these systems are identified. The future is speculated upon with the identification of the emergence of a "position oriented society".

1. INTRODUCTION

It is natural to discuss satellite and inertial techniques together when one considers the task of positioning within the context of national and engineering surveys. The reason for this is that one is a discrete point to point operation, while the latter is a continuous interpolator of position. Further, satellite methods yield high proportional accuracy over large distances (100's of km) and, now, are even considered for positioning shorter lines (a few 10's of km). Inertial Survey Systems (ISS) do, however, have an accuracy that deteriorates with time but when controlled by satellite positions show an improved accuracy. This symbiotic relationship comes to the fore when one considers the task of (kinematic) positioning ships, ground vehicles and aircraft. On the other hand, ISS as stand alone systems are more economical but less accurate.

Two factors that have lead to the intense usage of these two methods are those of accuracy and cost effectiveness. Also, they produce three dimensional positions and even velocity information within the context of kinematic positioning. Further, electronic satellite methods (eg. GPS) are all weather systems unlike the former optical satellite methods which were plagued by bad weather and vast amounts of post processing rendered them cost ineffective.

Satellite and inertial equipment have undergone vast improvement due to the recent competition among manufacturers and suppliers which vies well for the user and this trend will continue.

Another development that has helped the profession make the great stride it has, is the development and implementation of mathematical modelling and statistical techniques such as filtering and smoothing algorithms.

Discussed in the remainder of this paper is a categorization of positioning tasks and their application in society (Section 2). Then in Section 3 the obstacles standing in the road of further progress are

Table 1: Positioning Tasks, Applications and User Accuracy Requirements

POSITIONING TYPE				Application	User Accuracy Requirement	Comment
	static	point and relative		consumer positioning: hikers, bikers and campers	50 m to 200 m	GPS point positioning mode: single frequency receiver.
				legal, control and concession surveys	1.5 m to 10 m	GPS point and relative positioning mode: one frequency receiver. Inertial Survey System (ISS).
				precise engineering surveys	0.01 m to 0.10 m	GPS relative positioning mode: two frequency receiver and complete estimation for timing and orbit biases. ISS (Honeywell).
	kinematic	slow		glacier flow; post glacial rebound; local deformations; mining subsidence		
		fast	land	private cars to truck and taxi fleets	20 m	GPS point positioning mode: single frequency receiver. ISS.
				exploration vehicles	1 m	GPS differential mode: integrated with Inertial Navigation System. (INS).
			sea	fishing boats to super tankers	10 m	GPS point positioning mode: single frequency receiver.
				exploration ships	2 m; 5 $cm \cdot s^{-1}$	GPS differential mode: integrated with INS for reliability and accuracy.
			air	commercial and business aircraft	20 m	GPS point positioning mode: single frequency receiver.
				exploration aircraft; airborne laser profiling; aerial photogrammetry	1 m; 5 $cm \cdot s^{-1}$	GPS differential mode: integrated with INS.

identified and prospects for their removal is speculated upon. In the last section of the paper, a look into the future reveals the emergence of a "position oriented" society.

2. POSITIONING TASKS AND APPLICATIONS

The two broad types of positioning tasks are static and kinematic (Table 1). Within static positioning, point (e.g., single receiver) and relative (e.g., two receivers) positioning are the two main tasks. From Table 1, one can see that point positioning is associated with applications with a lower accuracy requirement, while relative positioning is used in applications demanding higher accuracy. Networks of points fall within the realm of relative positioning. Both NAVSTAR Global Satellite Positioning (GPS) and Inertial Surveying Systems (ISS) are applicable for this task.

Kinematic positioning is divided into slow kinematic and fast kinematic. Slow kinematic is associated with applications such as crustal deformations and actually overlaps with precise relative (static) positioning of different epochs. Fast kinematic is essentially the positioning of moving vehicles on land, sea and in the air. Within this category of application low accuracy requirements can be met by stand alone GPS or Inertial Navigation Systems (ISS) or can be integrated for reasons of accuracy and reliability. In the case of positioning of exploration vehicles (aircraft in particular) GPS is proposed to be used in the differential mode and integrated with an INS device ***[Goldfarb and Schwarz, 1985]***. With this combination (Figure 1), using GPS phase measurements and inertially determined position differences, kinematic positioning of the aircraft can be obtained with an accuracy of 1 m. The implications of this breakthrough is that no ground control is needed except for the control station needed in the differential GPS mode.

Inertial techniques for static positioning have matured to the stage that they are routinely used in production work, see e.g. Babbage [1981], Webb and Penney [1981], and Gore [1981]. The error

characteristics of these systems have been analyzed and appropriate estimation procedures have been designed, see e.g. Schwarz [1983, 1985]. Relative accuracies of a few ppm can be reached on distances above 30 km while the relative accuracy on shorter distances seems to be poorer due to a relatively large 'zero error' ***[Schwarz et al., 1984]***. However, accuracies of a few centimeters over distances of up to 5 km have been reported by Rueger [1984]. Although accuracy improvements are still possible, the present performance seems to be quite adequate for standard applications.

The use of inertial systems in kinematic positioning has a long tradition, albeit at an accuracy level which is insufficient for surveying applications. The combination of inertial navigation system (INS) with GPS promises a real breakthrough in kinematic positioning. The work in this area was pioneered by Wong and Schwarz [1982] and further reported upon in Schwarz et al. [1984]. Based on these results, a new approach has been taken which will be reviewed in the following.

3. PROBLEMS NEEDING SOLUTION IN GPS

Even though there has been substantial progress in implementing and applying GPS technology, several unresolved problems remain. Foremost amongst these is the removal of a host of systematic errors which bias present results. These are categorized in Table 2 as being satellite, tracking station or observation dependent.

As far as timing errors are concerned, both satellite and receiver clocks are modelled by separate second order polynomials. Satellite clock coefficients are broadcasted and treated as weighted parameters ***[e.g., Remondi, 1984]***. Receiver clock parameters are also treated as weighted parameters and are dependent upon oscillator quality. Usually an offset and drift (only) is solved for relative to a one master station in the network ***[Wanless, 1985]***. Further research is needed to resolve timing biases simultaneously with other parameters such as orbital biases - the along track bias being the most troublesome within this context.

Table 2

Possible Biases and Errors

SATELLITE DEPENDENT:
- Orbit Representation Biases (i.e. Initial Condition Biases
- Satellite Clock Model Coefficients

STATION DEPENDENT:
- Receiver Clock Model Coefficients
- Tropospheric Scale Parameter
- Station Coordinates

OBSERVATION DEPENDENT:
- Continuously Integrated Doppler Lock-on Range Biases
- Phase Measurement Ambiguity
  - Instantaneous
  - Single Difference
  - Double Difference
- Random Observation Error

Atmospheric effects are of two varieties - the effect of the ionosphere and that of the troposphere. As far as the ionospheric effect is concerned, a correction can be made apriori as a function of the two GPS frequencies. Strange as it seems, however, the results to date ***[e.g., Lachapelle and Cannon, 1985]*** have indicated that the results are better when neglected, i.e., one frequency data yields better results. More research is needed in this domain before the high accuracies can be achieved.

The tropospheric effect is usually taken care of by the Hopfield [1971] model in which surface measurements of the atmospheric conditions are needed to define the wet component of this correction. In accurate work, the unaccounted for portion is usually taken care of by an unknown scale parameter which needs to be solved for, along with other parameters, in the least squares estimation process. Another solution to this problem is being talked about, namely the use of a wet bulb radiometer to sample the atmosphere, but, indications are that the cost of this equipment will be greater than that of the GPS receiver itself.

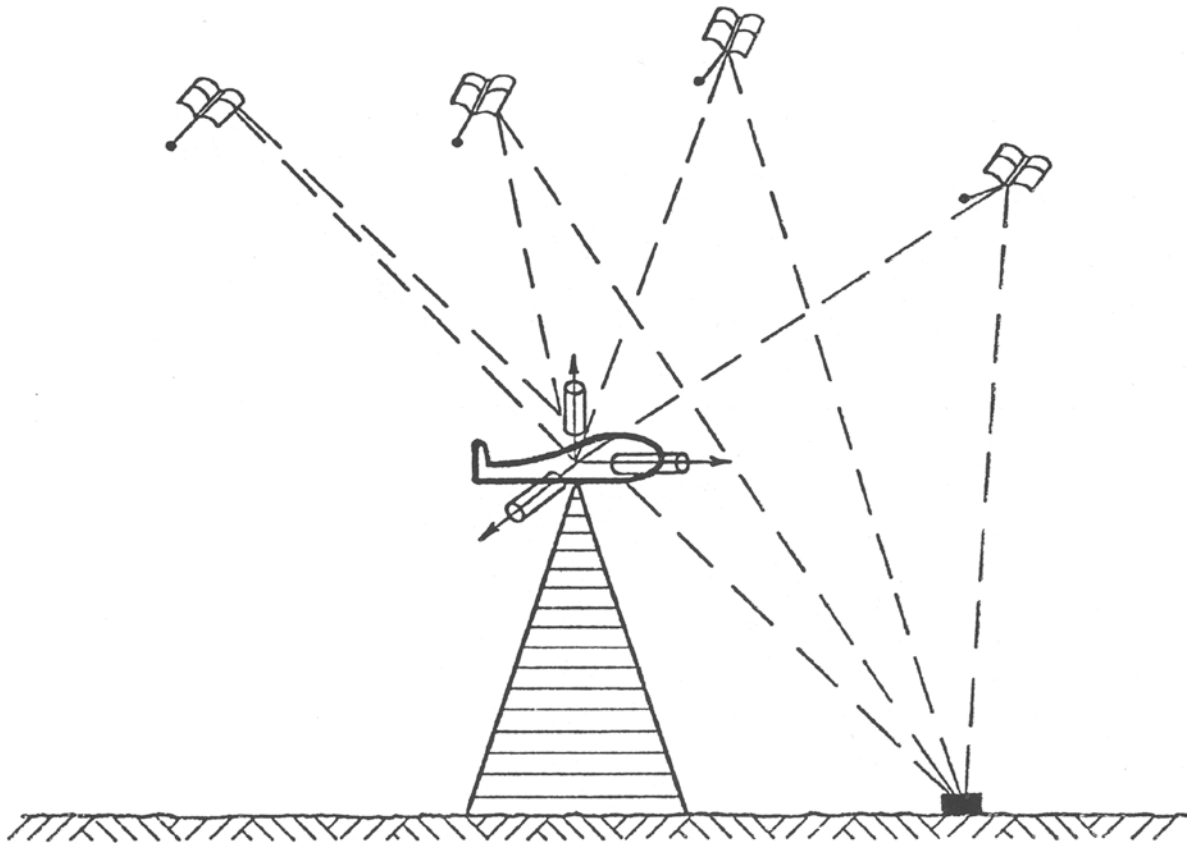

Figure 1: Integrated GPS and INS
Differential Positioning
[From Schwarz et al., 1984c]

Harring [1985] has indicated a possible solution to this problem by observing that in VLBI solutions the observations between 10 and 20 degrees above the horizon help one determine the tropospheric correction. GPS instruments such as the Macrometer do not measure below 15° because of antenna design. A possible improvement of results with TI4100 and other GPS instrumentation is to make sure that data is also collected in this critical region.

Next, let us turn to orbit biases. For long lines (100's of km) and shorter lines where extreme accuracy is required (less than 1 cm), orbital biases can destroy relative positioning results. Shown in Table 3 are baseline length errors (db) corresponding to orbit errors (dr). For example one can deduce that for a 100 km baseline and a baseline accuracy of only 20 cm, an orbital error of about 40 m can be tolerated. If you desire, however, a baseline accuracy of 1 cm, then an orbit is needed to an accuracy of 2 m. For longer baselines, e.g., 1000 km, the extreme orbital accuracy of 0.2 m is needed to determine a baseline accurate to 1 cm. Even an accuracy of 5 cm requires the orbit to be accurate to 1 m. For very short lines of say 1 km the orbit need be accurate to only 200 m if a 1 cm baseline accuracy is desired. For lines of medium length, say 10 km, an orbit accuracy of 20 m is needed for a "1 cm survey".

The relevance of the above immediately becomes apparent when one learns that, even the U.S. Defence Mapping Agency (DMA) computed GPS orbits are only accurate to about 20 to 30 m ***[Goad, 1984]***. This implies that present GPS broadcast ephemerides could be in error by as much as 50 m. Ephemerical results seem to confirm this observation. Beutler et al. [1984] report results for the Ottawa test network with unexplained coordinate differences of 7.2, -9.0, 13.7 cm and as much as -16.3 cm between two sets of solutions. No solution for orbit biases was made.

Taking another set of results reported by Beck et al. [1984] for the same network, we see similar magnitudes for the unexplained discrepancies. Again, the orbit was treated as fixed and errorless. The Goad and Remondi [1984] results are yet another example of the

problem with orbit biases. Recently, the results presented by Lachapelle and Cannon [1985] show a clear deterioration of accuracy, as compared to a terrestrial survey, with an increase in baseline length; the orbit was considered as fixed and errorless.

Research into helping resolve GPS orbit biases was first recognized by an Australian group ***[Stolz et al., 1984]***, band by The University of Calgary GPS Group ***[Nakiboglu et al., 1984; Krakiwsky et al., 1985]***. A prototype software package has been developed under contract by the U of C group for the Canadian Geodetic Survey ***[Nakigloblu et al., 1985; Buffet, 1985; Wanless, 1985]***. A production computer program package is presently being developed by U of C for CGS. The intended use of this pacjage is to implement it into the Canadian scheme of ACP's - Active Control Points ***[Delikaraoglou and Steeves, 1985]***, see Figure 2.

Primary to this proposed ACP System is the establishment of four permanent tracking systems for orbit improvement. Nakiboglu et al. [1985] have shown that it is possible to solve for multiple sets of Keplerian orbital elements from pseudo range, Doppler and phase GPS measurements over Canadian territory. This capability takes on even further significance if the GPS orbital data is degraded by the U.S. Department of Defence. There is a move, if not a trend, for certain countries to set up small "national" networks for monitoring GPS orbits over their respective territories.

Another challenge in connection with such a monitoring network is the definition and maintenance of the coordinates for the main stations. Simulations performed by the U of C GPS group have shown that a relative baseline accuracy of about 0.4 ppm is needed to improve orbits over Canadian territory to the 2.5 m level ***[Krakiwsky et al., 1985; Nakiboglu et al., 1985]***. LBI results will undoubtedly play a key role in this regard.

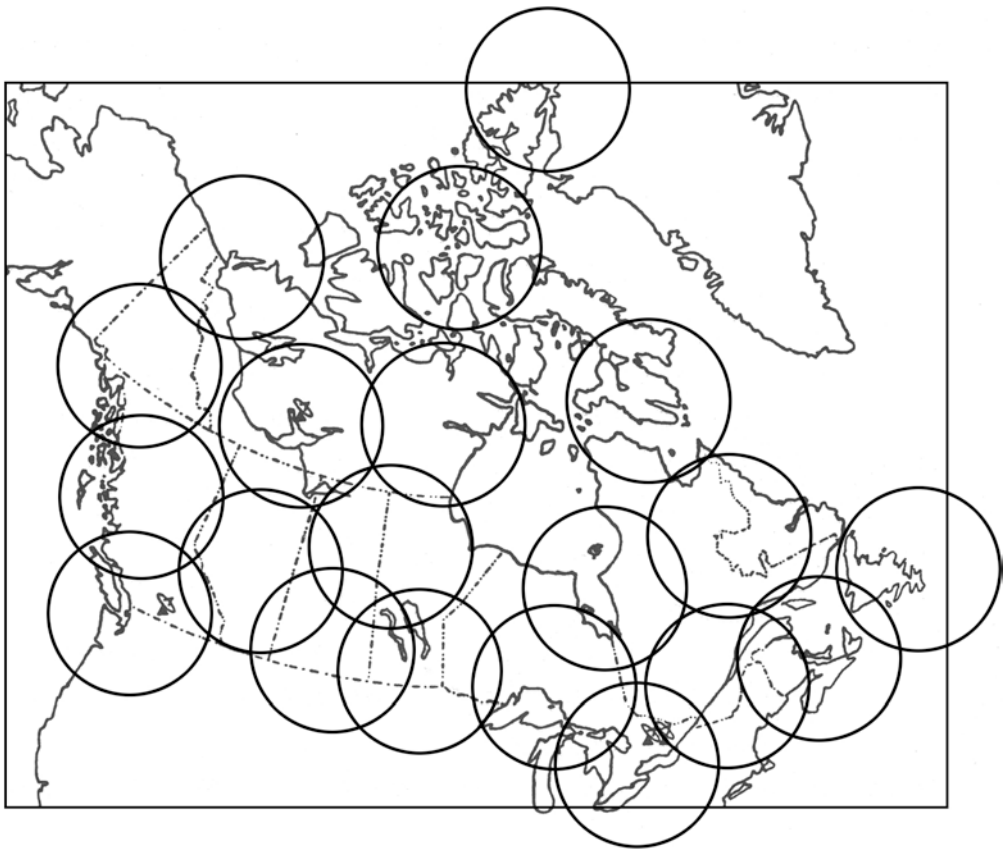

Figure 2: A National ACP System

[from Delikaraoglou and Steeves, 1985]

Figure 2: A National ACP System

[from Delikaraoglou and Steevens, 1985]

Table 3

ORBIT BIASES

[from Krakiwsky et al., 1985]

Effect on Baseline:

$$\frac{db}{b} = \frac{dr}{r} \quad ,$$

where dr is orbit error
db is baseline error

dr	$\frac{db}{b}$
100 m	5 ppm
20 m	1 ppm
10 m	0.5 ppm
2 m	0.1 ppm

Other challenges that need to be faced vis-a-vis GPS and INS technology is the successful integration of these two systems ***[Goldfarb and Schwarz, 1985]***. Also within this context, Lachapelle [1985] has discussed the development of GPS instrumentation for the positioning of aircraft carrying out geophysical surveys.

4. A LOOK INTO THE FUTURE

One fact is certain, the use of space (GPS) and inertial methods will continue to increase. The cost will come down drastically as a result of competition between equipment manufacturers. Present GPS receivers cost about $150 000 US; by the year 2000 equipment manufacturers predict that the cost will be about $500. Further competition, thus reducing the cost of positioning, will come from other satellite systems, e.g. GEOSTAR (U.S. Commercial), GLONASS (USSR GPS-type system), NAVSAT (ESA), GRANAS (German) and COSPAS-SARSAT (International Search and Rescue).

Positioning will become more of a point-like operation with classical networks playing a less important role. Nevertheless, when reliability and accuracy are of interest and redundant measurements are available, the observed three dimensional coordinate differences will be processed in a standard network fashion to yield improved results.

One important parameter that will change the entire mosaic of positioning is the interest in "positions" by the population at large (see Table 1). This means that the traditional user population will increase by two or three orders of magnitude bringing geodesy into the mainstream of the information revolution where "positions" will be an indispensable commodity for the emerging "position oriented society".

ACKNOWLEDGEMENTS

The author has had valuable discussions on this topic with fellow members of the U of C GPS Research Group; namely M. Nakiboglu, K.P. Schwarz, B. Buffet and B. Wanless. Discussions were also held with D. Delikaraoglou and R. Steeves, GPS Contract Officers, Canadian Geodetic Survey, Ottawa. The collaboration with colleagues R. Langley, D. Wells and P. Vanicek of the UNB GPS research group is also acknowledged.

REFERENCES

Babbage, G., ***Inertial surveying – a study in accuracy and versatility***. Proceedings Second International Symposium on Inertial Technology for Surveying and Geodesy, Banff, June 1 to 5, 1981.

Beck, N., D. Delikaraoglou, T. Lockhart, D.J. McArthur, and G. Lachapelle, ***Preliminary results on the use of differential GPS positioning for geodetic applications***. A paper presented to IEEE PLANS 1984, Position Location and Navigation Symposium, San Diego, 1984.

Beutler, G., D.A. Davidson, R.B. Langley, R. Santerre, P. Vanicek, and D.E. Wells, ***Some theoretical and practical aspects of geodetic positioning using carrier phase difference observations of GPS satellites***. Mitteilungen der Satellitenbeobachtungsstation Zimmerwald, No. 14, 1984.

Buffet, B. (in preparation), ***Short-arc determination for the Global Positioning System***. M. Sc. thesis, Division for Surveying Engineering, The University of Calgary.

Delikaraoglou, D. and R.R. Steeves, ***The impact of VLBI and GPS on geodesy in Canada***. A paper presented to the CSEG-CGU meeting, Calgary, May 1985.

Goad, C.C., Personal Communication, February 1985.

Goad, C.C. and B.W. Remondi, ***Initial relative positioning results using the global positioning system***. Bulletin Géodésique, Vol. 58, 1984.

Goldfarb, J.M. and K.P. Schwarz, ***Kinematic positioning with an integrated INS-differential GPS***. A paper presented to the First International Symposium with the Global Positioning System, Rockville, Maryland, April 15 to 19, 1985.

Gore, G.L., ***Some field applications of inertial technology***. Proceedings Second International Symposium on Inertial Technology for Surveying and Geodesy, Banff, June 1 to 5, 1981.

Harring, T., Personal Communication, May 1985.

Hopfield, H.S., ***Tropospheric effect on electromagnetic measured range: prediction from surface data***. Radio Science, Vol. 6 (3), 1971.

Krakiwsky, E.J., B. Wanless, B. Buffet, K.P. Schwarz, and M. Nakiboglu, ***Orbit Improvement and Precise Positioning***. A paper presented to the First International Symposium on Precise Positioning with the Global Positioning System, Rockville, Maryland, April 15 to 19, 1985.

Lachapelle, G. and E. Cannon, ***Centimetre accuracy GPS positioning with the TI 4100 receiver***. A paper presented to the CSEG-CGU meeting, Calgary, May 1985.

Nakiboglu, M., B. Buffet, K.P. Schwarz, E.J. Krakiwsky, and B. Wanless, ***A multi-pass, multi-station approach to GPS orbital improvement and precise positioning***. A paper presented to IEEE PLANS '84, Position Location and Navigation Symposium, San Diego, November 1984.

Nakiboglu, M., E.J. Krakiwsky, K.P. Schwarz, B. Buffet, and B. Wanless, ***A Multi-Station, Multi-Pass Approach to Global Positioning System Orbital Improvement and Precise Positioning***. Final contract report to the Canadian Geodetic Survey by the Division of Surveying Engineering, The University of Calgary, April 30, 1985.

Remondi, W., ***Using the global positioning system (GPS) phase observable for relative geodesy: modelling, processing, and results***. Doctoral Dissertation, University of Texas at Austin, 1984.

Rueger, J.M., ***Evaluation of an inertial survey system***. The Australian Surveyor, Vol. 32 (2), 1984.

Schwarz, K.P., ***A unified approach to post-mission processing of inertial data***. Bulletin Géodésique, Vol. 59 (1), 1985.

Schwarz, K.P., ***Inertial surveying and geodesy***. Reviews of Geophysical and Space Physics, Vol. 21 (4), 1983.

Schwarz, K.P., D.A.G. Arden, and J.J.H. English, ***Comparison of adjustment and smoothing methods for inertial networks***. USCE Report No. 30006, The University of Calgary, 1984a.

Schwarz, K.P., R.V.C. Wong, J. Hagglunf, and G. Lachapelle, ***Marine positioning with a GPS-aided inertial navigation system***. Proceedings 1st National Technical Meeting of the Institute of Navigation, San Diego, January 17 to 19, 1984b.

Schwarz, K.P., C.S. Fraser, and P.C. Gustafson, ***Aerotriangulation without ground control***. International Archives of Photogrammetry and Remote Sensing, 25, Part A1, Rio de Janeiro, June 16-29, 1984c.

Stolz, A., E.G. Masters, and C. Rizos, ***Determination of GPS satellite orbits for geodesy in Australia***. Aust. J.Geod.Photo.Surv., No. 40, June 1984.

Wanless, B. (in preparation), ***A prototype multi-station, multi-pass satellite data reduction program***. M.Sc. thesis, Division of Surveying Engineering, The University of Calgary, 1985.

Webb, J.D. and R.C. Penney, ***Six years of inertial surveying at Geodetic Survey of Canada***. Proceedings Second International Symposium on Inertial Technology for Surveying and Geodesy, Banff, June 1 to 5, 1981.

Wong, R.V.C. and K.P. Schwarz, ***Offshore positioning with an integrated GPS/inertial navigation system***. Proceedings 3rd International Geodetic Symposium on Satellite Doppler Positioning, Las Cruces, New Mexico, February 8 to 12, 1982.

A C/A CODE GPS-RECEIVER FOR NAVIGATION

by

Wolfgang BEIER

Standard Elektrik Lorenz AG
Lorenzstrasse 10
D-7000 Stuttgart 40
Fed. Rep. of Germany

ABSTRACT

A lab model of a 1.5-channel C/A code GPS-receiver was developed in 1983 and 1984. For this receiver analogue correlation and tracking circuitry was used in both channels. The hardware was mainly intended as testbed to enable the accumulation of the GPS software know-how. This includes the processing of the GPS message, the measured data as well as the computations to determine the position and the navigation data for a mobile user. To determine the position four measured pseudoranges (or three pseudoranges for known altitude) are used together with dead reckoning using the velocity as derived from the measured doppler of the satellite signals. The measured accuracy of 40 m (SEP) is as expected for a C/A code receiver.

In a follow on effort the software was extended to determine position updates by means of a Kalman filter using measured pseudoranges to individual satellites. This eliminates the need for simultaneous visibility of 4 (or 3) satellites to enable the determination of a new position and improves the performance of the receiver when the visibility of single satellites is not given from time to time as it may happen due to constructions, trees etc. This improvement was verified by simulations which demonstrated the benefits of the new software for operational receivers.

A condition for the improvement of the hardware towards reduced cost, was the application of a new receiver concept. By means of early digitalization a maximum of functions could be performed by programmable circuits. This reduced the number of functions needed within the RF part of the receiver, and a simple RF part is the main key for low production costs. The new concept was validated by means of experimental and theoretical investigations. The receiver can be packed into a volume comparable to that of a car radio. Using general terminology the receiver is characterized as four channel, fast scan multiplex receiver. It measures the pseudoranges and decodes the data of four satellites to determine the position and navigation data.

An interesting feature of the receiver is that it reconstructs simultaneously the carrier phases and the pseudoranges of the four satellites.

This work was supported by the Bundesministerium für Forschung und Technologie.

1. INTRODUCTION

The traditional engagement of Standard Elektrik Lorenz AG in the field of Radio Navigation was extended in the early seventies to include satellite navigation. This effort actually started with a program called NAVEX where for the D1 mission of the spacelab navigation experiments were executed. For these experiments no use of the GPS satellites was made, however, through the use of GPS-like signal formats and consequently through the development of GPS (-receiver)-like hardware as well as through the use of GPS-like methods to determine the position of the spacelab, the basis of the GPS know how was accumulated in this program.

In 1983 and 1984 a lab model of a 1.5-channel C/A code GPS-receiver was developed using mainly this hardware. The aim was to produce hardware that could be used as testbed for the development of the GPS software which was the main task in 1983 and 1984 and which was accomplished by the end of 1984. It was clearly understood that the hardware used for that lab model could not lead to GPS receivers for series production. However, during the development phase we learned that it would be almost impossible to shrink the size (and cost) of the receiver by pure technological measures to meet the requirements of the civil market in relation to production costs.

The need for a low cost GPS receiver lead to the application of a new GPS-receiver concept. The main condition for a low cost GPS receiver is a signal processing concept that allows the application of low cost technologies. The new concept avoids as far as possible analogue signal processing which is mainly used so far and we therefore consider this GPS receiver which is currently under development, a GPS receiver of the second generation.

Section 2 describes the lab model of the 1.5-channel receiver and the accomplishments reached so far towards the development of a low-cost GPS receiver are described in section 3. Section 4 dwells on other applications of the low-cost receiver that are seen beyond its primary intend as navigation receiver.

2. DESCRIPTION OF THE 1.5-CHANNEL-GPS RECEIVER

2.1 The main operational features

One channel of the receiver scans at medium speed (100 ms dwell per satellite) from one visible satellite to another to measure the pseudoranges and the doppler frequency for each satellite. The other channel dwells for longer periods on selected satellites to collect the GPS data and as this channel does not contain facilities to measure the pseudoranges it is called a half channel which explains the designation in the heading to this chapter. The receiver determines the users position (SEP < 40 m) using measured pseudoranges to maximal 5 visible satellites. Two dimensional positions will be determined for only 3 visible satellites. Together with each pseudorange the doppler frequency is also determined and this is used for dead reckoning.

The position can be displayed for selectable earth ellipsoides in LAT/LONG or in UTM coordinates plus altitude.

Besides the position the following information is derived:

- velocity (ground speed, track and vertical velocity),
- time (day of the week and time of the day),
- navigational data (to and between selectable way points).

2.2 The electrical design of the receiver

Fig. 1 shows the block diagram of the receiver. The set consists of four separate units:

- the antenna (A),
- the antenna preamplifier (AE),
- the actual receiver unit,
- the CDU.

The following description highlights the main design features of the actual receiver unit. For the reasons described in chapter 1 the design of the receiver set is quite straight forward and detailed descriptions and results of analytical investigations for the various solutions may be found in the literature.

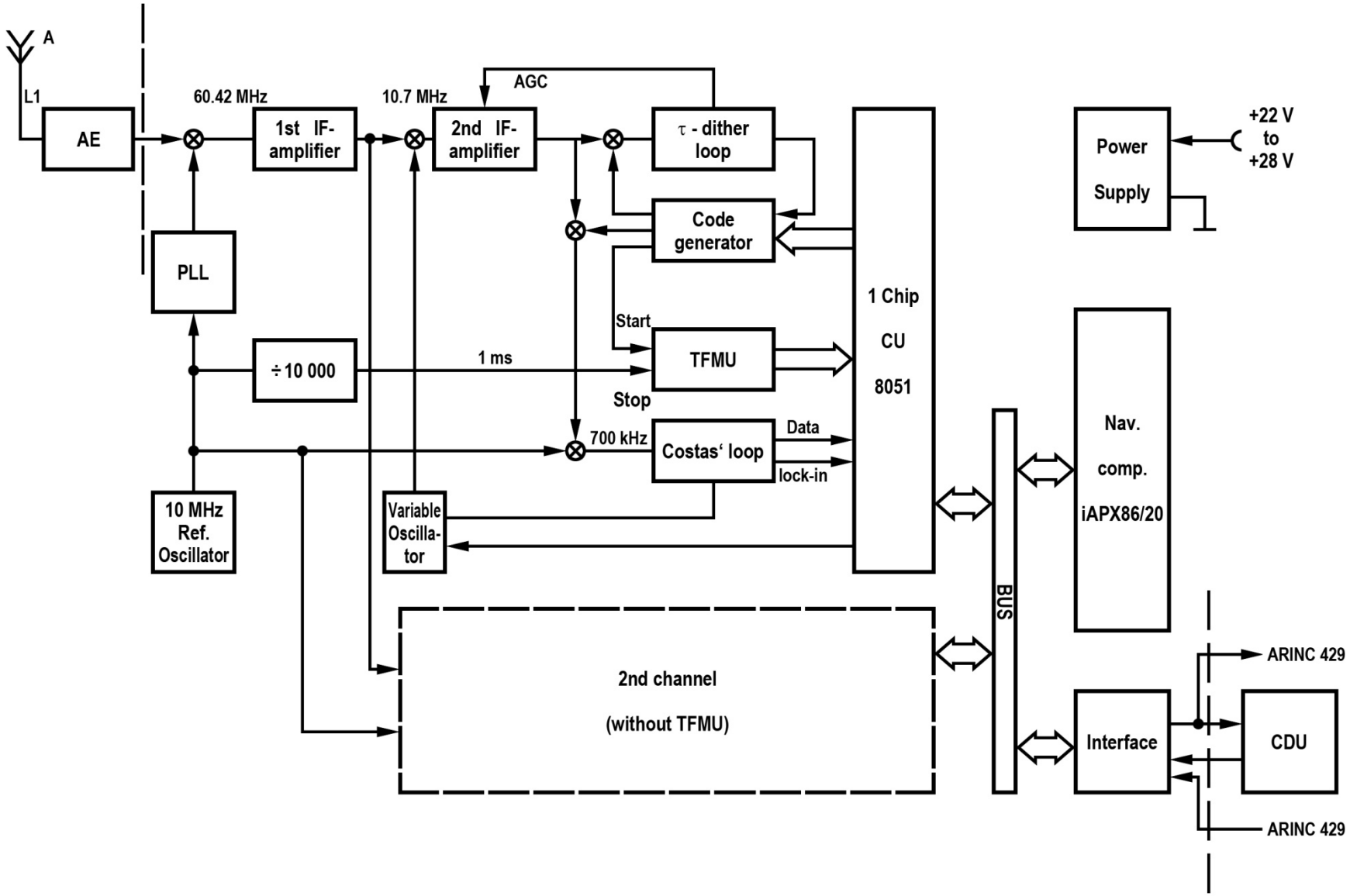

FIGURE 1 The block diagram of the 1.5-channel receiver

The actual receiver contains the following moduls:

- HF/IF unit,
- τ-dither loop and C/A code generator,
- time and frequency measurement unit (TFMU),
- Costas' loop,
- control unit (CU),
- navigational computer (Nav. Comp.).

The HF unit with the highly stable reference oscillator (10^{-9}/day) is common to both channels. At the output of the first IF stage to the BUS the hardware is separated in two channels and both channels contain the same hardware except that channel 2 does not have a TFMU. Also the software of the CU in both channels is identical. However, on command of the nav. comp. different routines are executed in both channels and they depend on the tasks assigned to a channel at a given time during operation. For the initial acquisition and during the scanning mode the CU selects the proper C/A code, preadjusts the timing of the code generator and the frequency of the variable oscillator. When "lock-in" is achieved, the CU reads the measured time and frequency data from the TFMU after a waiting time (to allow for dwell-in) of about 50 ms. This data is transmitted to the nav. comp. for further processing.

The τ-dither loop uses envelope detection and the predetection filter bandwidth of this loop is 1 kHz. Larger bandwidths would result in increased signal losses at the envelope detectors. The 1 kHz is a trade-off between acceptable loss and reduced initial acquisition time for cases when Doppler uncertainties are not predictable. The loop bandwidth of the τ-dither loop is controlled by the CU and different bandwidths are used in the search and in the track mode. The selected loop bandwidth of the Costas' loop (25 Hz) allows for rapid pull-in given the frequency uncertainty of the carrier frequency as preadjusted by the CU and keeps the phase jitter at an acceptable level during track.

The TFMU measures the displacement of the received code epoch relative to the internal clock with a resolution of 2 ns.

The receiver communicates to other systems and to the CDU via an ARINC 429 interface. This interface contains also a battery buffered clock that delivers the date and the time to the nav. comp. which it needs to compute

the satellite positions using almanach data that it can read from a battery buffered store following a switch-off of the receiver.

2.3 The mechanical design of the receiver

The key features of the mechanical design of the main units, the actual receiver and the CDU will be seen from Fig. 2. Standard avionic packages have been selected and the packing densities achieved within the boxes represent an optimum for the conventional technology available for this program.

2.4 Description of the mathematical methods

To determine the position and the navigation data, a GPS receiver has to solve various mathematical routines like:
Computation of the positions of the satellites, conversion from WGS to UTM, computation of navigation data to preselected way points etc.
The most important method that determines the performance of the receiver is, however, the procedure to compute the position from the measured data (pseudoranges and doppler frequency).

For the 1.5-channel receiver the method to compute the four unknowns x_u, y_u, z_u and Δt, where Δt is the time error of the users clock, is described by the following set of equations which will be solved using iterative methods.

$$(x_{sn} - x_u)^2 + (y_{sn} - y_u)^2 + (z_{sn} - z_u)^2 = (R_n + \Delta t \cdot c)^2 \qquad (2\text{-}1)$$
$$\text{for } n = 1 \text{ to } 4$$

R_n represents the measured pseudoranges, x_u, y_u, z_u estimated values of the users' position, and x_{sn}, y_{sn}, z_{sn} the position of the n'th satellite. The same set of equations is used for only three visible satellites and in this case an artificial satellite with a known vertical range is assumed.

All measured values R_n will be related (scaled) to a common time reference point and the solution is straight forward for a stationary user. For a moving user dynamic interpolation methods are necessary to avoid position errors for the case that the users dynamic contributes to position changes of more than let's say 10 m during one scan period of four satellites which takes about 0.5 sec. The coefficients of the filter used for the dynamic and linear interpolation are determined through recursive computations.

Dimensions: 50 cm x 19 cm x 19 cm

FIGURE 2 Photos of the actual receiver and the CDU

However, a necessary condition for sufficient accuracy of the method described above is that four (or three) measured pseudoranges are available from four successive dwells during one scan period.

As will be discussed in section 2.6 this requirement leads to constraints for the operational use of the receiver.

Before this constraint is discussed further it shall be mentioned that also a dead reckoning method has been implemented. For this the doppler frequency is measured for each dwell on a specific satellite shortly following the measurement of the pseudorange. From this velocity vector pointing to the satellite the contribution to the users' covered way can be determined after integration. If in the extreme the user moves orthogonal to the satellite no measurement update can be derived. However, on average valid updates will be obtained and these are used to update the display of the position following each dwell (i.e. each 100 ms). This reduced considerably the drag error on the display of a moving user.

To avoid the above mentioned necessity that four measured pseudoranges during one scan period must be available before a position value can be computed, a Kalman filter was designed. This algorithm allows the derivation of correction terms for the position using single measured pseudoranges and each measured value contributes to position updates. The improvement of the receiver in this respect has been demonstrated by means of simulations. A full demonstration of the performance in field trials will be performed with the low cost receiver described in section 3.

2.5 Some statements to the software

Three main software packages have been produced:

- The software for the CU (Assembler, one 8051 µP in each channel)
- The software for the CDU and the ARINC interface (Assembler, four 8051 µP's)
- The software for the nav. comp. (PASCAL, one 8086/8087 µP).

The volume of the software for the nav. comp. is about 80 kByte and it is obvious that a more detailed description is beyond the scope of this paper.

In brief, the main achievements are:

- After switch-on, the receiver for the various conditions will always find an optimal satellite configuration if enough satellites are visible and for a given set of conditions it will proceed in an optimal way.

- The receiver executes the methods to determine position, velocity and navigation data and he changes satellite configurations to select the optimum configuration during operation.

- The receiver responds during operation also to operator inputs via the CDU.

2.6 Results of the tests with the 1.5-channel receiver

Extensive stationary as well as dynamic tests have been performed and for the dynamic tests the receiver was installed in a car. The test criteria were seen in relation to the receivers performance to determine positions, to measure the user's velocity, to execute the various satellite acquisition strategies and to determine the navigation data. The results are summarized as follows:

- When at least four satellites (three when the altitude is known) can be seen by the antenna, the accuracy of the position determination for a stationary user is as expected for a C/A code receiver (SEP < 40 m). For this statement a GDOP value is assumed that will be existent for more than 50 % of the time following the FOC of the GPS system in 1989.

- The same accuracy is measured for a user that moves at velocities less than 200 km/h when the same conditions as described above apply.

However, as described in section 2.4 the following constraints that result from the receivers' inherent design features must also be stated:

- When for example due to constructions the visibility of four satellites (three when the altitude is known) during one scan period is not given, the 4 x 4 matrix to determine the position cannot be solved. In this case the last valid position will be displayed to the user and a lamp indicates the disruption of the position computing process. However, as the receiver further attempts to acquire the shadowed satellite during a scan cycle a new position will be computed immediately when the visibility

is given again.

New mathematical procedures (see section 2.4) to overcome these constraints have been developed and these will be implemented into the low cost receiver described next.

3. A LOW COST GPS-RECEIVER

3.1 The design criteria for the new receiver concept

As described in chapter 1 the main condition for a low cost receiver is a signal processing concept that allows the application of low cost technologies and the main features of this new concept are described in this chapter.

The key words for the new concept are in relation to the RF circuitry

- quasi "zero IF"
- simple frequency conversion techniques

and in relation to the signal processing unit

- one hardware channel
- early digitalization and
- the use of commercially available integrated technology (i.e. µP's).

Fig. 3 shows a block diagram of the new concept. The RF unit converts the input signal to an IF of 10 kHz and the IF bandwidth is about 1 MHz. The digitalization (1 bit quantization) is performed directly at the IF output and the following process performed by an exclusive-OR is the multiplication of the received signal with the locally generated C/A code, and all GPS codes are derived from one ROM. This completes the description of the main functions performed by dedicated hardware. All other main functions like

- carrier acquisition and tracking
- code acquisition and tracking
- data demodulation

are performed by the µP and a digital Costas' loop and a digital τ-dither loop are realized by software.

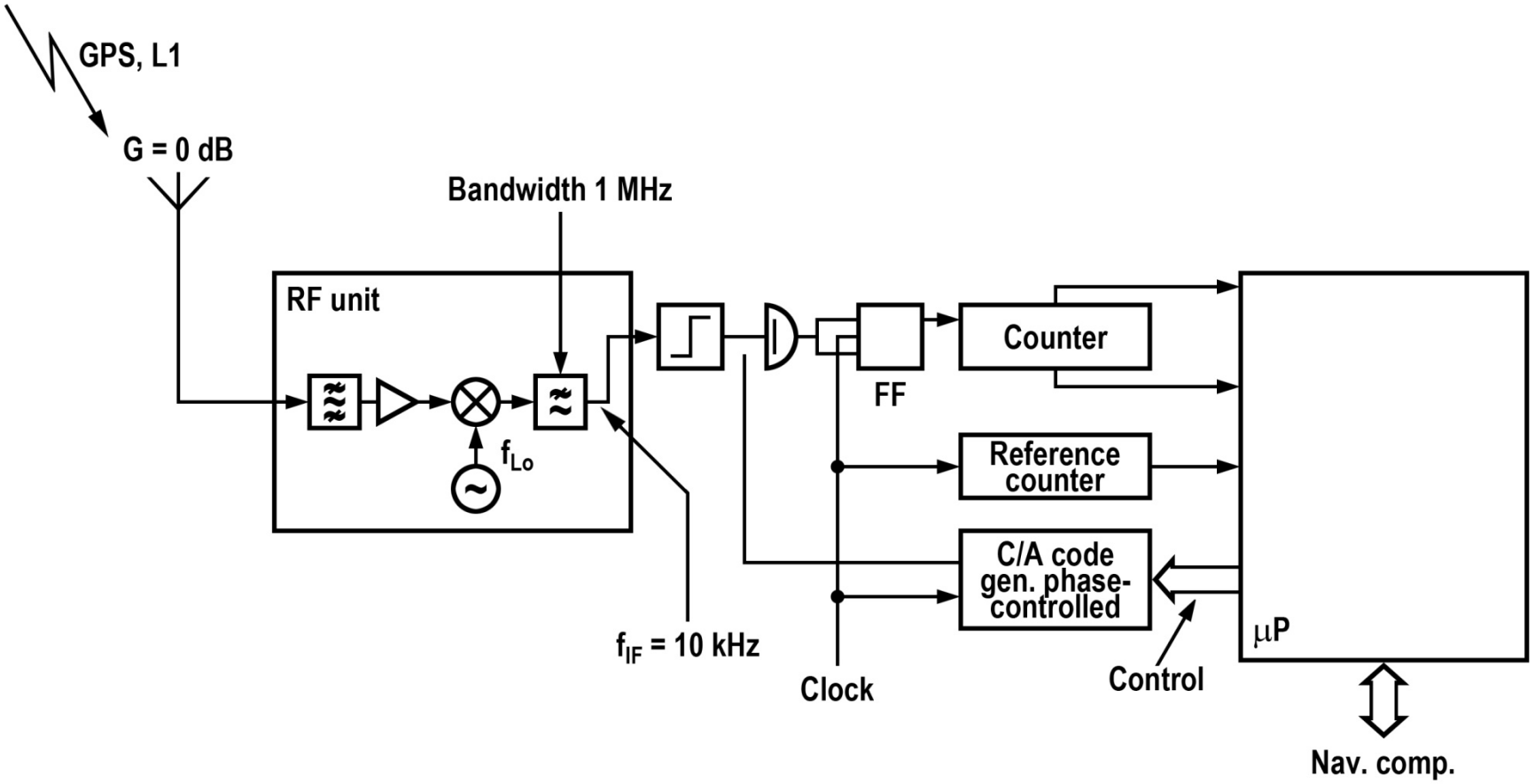

FIGURE 3 The new low cost receiver concept

It is noted that no AGC is needed within the RF unit and due to the software solutions there is no need for frequency agile or phase controlled oscillators both for carrier and for code tracking. So a maximum of functions are performed in software with the result that the hardware configuration is as simple as possible. Through the early digitalization the possibility to apply readily available techniques to increase the degree of integration beyond the level that could be achieved for analogue techniques has been achieved.

The one hardware channel is operated in the fast scan mode with a dwell time of 1 ms per satellite. As for this solution four Costas' loops and four code tracking loops remain quasi locked to the four selected satellites, this receiver is called to have four pseudo channels.

As the loops are realized in software it is easy to implement variable loop bandwidths and this feature is exploited to optimize the receivers' performance during the acquisition and during the tracking phase. Narrowing the loop bandwidth during tracking for example reduces the error of the pseudorange measurement due to noise and a wider loop bandwidth enables rapid pull-in during acquisition.

3.2 Performance prospects of the low cost receiver

Following the definition of the concept we are concerned with questions relating to the performance of the receiver. The following statements to the performance are based on the results of an experimental validation and of an intensive numerical simulation. One goal of the experimental validation was to find out if a commercial available µP can handle the tasks to acquire and to track simultaneously up to four satellites and the main question was in relation to its computing speed. Another goal was to verify the results of the computer simulation and these results stem from different objectives for the investigations. On one hand the results were used for the design of the loops and on the other hand the losses due to the signal processing concept selected were computed. For this the specified received GPS power of -130 dBm and a receiver noise figure of 4 dB were assumed. A further focal point of interest was the investigation of the dynamic performance and the same signal-to-noise ratio was used for this simulation. The experimental validation successfully demonstrated the questioned capability of the µP and with an experimental setup up to four satellites were

acquired and tracked. In addition the results of the computer simulation were verified and details are described below. It is noted that all statements to these results are valid for the hardware configuration shown in Fig. 3. For all losses given means to avoid them are known and these means can be implemented at the expense of additional hardware and we therefore call the configuration shown in Fig. 3 the minimum version of the low cost GPS-receiver. The losses quoted below have been derived by comparing the actual computed performance to an ideal signal processing concept. Therefore if one attempts to compare these losses to practical analogue receivers, their implementation loss that amounts to some dß's has to be considered as well.

Loss due to one-bit quantization of the IF

The quantization of the IF signal involves two different contributions to this loss. One is due to the fact that no phase-coherent reference is used for the conversion to the IF and this loss amounts to 4 dB. Another contribution is due to the one-bit quantization alone and this amounts to 2 dß. In total therefore is 6 dB loss due to the one-bit quantization of the IF.

Loss due to the 1 ms dwell time per satellite

One specific satellite is only observed for a quarter of the time (for four satellites of one sequence). This impacts the tracking capability of the loops and hence the dynamic performance of the receiver as no tracking information is available during a period of 3 ms. In terms of signal to noise this degradation is described by a loss of 6 dß for the signal to noise in the loops.

Loss due to fact that no in-time code is used for decorrelation

The concept foresees the realization of a τ-dither loop and (for the minimum hardware configuration) no separate correlator with an in-time code is used. For a dither of ±0.25 chips this amounts to a loss of 2.5 dB compared to the case where an in-time code is used. However, as the addition of an in-time code can be performed with little extra hardware, this will be done for future applications. This loss is therefore not applicable for future practical applications.

Dynamic simulation of the Costas' loop

Due to the losses described above the Costas' loop will only remain locked with a sufficient low cycle slipping rate when the dynamic of the vehicle does not exceed a fraction of 1 g. Normally the receiver will require aiding for non stationary uses. However, aiding will normally be required also for other reasons for mobile use. For most civil applications we therefore are able to handle the dynamic performance of the minimum hardware configuration.

Dynamic simulation of the code tracking loop

As expected the code tracking loop withstands high user dynamics without loss of lock and without impact on the acquisition performance. Compared to the performance of the Costas' loop this increased resistance is due to the ratio of the code clock frequency to the L1 frequency of GPS.

3.3 Prospects to the construction of the low cost receiver

Based on the experimental units produced and tested so far and based on investigations how the (simple) RF unit could be realized, the overall dimensions of the receiver were estimated. Without the antenna and the antenna pre-amplifier, however with the CDU the receiver dimensions will be comparable to a size of a car radio (Fig. 4).

FIGURE 4 Mechanical conception of the low cost receiver

4. APPLICATIONS OF THE LOW COST GPS-RECEIVER

The achievements described are the basis for the on-going effort to develop a GPS-receiver for civil applications. The first goal is a navigation receiver with the optional capability for differential operation.

The interesting feature that the carrier phases of all satellites acquired and tracked during a scan period are simultaneously available in relation to an exact time reference challenges the exploitation to extend the receivers' capability to be used as geodetic positioning instrument.

OPTIMAL DESIGN FOR GPS 3-D DIFFERENTIAL POSITIONING

by

Harald BORUTTA and Hansbert HEISTER

Institut für Geodäsie
Universität der Bundeswehr München
Werner-Heisenberg-Weg 39
D-8014 Neubiberg
Fed. Rep. of Germany

ABSTRACT

The optimization problem of second order design of 3 dimensional geodetic networks is formulated as an allocation problem. The solution is obtained by applying the dynamic programming method. Considered observations are GPS baseline vectors and slope distances. The objective function, being minimized is the trace of the covariance matrix of the coordinate parameters (A-optimality) as a global measure of accuracy of the network. The optimal configuration of the observations is found under a given cost restriction. The optimization procedure is apt to account for prior information on the coordinates of the points, and it can be used in any geodetic datum. The proposed method is illustrated at different examples.

ZUSAMMENFASSUNG

Die Optimierung des Designs zweiter Ordnung 3-dimensionaler geodätischer Netze wird als Zuteilungsproblem formuliert. Die Lösung wird durch Anwendung der dynamischen Optimierung erhalten. GPS Vektoren und EDM Schrägstrecken werden als mögliche Beobachtungen in Betracht gezogen. Die zu minimierende Zielfunktion ist die Spur der Varianz-Kovarianz-Matrix des unbekannten Koordinatenparameters (A-Optimalität) als globales Maß für die Genauigkeit des Netzes. Die optimale Anordnung der Beobachtungen wird unter Berücksichtigung einer vorgegebenen Kosten-Restriktion angegeben. Das Optimierungsverfahren ist für die Berücksichtigung von Vorinformationen über die Koordinatenparameter bearbeitet worden. Die Optimierung kann in jedem beliebigen Datum durchgeführt werden. Die vorgeschlagene Methode wird anhand von verschiedenen Beispielen veranschaulicht.

1. INTRODUCTION

Since the advent of GPS differential positioning satellite methods have become applicable for precision survey purposes. Recent papers report on baseline determinations in conventional triangulation networks (***SCHMIDT 1983, SCHWINTZER et al., 1985***) and on the observation of networks for deformation analyses (***SCHUSTER, 1984***). It seems that this new observation technique is attractive for a variety of surveying tasks (***NIEMEIER et al., 1985***). Its main advantages are, that no line of sight between the stations is necessary for the observation, and that it is independent of weather conditions. These properties and the automized observation procedure allow for a fast completion of the field work. On the other hand the renting or buying of the equipment is very costly. Therefore the optimization of hybrid network designs deserves attention in order to attain a pre-given accuracy at a minimum of cost.

In many applications, especially in network densification, it is necessary to consider the quality of the given points. This has been made possible in the proposed optimization procedure, thus providing realistic results for a wide range of applications.

2. DEFINITION OF THE OPTIMIZATION MODEL

If a new network or the densification of an existing network is planned the configuration has to be designed considering the purpose of the network and the restrictions of topography and of surveying methods. In the literature this procedure is known as the first order design problem.

The second step is the optimization of the observation plan (second order design). This paper proposes a procedure for the determination of an optimal observation scheme using the global accuracy of the network as the target function. The solution is restricted by the maximum number of measurements (cost-restriction). The approach is based on the dynamic programming method which has already been applied to the optimization of second order design of geodetic networks (***HEISTER, 1976 and 1978***). GPS interstation vectors and slope-distances are considered as observables. The coordinates of the points refer to a local geodetic coordinate system. The geodetic datum can be chosen arbitrarily and prior information about the coordinates can be introduced into the model.

2.1 The Functional Model

The GPS-observable of the optimization approach is the interstation vector derived from phase measurements (vector observable). The basic relation between the Cartesian ccordinates of point i in the GPS system (WGS 72) and the local geodetic coordinate system is given by the transformation equation

$$\mathcal{X}_{G_i} = \mathcal{X}_0 + \lambda \mathcal{D} \mathcal{X}_{T_i} \tag{1}$$

with

$\mathcal{X}_{G_i}$ ... coordinate vector of point i in the GPS system

$\mathcal{X}_0$ ... translation vector

λ ... scale factor

$\mathcal{D}$ ... rotation matrix $\mathcal{D} = \mathcal{D}(\alpha,\beta,\gamma)$

$\mathcal{X}_{T_i}$ ... coordinate vector of point i in the local system.

In terms of coordinate differences the observation equation for an interstation vector from station i to station k reads

$$\Delta\mathcal{X}_{iG}^{k} = \lambda \mathcal{D} \left(\mathcal{X}_{T_k} - \mathcal{X}_{T_i}\right) \tag{2}$$

$\Delta\mathcal{X}_{iG}^{k}$ contains the "observed" coordinate differences in the GPS system

$$\Delta\mathcal{X}_{iG}^{k} = \begin{vmatrix} x_k - x_i \\ y_k - y_i \\ z_k - z_i \end{vmatrix}_G = \begin{vmatrix} \Delta x_i^k \\ \Delta y_i^k \\ \Delta z_i^k \end{vmatrix}_G$$

The observation equation for distances is given by

$$s_i^k = \sqrt{\left(x_k - x_i\right)^2 + \left(y_k - y_i\right)^2 + \left(z_k - z_i\right)^2} \tag{3}$$

Linearization of the equations leads to the functional model

$$\ell + v = [\mathcal{A}_1 \vdots \mathcal{A}_2] \begin{bmatrix} x_1 \\ \cdots \\ x_2 \end{bmatrix} = \mathcal{A}x \tag{4}$$

with

ℓ ... observation vector
v ... residual vector
$\mathcal{A}_1$ ... design matrix (part for coordinate unknowns)
$\mathcal{A}_2$ ... design matrix (part for scale and rotations)
x_1 ... parameter vector (coordiante unknowns)
x_2 ... parameter vector (scale and rotations)

The decomposition of the parameter vector is introduced in order to elimi-nat the nuisance parameters.

Besides this observations prior informatgion about the coordinates may be introduced. The prior information is given by ℓ_x , the vector of coordi-nates of net points and the corresponding variance-covariance matrix Σ_x .

2.2 The Stochastic Model

The baseline vector is estimated from phase measurements of satellite sig-nals in respect to a receiver reference signal. The results of the esti-mation procedure are the components of the baseline vector along with the covariance matrix and some clock bias parameters. For pre-analysis purposes, such as design optimization, assumptions about the stochastic properties of the measurements are necessary. They are based on the analysis of prior measurements in similar situations. The assumptions in this article stem from baseline measurements with Macrometer TM equipment in middle Europe (***BOCK et al. 1984, SCHWINTZER et al. 1985, HEISTER et al. 1985***). The variances of the baseline components increase with the distance between the stations. Therefore it is assumed that

$$s_{x,y,z} = a + b \cdot s \qquad s\text{: slope distance} \qquad (5)$$

with $s_{x,y,z}$ being the standard deviation of the coordinate difference and a,b being constants. At the time being the observation window allows only 4 - 5 hours of observation per day. Hence only one interstation vector is observable per day with a pair of receivers. Therefore it is justified to consider a and b of Equation (5) as constants. Later on when the system is complete with 18 satellites individual observation times will be possible. Then a and b can be treated as variables depending on the observation time.

For the numerical examples in this paper the constants a and b were chosen to be

$$a = 0.5 \text{ cm} \qquad \text{and} \qquad b = 1.5 \text{ ppm}$$

Further assumptions are necessary as to the correlations between the components of the vectors. They depend on the number of phase differences, the constellation of satellites and of the ground stations. According to available data they vary in a broad range. But mostly high positive correlations were obtained. For the examples the assumptions

$$r_{xy} = 0.6 \qquad r_{xz} = 0.7 \qquad r_{yz} = 0.8$$

were made. Furthermore it is assumed that the interstation vectors are independent.

The standard deviation of distances are given by the well known formula

$$s_d = a + b \cdot s \tag{6}$$

For the numerical examples the constants $a = 0.5$ cm and $b = 2.0$ ppm were used. Additionally, it is assumed that there are no correlations between different distances.

The covariance matrix of the a priori known coordinates is assumed to be positive definite so that the weight matrix is given by

$$\mathcal{P}_x = \Sigma_x^{-1} \tag{7}$$

Combining all observations the stochastic model takes the form

$$\mathcal{P}_L = \Sigma_L^{-1} \tag{8}$$

with Σ_L being the covariance matrix of the observation vector.

2.3 The Cost Model

In order to get an efficient solution in the economic sense it is necessary to introduce a realistic cost model. The optimization of the observation plan under the objective function of maximum accuracy is useless if no cost restriction is given. Particularly if hybrid configurations are considered the specific cost of different types of observations must be estimated

thoroughly. In general it is even better to take the individual cost of each observation into account. For this purpose the cost for each observation is to split up in cost factors. For example:

- costs for renting or buying the equipment
- costs for transportation
- costs for the operating personal
- costs for signal building

The different cost factors are to put together in a cost function which yields the total cost for the planned observation. The cost for the whole project is simply the sum of the costs of the single observations. For further discussion of this topic it is referred to the textbook of ***GRAFAREND et al., 1979***. For simplicity a very coarse cost model has been chosen for the numerical examples. It is assumed that in each group all possible observations require the same cost.

Type of observation	Cost
GPS interstation vector	4 Cost Units (CU)
slope distance	1 Cost Unit (CU)

Tab. 1

As the optimization results are very sensitive to the cost assumptions it is important for practical applications to investigate the costs very carefully.

3. FORMULATION OF THE DYNAMIC PROGRAM

The LS estimator for the parameter vector of the functional and stochastic model presented in chapter 2 is given by

$$x = \left(\mathcal{A}^T \mathcal{P}_L \mathcal{A}\right)^+ \mathcal{A}^T \mathcal{P}_L \ell = \mathcal{R}\ell \qquad (9)$$

According to the decomposition of Equation (4) the normal equations are partitioned.

$$\begin{bmatrix} \mathcal{A}_1^T \mathcal{P}_L A_1 & \mathcal{A}_1^T \mathcal{P}_L A_2 \\ \mathcal{A}_2^T \mathcal{P}_L A_1 & \mathcal{A}_2^T \mathcal{P}_L A_2 \end{bmatrix} \begin{bmatrix} x_1 \\ x_2 \end{bmatrix} - \begin{bmatrix} \mathcal{A}_1^T \mathcal{P}_L \ell \\ \mathcal{A}_2^T \mathcal{P}_L \ell \end{bmatrix} = 0$$

or shorter (10)

$$\begin{bmatrix} \mathcal{N}_{11} & \mathcal{N}_{12} \\ \mathcal{N}_{21} & \mathcal{N}_{22} \end{bmatrix} \begin{bmatrix} x_1 \\ x_2 \end{bmatrix} - \begin{bmatrix} n_1 \\ n_2 \end{bmatrix} = 0$$

Applying the rules for the elimination of x_2

$$\begin{aligned} \bar{\mathcal{N}}_{11} &= \mathcal{N}_{11} - \mathcal{N}_{12} \mathcal{N}_{22}^{-1} \mathcal{N}_{21} \\ \bar{n}_{11} &= n_1 - \mathcal{N}_{12} \mathcal{N}_{22}^{-1} n_2 \end{aligned} \qquad (11)$$

yields

$$x_1 = \bar{\mathcal{N}}_{11}^{+} \bar{n}_1 = \mathcal{Q} \bar{n}_1 \qquad (12)$$

and finally

$$x_1 = \mathcal{Q} \left(\mathcal{A}_1^T \mathcal{P}_L - \mathcal{N}_{12} \mathcal{N}_{22}^{-1} \mathcal{A}_2^T \mathcal{P}_L \right) \ell = \bar{\mathcal{R}} \ell \qquad (13)$$

The estimate for x_1 is a linear function of ℓ. Therefore simple error propagation results in

$$\mathcal{Q}_x = \bar{\mathcal{R}} \mathcal{Q}_L \bar{\mathcal{R}}^T \qquad (14)$$

As already mentioned the objective function to be minimized is the trace of the covariance matrix

$$\mathrm{tr}(\mathcal{Q}_x) = \mathrm{tr}\left(\bar{\mathcal{R}} \mathcal{Q}_L \bar{R}^T\right) \qquad (15a)$$

Because of $\mathrm{tr}(\mathcal{AB}) = \mathrm{tr}(\mathcal{BA})$ Equation (15a) can be written as

$$\mathrm{tr}\left(\bar{\mathcal{R}} \mathcal{Q}_L \bar{\mathcal{R}}^T\right) = \mathrm{tr}\left(\bar{\mathcal{R}}^T \bar{\mathcal{R}} \mathcal{Q}_L\right) \qquad (15b)$$

The right side of Equation (15b) represents an additive decomposition of the objective function containing one term for each observation. The contribution of observation i to $\mathrm{tr}(Q_x)$ is given by $\mathrm{diag}(\bar{R}^T \bar{R} Q_L)$. On the other hand the cost model allocates a most A_i to each observation.
The total sum of cost is given by

$$A_G = \sum A_i$$

Therefore the second order design problem can finally be formulated as

$$\mathrm{tr}(Q_x) \rightarrow \min$$

under the restriction (16)

$$A_G \leq A_B$$

where A_B denotes the given cost bound.

Including prior stochastic information about the coordinates the LS estimator for the parameter vector takes the form

$$\begin{aligned} x &= (A^T P_L A + P_x)^{-1} (A^T P_L \ell + P_x \ell_x) \\ &= (A^T P_L A + P_x)^{-1} [A^T P_L \vdots P_x] \begin{bmatrix} \ell \\ \cdots \\ \ell_x \end{bmatrix} \qquad (17) \\ &= [Q A^T P_L \vdots Q P_x] \begin{bmatrix} \ell \\ \cdots \\ \ell_x \end{bmatrix} \end{aligned}$$

Error propagation results in

$$\begin{aligned} Q_x &= [Q A^T P_L \vdots Q P_x] \begin{bmatrix} \Sigma_L & 0 \\ 0 & \Sigma_x \end{bmatrix} \begin{bmatrix} P_L A Q \\ \cdots \\ P_x Q \end{bmatrix} \\ &= Q A^T P_L \Sigma_L P_L A Q + Q P_x Q \qquad (18) \\ &= R \Sigma_L R^T + Q P_x Q \end{aligned}$$

Hence the objective function as given by the trace operator

$$\begin{aligned} \mathrm{tr}\,(\mathcal{Q}_x) &= \mathrm{tr}\left(\mathcal{R}\,\Sigma_L\,\mathcal{R}^T + \mathcal{Q}\,\mathcal{P}_x\,\mathcal{Q}\right) \\ &= \mathrm{tr}\left(\mathcal{R}\,\Sigma_L\,\mathcal{R}^T\right) + \mathrm{tr}\,(\mathcal{Q}\,\mathcal{P}_x\,\mathcal{Q}) \\ &= \mathrm{tr}\left(\mathcal{R}^T\mathcal{R}\,\Sigma_L\right) + \mathrm{tr}\,(\mathcal{Q}\,\mathcal{P}_x\,\mathcal{Q}) \end{aligned} \qquad (19)$$

shows that the first term comprises the influence of the observations and the second one reflects the influence of the prior information.

It is obvious that only the first term is affected by the choice of Σ_L . Therefore the matrix $\bar{\mathcal{R}}$ results in

$$\bar{\mathcal{R}} = (\bar{\mathcal{N}}_{11} + \mathcal{P}_x)^{-1}\left(\mathcal{A}^T\mathcal{P}_L - \mathcal{N}_{12}\,\mathcal{N}_{22}\,\mathcal{A}_2^T\,\mathcal{P}_L\right) \qquad (20)$$

The optimization problem (16) can be treated as an allocation problem. Using the terminology of dynamic programming the state variable of the problem is given by the cost model. The problem has N stages according to the number of possible observations. On each stage a decision is required whether or not the corresponding observation is to carry out. The sequence of observations which generates the minimum of the objective function is the optimal policy to be determined.

The initial state variable is given by the initial cost sum amount

$$x^0 = A_g \qquad (21)$$

The state variable is transformed on each stage

$$x^\nu = x^{\nu-1} - y^\nu \qquad (22)$$

and restricted to

$$0 < x^\nu < x^0\,. \qquad (23)$$

The decision y^ν represents the cost for the observation ν . If "no measurement" is decided $y^\nu = 0$ otherwise $y^\nu = A_\nu$. On each stage the contribution to the objective function is given by

$$g_\nu = \underset{\nu}{\mathrm{diag}} \left(\bar{\mathcal{R}}^T \bar{\mathcal{R}} \Sigma_L \right) . \qquad (24)$$

The sequence of decision y which minimizes

$$\sum_{u=1}^{N} g_\nu = \mathrm{tr} \left(\bar{\mathcal{R}}^T \bar{\mathcal{R}} \Sigma_L \right) = \mathrm{tr} \left(\mathcal{Q}_x \right) \qquad (25)$$

is the solution of the optimization problem. For a more detailed description of the method of dynamic programming see ***HEISTER 1978, GESSNER/ WACKER 1972*** and ***LARSON/CASTI 1979***.

4. COMPUTATIONAL ASPECTS

For practical computation it is necessary to introduce an iterative algorithm because of the dependence of $\bar{\mathcal{R}}$ on $\mathcal{P} = \Sigma_L^{-1}$. In the first step a start solution is to be set up. The corresponding total sum of costs is A_0 . Then a reduction rate ΔA is defined. The optimum is computed for $A_n = A_0 - \Delta A$ If A_n is still larger than the given final cost, in the next step a new start solution is used. The computations are repeated until the optimal configuration for the given cost bound is found. It may be noticed that on each step of computation in respect to the cost A_n an optimal configuration is present for analysis.

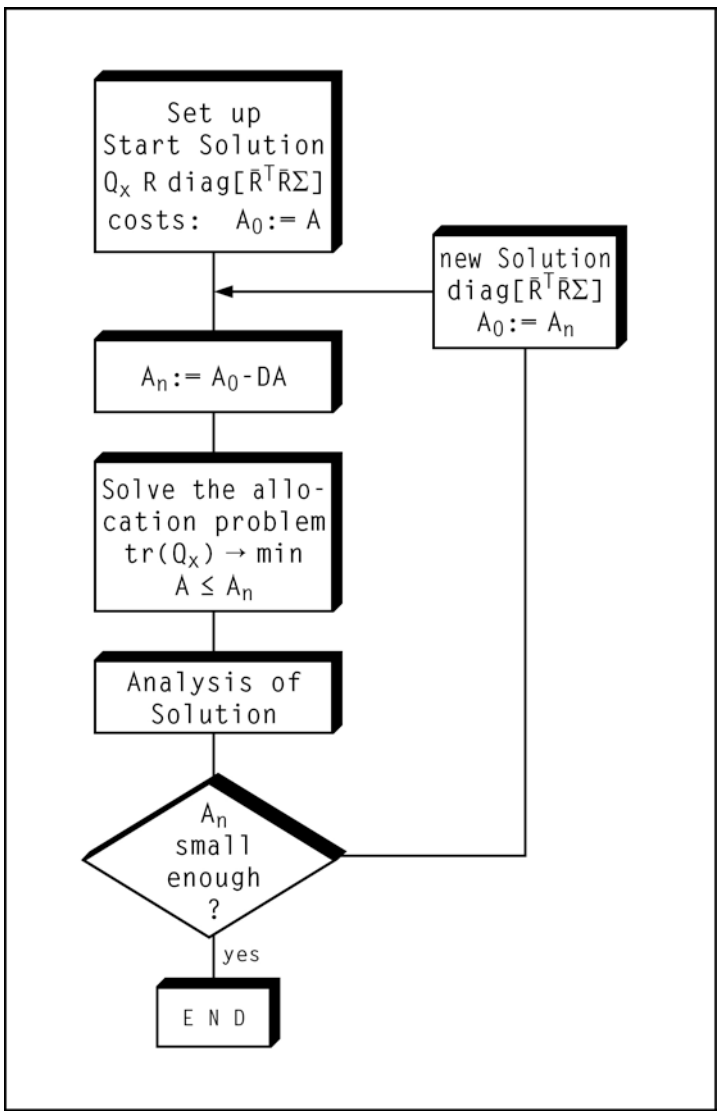

Fig. 1: Computational scheme

5. EXAMPLES

In order to give an idea of the capability of the proposed method some examples follow. The examples are based on real networks with a given first order design. But no restrictions as to the intervisibility of stations are imposed and no individual cost analysis has been carried out.

5.1 Inntal Network

The first example treats the Inntal Network which consists of 8 points with an average spacing of 9 km. The start solution for all versions includes all 28 possible vectors. Two different versions were calculated. In the first version the network was optimized using only GPS interstation vectors. The second one is based on GPS vectors and EDM distances. The cost relation between GPS vectors and EDM distances was chosen at 4:1. The assumptions on the precision $s_{GPS} = 0.5 + 1.5$ ppm and $s_{EDM} = 0.5 + 2.0$ ppm.

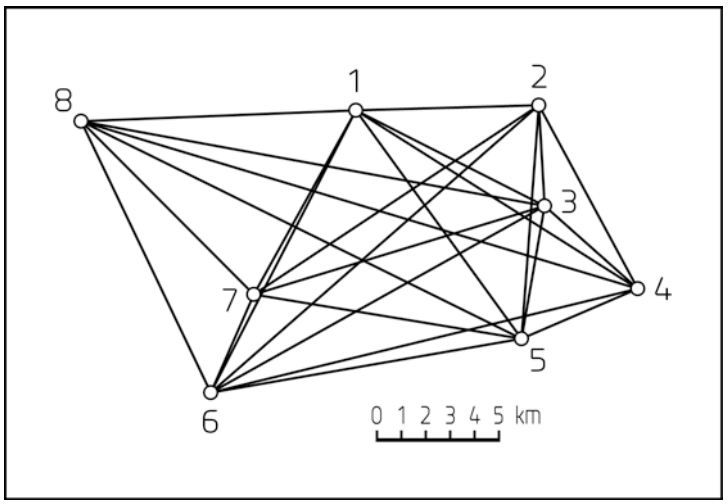

Fig. 2: Inntal Network

The examples are based on the inner constraint solution. The results of both versions are plotted on the following figures. The first plot (Fig. 3) shows the optimal design for 10 GPS-vectors (≙ 40 Cost Units). It is obvious that short lines are preferred because of the dependence of the precision on the distance. Fig. 4 is the plot of the optimal configuration for 72 CU (≙ 18 vectors). The mean point error (MPE)

$$\overline{s}_P = \sqrt{\frac{\mathrm{tr}(Q_x)}{n}} \qquad n: \text{ number of points} \qquad (26)$$

decreases from 1.7 cm for 40 CU to 1.3 cm (see Tab. 1). The plot displays a homogeneous distribution of observations.

In order to investigate combined network designs optimal plans were computed for 40 and 72 CU.

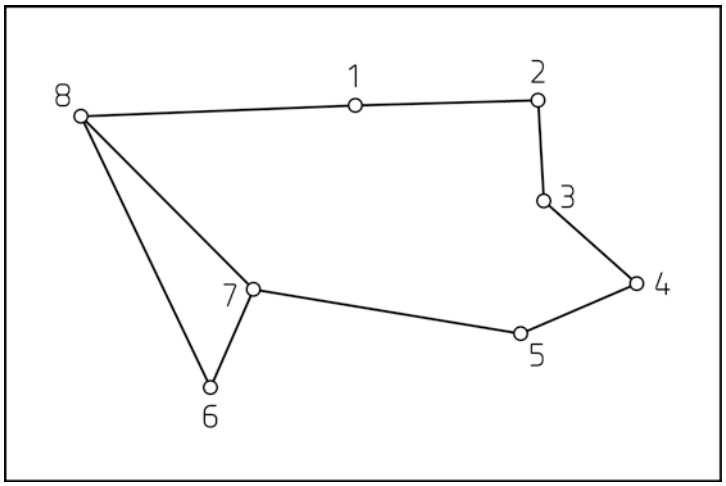

Fig. 3: Version 5.1.1 (40 CU)

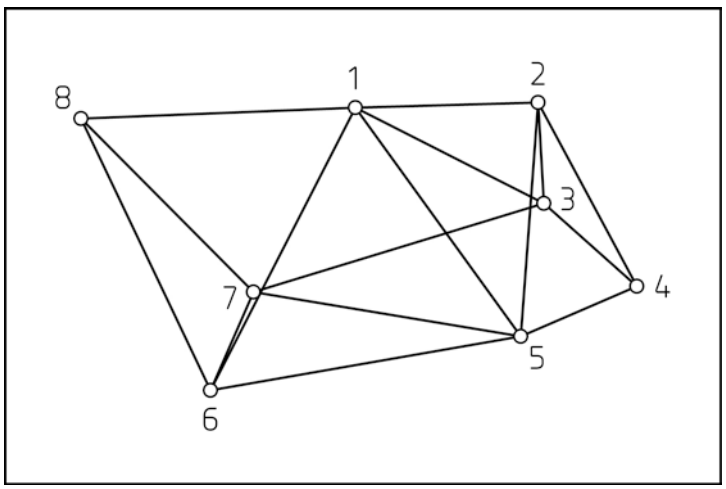

Fig. 4: Version 5.1.1 (72 CU)

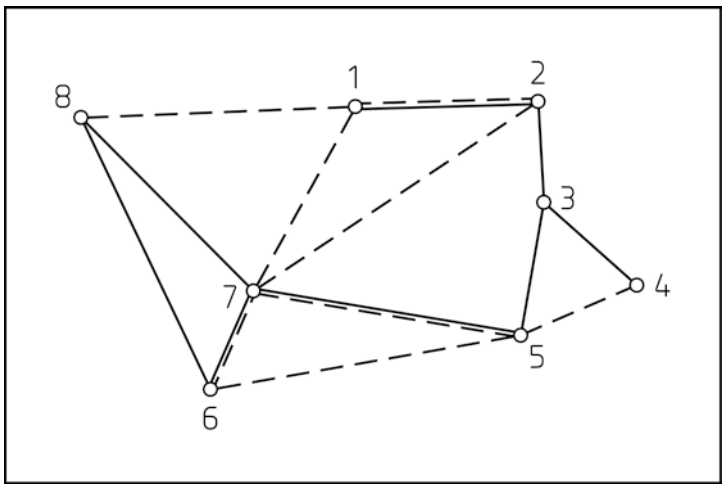

Fig. 5: Version 5.1.2 (40 CU)

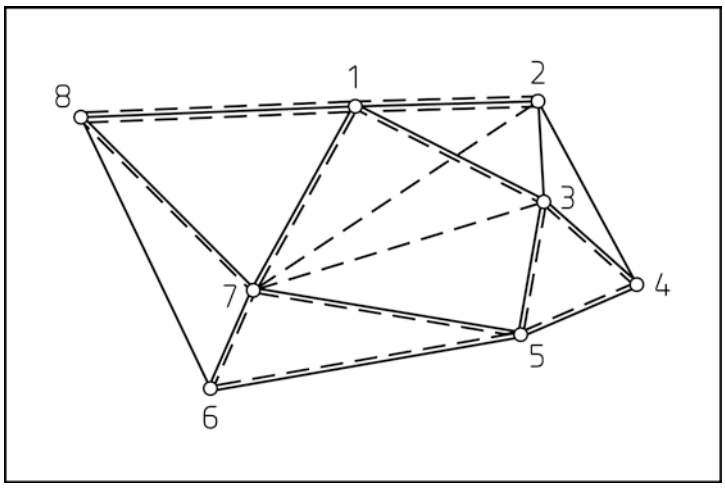

Fig. 6: Version 5.1.2 (72 CU)

The solution for 40 CU consists of 8 vectors and 8 EDM-distances. In comparison with the pure GPS solution some vectors, especially the long ones, are replaced or bordered by distances. The precision of the network has increased slightly from 1.7 cm to 1.6 cm. From the viewpoint of reliability the second version is preferable because of its higher redundancy.

The combined solution for 72 CU shows a homogeneous distribution of the observations. There are 14 vectors and 16 distances again concentrated on short connections. The global measure of accuracy has decreased from 1.3 cm to 1.2 cm in comparison to version 5.1.1.
All results for this example are compiled in table 1.

Expl.	$\overline{s}_P$	$s_{P_{max}}$	$s_{P_{min}}$	Number (CU)				Sum
	[cm]	[cm]	[cm]	Dist.		Vect.		[CU]
5.1.1	1.7	2.0	1.5	-		10	(40)	40
	1.3	1.5	1.2	-		18	(72)	72
5.1.2	1.6	2.0	1.3	8	(8)	8	(32)	40
	1.2	1.4	1.1	16	(16)	14	(56)	72

Tab. 1: Results of example 1 (Inntal Network)

5.2 Eifel-Network

In order to show the optimization effect in larger networks with special consideration of prior information about the coordinates the Eifel network (***SCHMIDT 1983***) has been chosen. The network consists of 19 points with an average distance of 5 km. This example was optimized as a pure GPS network and as a combined GPS-EDM net. The same assumption as in example 5.1 were used and additionally prior information of different quality was introduced. The start solution for all versions of this example consists of 48 connections as depicted in Fig. 7. For the combined network it is assumed that all drawn connections can be measured with EDM equipment.

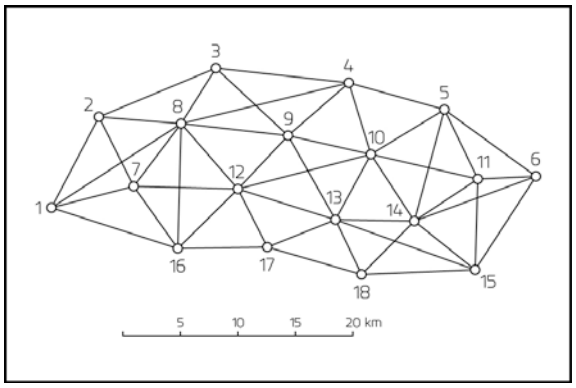

Fig. 7: Eifel network "Start solution"

The results of six different pure GPS solutions are plotted in Fig. 8. The graphs 8a and 8b show the results of the inner constraint solution with 20 and 29 vectors, respectively. If only a small number of observations is available (17 vectors are necessary to determine all points), the solution consists of traverses so that nearly all points are connected by two vectors with adjacent point. If more vectors are allowed the figure is strengthened with diagonals in a homogeneous manner. The average point error decreases from 3.0 cm (20 vectors) to 2.2 cm (29 vectors). The objective function is plotted against the number of vectors in Fig. 9.

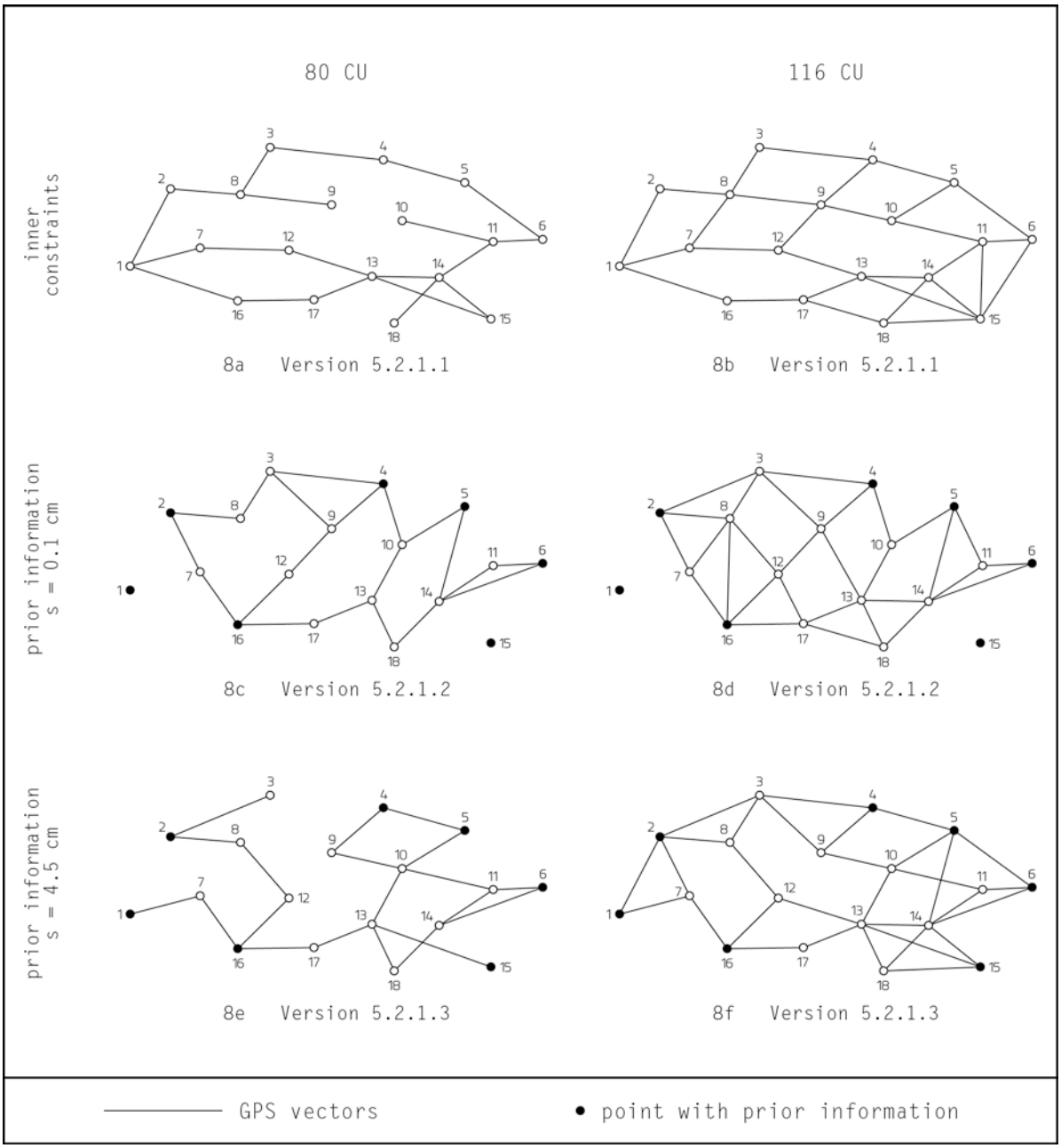

Fig. 8: Optimized solutions of the Eifel network (GPS vectors)

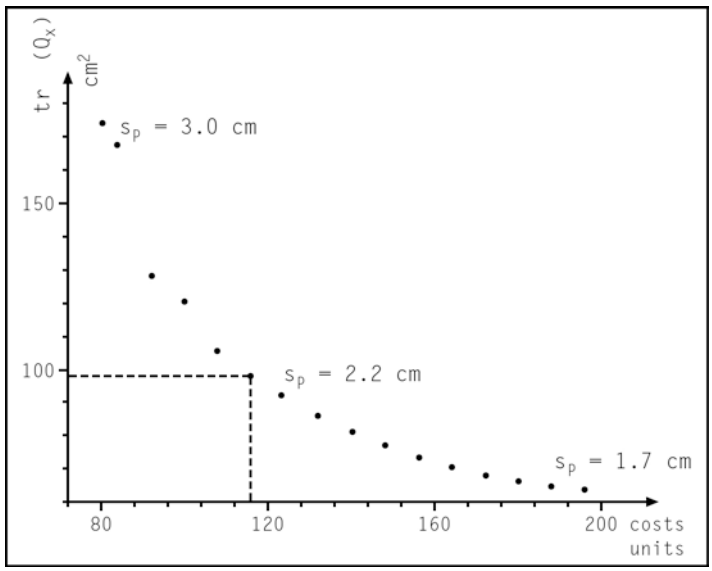

Fig. 9: Objective function

The two plots 8c and 8d show the results for two versions of network densification. For the marked points prior information in form of a standard deviation of 0.1 cm in each coordinate was introduced. The optimal observation plans for 20 and 29 vectors, respectively, contain no connections of point 1 and 15 to other points.

The inner points are linked with their nearest neighbors. None of the versions includes a line between points with prior information. The MPE decreases from 2.5 cm to 2.0 cm (points with prior information excluded) when the costs increase from 20 to 29 vectors.

The last two points display the results for the case that the prior standard deviation of the marked points is set at s = 4.5 cm (no correlations). As opposed to the previous versions, now all points are connected as the prior information is too weak to determine the border points with sufficient accuracy. The solution with 29 vectors even contains several connections between points with prior information. The MPE decreases from 5.3 cm for 20 vectors to 4.9 cm (for 29 vectors). It may be noticed that the accuracy measures of the three versions must not be compared because they refer to different datum choices. The prior information was introduced as an absolute one in order to simulate the situation of network densification with given points.

This example was also optimized as a combined GPS-EDM network. The assumptions on accuracy and cost were taken from the Inntal example. The optimized designs are compiled in Fig. 10 in the same order as in Fig. 8.

The plots 10a and 10b show the results for 117 CU and 149 CU, respectively, for the inner-constraint-datum. The less expensive version consists of 21

GPS vectors and 33 EDM distances. This design can be compared with the 29-vector-solution of figure 8 as both solutions are based on 117 CU. The combined solution is more accurate than the pure GPS design (see Tab. 2) and also preferable under the criterion of reliability. The plan for 149 CU differs from the combined 117 CU design by additional GPS vectors. The mean point error decreases from 1.9 to 1.6 cm which is only a poor gain in comparison with the increase of the costs.

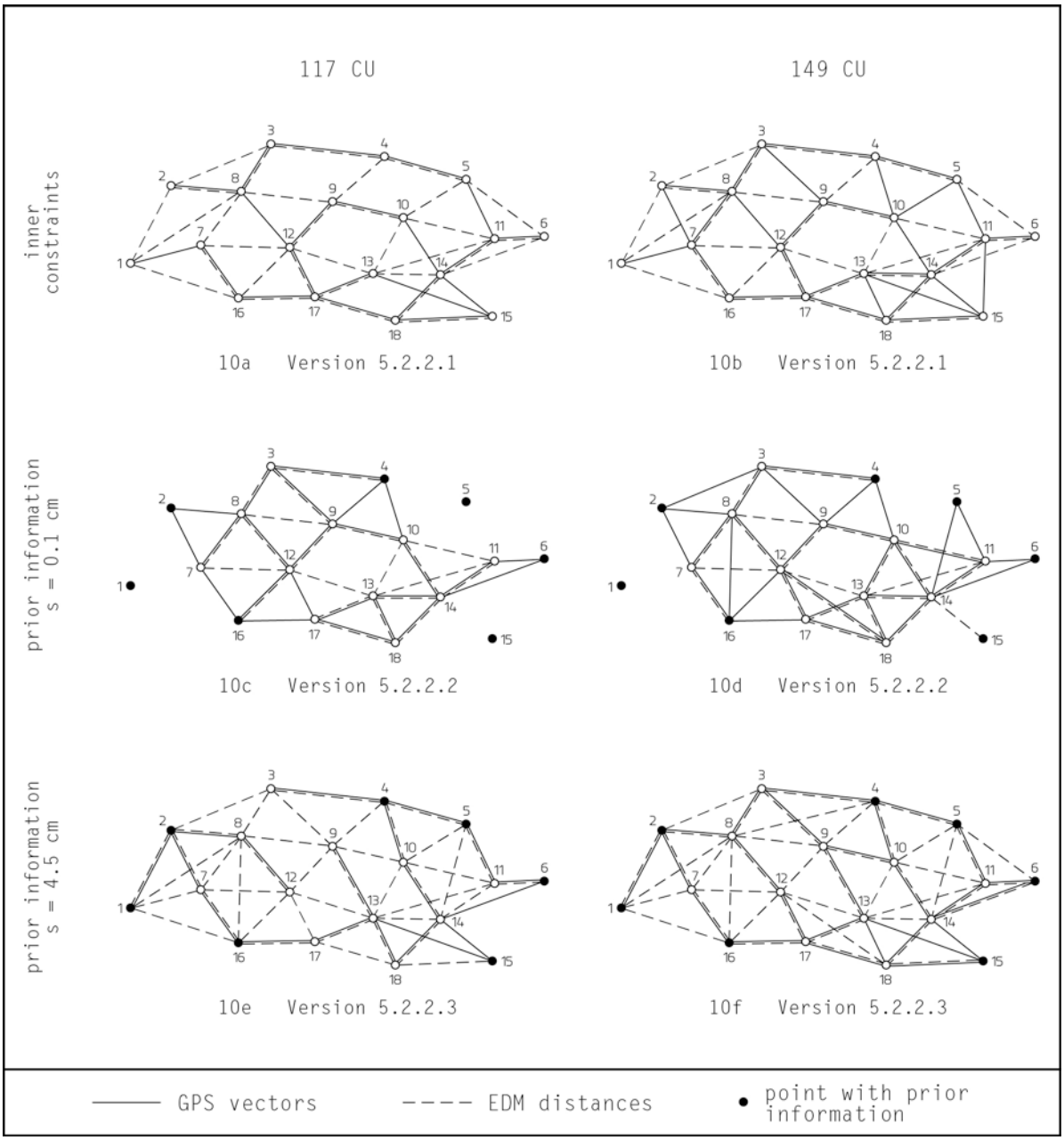

Fig. 10: Optimized design of the Eifel net for six different sets of model assumptions

The two plots 10c and 10d show the results of the versions where prior information about the coordinates of the marked points was introduced with a standard deviation of 0.1 cm. Again some points are not linked with the inner part of the network. The first version (117 CU) consists of 24 vectors and 21 distances and is 40% more accurate than the version without distances. The design based on 149 CU comprises 31 vectors and 25 distances. It includes vector connections to point 5 and a distance to point 15. If the prior information is introduced with a standard deviation of 4.5 cm then the observations can improve the accuracy of the given points. This situation was a simulated in the last version having led to the designs depicted in Fig. 10e and 10f.

Expl.	$\overline{s}_P$	$s_{P_{max}}$	$s_{P_{min}}$	Number (CU)		Sum
	[cm]	[cm]	[cm]	Dist.	Vect.	[CU]
5.2.1.1	3.0	5.3	1.8		20 (80)	80
	1.7	3.9	1.2	–	49 (196)	196
	2.2	4.1	1.6		29 (116)	116
5.2.1.2	2.5	3.4	2.0		20 (80)	80
	1.7	2.7	1.4	–	49 (196)	196
	2.0	3.0	1.7		29 (116)	116
5.2.1.3	5.3	7.7	4.1		20 (80)	80
	4.7	7.1	3.4	–	49 (196)	196
	4.9	7.3	3.8		29 (116)	116
5.2.2.1	1.9	3.4	1.3	33 (33)	21 (84)	117
	1.4	2.8	1.0	49 (49)	49 (196)	245
	1.6	3.1	1.3	33 (33)	29 (116)	149
5.2.2.2	1.7	2.8	1.3	21 (21)	24 (96)	117
	1.5	2.5	1.2	49 (49)	49 (196)	245
	1.6	2.6	1.3	25 (25)	31 (124)	149
5.2.2.3	3.8	5.3	3.3	41 (41)	19 (76)	117
	3.5	4.8	2.8	49 (49)	49 (196)	245
	3.6	5.2	3.0	45 (45)	26 (104)	149

Tab. 2: Collected results of example 2 (Eifel Network)

The solution based on 117 CU, consists of 41 distances amd 19 vectors, which is nearly the minimum to guarantee a proper height solution. The MPE of this solution is 3.8 cm being much smaller than the same measure of accuracy of the pure GPS solution (4.9 cm). The consideration of distance measurements seems to effectively improve GPS interstation vector networks.

The results of all versions of optimal design of the Eifel network are given in Tab. 2.

6. CONCLUSIONS AND PROSPECTS

The proposed method is an effective tool for the optimization of 3D networks containing GPS-interstation vectors. It is applicable to optimize the design of new networks and to optimize the densification of existing networks when the knowledge about the old points is introduced as prior information. The optimization procedure is based on dynamic programming regarding the trace of the covariance matrix of the coordinates as the objective function to be minimized. The method can easily be extended to use the trace of the covariance matrix of a set of optional functions of the coordinates as the objective function. At the present time the daily observation window is so narrow that only a decision on whether or not to observe a considered baseline vector is possible. When all satellites of the Global Positioning System are orbiting it will be no problem to sophisticate the model in order to consider different observation lenghts, different accuracy and cost in the process of optimizing the configuration.

REFERENCES

BOCK, J., R.I. ABBOT, C.C. COUNSELMANN III, S.A. GOUREVITCH, R.W. KING (1985): ***Establishment of Three-Dimensional Geodetic Control by Interferometry with the Global Positioning System***. Submitted to Journal of Geophysical Research, December 1984

BORUTTA, H. (1985): ***Discrete Dynamic Optimization of Relative GPS Positioning***. Presented Paper to the 7th International Symposium on Geodetic Computations, Cracow 1985

GESSNER, P., H. WACKER (1972): ***Dynamische Optimierung***. München 1972

GRAFAREND, E., H. HEISTER, R. KELM, H. KROPFF, B. SCHAFFRIN (1979): ***Optimierung geodätischer Meßoperationen***. Karlsruhe 1979

HEISTER, H. (1976): ***Bestimmung der günstigsten Beobachtungsanordnung in lokalen Lagenetzen mit Hilfe der dynamischen Optimierung***. Diss. München 1976

HEISTER, H. (1978): ***Die diskrete dynamische Optimierung und ihre Anwendung beim geodätischen Netzentwurf***. Allgemeine Vermessungsnachrichten, pp. 64

HEISTER, H., A, SCHÖDLBAUER, W. WELSCH (1985): ***Macrometer Measurements 1984 in the Inn Valley Network***. First International Symposium on Precise Positioning with the Global Positioning System, Rockville 1985

LARSON, R.E., J.L. CASTI (1978): ***Principles of Dynamic Programming***. Part I and Part II, New York 1978

LEICK, A. (1984): ***Macrometer TM Satellite Surveying***. FIG Engineering Surveys Conference, Washington, D.C. 1984

NIEMEIER, W., K. FRITZENSMEIER, G. KLOTH, K. EICHHOLZ (1985): ***Simulation Studies on the Improvement of Terrestrial 2D Networks by Additional GPS Information***. Proceedings of the Joint Meeting of FIG Groups 5B and 5C, Munich 1985, Schriftenreihe des Wissenschaftlichen Studienganges Vermessungswesen an der Universität der Bundeswehr München, Heft 20

SCHMIDT, R. (1983): ***Das neue interferometrische GPS-Vermessungsgerät Makrometer und sein Einsatz in der TP-Netzerneuerung 2. Ordnung Nordeifel***. Nachrichten aus dem öffentlichen Vermessungsdienst des Landes Nordrhein-Westfalen 1983, S. 138-148

SCHWINTZER, P., CH. REIGBER, R. STRAUSS (1985): ***Macrometerbeobachtungen im Deutschen Hauptdreiecksnetz (Macrometer-Netz "Hessen")***. Deutsche Geodätische Kommission, Reihe B, Heft 273, München 1985

THE ESTIMATION OF ORTHOMETRIC HEIGHTS FROM GPS BASELINE VECTORS USING GARVITY FIELD INFORMATION AND LEAST-SQUARES COLLOCATION

by

Bernd EISSFELLER

Institut für Astronomische und Physikalische Geodäsie
Universität der Bundeswehr München
Werner-Heisenberg-Weg 39
D-8014 Neubiberg
Federal Republic of Germany

ABSTRACT

The adjustment of GPS baseline vectors in geodetic networks yields (among) other quantities) very precise ellipsoidal height differences. Due to the fact that the (orthometric) heights in classical geodetic networks are defined physically referring to the geoid as vertical reference surface, heights above the ellipsoid are in principle of no use for geodetic and surveying applications.

The topic of this paper is to discuss a solution strategy for the separation of orthometric heights and relative geoidal heights which can be done only by taking into account additional gravity field data in such an approach.

Starting with the basic observations equation of Cartesian baseline vectors, a least-squares collocation solution strategy is presented. Minimizing the hybrid quadratic norm of observational noise and the functionals of the gravity disturbing potential (signals) ellipsoidal coordinates B, L, orthometric heights H , and geoidal undulations N can be estimated in a unified model approach.

Will be published in:
GPS Research at the Institute of Astronomical and Physical Geodesy.
Schriftenreihe des Wissenschaftlichen Studiengangs Vermessungswesen,
Universität der Bundeswehr München, Heft 19, 1985

THE GLOVAL POSITIONING SYSTEM:

AN ALTERNATIVE TO

SIX DEGREES-OF-FREEDOM INERTIAL NAVIGATION

by

Alan G. Evans

Naval Surface Weapons Center
Dahlgren, Virginia 22448-5000
United States of America

ABSTRACT

This paper demonstrates the potential capabilities of the Global Positioning System (GPS) for determining a platform's orientation. Orientation plus positioning capabilities qualify GPS as an alternative to inertial navigation. Phase measurements were obtained from two TI4100 Geodetic Receivers connected to the same frequency standard and to two antennas on a static 25m baseline. It is shown that if the integer number of cycles between the initial phase measurements is determined, the orientation of a platform can be calculated using phase measurements taken at the same time instant from four satellites.

The paper discusses conditions and potential procedures for determining this integer number of cycles. Instantaneous azimuth and elevation (yam and pitch) estimates are obtained from a series of measurements; the accuracy of these unfiltered estimates is discussed. The test case accuracies were found to be very close to values predicted by simulation.

1. INTRODUCTION

Before the development of the NAVSTAR Global Positioning System (GPS), only inertial measurement systems had the potential to provide both position and platform orientation, six degrees-of-freedom information, as a stand-alone system (Reference 1). Initial demonstrations using measured data have demonstrated an accurate navigation capability of GPS (Reference 2), and much emphasis has been given to both static and dynamic positioning (Reference 3). This paper emphasizes GPS's capability to determine platform orientation.

Initially, change-in-phase measurements for an antenna rotating in a plane were used to demonstrate GPS's capability to determine platform orientation (Reference 4 and a slightly later demonstration in Reference 5). At that time, the available GPS receivers did not output coherent phase measurements. That is, the initial phase measurements between two receivers on the same antenna and clock were completely random, rather than related to each other. The change-in-phase procedure appears to be potentially useful for a rotating antenna on a helicopter or a ship, since it requires only one antenna and the standard tracking capability of a single, currently available receiver. Also, change-in-phase measurements remove many bias errors, are readily available from the receivers, and may be used directly in simple computational algorithms. The main disadvantage of this procedure is that it requires mechanical motion of the antenna.

With the advent of coherent phase measurement receivers, GPS could be used to determine platform orientation using three antennas fixed relative to each other on the vehicle. The conclusions of this paper are based on measurements from two Texas Instruments Model 4100 Geodetic GPS Receivers (Reference 1) connected to the same clock and two antennas with a static 25m baseline. The receivers measure coherent phase on both L1 and L2 GPS frequency channels and track up to four satellites. The paper demonstrates that instantaneous elevation and azimuth (pitch and yam) estimates can be obtained from one time line of phase measurements is determined. For a moving platform, unless the orientation is approximately known, the integer number of cycles measurements may be difficult to obtain. Iterative initialization procedures are under investigation to determine the integer number of cycles. It is theoretically shown that if both L1 and L2 phase measurements are available, the integer cycle resolution length increases from either the L1 or L2 wavelength to 86cm when using the L1 and L2 phase measurement differences.

The TI4100 Geodetic Receiver was developed by Texas Instruments, Inc. of Lewisville, Texas, for the Defense Mapping Agency and the National Oceanic and Atmospheric Administration. The tests described in the next section were performed at the Applied Research Laboratories of the University of Texas (ARL/UT) in Austin.

The procedure described in the paper uses phase measurements from four satellites tracked simultaneously by the receiver. The procedure is similar to the interferometric procedures described in References 6 and 7. However, it was found necessary to difference the measurements, and corresponding range equations, from one satellite with the other three being tracked. This procedure eliminates antenna cable bias, and receiver bias and drift. The phase relationships and estimation procedures are presented in Sections 3 and 4 respectively, and the orientation test results are given in Section 5. The conclusion discusses the test accuracy and current dynamic orientation tests.

2. TEST DESCRIPTION

The data used for the orientation test was obtained on 16 July 1984, as part of a series of collocation tests to analyze the TI4100 Geodetic Receiver performance (Reference 6). The test configuration used in this paper is illustrated in Figure 1. Two receivers were operated simultaneously in Geodetic User Class for approximately 90 min, while there were four GPS satellites in view (PRN-6, -8, -9 and -11). Two antennas, separated by 25m, were placed on the roof at ARL/UT. A rubidium frequency standard locked both receivers to a common time reference. Two frequency pseudo-range and phase observations were collected and recorded on cassettes tapes for post-processing. The data was recorded at one second (1-s) intervals. However post-processing was done at 6-s intervals. The data collection software program, ASDAP (ARL/UT Simplified Data Acquisition Program), also recorded receiver status information and broadcast ephemerides from the four satellites. For analysis, post-fit trajectories were used, instead of trajectories derived from the broadcast ephemerides. Since the baseline was so short, the two trajectories were expected to produce very nearly the same results.

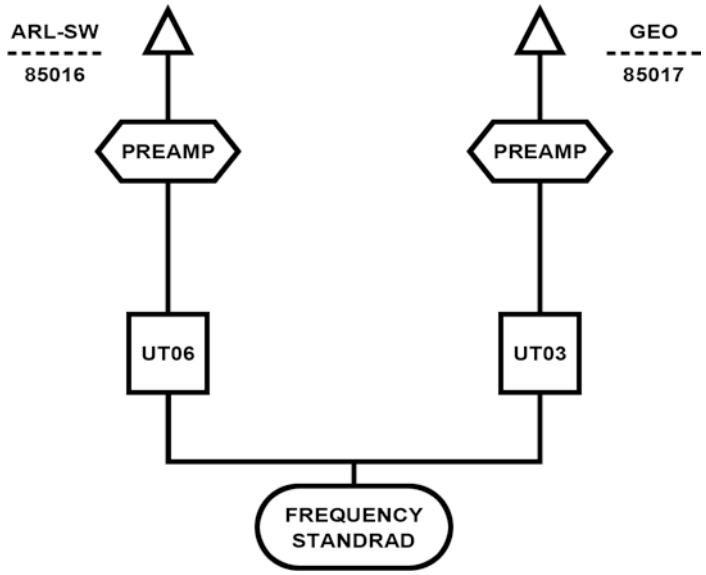

FIGURE 1. ARL/UT rooftop test: 16 July 1984

The collocation tests (Reference 6) showed that the geodetic receivers experience some drift. This drift was very nearly the same on each tracker within the given receiver. Consequently, to remove this unknown drift, the measurements and corresponding range equations are differenced. This also removes antenna cable and receiver biases.

3. PHASE RELATIONSHIPS FOR A SINGLE TIME INSTANT

At a single instant in time, the phase relationship of a satellite transmitted signal between two closely located antennas is shown in Figure 2. The fractional parts of the Geodetic Receiver phase measurements of the k^{th} tracker are designated as F_A^k and F_B^k for each receiver, respectively, and are depicted in the figure. At this point, the integer number of cycles between the measurements is not known. Determination of this integer is discussed below.

The first procedure is to assume the approximate location of the antennas is known or can be determined. If the antennas are stationary, Reference 6 demonstrates that the approximate relative location of the antennas on the 25m baseline can be obtained using GPS with less than an hour of data. For GPS, the accuracy must be known to some what less than the signal wavelength, which is λ_1 = 0.19029m

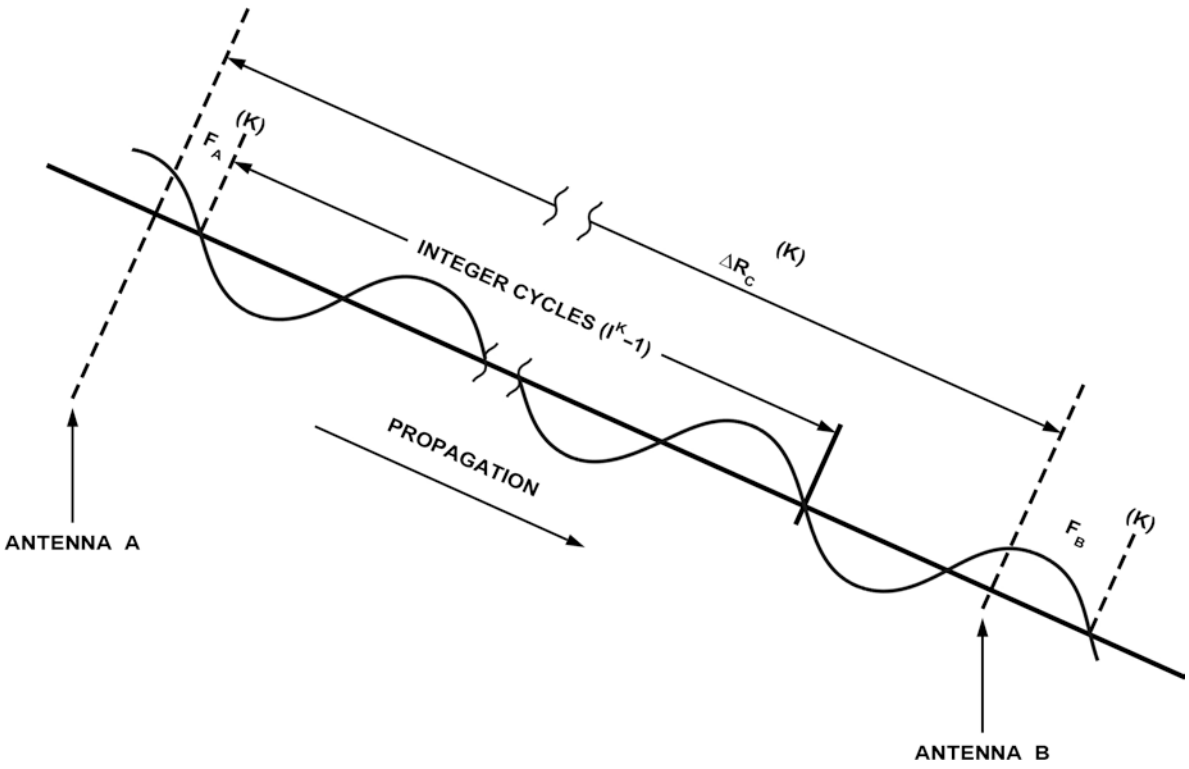

Figure 2. Single time instant phase diagram

for L_1 channel and $\lambda_2 = 0.24421$m for L_2 channel. Here, the surveyed locations of the antennas are used. The calculated difference in range between the antennas for the k^{th} tracker, i.e., for a particular satellite, is given in cycles by

$$\frac{\Delta R_c^k}{\lambda_1} = I^k + F_A^k - F_B^k + e^k \tag{1}$$

where I^k is the unknown integer and e^k is the error which includes a cable bias and receiver measurement errors. Now, subtracting the k^{th} tracker from the l^{th}

$$\frac{\Delta R_C^l - \Delta R_C^k}{\lambda_1} = I^{l,k} + F_A^l - F_B^l - \left(F_A^k - F_B^k\right) + e^{l,k} \tag{2}$$

procedures where

$$I^{l,k} = I^{l} - I^{k} \quad \text{and}$$

$$e^{l,k} = e^{l} - e^{k}$$

Here, it is important to note that $e^{l,k}$ has the bias due to antenna cable and the receiver removed. The receiver drift, which can be considered as a randomly changing bias, is also removed, since it is common to all trackers on the TI4100 Geodetic Receiver. Consequently, the error $e^{l,k}$ shouldbe much smaller than one wavelength.

$$I^{l,k} = \frac{\Delta R_C^l - \Delta R_C^k}{\lambda_1} - \left[F_A^l - F_B^l - \left(F_A^k - F_B^k\right) + e^{l,k}\right] \tag{3}$$

To check this procedure and the receiver's coherent phase measuring capability, the substitution of measured fractional phase values and calculated range differences into the above equations should produce approximate integer values for the $I^{l,k}$. This was done for the initial time line for the test case described above. Surveyed locations were used to compute the calculated ranges. The approximate and actual integer values are given in Table 1. For the values in the table, the tracker values are l = 1 and k = 2, 3 and 4. These integer values are applied in Section 4, to estimate relative antenna position.

The integer $I^{l,k}$ needs to be determined only for the initial common measurement time, as long as the receivers are locked to the same common satellite. Integer cycle phase measurements of the receivers can be used directly to determine the $I^{l,k}$ for subsequent measurement times.

For the above discussion the accuracy tolerance, to which the calculated range difference must be known, was less than a wavelength. Thus, λ_1 and λ_2 are the ambiguity lengths for the L_1 and L_2 frequency channels, respectively. This ambiguity length can be increased if both L_1 and L_2 phase measurements are available. For example let n_1 and n_2 be the integer and fractional part of the number of cycles between antennas as shown in Figure 2 for L_1 and L_2, respectively. Then,

$$n_1 = \frac{\Delta R_C}{\lambda_1}$$

and

$$n_2 = \frac{\Delta R_C}{\lambda_2}$$

The difference in these measurements is

$$n_1 - n_2 = \left(\frac{1}{\lambda_1} - \frac{1}{\lambda_2}\right) \Delta R_C$$

$$= \frac{1}{\lambda_{1,2}} \Delta R_C$$

where substitution λ_1 of and λ_2 produces

$$\lambda_{1,2} = 0.861846\text{m}$$

which is significantly larger than either λ_1 or λ_2. This indicates, at least ideally, that if the antennas are separated by a very short baseline less than $\lambda_{1,2}$, and if there is no antenna interference, the orientation phase measurements, can be used directly. Note, however, that receiver biases are not removed.

Alternatively, iterative procedures are also under investigation to determine the integer cycle ambiguity number. Here, all possible integer values, which when multiplied by the wavelength, are substituted. The integers which produce solutions with the proper baseline length are considered as possibilities. Further eliminations occur at successive time lines.

4. ORIENTATION ESTIMATION

In this section the integer number of cycles between the initial phase measurements given in Table 1 are assumed to be known.

TABLE 1. Approximate and actual integer numbers of cycles between differenced phase measurements

Trackers l,k	Approximate Value $I^{l,k}$	Integer Value $I^{l,k}$
1, 2	-45.03	-45
1, 3	49.03	49
1, 4	45.90	46

Also, the location of the antenna at site 85016 is assumed to be known perfectly. Based on the measured data, the position of site 85017 of Figure 1 is corrected. For the initial time line estimate, F_A^k and F_B^k of Figure 2 are used. Receiver change-in-phase measurements are then added to F_A^k and F_B^k to produce successive phase measurements. The range equation for the k^{th} tracker is

$$\Delta R_0^k - \Delta R_C^k = \frac{\partial R_C^k}{\partial d}\Delta d + \frac{\partial R_C^k}{\partial p}\Delta p + \frac{\partial R_C^k}{\partial h}\Delta h + e^k$$

where

Δd = north correction
Δp = east correction
Δh = vertical correction
R_0^k = the obserced difference in range
R_C^k = the calculated difference in range

Here,

$$\Delta R_0^k = I^k + n_A^k - n_B^k$$

where n_A^k and n_B^k are the phase measurements in cycles such that for the initial phase measurement $n_A^k = F_A^k$ and $n_B^k = F_B^k$, where I^k, F_A^k and F_B^k are shown in Figure 2. To remove the bias term of e^k, the k^{th} tracker values are differenced from the l^{th} tracker values to produce a double difference relationship where

$$\left(\Delta R_0^l - \Delta R_C^l\right) - \left(\Delta R_0^k - \Delta R_C^k\right) = \left(\frac{\partial R_C^l}{\partial d} - \frac{\partial R_C^k}{\partial d}\right)\Delta d +$$

$$+ \left(\frac{\partial R_C^l}{\partial p} - \frac{\partial R_C^k}{\partial p}\right)\Delta p + \left(\frac{\partial R_C^l}{\partial h} - \frac{\partial R_C^k}{\partial h}\right)\Delta h + e^{l,k}$$

Now,

$$\Delta R_0^l - \Delta R_0^k = I^{l,k} + n_A^l - n_B^l - \left(n_A^k - n_B^k\right)$$

and where $I^{l,k}$ are given in Table 1. Since there are three such equations formed by differencing the data from one tracker from the remaining three, there is sufficient information to determine Δd, Δp and Δh at each time line. These values are added tom the assumed corresponding values for site 85017 and denoted as $\hat{\Delta} d$, $\hat{\Delta} p$ and $\hat{\Delta} h$. The elevation and azimuth can then be written as

$$\text{elevation} = \arcsin \frac{\hat{\Delta} h}{b}$$

and

$$\text{azimuth} = \arcsin \frac{\hat{\Delta} p}{b}$$

where b is the fixed baseline length between the antennas.

5. TEST RESULTS ACCURACY

Measured phase data from the test configuration described in Section 2 was processed during a span of 48 minutes at 6 second intervals. Time lines estimates were obtained of the position corrections to the survey location of 85017. Since the fixed antenna location sites were very nearly level, and somewhat close to being in the East-West direction, the orientation estimation errors can be approximated by

$$\Delta \text{elevation} = \arcsin \frac{\Delta h}{b}$$

and

$$\Delta \text{azimuth} = \arcsin \frac{\Delta p}{b}$$

Plots of these errors as a function of time are given in Figures 3 and 4. The standard deviation of these estimates is $\sigma_{\Delta Elev.} = 0.14$ and $\sigma_{\Delta Az.} = 0.09$ milliradians, respectively.

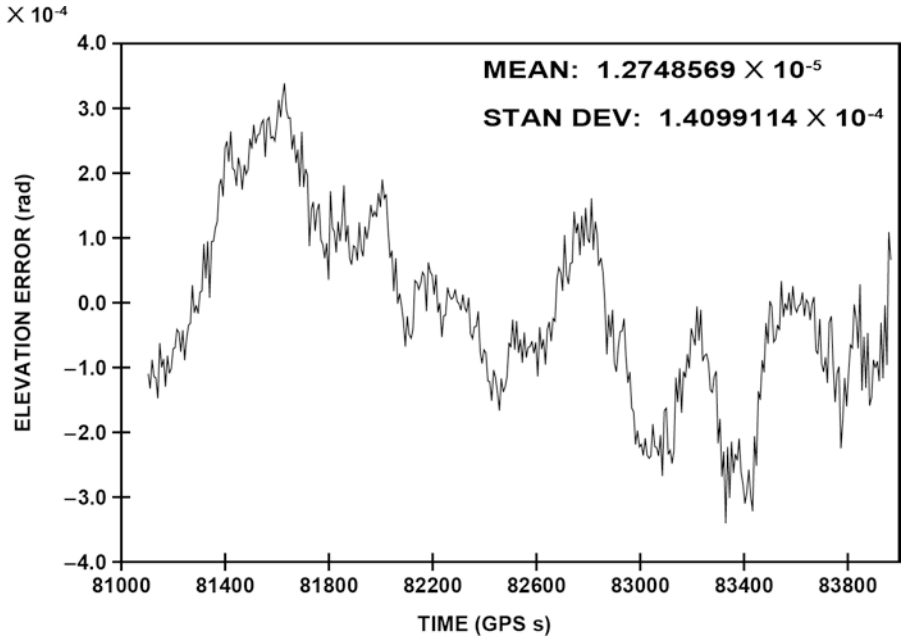

FIGURE 3. Elevation estimation error for a static 25m baseline.

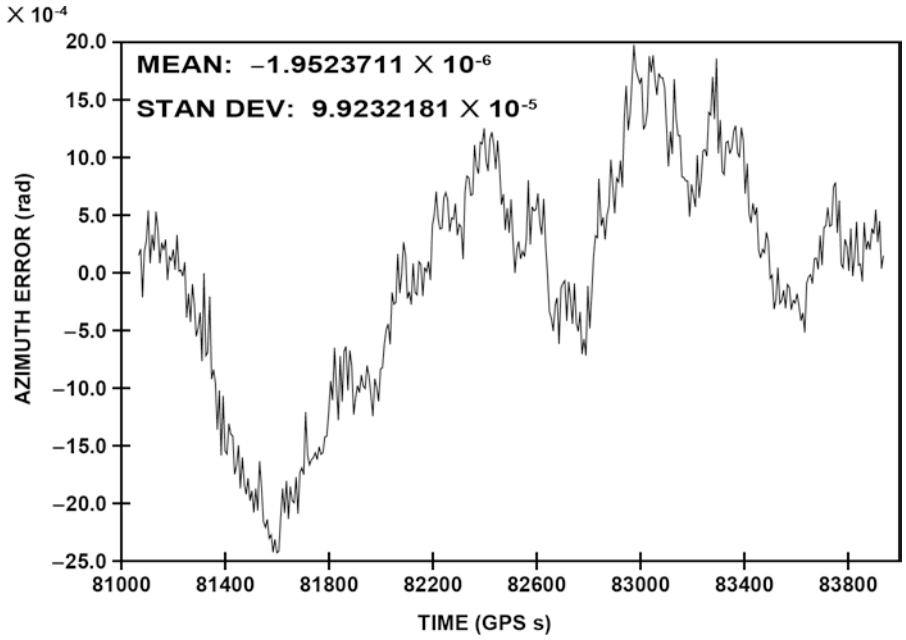

FIGURE 4. Azimuth estimation error for a static 25m baseline.

6. CONCLUSION

This paper examines the application of GPS to determine the orientation of a platform. This application is in addition to its more standard use, positioning. The combined position and orientation information indicates that GPS can in the future be regarded as a complete alternative to the six degree-of-freedom inertial navigation system for the low dynamic user.

The potential orientation accuracy of GPS has been demonstrated. If the initial integer number of cycles between the phase measurements is obtained, the orientation of a platform can be determined at each measurement time instant. Currently, the initial integer number of cycles can be obtained by keeping the platform fixed for a sufficient time to enable the integers to be determined; more sophisticated procedures are under investigation.

The accuracy of the orientation procedure varies linearly with the length of the baseline (Reference 1). The advantge of the coherent phase procedure over the change-in-phase procedure of Reference 2 is that the fixed length baseline can be more easily be increased over the rotating antenna procedure to provide greater accuracy. The disadvantage is that the integer cycle number must be resolved and the satellite trackers must be kept in lock; otherwise, the integer cycle number must be resolved again. This is not necessary for the change-in-phase procedure.

For the series of L_1 phase measurements in the static 25m baseline experiment, the standard deviation of the elevation (pitch) and azimuth (yaw) were found to be 0.14 and 0.09 miilradians, respectively. These values very closely match the predicted accuracy of Reference 9. There, simulation results predicted an orientation error of about 0.15 milliradians for roll, pitch and yaw for a 25m baseline. The simulation modeled the same receiver used in the experiment for both measurement accuracy and tracking capability. The test accuracy values also fall in the more accurate end of the range of predicted performance given in Reference 1 for the case using two receivers.

The procedure described above for two antennas can be extended to three antennas and receivers. Dynamic laboratory tests of this three-antenna configuration have been performed at ARL/UT and will be analyzed in the future.

7. REFERENCES

1. C. R. Johnson et al., "Applications of a Multiplexed GPS User Set," *Navigation*, Vol. 29, No. 4, pp. 353-369, Winter 1981-82.

2. A. G. Evans, B. R. Hermann and P. Fell, "Global Positioning System Sensitivity Experiments," *Navigation*, Vol. 28, No. 7, pp. 74-84, Summer 1981.

3. First International Symposium on Precise Positioning with the Global Positioning System, Vol. I and II, Rockville, Maryland, April 1985.

4. A. G. Evans, "Roll, Pitch and Yaw Determination Using a Global Positioning System Receiver and an Antenna Periodically Moving in a Plane," *Marine Geodesy*, to be published.

5. K. M. Joseph and P. S. Deem, "Precision Orientation: A New GPS Application," International Telemetering Conference, San Diego, California, October 1983.

6. A. G. Evans, B. R. Hermann, D. S. Coco, J. R. Clynch, "Collocation Tests of an Advanced Geodetic Global Positioning System Receiver," First International Symposium on Precise Positioning with the Global Positioning System, Rockville, Maryland, April 1985.

7. V. W. Spinney, "Applications of the Global Positioning System as an Attitude Reference for Near Earth Uses," ION, Warminster, Pennsylvania, April 1976.

8. A. K. Brown and W. M. Bowles, "Interferometric Attitude Determination Using the Global Positioning System," Third Geodetic Symposium on Satellite Doppler Positioning, Las Cruces, New Mexico, pp. 1289-1302, February 1982.

9. B. R. Hermann, "A Simulation of the Navigation and Orientation Potential of the TI-AGR," *Marine Geodesy*, Vol. 9, No. 2, pp. 133-143, 1985.

SIMULATION STUDIES ON THE IMPROVEMENT OF TERRESTRIAL 2-D-NETWORKS BY ADDITIONAL GPS-INFORMATION

by

Klaus FRITZENSMEIER
Gerhard KLOTH
Wolfgang NIEMEIER
Geodätisches Institut
Universität Hannover
Nienburger Straße 1
D-3000 Hannover 1
Fed. Rep. of Germany

Klaus EICHHOLZ
Institut für Markscheidewesen
Westfälische Berggewerkschaftskasse
Herner Straße 45
D-4630 Bochum
Fed. Rep. of Germany

ABSTRACT

In this paper it is shown that GPS-information can be treated as observables with same role as terrestrial information, i.e. as relative position information with a precision of about 1 ppm. This precise GPS-information is a useful addition to terrestrial information and often will replace the terrestrial observations. For a systematic control network and a tunneling network simulation studies are performed to compare different types of networks using terrestrial, satellite or combined information.

1. INTRODUCTION

With the Navy Navigation Satellite System (NNSS) the inclusion of satellite-based-observations in terrestrial networks was a useful tool for purposes of datum definition and - for lower accuracy requirements - for coordinate determinations (***SEEBER 1984***). With the establishment of the Global Positioning System (GPS) and its high precision for relative positioning this situation has changed, the satellite information now can be treated as additional observables in competition to terrestrial observables.

Besides other examples, for the network "Emschermulde" in the Ruhrgebiet area a Macrometer survey was performed in 1984 and by comparison with terrestrial techniques the assumed high precision of 1-2 ppm was confirmed. A detailed study in this network and the comparison between terrestrial and satellite results will be given in ***KLAKA and KORITTKE (1985)***. These convincing results encouraged us to study the potential of relative GPS-positioning for the improvement of 2D-networks.

In this paper we want to show that it is possible to use GPS-coordinate-differences in a combined 2D-network adjustment program just as an additional type of observables. Furtheron the optimization of 2D-networks by adding GPS-satellite-information is discussed in respect to precision and reliability criteria. There are different strategies outlined:

- improvement of the precision and reliability of the terrestrial network by adding GPS-information
- replacement of terrestrial observations by GPS-information, preserving the quality of the net.

For both strategies of optimization simulated examples are given. The GPS-information is used as 2D-coordinate-differences with a precision between 0.1-1.0 ppm or as derived quantities distances and azimuths. Our objective is to demonstrate the possibilities given nowadays for including satellite information in the design and adjustment process of 2D-geodetic networks.

2. THEORETICAL BACKGROUND

2.1 General

The combination of satellite information and traditional terrestrial observations in a combined model cannot be done without problems, as both

types of observables are defined in different reference systems (***BÄUMKER 1984***). Furtheron in classical geodetic networks a rigorous separation between the horizontal and height components is used. The reference system for horizontal control networks is in general a geometrically defined reference ellipsoid (best fit to the area under discussion). The reference system for the vertical control is in general the geoid, which is defined purely by physical parameters. As reference system for the satellite observations a cartesian, earth fixed, geometric coordinate system is used, i.e. a 3D-model based on well defined assumptions on its origin, orientation and scale.

For a combined solution of terrestrial and GPS-observations therefore a common reference system has to be defined or selected. In the literature different approaches for this problem can be found ***(see e.g. WELSCH and OSWALD 1984)***. Essentially the proposed one-, two- and three-dimensional models can be described as follows:

2.2. Three-Dimensional-Solution

For a 3D-solution a transformation of the terrestrial and the satellite observations into a common 3D-reference-system has to be carried out (see Fig. 1).

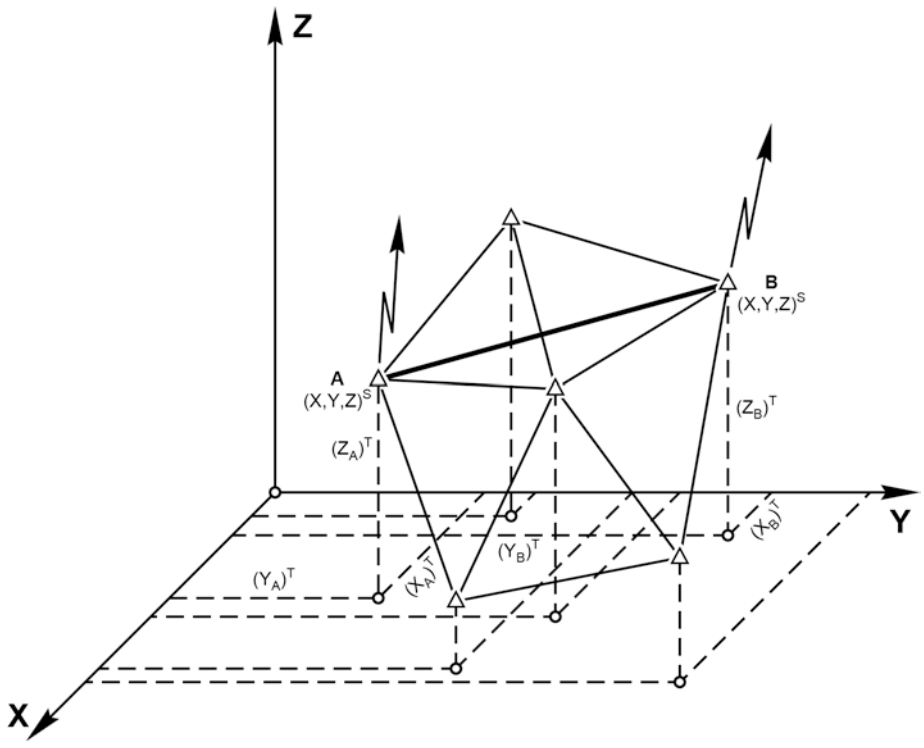

Fig. 1: 3D-combined-solution

The main advantage is the use of the entire GPS-information. Critical is the selection of a suitable reference system, which has to be stable for a longer period of time. Critical for the transformation of terrestrial observations is the inaccurate determination of the geoid.

2.3 Two-Dimensional-Solution

In this approach a transformation of the 3D-satellite-information into a 2D-reference-system has to be carried out.

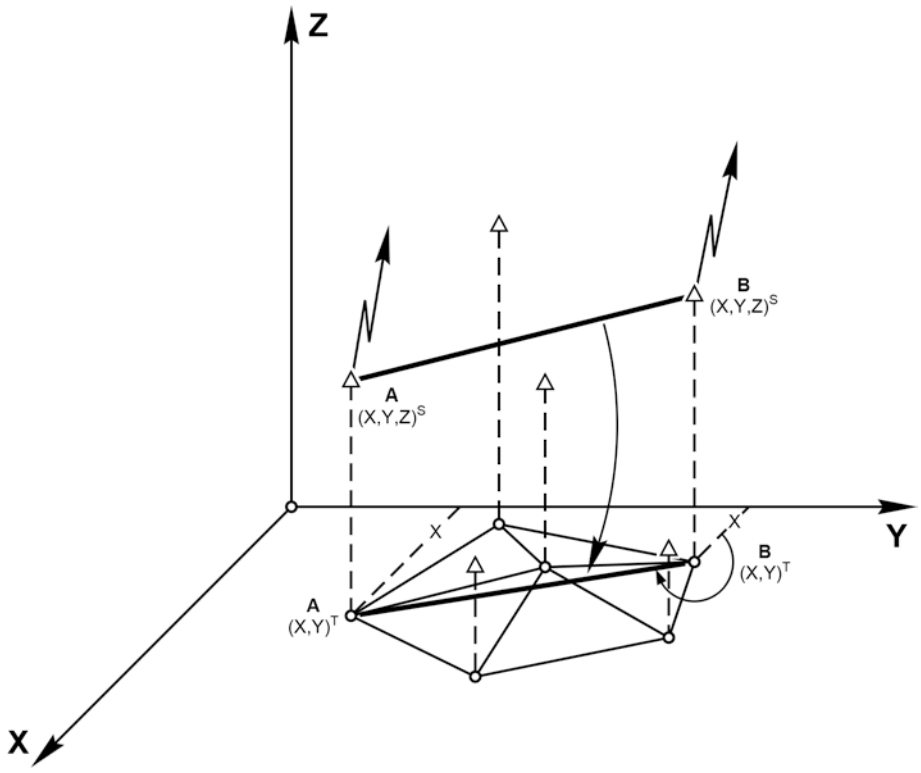

Fig. 2: 2D-combined-solution

The main advantage is that the existing reference system for horizontal control, as used e.g. by the state survey authorities, can be maintained. Existing software packages for the adjustment can be used. A problem is the transformation for the functional and stochastic components of the 3D-information into the 2D-reference-system, and here especially the elimination of the height components has to be mentioned ***(WOLF 1980, 1982)***. This approach is outlined in some detail in chapter 3. Unsatisfactory remains the loss of information due to the transformation into a 2D-system.

2.4 One-Dimensional-Solution

The one-dimensional approach - in consequence with the preceding approaches - is using the satellite information as support for extended height control networks. Due to the high relative and almost distance independent precision the GPS-information can be used for separate checks in extended levelling networks. The problem here is of course the definition of the geoid and the choice of a suitable reference system for both kinds of observables.

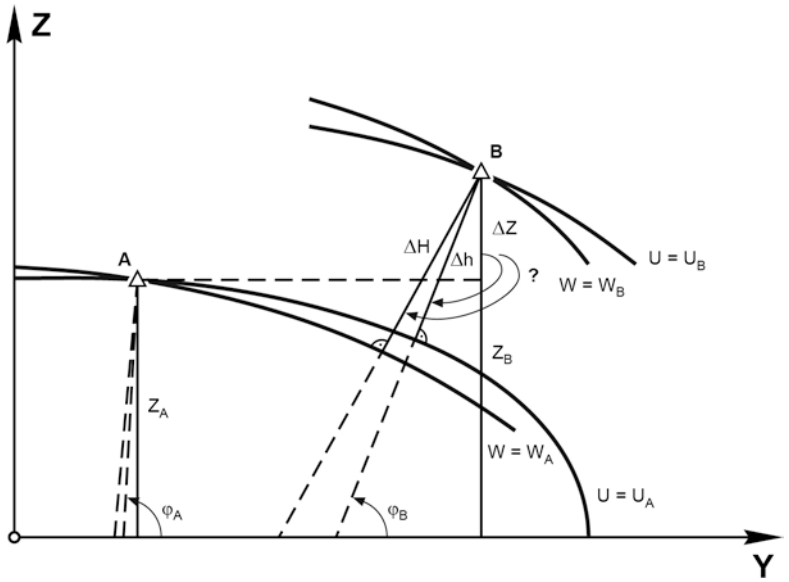

Fig. 3: 1D-combined-solution

3. TRANSFORMATION OF 3D-GPS-INFORMATION FOR 2D-UTILIZATION

The simulation studies, given in the next chapter, are based on the 2D-combination-model, as outlined in section 2.3. As starting point we consider the coordinate differences ΔX, ΔY, ΔZ and the corresponding covariance matrix $(C_{\Delta XYZ})_S$ for a single baseline. Following the techniques of double or triple differences ***(GOAD 1985, REMONDI 1984)*** this is the commonly used derived observables after preprocessing of the original data. For the treatment of these 3D-coordinate-differences in a 2D-adjustment process a transformation into the 2D-reference-system, e.g. the Gauß-Krüger-plane, is necessary. This transformation can be split up into four steps, see Fig. 4:

As a first step the 3D-cartesian-coordinate-differences of the satellite system, defined e.g. in the WGS 1984, has to be transformed into ellipsoidal-

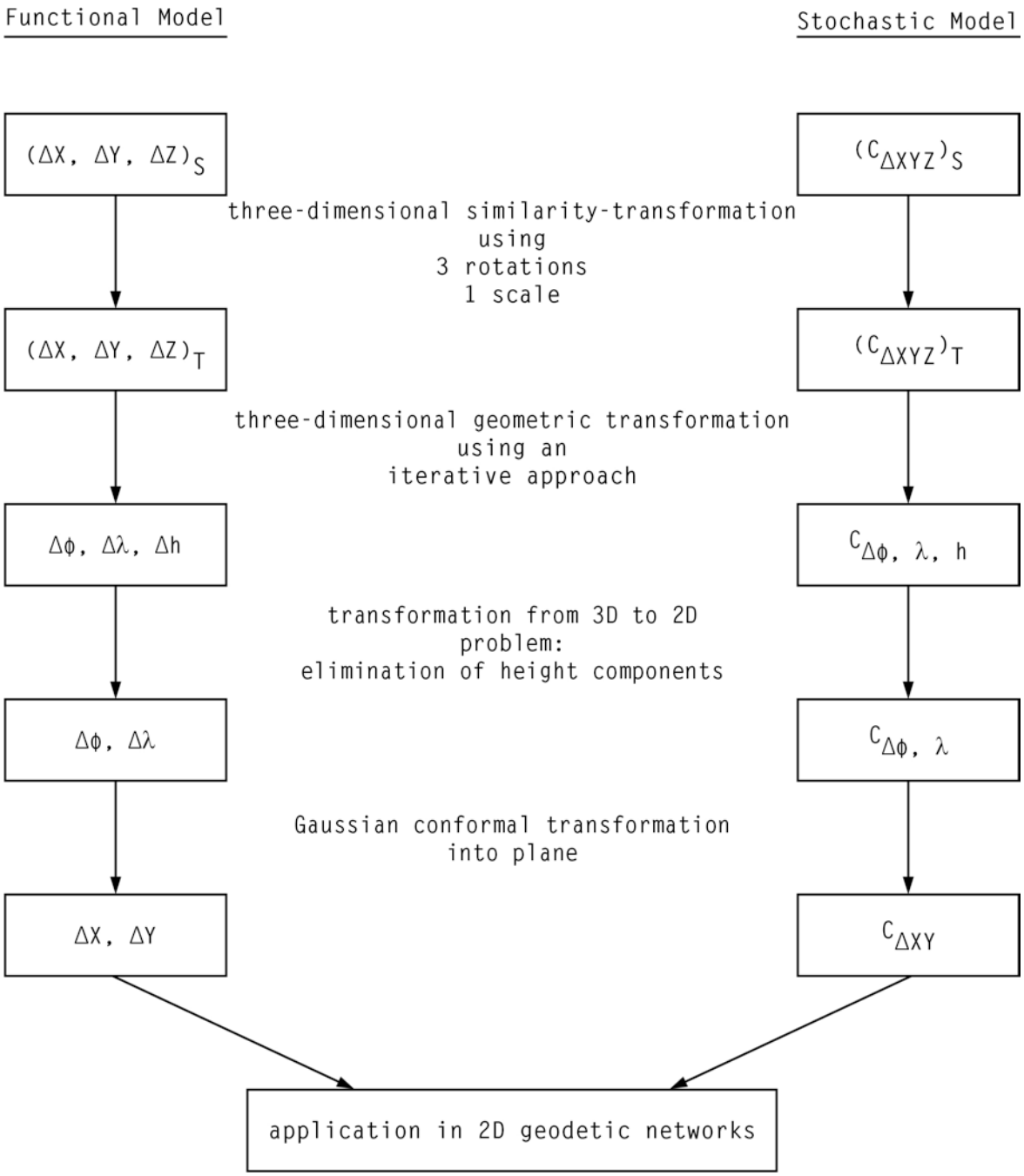

Fig. 4: Transformation of GPS-coordinate differences from 3D into 2D

cartesian-coordinate-differences of the reference ellipsoid, e.g. the Bessel-ellipsoid. This 4-parameter-transformation is given by

$$\Delta X_S = (1+m)\, R(\varepsilon)\, \Delta X_T \qquad (3\text{-}1)$$

ΔX_S : coordinate differences in the satellite system
ΔX_T : coordinate differences in the terrestrial system
m : scale factor
$R(\varepsilon)$: matrix of rotation

In principle this is a 7 parameter transformation. Due to the use of coordinate differences the translation parameters between both systems vanish. The covariance-matrices $(C_{\Delta XYZ})_S$ have to be transformed, too. These formulae can be derived applying the law of error propagation to Eq.(3-1). A problem is the determination of the transformation parameters. For our relative 2D-applications approximate values should be sufficient, which can be taken from (theoretical) global definitions of the different systems or from a local determination via identical points.

The next step is the transformation of the ellipsoidal cartesian into ellipsoidal geographical coordinate differences. This can be done on the basis of the well-known iterativ relations ***(e.g. TORGE 1975)***:

$$\phi = \arctan\frac{Z}{\sqrt{X^2+Y^2}}\left(1+e^2\,\frac{N}{N+h}\right)^{-1} \qquad (3\text{-}2)$$

$$\lambda = \arctan\frac{Y}{X} \qquad (3\text{-}3)$$

$$h = \frac{\sqrt{X^2+Y^2}}{\cos\phi} - N \qquad (3\text{-}4)$$

Here X, Y, Z are ellipsoidal cartesian coordinates, ϕ, λ, h are ellipsoidal geographical coordinates, N is the radius of normal curvatures and e is the 1st numerical eccentricity. The covariance matrix has to be transformed by using again the law of error propagation

$$C_{\Delta\phi,\lambda,h} = F\, C_{\Delta XYZ}\, F^T \qquad (3\text{-}5)$$

where the matrix F has to be derives according e.g. to ***HOYER (1982)***.

The third step concerns the elimination of the height component. Here the following apporaches are mentioned in the literatur ***(WOLF 1980, 1982, WELSCH***

and OSWALD 1984):

- algebraic elimination of the heights out of the normal equations
- geometric elimination by crossing out the height information
- fixing the ellipsoidal heights

The most elegant and rigorous approach is the algebraic elimination, suggested by ***WOLF (1982)***, as here no loss of information has to be taken into account.

The last step is the transformation of the 2D-ellipsoidal geographical coordinates $\Delta\phi$, $\Delta\lambda$ into Gauß-Krüger-differences by the well-known formulae, given in any textbook on mathematical geodesy. Again the corresponding covariance matrix is derived by applying the law of error propagation.

This method of transformation is not free of problems. Especially the determination of the transformation parameters and the transformation of the stochastic part should be mentioned. A further discussion of this topic is without the scope of this paper. Anyway, it should be pointed out that under certain conditions the transformation from 3D to 2D coordinate differences is rigorously possible.

4. DIFFERENT WAYS TO USE 2D-GPS-INFORMATION IN AN ADJUSTMENT PROCESS

To use the 2D-GPS-coordinate-differences in a common adjustment program, different ways can be selected.

a) The most direct way would be the use of 2D-coordinate-differences as an additional type of observables in the adjustment program. The error equations then would be:

$$\Delta X_{ij} + v_{\Delta X_{ij}} = \hat{X}_j - \hat{X}_i \qquad (4\text{-}1)$$

$$\Delta Y_{ij} + v_{\Delta Y_{ij}} = \hat{Y}_j - \hat{Y}_i \qquad (4\text{-}1)$$

The stochastic model is given by the non-diagonal matrix

$$C_{\Delta XY} = \begin{bmatrix} \sigma_{\Delta X\Delta X} & \sigma_{\Delta X\Delta Y} \\ \sigma_{\Delta Y\Delta X} & \sigma_{\Delta Y\Delta Y} \end{bmatrix} \qquad (4\text{-}3)$$

Eq.(4-3) shows that even for a single baseline off-diagonal elements exist, which have some influence on the formation of the normal equations and e.g. the technique used for "data snooping".

To treat the GPS-information only as relative information we have to introduce some additional parameters in the above model, which take into account the uncertainty of the transformation parameter used between the 3D- and the 2D-information.

b) A further technique, used for the simulation studies in chapter 5, is the use of derived quantities instead of the original coordinate differences. In the most simple case these may be distances D_{ij} and azimuths A_{ij} leading to the error equations

$$D_{ij} + v_{D_{ij}} = m \left((X_j - X_i)^2 + (Y_j - Y_i)^2 \right)^{1/2} \qquad (4\text{-}4)$$

$$A_{ij} + v_{A_{ij}} = \arctan \frac{Y_j - Y_i}{X_j + X_i} + O \qquad (4\text{-}5)$$

The cooresponding covariance matrix has to be computed using the usual error propagation techniques.

$$C_{DA} = \begin{bmatrix} \sigma_{DD} & \sigma_{DA} \\ \sigma_{AD} & \sigma_{AA} \end{bmatrix} \qquad (4\text{-}6)$$

In this model the often found scale differences between terrestrial and satellite systems are accounted for by the scale factor m in Eq.(4-4), whereas for possible orientation differences the orientation parameter O is used, which should be introduced for all derived azimuths.

For both techniques the stochastic model is restricted to the components of one baseline. In theory there should be estimates for the correlation between different baselines as well, but - al least as the authors are aware - no information for this inter-baseline correlation is computed in the common preprocessing software packages.

The advantage of the techniques presented here is the ability to use common 2D-adjustment programs (e.g. our system PAN) for the combination of terrestrial and satellite observations. Furtheron it is possible to optimize these combined networks in respect to precision and reliability using any techniques and algorithms developed for terrestrial networks ***(see e.g. NIE-***

MEIER 1985). Therefore it was relatively easy to carry out the following simulation studies using just the well established program system PAN to simulate the GPS- and the terrestrial observations, to perform the adjustment, to carry out the optimization and to represent the results graphically.

5. SIMULATION STUDIES

5.1 Example 1: Ideal Control Network

Here the strategy was to improve the precision and reliability by additional GPS-information. The datum of all adjustments are defined by the minimum constraint solution. The systematic control network consists of 61 points with a point distance of 10 km. All distances and sets of directions to neighboring points are assumed to be observed. The scheme of this net and the error ellipses are depicted in Fig. 5. For the simulated terrestrial observations the following standard deviation were selected:

directions σ_R = 0.2 mgon

distances σ_D = 5 mm + 5 ppm

For the GPS-information at first a precision of 1 ppm for single baselines was chosen, but with this precision only a minor improvement of the quality of this almost ideal control network was found. Therefore the nowadays still too optimistic precision of 0.1 ppm was taken for the GPS-baselines and derived quantities. A detailed study was carried out with a lot of different variants for the additional GPS-information *(KLOTH 1985)*. As representative for all variants only the results of a combined network with 6 outer and 6 diagonal baselines are given in Table 1 and Fig. 5. It can easily be seen that an improvement of the precision of such an almost homogeneous and isotropic network can only be found at the outer points of redundancy as measures for the "inner" reliability, but there is an effective reduction of the nabla-values ∇X and ∇Y for the corner points.

It may seem not to be useful just to add GPS-observations to such a good terrestrial network. Therefore the way for the future will be to reduce the number of terrestrial observations, preserving the high quality of the net-

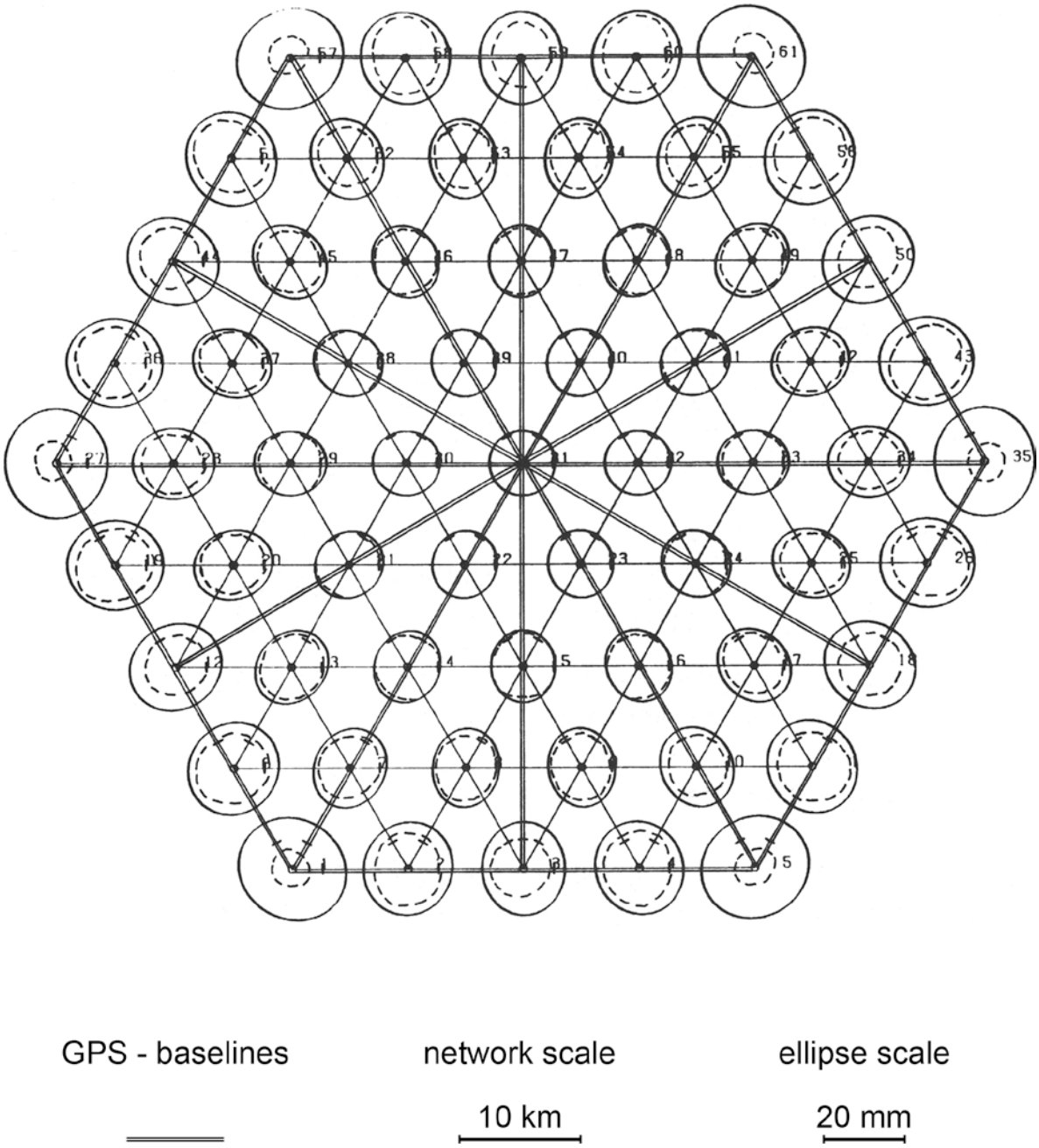

Fig. 5: Simulated control network
Error ellipses :
- full lines : pure terrestrial network
- dashed lines : terrestrial plus GPS network

work. This strategy to replace terrestrial observations by GPS is used in the next examples.

	precision		reliability			
	error ellipses		inner		outer	
	major axis [mm]	minor axis [mm]	distance [ ]	direction [ ]	∇X [mm]	∇Y [mm]
Terrestrial Network						
max	15.71	14.43	0.53	0.73	53.5	61.2
min	9.38	9.38	0.33	0.56	16.6	19.1
Combined Network						
max	11.18	9.78	0.55	0.73	37.0	31.0
min	6.05	5.42	0.49	0.59	9.3	10.1

Table 1: Measures for precision and reliability for a simulated control network ***(KLOTH 1985)***

5.2 Example 2: Systematic Tunneling Network

As example for a network in engineering surveying a tunneling network was selected. These networks are in general designed independently from geodetic control and are computed within the model of minimum constraints or as free networks. For a tunneling network homogeneity or isotropy is no meaningful traget function for optimization; the essential measure for precision is the break-through error or the relative error ellipse of the break-through points ***(see e.g. KRÜGER and NIEMEIER 1984)***.

A typical scheme is depicted in Fig. 6. The surface network has to connect the two portal areas, which are the starting points for the construction of the tunnel. In practice expensive work for the set-up of the high signals and the cutting of trees to get free lines of sight has to be done very often. Here the idea was to replace at least parts of the surface network by GPS-observations and to study the effect on the quality of the net, resp. the break-through error.

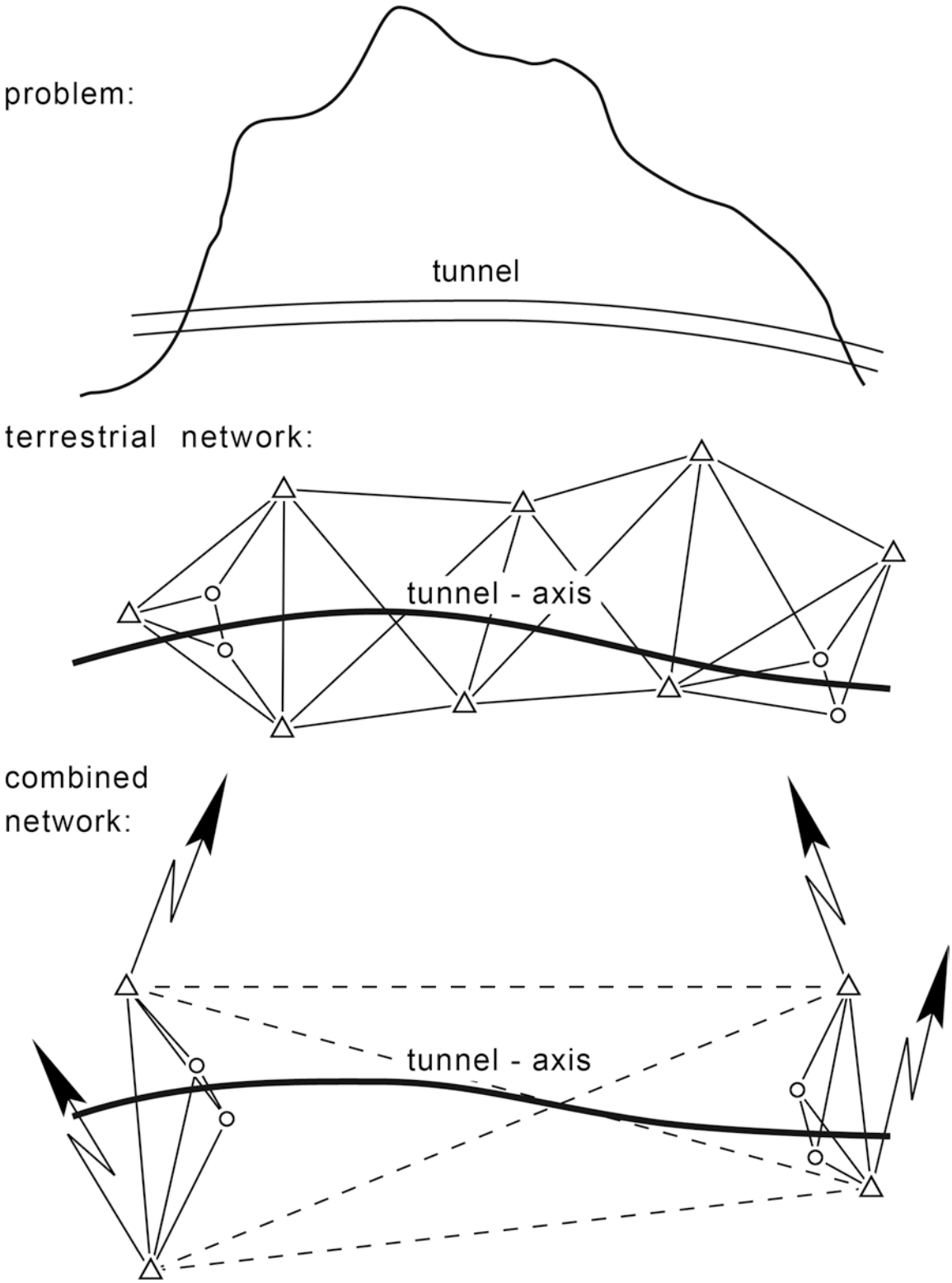

Fig. 6: Basic ideas for tunneling networks using terrestrial or GPS networks

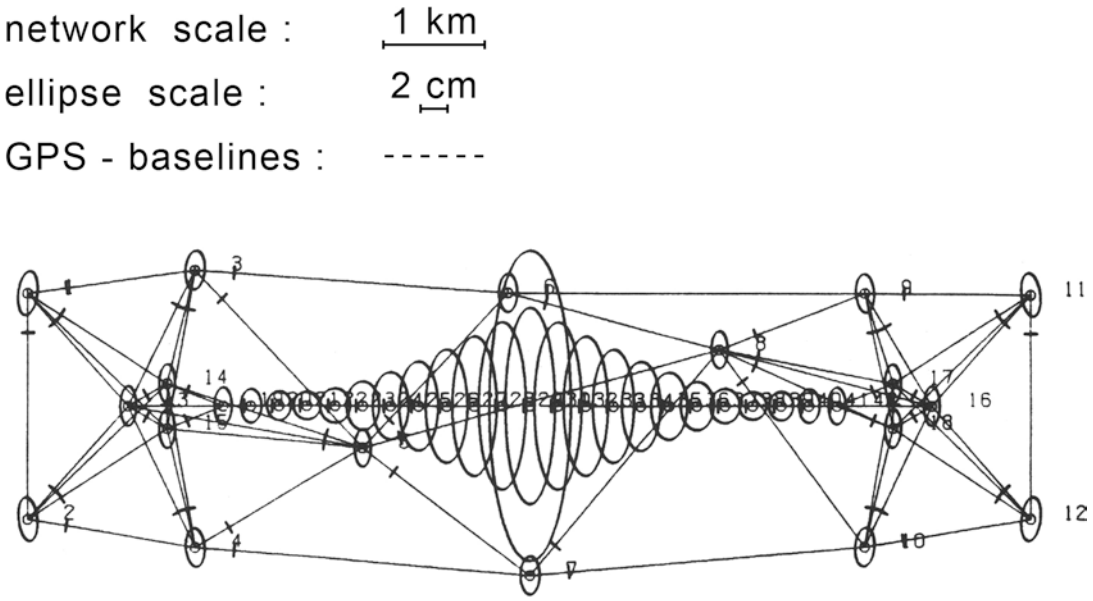

Fig. 7: Variants of the simulated tunneling network with error ellipses and the break-through relative error ellipse

variant	1. Precision and Reliability of the Main Portal Points						
		precision			reliability		
	point no.	A	B [cm]	P	$\nabla_{X_{max}}$	$\nabla_{Y_{max}}$	$\nabla_{P_{max}}$
0	14	1.72	0.71	1.86	1.53	0.78	1.72
	18	1.72	0.72	1.86	1.52	0.83	1.73
1	14	1.87	0.71	2.00	1.67	0.98	1.94
	18	1.88	0.71	2.01	1.67	0.83	1.96
2	14	2.14	0.83	2.30	2.17	1.41	2.59
	18	2.14	0.83	2.30	2.17	1.41	2.59

	2. Precision and Reliability of the Break-Through Points						
0	30, 31	8.70	2.24	8.98	5.36	0.77	5.42
1	30, 31	8.61	2.19	8.88	5.26	0.78	5.32
2	30, 31	8.66	2.17	8.93	8.18	0.96	8.24

variant	3. Break-Through Error	
	orthogonal [cm]	longitudinal [cm]
0	13.74	3.65
1	13.76	3.61
2	14.13	3.64

variant	4. Values of Reliability for the Entire Network											
	directions			distances			GPS-distances			GPS-azimuths		
	z_{min}	z_{mean}	∇_{max}	z_{min}	z_{mean}	∇_{max}	z_{min}	z_{mean}		z_{min}	z_{mean}	∇_{max}
0	0.33	0.68	2.87	0.46	0.71	6.82	-	-	-	-	-	-
1	0.32	0.64	2.91	0.61	0.73	4.48	0.23	0.27	5.14	0.52	0.53	0.37
2	0.29	0.57	3.05	0.67	0.70	4.31	0.24	0.26	7.51	0.62	0.62	0.34

variant	5. Expenditure			
	points	directions	distances	GPS-baselines
0	18	110	56	0
1	14	72	36	4
2	10	40	20	4

Table 2: Results of the simulation variants for the tunneling network

In Fig. 7 different network configurations and their corresponding error ellipses are depicted. For the observations in the surface network the following a priori standard deviations were chosen:

directions	σ_R = 0.4 mgon
distances	σ_D = 3 mm + 3 ppm
GPS baseline information	σ_{GPS} = 1 ppm

As usual in tunneling for the underground network these values were doubled.

For the networks in Fig. 7 the typical weakness of long networks orthogonal to its extension can be found. The main portion of the break-through error is caused by the weak underground net - simple polygons -; for the discussion of different variants in Table 2 the values for the portal points should be given more evidence. In terms of precision the variants with GPS-observations have just little larger error ellipses, whereas the break-through error is almost unchanged. Considering reliability we can state that the external reliability is reduced a little bit, especially in variant 2, while the ∇_{max}-value for distances is 35% down. Looking at the costs for the different variants, Table 2 shows the tremendous reduction for the terrestrial field work. This reduction for the surface network combined with just a minor loss of quality was possible by adding only 4 GPS-baselines! As the relation in costs between terrestrial and GPS-observations cannot be given exactly, we restricted ourselves to the number of points and observations rather than to the money behind it.

5.3 Example 3: Tunneling System No. 7 of the New Railroad Route Hannover - Würzburg

Finally, as a practical example the tunneling system no. 7 of the new railroad route Hannover - Würzburg will be discussed. The combined net for the Sohlberg-tunnel and the Krieberg-tunnel has a length of about 7.5 km and was established in 1983. It can be seen in Fig. 8, variant 0, that the topography is the limiting factor for the configuration of this network. The variant 0 is the original net and the values for the precision of the observations used in Example 2 and 3 are taken from this net. The error ellipses of this net are depicted in Fig. 8, while measures for the quality are given in Table 3.

In the variant 1 and 2 the connection between the portal points is realized by 8 GPS baselines. In variant 1 eight points of the original network are

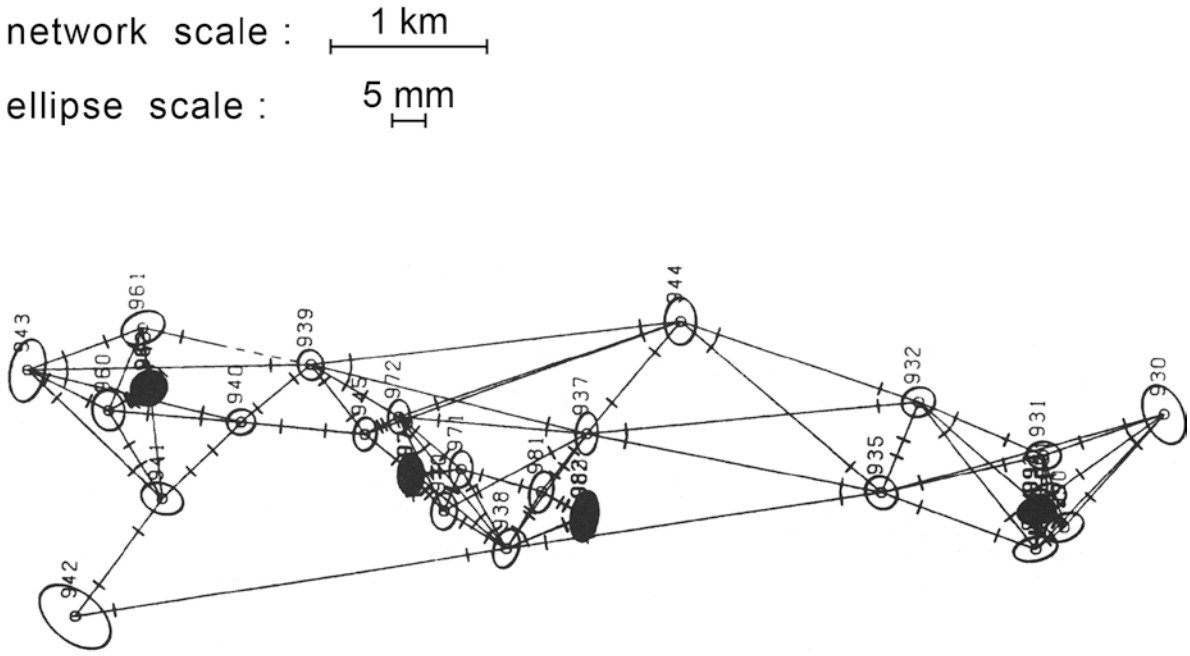

Fig. 8: Different variants for the tunneling system 7 using pure terrestrial or combined networks

variant	1. Precision and Reliability of the Main Portal Points						
		precision			reliability		
	point no.	A	B [cm]	P	$\nabla_{X_{max}}$	$\nabla_{Y_{max}}$	$\nabla_{P_{max}}$
0	962	0.31	0.28	0.42	0.50	0.43	0.66
	973	0.34	0.22	0.40	0.22	0.55	0.59
	982	0.42	0.23	0.48	0.25	0.72	0.76
	993	0.32	0.21	0.38	0.39	0.27	0.47
1	962	0.25	0.22	0.33	0.46	0.47	0.66
	973	0.31	0.19	0.36	0.21	0.47	0.51
	982	0.25	0.17	0.38	0.23	0.65	0.69
	993	0.16	0.10	0.19	0.49	0.17	0.52
2	962	0.22	0.15	0.27	0.59	0.54	0.80
	973	0.47	0.19	0.51	0.38	0.97	1.04
	982	0.34	0.15	0.37	0.18	0.72	0.74
	993	0.17	0.15	0.23	0.47	0.33	0.57

variant	2. Values of Reliability for the Entire Network											
	directions			distances			GPS-distances			GPS-azimuths		
	z_{min}	z_{mean}	∇_{max}	z_{min}	z_{mean}	∇_{max}	z_{min}	z_{mean}		z_{min}	z_{mean}	∇_{max}
0	0.23	0.61	3.43	0.55	0.84	5.51	-	-	-	-	-	-
1	0.30	0.55	3.04	0.72	0.85	3.02	0.33	0.44	2.11	0.34	0.53	0.45
2	0.27	0.46	3.15	0.72	0.83	2.19	0.34	0.41	2.13	0.58	0.61	0.35

variant	5. Expenditure			
	points	directions	distances	GPS-baselines
0	30	159	159	-
1	22	92	52	8
2	16	54	54	8

Table 3: Results of the simulation variants for the network of the tunnel system 7

cancelled. In variant 2 even 14 points are cancelled, here the GPS baselines are directly observed between the portal points. This replacement of a number of points and a lot of the terrestrial observations by just 8 GPS baselines does not really weaken the quality of the network, as can be seen in Table 3: The precision of the portal points 962 and 973 for the Sohlberg-tunnel and 982 and 993 for the Kriegberg-tunnel is better (variant 1) or almost as good (variant 2) as in the original variant! The same statement can be made for the external reliability of these points and for the average reliability of the whole network.

6. SUMMARY AND PROSPECT

With the set-up of the Global-Positioning-System very precise information for geodetic positioning is or will be available. The GPS observables cannot only be used for the establishment and checking of global 3D-networks, this information is as well useful for the improvement of regional and local 2D-networks. It is shown that the transformation of 3D-baseline vectors into 2D-coordinate differences is possible, and that these differences can be simply included into the common 2D-adjustment programs.

For the many problems involved generally with the design of tunneling networks we have proved that the use of GPS-information will bring many advantages and probably will be less expensive than the classical terrestrial techniques: To achieve the same quality for the nets a reduction of about 50% for terrestrial observations is possible.

The inclusion of GPS-observations in well designed, homogeneous terrestrial control networks will give only minor improvements, but it provides the possibility to replace a lot of terrestrial observations without any substantial loss in the quality of the net. As a consequence of these replacements perhaps a completely new structure of control schemes will be established in the future. At least the higher order networks will be observed by GPS only. In a further step it is possible that the hierarchical structure of control networks will vanish completely. As proposed by ***VANIČEK et al. (1983)*** perhaps only a few permanent GPS-stations will serve as reference stations, and will dispose the coordinate information for a whole country. For each surveying activity the coordinate link to these stations will be made by GPS measurements, while the detailed surveying will be performed either by GPS or by terrestrial techniques ***(EICHHOLZ et al. 1985)***.

This is a concept for the future, but perhaps these ideas will come through faster that even optimists may expect.

7. REFERENCES

BÄUMKER, M.: ***Zur dreidimensionalen Ausgleichung von terrestrischen und Satellitenbeobachrtungen.*** Wiss. Arb. d. Fachr. Verm. der Universität Hannover, Nr. 130, Hannover, 1984

EICHHOLZ, K.; KORITTKE, N.; NIEMEIER, W.: ***Zur Optimierung markscheiderischer Messungen über und unter Tage.*** Mitt. Westf. Berggewerkschaftskasse, Nr. 50, Bochum, 1985

GOAD, C.C.: ***Precise Relative Position Determination Using Global Positioning System Carrier Phase Measurements in a Nondifference Mode.*** Proceedings "Positioning with GPS - 1985", Vol. I, pp. 347 - 356, 1985

HOYER, M.: ***Satelliten-Dopplermessungen als unterstützende Beobachtungen bei der Kontrolle und Verbesserung eines geodätischen Netzes in Venezuela.*** Wiss. Arb. d. Fachr. Verm. der Universität Hannover, Nr. 111, Hannover, 1982

KLAKA, H.; KORITTKE, N.: ***Einsatz eines neuen Satellitenmeßsystems im Befliegungsnetz Emschermulde.*** Merkscheidewesen, 1985, in press.

KLOTH, G.: ***Simulationsstudien zur Verknüpfung von GPS- und terrestrischen Meßinformationen am Beispiel zweidimensionaler geodätischer Netze.*** Diplomarbeit am Geodätischen Institut der Universität Hannover, unveröffentlicht, 1985

KRÜGER, J.; NIEMEIER, W.: ***Zur Genauigkeits- und Zuverlässigkeitsanalyse bei der Anlage von Tunnelabsteckungsnetzen.*** IX. Int. Kurs f. Ingenieurvermessung, Graz, 1984

NIEMEIER, W.: ***Netzqualität und Optimierung.*** In: H. Pelzer (Hrsg.): Geodätische Netze in Landes- und Ingenieurvermessung II, Verlag Konrad Wittwer, Stuttgart, 1985

REMONDI, B.W.: ***Using the Global Positioning System (GPS) Phase Observable for Relative Geodesy: Modeling, Processing and Results.*** Ph. D. Dissertation, University of Texas, 1984

SEEBER, G.: ***Das Navy Navigation Satellite System und seine geodätische Nutzung.*** Schriftenreihe der Hochschuel der Bundeswehr München, Heft 15, München, 1984

TORGE, W.: ***Geodäsie.*** Verlag Walter de Gruyter, Berlin, New York, 1975

VANICEK, P.; WELLS, D.; CHRZANOWSKI, A.; HAMILTON, A.C.; LANGLEY, R.B.; McLAUGLIN, J.D.; NICKERSON, B.G.: ***The Future of Geodetic Networks.*** Proceedings of the IUGG-Congress, Hamburg, 1983

WELSCH, W.; OSWALD, W.: ***Kombinierte Ausgleichung von Doppler-Satellitennetzen und terrestrischen Netzen.*** Schriftenreihe der Hochschule der Bundeswehr München, Heft 15, München, 1984

WOLF, H.: ***Scale and Orientation in Combined Doppler and Triangulation Nets.*** Bulletin Géodésique 54, pp. 45 - 53, 1980

WOLF, H.: ***Stochastic Aspect in Combined Doppler and Triangulation Nets.*** Bulletin Géodésique 56, pp. 63 - 69, 1982

SCHRIFTENREIHE

des Wissenschaftlichen Studienganges Vermessungswesen an der HSBwM

Bisher erschienene Hefte :

Nr. 1/78 A. Schödlbauer:
Curriculum für den wissenschaftlichen Studiengang Vermessungswesen der Hochschule der Bundeswehr München;
53 Seiten, DM 10.--

Nr. 2/78 A. Chrzanowski and E. Dorrer (Eds.):
Proceedings "Standards and Specifications for Integrated Surveying and Mapping Systems", Workshop held in Munich,
1-2 June 1977;
181 Seiten, DM 20.--

Nr. 3/78 W. Caspary und A. Geiger:
Untersuchungen zur Leistungsfähigkeit elektronischer Neigungsmesser;
62 Seiten, DM 10.--

Nr. 4/79 E. Baumann, W. Caspary, H. Dupraz, W. Niemeier, H. Pelzer, E. Kuntz, G. Schmitt, W. Welsch:
Seminar über Deformationsanalysen;
106 Seiten, DM 15.--

Nr. 5/81 K. Torlegård:
Accuracy Improvement in Close Range Photogrammetry;
68 Seiten, DM 10.--

Nr. 6/82 W. Caspary und W. Welsch (Herausgeber):
Beiträge zur großräumigen Neutrassierung;
268 Seiten, DM 20.--

Nr. 7/82 K. Borre and W.M. Welsch (Editors):
Proceedings "Survey Control Networks",
Meeting of FIG-Study Group 5B, Aalborg, 7 - 9 July 1982;
428 Seiten, DM 35.--

Nr. 8/82 A. Geiger:
Entwicklung und Erprobung eines Präzisionsneigungstisches zur Kalibrierung geodätischer Instrumente;
124 Seiten, DM 10.--

Nr. 9/83 W. Welsch (Herausgeber):
Deformationsanalysen '83;
336 Seiten, DM 25.--

Nr. 10/84 W. Caspary, A. Schödlbauer und W. Welsch (Herausgeber):
Beiträge aus dem Institut für Geodäsie;
241 Seiten, DM 20.--

SCHRIFTENREIHE

des Wissenschaftlichen Studienganges Vermessungswesen an der HSBwM

Nr. 11/84 W. Caspary und H. Heister (Herausgeber):
Elektrooptische Präzisionsstreckenmessung;
268 Seiten, DM 20.--

Nr. 12/84 P. Schwintzer:
Analyse geodätisch gemessener Punktlageänderungen
mit gemischten Modellen;
155 Seiten, DM 15.--

Nr. 13/84 G. Oberholzer:
Landespflege in der Flurbereinigung;
80 Seiten, DM 10.--

Nr. 14/84 G. Neukum mit Beiträgen von G. Neugebauer:
Fernerkundung der Planeten und kartographische Ergebnisse;
100 Seiten, DM 25.--

Nr. 15/84 A. Schödlbauer und W. Welsch (Herausgeber):
Satelliten-Doppler-Messungen,
Beiträge zum Geodätischen Seminar 24./25. September 1984;
394 Seiten, DM 30.—

Nr. 16/85 M.K. Szacherska, W.M. Welsch:
Geodetic Education in Europe;
230 Seiten, DM 20.—

Nr. 17/85 B. Eissfeller, G.W. Hein:
A Contribution to 3d-Operational Geodesy.
Part 4: The Observation Equations of Satellite Geodesy in
the Model of Integrated Geodesy;
(in Vorbereitung)

Nr. 18/85 G. Oberholzer:
Landespflege in der Flurbereinigung, Teil II;
114 Seiten, DM 12.—

Nr. 19/86 H. Landau, B. Eissfeller and G.W. Hein:
GPS Research 1985 at the Institute of Astronomical
and Physical Geodesy;
210 Seiten, DM 20.—

Nr. 20/85 W. Welsch and L.A. Lapine (Editors):
Proceedings "Inertial, Doppler and GPS Measurements for
National and Engineering Surveys"
Joint Meeting of Study Groups 5B and 5C, July 1-3, 1985;
2 Bände, 630 Seiten, DM 50.—